1. Report No. CR-165205	2. Government Accession No.	3. Recipient's Catalog No.

4. Title and Subtitle

SKF COMPUTER PROGRAM "SPHERBEAN"
VOLUME III: Program Correlation with
Full Scale Hardware Tests

5. Report Date DECEMBER 1980

6. Performing Organization Code AT81D008

7. Author(s)

R.J. KLECKNER
J.W. ROSENLIEB
G. DYBA

8. Performing Organization Report No.

9. Performing Organization Name and Address

SKF Industries, Inc.
Technology Services
1100 First Avenue
King of Prussia, Pa. 19406

10. Work Unit No.

11. Contract or Grant No. NAS3-20824

12. Sponsoring Agency Name and Address

NASA/Lewis Research Center
21000 Brookpark Road
Cleveland, Ohio 44135

13. Type of Report and Period Covered Final Report/ June 1978-December 1980

14. Sponsoring Agency Code

15. Supplementary Notes

16. Abstract

The objective of this three volume report is to describe the use of a fully operational computer program which will predict the thermomechanical performance characteristics of high speed lubricated double row spherical roller bearings. The analysis allows six degrees of freedom for each roller and three for each half of an optionally split cage. Roller skew, free lubricant, inertial loads, appropriate elastic and friction forces, flexible outer ring, etc. are considered. Roller quasidynamic equilibrium is calculated for a bearing with up to 30 rollers per row, and distinct roller and flange geometries are specifiable. Software performance is verified by correlation with results of hardware testing.

Volume I describes the models and associated mathematics used within SPHERBEAN. The user is referred to the material contained there for formulation assumptions and algorithm detail.

Volume II is structured to guide the user in the correct and practical implementation of SPHERBEAN. Input and output, guidelines for program use and sample executions are detailed.

The material presented in this, Volume III, describes the results of a series of full scale hardware tests, and demonstrates the degree of correlation between performance predicted by SPHERBEAN and measured data. Experimental and calculated performance data is compared over a range in speed up to 19,4000 RPM (.8 MDN), under pure radial, pure axial and combined loads.

17. Key Words (Suggested by Author(s))	18. Distribution Statement
Spherical Roller Bearing Computer Simulation High Speed Tests Thermal Analysis	

19. Security Classif. (of this report)	20. Security Classif. (of this page)	21. No. of Pages	22. Price*

* For sale by the National Technical Information Service, Springfield, Virginia 22161

SPHERICAL ROLLER BEARING ANALYSIS

SKF COMPUTER PROGRAM "SPHERBEAN"

VOLUME III: PROGRAM CORRELATION WITH FULL SCALE HARDWARE TESTS

DECEMBER 1980

R.J. KLECKNER
J.W. ROSENLIEB
G. DYBA

Prepared: Robert J. Kleckner

Approved:

Released:

SKF REPORT NO.: AT81D008

SKF PROGRAM NO.: AT81Y001

SUBMITTED TO:

NATIONAL AERONAUTICS & SPACE ADMINISTRATION
LEWIS RESEARCH CENTER
21000 BROOKPARK ROAD
CLEVELAND, OHIO 44135

SUBMITTED BY:

SKF INDUSTRIES, INC.
TECHNOLOGY SERVICES
1100 FIRST AVENUE
KING OF PRUSSIA, PA 19406

FOREWORD

This, Volume III of the report "Spherical Roller Bearing Analysis" describes the results of full scale hardware tests and demonstrates the degree of correlation between performance predicted by SPHERBEAN and measured data.

Efforts involved in the generation of the computer code and hardware testing were accomplished under contract NAS3-20824 issued by the NASA-Lewis Research Center of Cleveland, Ohio, under the administration of the Structures and Mechanical Technologies Division. Funding was provided by the Product Assurance office of the Army Aviation Research and Development Command, St. Louis, Missouri. The technical monitor was Mr. H. H. Coe. The work was performed at SKF Industries, Inc., King of Prussia, Pennsylvania, during the Period June 1978 to December 1980.

Technical project leadership was executed by Mr. R. J. Kleckner, with contributions from Dr. J. Pirvics and Messrs. F. Morrison, N. Miller and T. Deromedi.

TABLE OF CONTENTS

LIST OF TABLES

LIST OF FIGURES

LIST OF FIGURES (CONTINUED)

LIST OF FIGURES (CONTINUED)

LIST OF FIGURES (CONTINUED)

LIST OF FIGURES (CONTINUED)

LIST OF FIGURES (CONTINUED)

LIST OF FIGURES (CONTINUED)

1.0 INTRODUCTION

The rolling element bearing, in today's technology, is being required to operate at ever increasing DN values. Ball bearings, for example, have seen numerous applications at the 2×10^6 DN level. Cylindrical and tapered configurations are being asked to follow in this regime. These new demands result from the requirements posed by advanced hardware missions and the increased emphasis on extracting maximum energy from a given process cycle.

The conventional spherical rolling element bearing design, Figure 1, meets all but one of the challenges posed by these emerging requirements. Operating speed has been restricted to maximum values on the order of 5000 rpm. DN values have peaked at about $.25 \times 10^6$. Efforts are now under way to reach higher speeds, with particular emphasis placed on reaching a 1.0×10^6 DN value.

Any one of several design methodologies may be employed to extend the practical speed range of spherical bearings. One particularly powerful method is load support system (LSS) analysis [1][1]. Here, thermomechanical performance of the LSS is simulated on a digital computer using a general purpose computer program. The method offers the advantage of numerical

[1]Numbers in brackets denote references at end of report.

exploration of a competitive variety of LSS concepts, prior to hardware commitment.

The SPHERBEAN computer program [2,3] was created to simulate spherical roller bearing LSS performance over a wide range of operating conditions. Program capabilities provide sufficient generality to allow the detailed simulation of both high speed (i.e. 1.0×10^6 DN) and conventional bearing operation. However the credibility of performance data calculated by SPHERBEAN cannot be established until program predictions are correlated with realistic experimental data.

This report compares SPHERBEAN predicted LSS performance data with data generated under full scale hardware tests. The close degree of correlation between simulated and actual performance provides the necessary credibility for the mathematical models used in the program.

This report begins with a description of the high speed rig used to perform the bearing tests. Its mathematical analog, the system model used with SPHERBEAN, is then detailed. Test conditions are described and measured performance values are compared to predicted values for radial and combined load cases. Effects of clearance and osculation are also quantified.

2.0 TEST RIG SYSTEM MODEL

The experimental data used for comparison was generated on the spherical bearing test rig shown in Figure 2.[2] The rig has the capability to load a 40mm bore test bearing both axially and radially, at inner ring speeds to 20,000 RPM. Instrumentation is provided to measure the bearing's: oil-in and oil-out temperature, inner and outer ring temperature, inner ring and cage speeds, operating torque, and oil flow rates, as well as the operating parameters of secondary equipment.

Lubrication is provided to the test bearing by way of a circumferential groove in the outer ring, where it enters the bearing cavity through three radial holes. Lubricant used in all tests was a type II ester, conforming to the MIL-L-23699 specification.

The information provided in Appendix A was used to reduce the test rig configuration to an equivalent, cross-coupled, lumped-mass nodal network containing 50 temperature nodes. Of these, the temperatures of 44 nodes are determined by SPHERBEAN, and the remaining six are specified as system boundary conditions, Table 1.

---

[2] A complete description of the test rig, test procedure, instrumentation and results can be found in Appendix A - "Full Scale Hardware Tests."

Figures 3 and 4 show the extent of the test rig that was thermally simulated. The model is bounded on the left side (nodes 1, 21, and 47 in Figure 3) by the axial hydrostatic bearing and ambient air. The actual test rig continues past this point in the form of (thermally) minor support hardware for the thrust bearing and a rotary transformer drive quill. Approximately 50% of the quill was modelled since its diameter (7mm)is small in comparison to the test bearing bore (40mm), and therefore contributes very little to the overall heat balance within the rig.

The thermal model is bounded on the right side by a "slave" cylindrical roller bearing. The additional modelling of the slave bearing was included to increase accuracy of the predicted test bearing inner ring temperatures, since the test bearing thermally communicates with the slave bearing by transferring heat through the drive shaft.

Three sources of heat generation, other than the test bearing, were considered. These are: labyrinth seals located at nodes 24 and 28, and the cylindrical roller bearing defined by nodes 32, 33, 44. The small quantity of heat created at the labyrinth seals was assumed to vary linearly with speed, from 2.2 to 11 watts each for inner ring speeds from 1000 to 5000 RPM. Heat generated at the cylindrical bearing was assumed to vary with speed and load. Heat

generation rate was computed as a function of these two parameters using a handbook equation [4].

Four independent lubrication systems were considered in the rig model, Figure 4. The two outermost loops (nodes 46, 42, 43 and 48, 40, 41) represent lubricant delivered to the axial and radial hydrostatic thrust bearings, respectively. The two innermost loops (nodes 45, 38, 39 and 50, 36, 37) simulate the lubricant delivered to the test and slave bearings. Flow rates, delivery temperature and heat transfer properties were individually specified for each of the loops listed in Table 2.

The four modes of heat transfer considered are listed in Table 3 with specific heat transfer coefficient values associated with each mode.[3]

---

[3]A complete set of input data used for the rig simulation, and the resulting program output, appears as Example 1 in Volume II [3] of this report.

3.0 CORRELATION OF CALCULATED WITH EXPERIMENTAL RESULTS

The test rig model was used to generate system performance data at the operating conditions listed in Table 4. Every combination of load and speed documented in Appendix A was not simulated. Steady state thermo-mechanical performance was examined, with the operating bearing clearance computed as a function of speed, interference fit pressure and operating temperature. Measured dimensions of the four bearings used for tests and simulation are given in Table 5.[4]

The five operating parameters used for comparison of measured and calculated performance are defined in Table 6. "Drag Torque" is computed from the program predicted heat generation rate:

$$\text{DRAG TORQUE(N-MM)} = 9549 \frac{Q}{W}$$

where:

Q - is the program predicted heat generation rate (Watts)

W - is the shaft speed (RPM)

---

[4] Also see Appendix B

The computed operating parameters are generated as single valued functions. Physical reality imposes a diffusion of that uniqueness. This could be simulated for example, by exploring the impact of dimension tolerance extremes, material property variations, and heat transfer coefficient differences. Computer bearing performance would then be represented by a "bandwidth," not a line. The extent and the crosscoupling of these variations within the load support system precludes full exploration within the scope of this effort. Therefore a minimum $\pm$ 5% bandwidth should be assumed to surround the computerized results presented.

No repeat-run experimental data was available for tests described in sections 3.A through 3.D and, thus, the absolute bandwidth spread, which represents experiment to experiment parameter variations is unknown. Based on the measured results it is prudent to assume that, for a particular test bearing, the experimental temperature bandwidth will be at least 5% of the minimum temperature value.

3.A PURE RADIAL LOAD[5]

Calculated predictions and experimental values obtained under pure radial load of 6672N (1500 LB) are presented for

[5]Test results appear in full in Table A2, Appendix A.

comparison in Figures 5 through 9, and for 13345N (3000 LB) radial loading in Figures 10 through 14.

Computed cage-to-shaft speed ratios are within 2% of measured values at each of the ten operating points investigated (Figures 5,10). This close correlation is seen because of the limited roller slip.

The computed temperatures at 6672N (1500 Lb) are within 3% of measured values for shaft speeds to 5000 RPM, Figures 6, 7, and 8. The largest difference between measured and calculated temperatures (3.5°C) is found at the inner ring, Figure 6, at 1000 RPM.

Measured temperatures are compared to calculated, under a 13345N (3000 Lb) radial load, in Figures 11, 12, and 13. Close agreement between predicted and measured inner ring temperature is seen over the entire speed range, Figure 11. Outer ring and lubricant outlet temperature predictions are within 4% of measured values for speeds to 4000 RPM. Between 4000 and 5000 RPM, the measured ring and lubricant outlet temperatures rise more slowly than the predicted values.

Predicted and measured drag torque values are presented in Figures 9 and 14. Close agreement is shown at a radial

load of 6672N (1500 Lb). Causes for scatter among measured data points at 13345N (3000 Lb) are discussed in Appendix A.

3.B COMBINED LOAD[6]

Comparison of predicted and measured data is presented in Figures 15 through 22. Calculated temperature data, at speeds of 1000,3000, and 5000 RPM, show the correct trend with speed, although generally increasing more quickly with speed than the measured data. Predicted temperature values are higher than those measured at all speeds under combined loading.

A possible cause for the general trend of higher predicted temperatures is related to the load distribution among rows of rollers during tests. Program output shows that the specified axial load will dominate the radial at all test conditions, and only one row of rollers need be loaded by the inner ring to maintain bearing equilibrium. Thus, the double row test bearing behaves like a single row bearing. During tests, the loaded row generates virtually all heat, creating a temperature gradient across the width of the bearing. The calculated temperature difference between rows, at the outer ring, for example, becomes

[6]Test results appear in Table A3, Appendix A.

significant at higher speeds, Table 7.

The bearing tester was designed with the capability to measure temperature at each row. During this test sequence, and sequence C, one of two thermocouples which sense temperature in the "hot" row failed. The measured outer ring temperature averages are therefore biased toward the lower row temperature (Figures 16,20).

The measured and calculated lubricant outlet temperatures are plotted as a function of speed in Figures 17 and 21. In general, the same trends are observed as for the outer ring temperature.

Inner ring temperature predictions are within 5% (5°C) of measured values at all speeds. Comparison of Figures 15 and 19 show that predicted inner ring temperatures follow the correct trend with load. For example, at 5000 RPM, a 9°C inner ring temperature increase is predicted; a 10°C increase is observed. The increase in temperature with respect to load compares well (within 2°C) over the entire speed range.

Measured drag torques are compared to calculated values for two operating loads in Figures 18 and 22. Instrumentation problems produced wide scatter in the torque measurements, and prevents meaningful comparison of the measured and predicted values at a given load. However, comparison of Figures 18 and 22 show that predicted torque values vary correctly with operating load.

3.C EFFECT OF CLEARANCE[7]

Calculated predictions and measured values obtained for bearing number 01 under pure radial and combined loads are shown for comparison in Figures 23 through 42. The effect of clearance is seen in Figures 39 through 42. Note that calculated values are only presented for extremes in speed.

Under 6672N (1500 Lb) radial load, the predicted ring and outlet lubricant temperatures are within 3% of measured values for all speeds, Figures 23 through 25. The largest difference between measured and calculated values (3°C) is found at the inner ring, at 1000 RPM, Figure 23.

Calculated temperatures are compared to measured under 13345N (3000 Lb) radial load in Figures 27 through 29. Steeper trends, with respect to speed, are seen under the higher load in both the predicted and measured data. Agreement is generally good, with a maximum deviation of 6%.

Predicted and measured data, under combined load, are shown in Figures 31 through 38.

Close agreement is seen between the test and calculated inner ring temperature data, Figures 31 and 35. The maximum discrepancy of 3% appears at 5000 RPM, under the 3114N (700 Lb) axial/6672N (1500 Lb) radial load.

---

[7] The complete test results appear in Table A4, Appendix A.

Outer ring temperatures are compared under two loads in Figures 32 and 36. Close agreement (within 2%) is seen at 1000 RPM. Calculated temperature trends with speed are steeper than measured, leading to a maximum 9°C difference at 5000 RPM. The steeper trend, and higher temperature predictions, may be related to an outer ring thermocouple which failed during testing.[8]

Lubricant outlet temperatures are compared in Figures 33 and 37. Agreement is good, within 5%, with the maximum temperature difference occurring at 5000 RPM.

Drag torque comparisons under combined load are shown in Figures 34 and 38. Scatter in experimental data prevents meaningful correlations at 3114N (700 Lb) axial/6672N (1500 Lb) radial load. An order of magnitude comparison of Figures 34 and 38 shows torque increasing with load. Torque data measured under pure radial load exhibits similar trends, Figures 26 and 30.

The effect of "off-the-shelf" clearance on temperature can be shown by comparing data generated for bearings Number 01 and 02, Figures 39 through 42.

Both the measured and predicted inner ring temperatures show an increase with increased clearance under radial and combined

---

[8]The same thermocouple failure occurred during test sequence B, "Combined Load." Its effect upon the measured data is described in Section 3.B.

load, Figures 39 and 41. The observed and calculated rises in inner ring temperature under radial load are in very close agreement, Figure 39.

The trend in outer ring temperature with clearance changed with applied load. Under combined load, outer ring temperature increased with clearance. However, under radial load, outer ring temperature decreased with clearance. This effect is seen in both the measured and calculated data, Figures 40 and 42.

3.D EFFECT OF OSCULATION[9,10]

Calculated predictions and measured values obtained for bearing number 03 under pure radial and combined loads are compared in Figures 43 through 59. The test sequence was executed with each hydrostatic bearing oil inlet temperature at ~89°C. (Table A5 Appendix A), therefore the predicted results were calculated with an 89°C boundary condition at nodes 46 and 48.

Results obtained under pure radial loads of 6672N (1500 Lb) and 13345N (3000 Lb) are shown in Figures 43 through 50. Agreement between experimental and calculated temperature at

---

[9] Osculation (O) is a measure of roller-to-raceway conformity, defined by

O= roller crown radius/raceway groove radius

[10] The complete test results appear in Table A5, Appendix A.

6672N (1500 Lb) is generally good. A maximum difference of 6°C is seen at 5000 RPM between measured and predicted lubricant outlet temperatures, Figure 45. Under 13345N (3000 Lb) radial load, the predicted temperature rise with increasing speed is steeper than that observed during tests, Figures 47 through 49. At 1000 RPM, agreement is within 2%; at 5000 RPM, agreement is within 10%.

Calculated and predicted component temperatures, under combined load, are compared in Figures 51 through 57. Generally close agreement, within 5%, is seen at extremes of speed and load. Both experimental and calculated inner ring temperature data, shown in Figures 51 and 55, indicate that the slope of the temperature vs. speed curve is a function of load. The same trend was seen in the calculated data for pure radial load, Figures 43 and 47, however, measured data for radial load did not show the same effect. Since repeat run temperature measurements were not available, the possibility of an inconsistency in measured data could not be checked.

Comparison of temperature data for bearings number 02 and 03 shows the combined effects of osculation and hydrostatic oil inlet temperature on inner ring temperature, Figure 59. Both experimental and predicted data points exhibit similar trends: under the higher load, ring temperature is nearly constant with respect to osculation and hydrostatic oil temperature; at moderate

loads, ring temperature increases with osculation and hydrostatic oil temperature.

The isolated effect of osculation on inner ring temperature was computed at 5000 RPM by simulating system performance with test bearing number 03 at a hydrostatic oil inlet temperature of 105°C. The resulting data is compared with the calculated data for bearing number 02 in Figure 60. Little change is seen in the calculated ring temperatures with respect to osculation.

Scatter in the measured drag torque values prevents meaningful comparison to calculated values at a given load, however drag torque was observed to consistently increase with load, and the same trend was seen in the calculated data (Figures 50, 54, and 58).

4.0 HIGH SPEED RIG CHECKOUT

The previous comparisons of experimental and calculated temperature data were made over an operating speed range having an upper bound near the bearing manufacturer's recommended "limiting speed" of about 5000 rpm. Conventional bearing operation above the limiting speed can result in overheating and thermal seizure. To avoid a possible catastrophic bearing failure, the SPHERBEAN program was used to explore high speed rig performance prior to the execution of full scale tests.

Performance of bearing number 06 was examined over a speed range of 5000 RPM to 20000 RPM.[11] The peak speed represents a value approximately four times greater than the limiting speed. Two load conditions were simulated: pure radial and pure axial.

Predicted results, under pure axial load of 4448N (1000 lb), are shown in Figures 61 through 64 as a continuous line. Bearing operating parameters, which were later measured, are indicated by single valued points. Note that the high speed simulations were executed for an average hydrostatic bearing inlet oil temperature of 90°C, a value at least 10°C higher than those later used in the actual test series. The 90°C value was chosen to simulate a conservative upper temperature limit of bearing performance.

---

11 Experimental results are presented in Appendix A, "Test Series F-H", pages 186-207.

Figure 61 shows ring temperatures to speeds of 20,000 RPM (.8 MDN). A peak temperature of 195°C is predicted for the inner ring, 182°C for the outer ring. Both temperatures are well within the material and lubricant oxidation limits.

The lubricant outlet temperature (Figure 64) follows essentially the same trend with speed as the ring temperatures.

The bearing diametral clearance remains positive over the speed range investigated, Figure 62. The predicted loss is attributed to the rise in rolling element temperature and rotation induced radial growth of the inner ring. The (maximum) 13°C temperature difference between inner and outer rings, Figure 61, has a negligible effect (-.005 mm) on operating clearance.[12]

Film thickness increases with speed by 50% at the inner ring and 30% at the outer ring, Figure 63. The improvement is due to increased rolling velocity, since lubricant viscosity will decrease with temperatures encountered at higher shaft speeds.

Calculated results for a pure radial load of 13345N (3000 Lb) are shown by continuous lines in Figures 65 through 68. A conservative hydrostatic oil inlet temperature of 90°C was again used for the high speed simulations, a value at least 10°C higher than was later used for the actual test series.

---

[12] Inner to outer ring temperature difference is stongly dependent upon the load support system geometry and lubrication method. It is not likely to be a secondary effect in designs such as pillow blocks or grease lubricated spherical bearings.

Predicted ring temperatures, shown in Figure 65, are seen to rise almost linearly with speed. Peak temperatures of 187°C at the inner ring and 176°C at the outer are achieved at 20,000 RPM. A stable temperature difference of 6 to 11°C is maintained over the entire speed range, and no indications of thermal seizure are seen.

Bearing diametral clearance remains positive, Figure 66, changing by 18% from its initial operating value of .056 mm (.0022 in) at 6000 RPM. The clearance trend with speed is similar to the trend seen under pure axial load. Clearance change is primarily due to rotation-induced ring growth and heating of the rolling elements.

Film thickness to surface roughness ratio at each raceway increases by 20% with speeds to 10,000 RPM, then maintains a nearly constant value to 20,000 RPM, Figure 67.

None of the predicted temperature data to 20,000 RPM was found to indicate a thermal or thermo-dimensional problem which would limit the test bearing speed. Also, the predicted cage speed was found to be near epicyclic, indicating skid would not be a problem.

The test bearing's torque transducer output was lost at elevated speeds under each load condition, therefore torque data was not available for later comparisons. The cause for instrument failure was found to be a loss of clearance in the radial

hydrostatic bearing. Figure 69 shows the program-predicted difference in the radial hydrostatic bearing's inner and outer ring temperatures (nodes 15 and 17 in Figure 3). A hand calculation shows the initial hydrostatic bearing geometry can tolerate an approximate 50°C temperature difference between inner and outer rings before losing all clearance. Referring to Figure 69, clearance, and therefore torque transducer output, will be lost in the anticipated test speed range.

5.0 CONCLUSIONS

The specific objective of assessing SPHERBEAN's utility as a practical design tool has been achieved. Calculated temperature data for four test specimens were found to correlate well with experimental measurements and no program anomalies were detected. Predicted temperatures were generally a few °C higher than the measured values. Predicted trends in temperature with bearing clearance and osculation were consistent with variations experimentally observed. The usefulness of the program was demonstrated by its ability to accurately simulate spherical bearing performance in conventional and high speed ranges.

6.0 LIST OF REFERENCES

1. Pirvics, J., "Numerical Analysis Techniques and Design Methodology for Rolling Element Bearing Load Support Systems", presented at the International Conference of Bearing Design: Historical Aspects, Present Technology and Future Problems, ASME Century 2 Publication (1980)

2. Kleckner, R.J. and Pirvics, J., "SKF Computer Program SPHERBEAN, Volume I: Analytic Formulation", SKF Report No. AT81D006, Submitted to NASA/Lewis Research Center under NASA Contract No. NAS3-20824, NASA CR-165203.

3. Kleckner, R.J. and Dyba, G., "SKF Computer Program SPHERBEAN, Volume II: User's Manual", SKF Report No. AT81D007, Submitted to NASA/Lewis Research Center under NASA Contract No. NAS3-20824, NASA CR-165204.

4. SKF Engineering Data, SKF Industries, Inc., © 1973, pp. 53-54.

5. Kreith, F., Principles of Heat Transfer, Intext Press, Inc., 3rd Ed, pp. 633-640 (1973).

6. General Electric Heat Transfer Data Book, G.E. Company, Corporate Research and Development, Schenectady, N.Y. (1976).

7. see Ref. 5, pp. 468-469.

8. Crecelius, W.J., and Pirvics, J., "A Computer Program for The Analysis of The Steady State and Transient Thermal Performance of Shaft-Bearing Systems," SKF Report No. AL76P030, Submitted to AFAPL, Wright-Patterson AFB, Ohio, and NAPTC, Trenton, N.J. under Air Force Contract No. F33615-76-C-2061 and Navy MIPR No. M62376-MP-00005.

NODE NUMBER	DESCRIPTION	TEMPERATURE (°C)				
		TEST A: PURE RADIAL LOAD	TEST B: COMBINED LOAD	TEST C: EFFECT OF CLEARANCE	TEST D: EFFECT OF OSCULATION	TEST E: HIGH SPEED RIG CHECKOUT
45	Lubricant Delivery Temperature (Test Bearing), a	93	93	93	93	93
46	Lubricant Delivery Temperature (Hydrostatic Thrust Bearing), a	108	105	104	89	90
47	Ambient Air Temperature	27	27	27	27	27
48	Lubricant Delivery Temperature (Radial Hydrostatic Bearing), a	108	105	104	89	90
49	Lubricant Sump Temperature	138	138	138	138	138
50	Lubricant Delivery Temperature (Slave Bearing)	93	93	93	93	93

a - ± 2°C

TABLE 1: SYSTEM BOUNDARY CONDITIONS

LOOP DESCRIPTION	NODES	FLOW RATE
Slave Bearing	50-36-37	.3 GPM
Test Bearing	45-38-39	.13 GPM
Radial Hydrostatic	48-40-41	3.7 GPM
Axial Hydrostatic	46-42-43	.8 GPM

TABLE 2: LUBRICATION NETWORK FLOW RATES

TYPE	COEFFICIENT VALUE	WHERE COEFFICIENT IS USED; COMMENTS
Conduction ($W/M-^oC$)	53.6	Used to simulate conduction through steel materials [5], a
Conduction ($W/M-^oC$)	69.8	Aluminum to steel (in series); quill coupling for rotary transformer [5]
Free Convection (W/M^2-^oC)	5.0	Outer surface of rig to ambient air [6]
Free Convection (W/M^2-^oC)	10.0	Inside rig surfaces to compartment air [6]
Forced Convection (W/M^2-^oC)	90.0	Outside surface of shaft to compartment air [7], b
Forced Convection (W/M^2-^oC)	98.4	Inner and outer rings of axial hydrostatic bearing to hydraulic fluid [6]
Forced Convection (W/M^2-^oC)	177.0	Inner and outer rings of radial hydrostatic bearing to hydraulic fluid [6]
Forced Convection (W/M^2-^oC)	196.5	Heat transferred to test bearing lubricant prior to entering bearing cavity [6], b
Forced Convection (W/M^2-^oC)	556.0	Test and slave bearing surfaces to lubricating oil [8]
Fluid Flow ($W/^oC$)	16.3	Heat transported through test bearing lubricant network [8]
Fluid Flow ($W/^oC$)	37.5	Heat transported through slave bearing lubricant network [8]
Fluid Flow ($W/^oC$)	100.0	Heat transported by hydraulic fluid through axial hydrostatic bearing [8]
Fluid Flow ($W/^oC$)	462.0	Heat transported by hydraulic fluid through radial hydrostatic bearing [8]
Fluid Flow ($W/^oC$)	616.0	Heat transported from oil sump [8]

TABLE 3: HEAT TRANSFER COEFFICIENTS USED IN TEST RIG MODEL

a - coefficients for heat transfer by conduction through the bearing are computed within SPHERBEAN

b - Non-linear function of shaft speed; value shown is for 5000 RPM

TEST SERIES	TEST DESCRIPTION	IDENTIFICATION NUMBER OF BEARING USED IN TEST a	SPEED RANGE (RPM)	APPLIED LOADS	
				RADIAL, (N)	AXIAL, (N)
A	PURE RADIAL LOAD	02	1000 - 5000	6672 (1500 Lbs)	0
		02	1000 - 5000	13345 (3000 Lbs)	0
B	COMBINED LOAD	02	1000 - 5000	6672 (1500 Lbs)	3114 (700 Lbs)
		02	1000 - 5000	13345 (3000 Lbs)	4448 (1000 Lbs)
C	EFFECT OF CLEARANCE	01	1000 - 5000	6672 (1500 Lbs)	0
		01	1000 - 5000	13345 (3000 Lbs)	0
		01	1000 - 5000	6672 (1500 Lbs)	3114 (700 Lbs)
		01	1000 - 5000	13345 (3000 Lbs)	4448 (1000 Lbs)
D	EFFECT OF OSCULATION	03	1000 - 5000	6672 (1500 Lbs)	0
		03	1000 - 5000	13345 (3000 Lbs)	0
E	HIGH SPEED RIG CHECKOUT	06	5000 - 20,000	311 (70 Lbs)	4448 (1000 Lbs)

a - Table 6 lists specific test bearing dimensions

TABLE 4: TEST CONDITIONS SIMULATED FOR COMPARISON OF CALCULATED AND MEASURED DATA

TABLE 5: TEST BEARING (MEASURED) DIMENSIONS USED AS INPUT TO SPHERBEAN

BEARING IDENTIFICATION NUMBER		01	02	03	06
INNER RING GROOVE RADIUS, inches [a]		1.5659 (39.774mm)	1.5709 (39.901mm)	1.6043 (40.749mm)	1.6260 (41.300mm)
OUTER RING, GROOVE RADIUS, inches [a]		1.5894 (40.371mm)	1.5886 (40.350mm)	1.5884 (40.345mm)	1.5898 (40.381mm)
ROLLER DIAMETER, inches [b]		.5117 (13.00mm)	.5118 (13.00mm)	.5117 (13.00mm)	.5122 (13.01mm)
ROLLER CROWN RADIUS, inches [b]		1.5520 (39.421mm)	1.5321 (38.915mm)	1.5322 (38.918mm)	1.5584 (39.583mm)
ROLLER TOTAL LENGTH, inches [b]		.4745 (12.05mm)	.4713 (11.97mm)	.4713 (11.97mm)	.4732 (12.02mm)
SURFACE ROUGHNESS	INNER RACEWAY, μin [c]	2.8 (.071μm)	2.6 (.066μm)	2.7 (.069μm)	5.1 (.13μm)
	OUTER RACEWAY, μin [d]	10.9(.277μm)	10.6(.269μm)	11.1(.282μm)	5.5 (.14μm)
	ROLLER, μin [e]	3.0(.076μm)	3.0(.076μm)	2.6(.066μm)	4.3(.11μm)
DIAMETRAL CLEARANCE, in [f]		.0039 (.0991mm)	.0029 (.0749mm)	.0030 (.0762mm)	.0029 (.0749mm)

a - Average for two rows

b - Average value for three rollers

c - Average for three equally spaced readings per row

d - Average for three equally spaced readings

e - Average for three rollers, three readings each

f - Average for three readings

OPERATING PARAMETER	HOW MEASURED ON TEST RIG	EQUIVALENT MEASUREMENT USING SPHERBEAN
CAGE SPEED	PROXIMITY PROBE AND COUNTER	DIRECT PROGRAM OUTPUT
INNER RING TEMPERATURE	AVERAGE OF SIMULTANEOUS READING OF FOUR RTD'S *	AVERAGE TEMPERATURE OF NODES 6 AND 7
OUTER RING TEMPERATURE	AVERAGE OF SIMULTANEOUS READING OF FOUR J TYPE THERMOCOUPLES	AVERAGE TEMPERATURE OF NODES 12 AND 13
OIL OUTLET TEMPERATURE	J TYPE THERMOCOUPLE	TEMPERATURE OF NODE 39
DRAG TORQUE	STRAIN GAUGED BEAM ON INNER RING OF RADIAL HYDROSTATIC BEARING	TORQUE COMPUTED FROM PROGRAM PREDICTED STEADY STATE HEAT GENERATION RATE

* RTD - Resistance Temperature Detector

TABLE 6: PREDICTED AND MEASURED OPERATING PARAMETERS

AXIAL LOAD 3114N (700 Lb)

RADIAL LOAD 6672N (1500 Lb)

SPEED (RPM):	1000	3000	5000
OUTER RING TEMPERATURE (°C)			
ROW 1*	101	106	112
ROW 2	100	104	107

AXIAL LOAD 4448N (1000 Lb)

RADIAL LOAD 13345 (3000 Lb)

SPEED (RPM):	1000	3000	5000
OUTER RING TEMPERATURE (°C)			
ROW 1*	103	111	118
ROW 2	102	106	111

* loaded row

TABLE 7: VARIATION IN RING TEMPERATURES BETWEEN ROWS OF ROLLERS UNDER COMBINED LOAD

BEARING NO	INNER RACE OSCULATION	OUTER RACE OSCULATION
02	.975	.964
03	.955	.965

TABLE 8: OSCULATIONS OF BEARINGS NO. 02 and 03

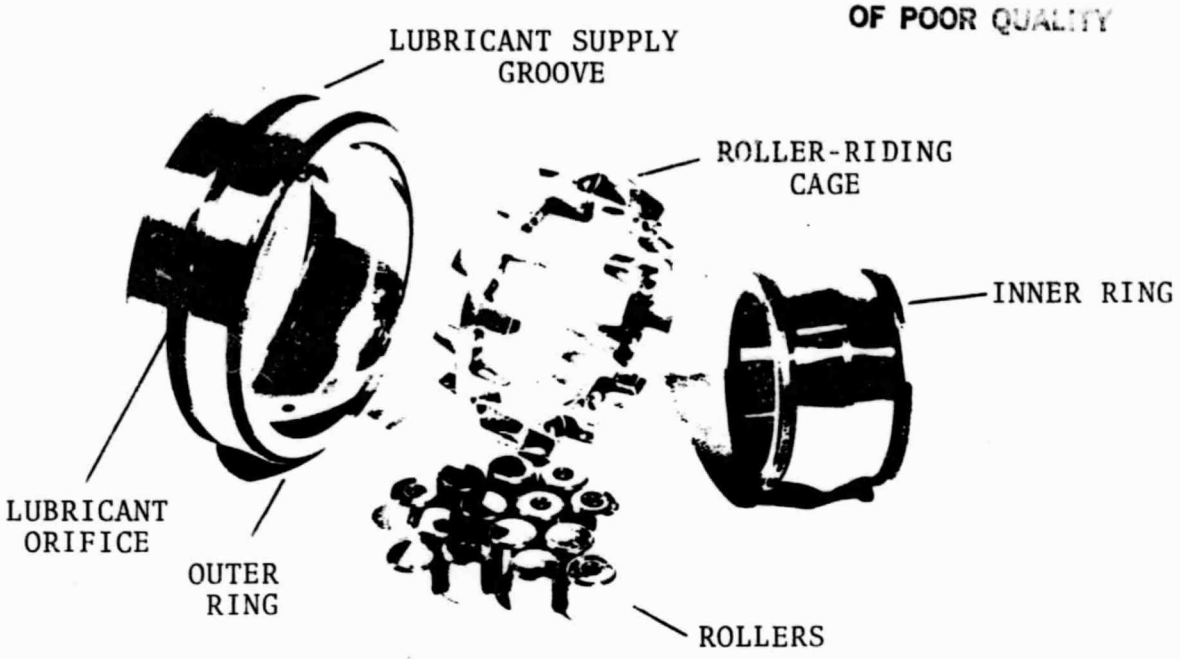

ASSEMBLED BEARING

FIGURE 1: SPHERICAL ROLLER BEARING

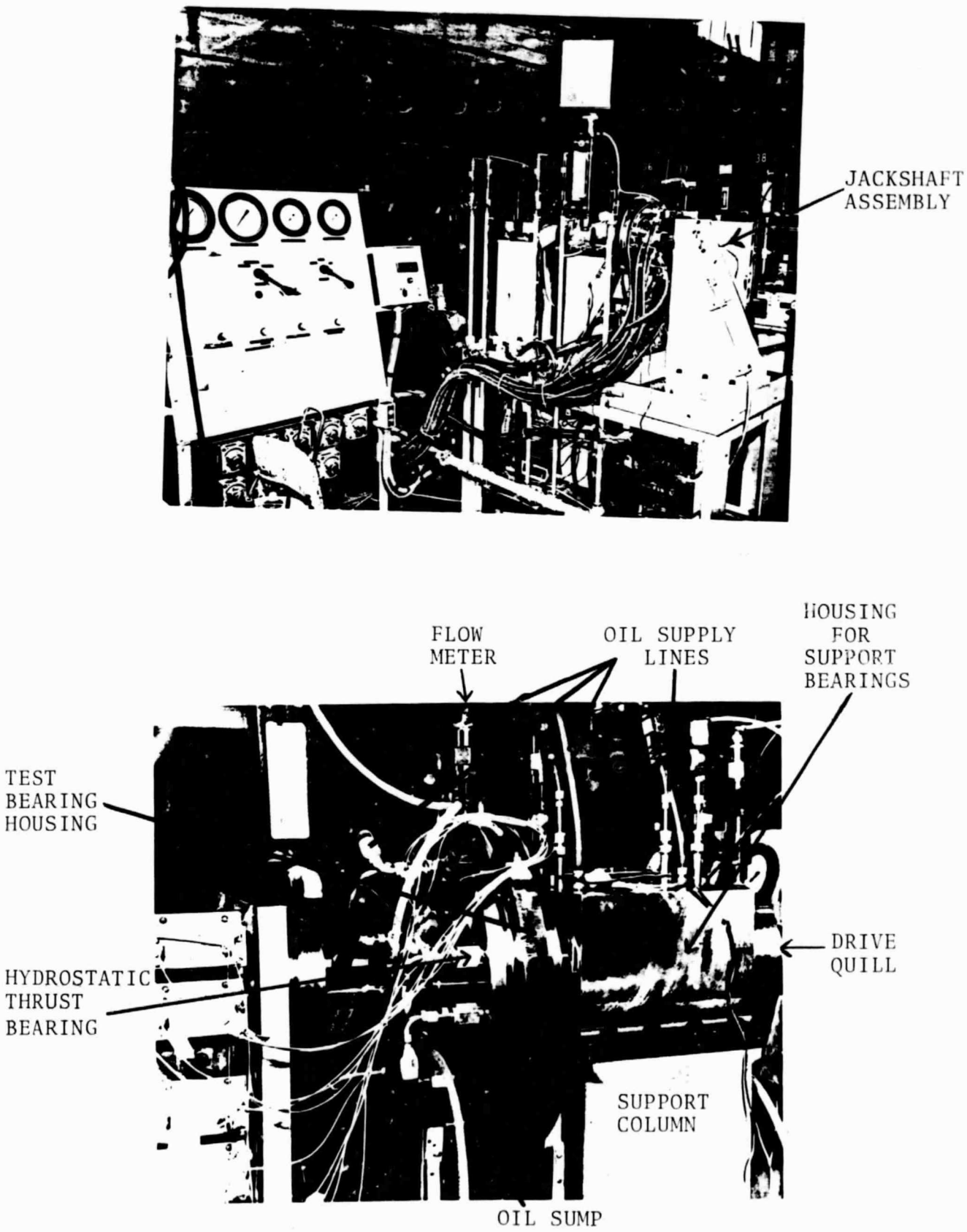

FIGURE 2: SPHERICAL ROLLER BEARING TEST RIG

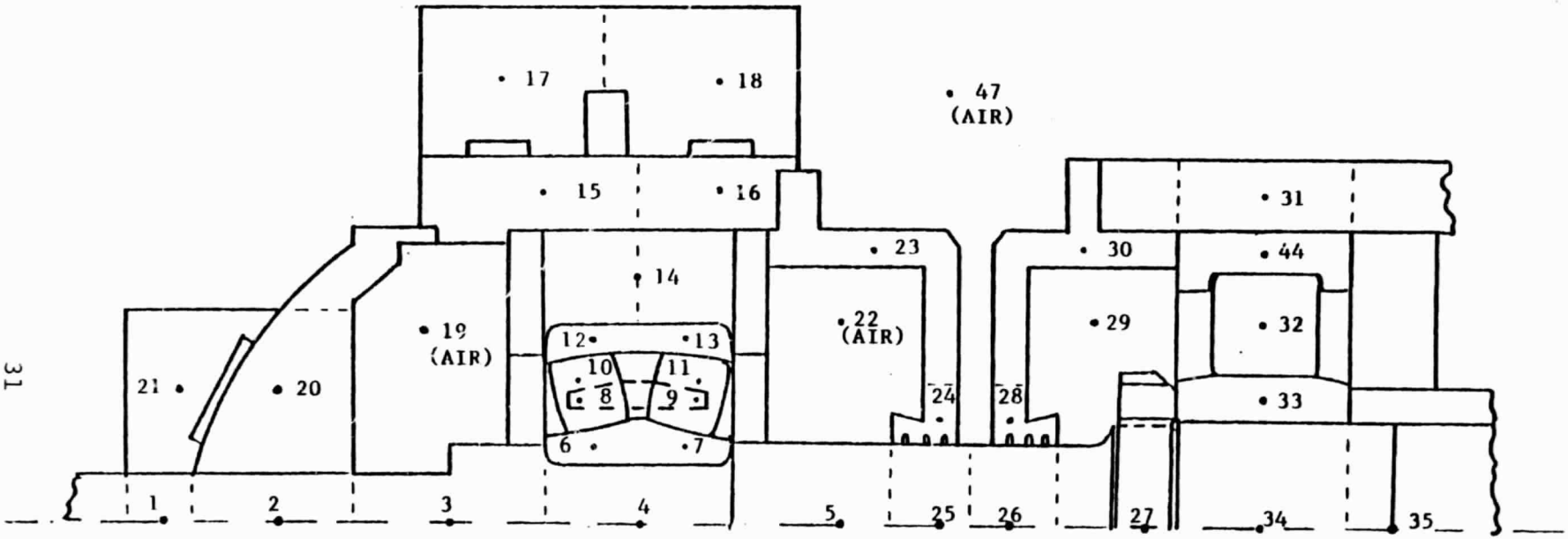

FIGURE 3

SYSTEM MODEL

(METAL AND AIR NODES)

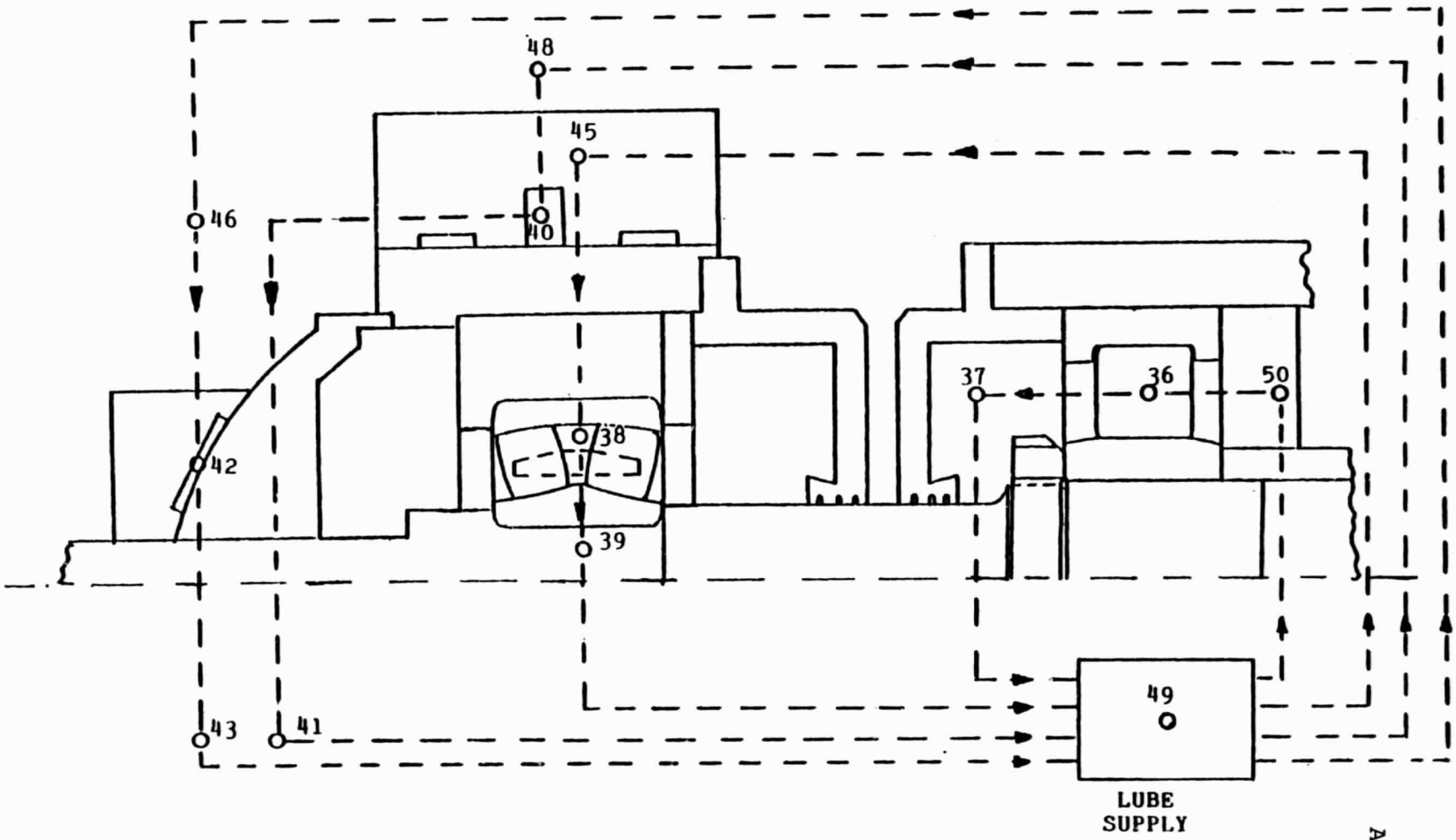

FIGURE 4

SYSTEM MODEL

(LUBRICANT SYSTEM NODES)

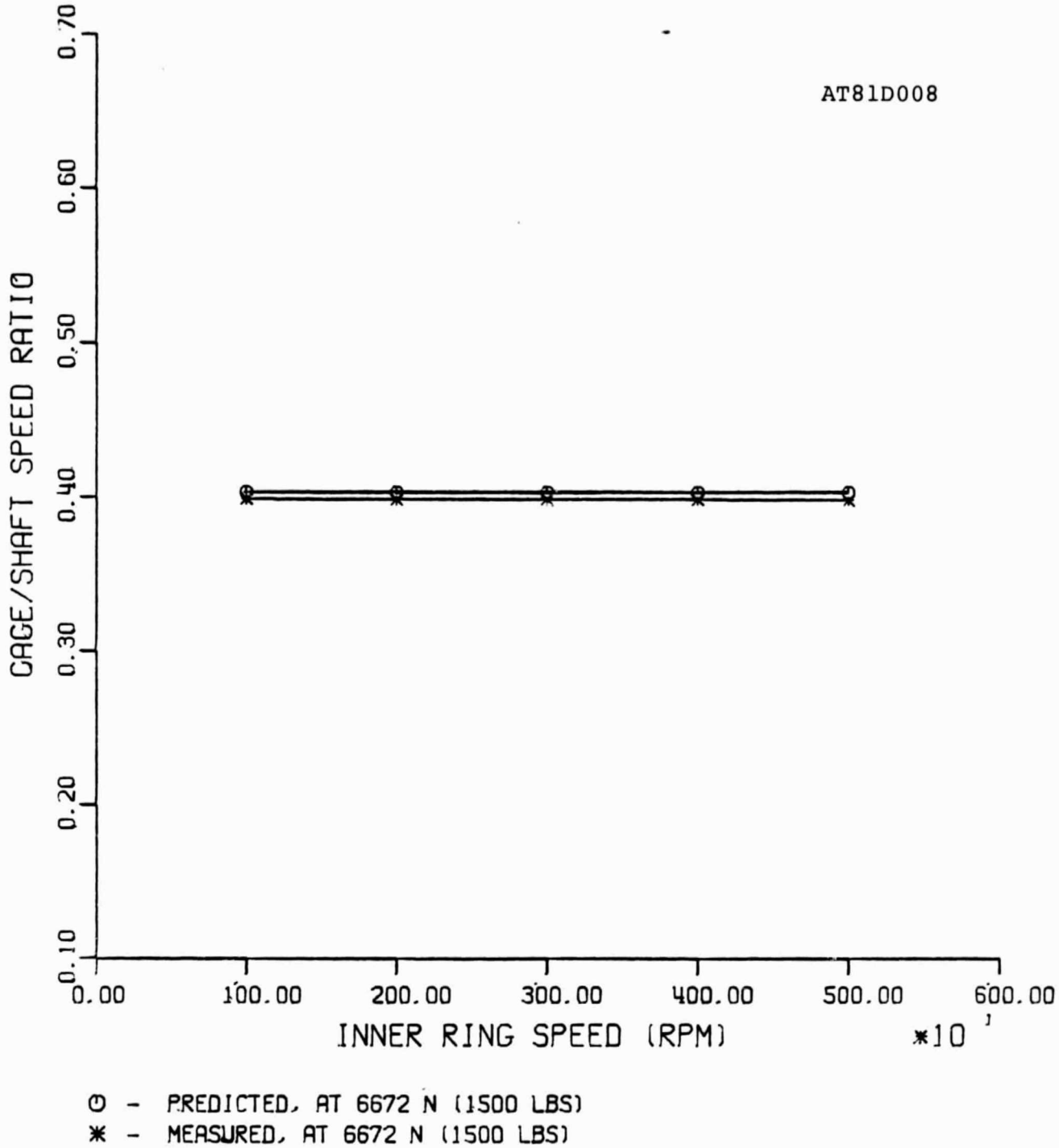

FIGURE 5:
COMPARISON OF PREDICTED AND MEASURED VALUES OF CAGE/SHAFT SPEED RATIO UNDER PURE RADIAL LOAD (BRG. NO. 02).

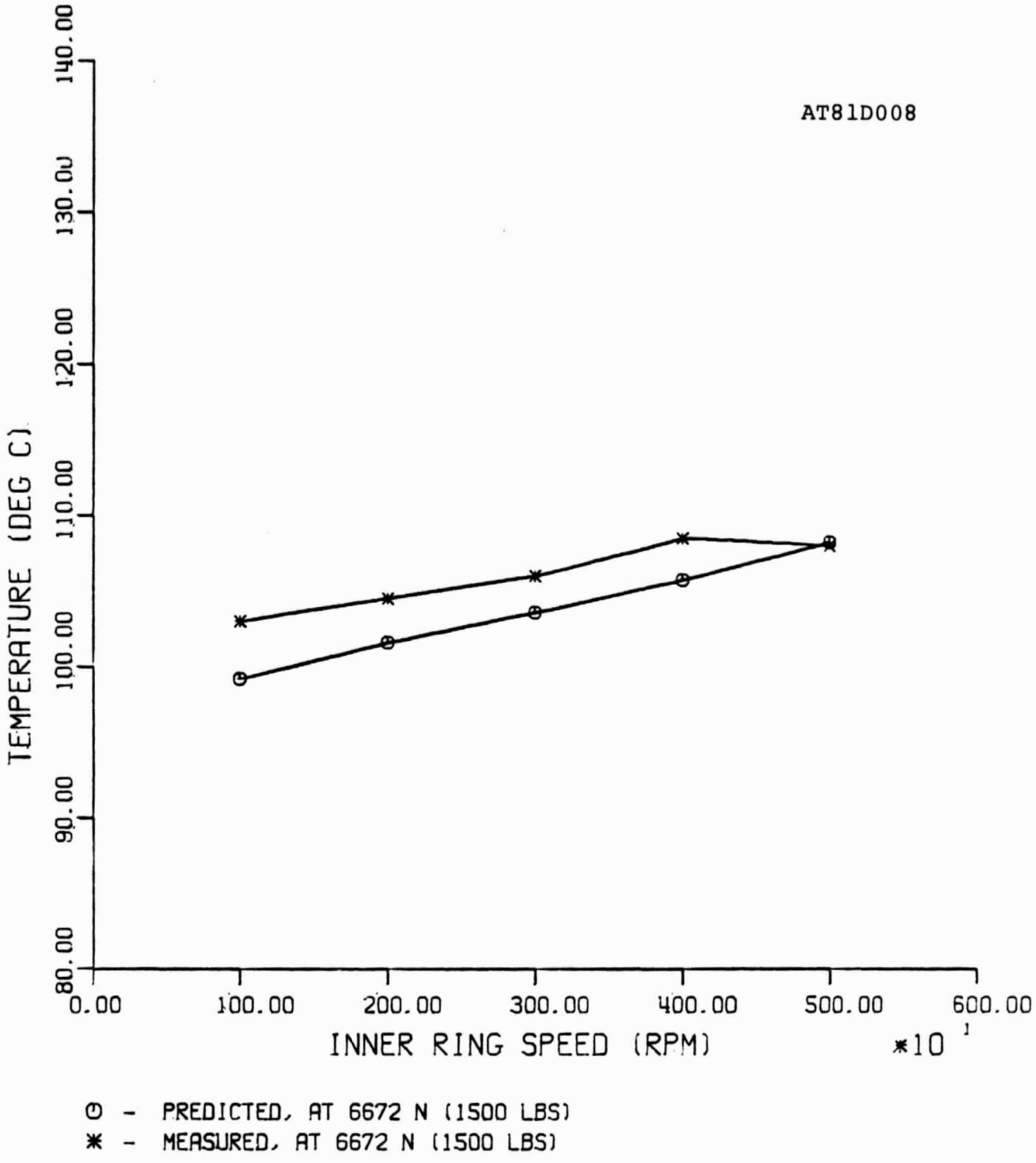

FIGURE 6:
COMPARISON OF PREDICTED AND MEASURED INNER RING TEMPERATURES UNDER PURE RADIAL LOAD (BRG. NO. 02).

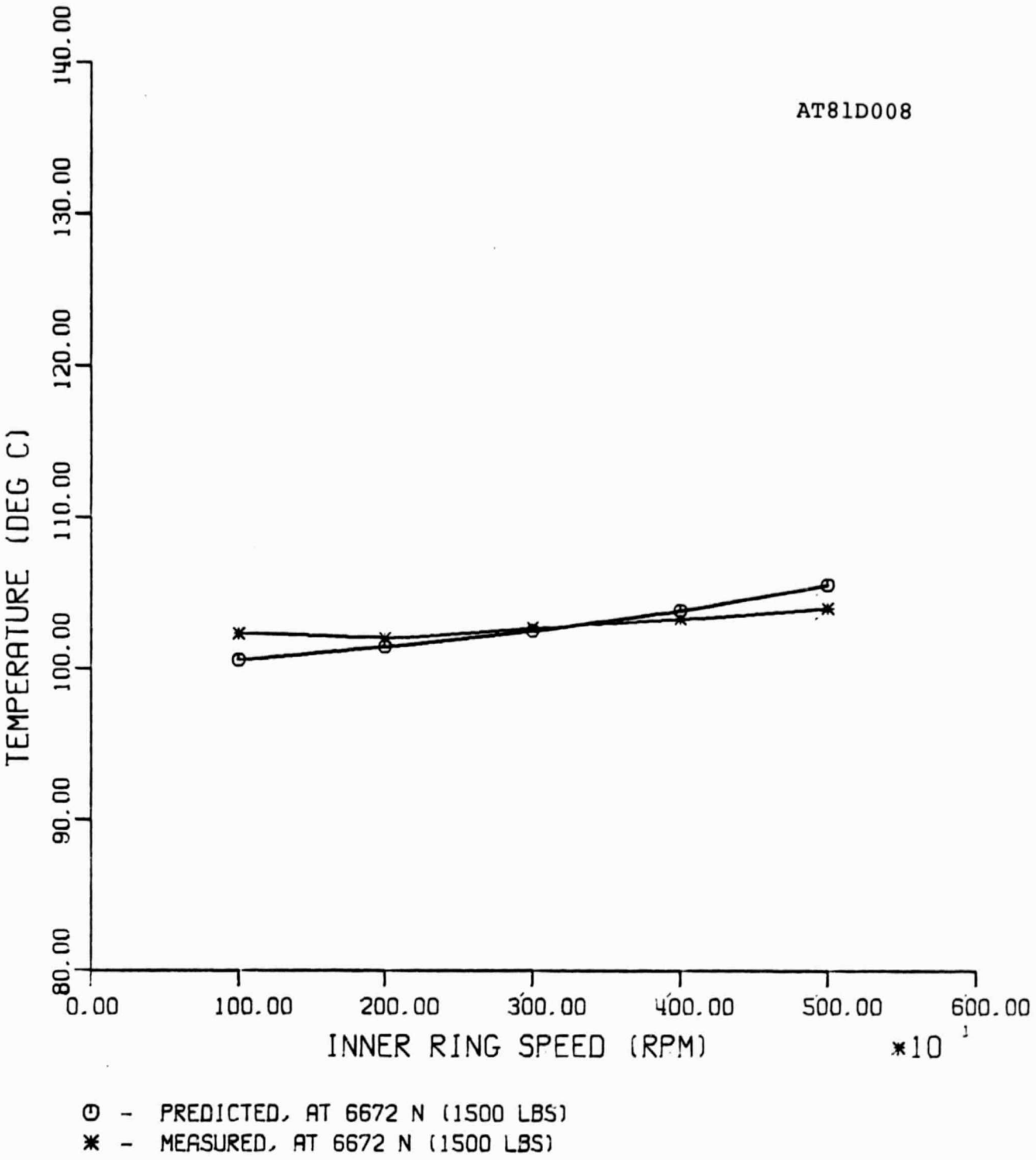

FIGURE 7:
COMPARISON OF PREDICTED AND MEASURED OUTER RING TEMPERATURES UNDER PURE RADIAL LOAD (BRG. NO. 02).

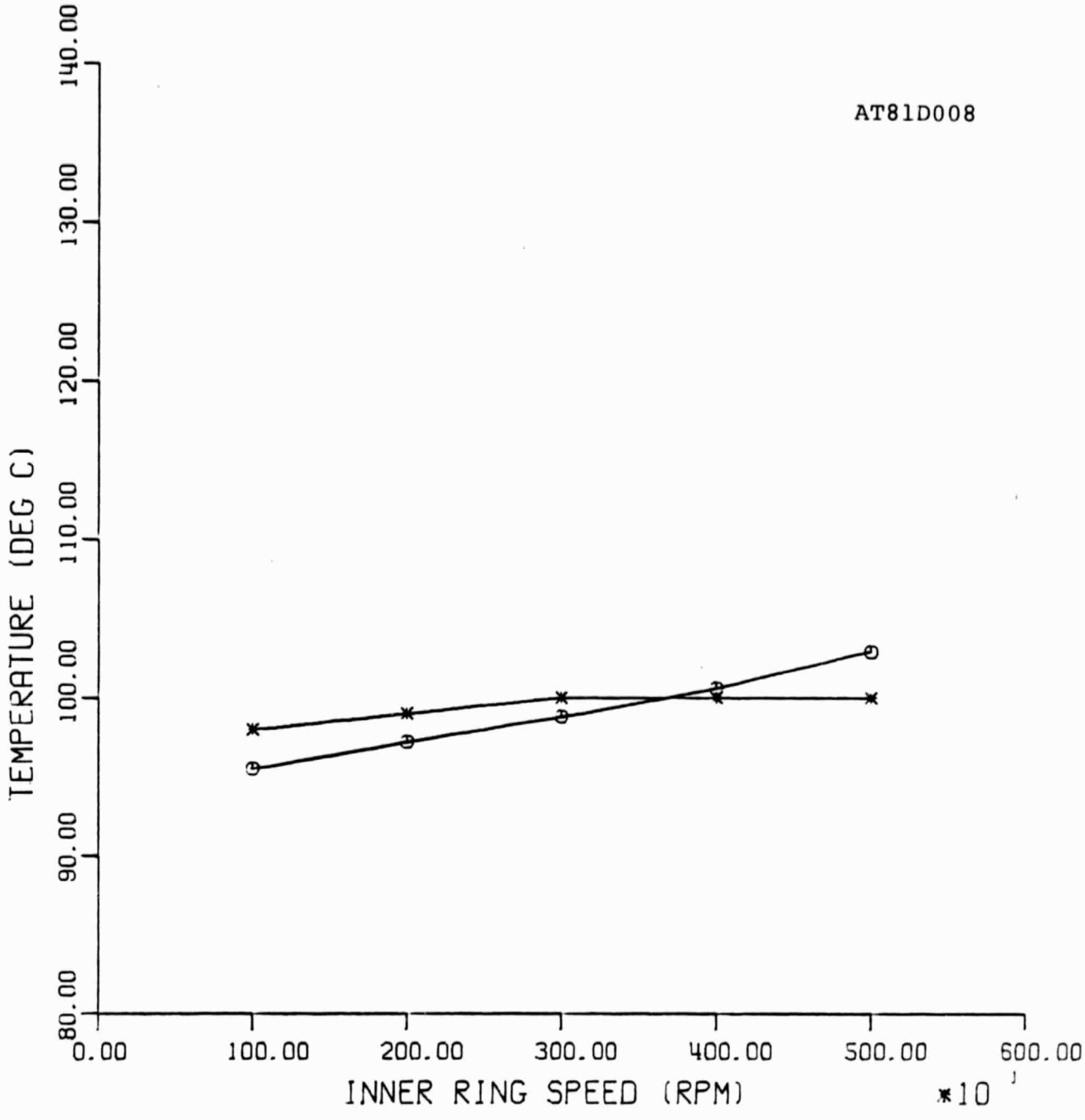

FIGURE 8:
COMPARISON OF PREDICTED AND MEASURED OUTLET LUBRICANT TEMPERATURES UNDER PURE RADIAL LOAD (BRG. NO. 02).

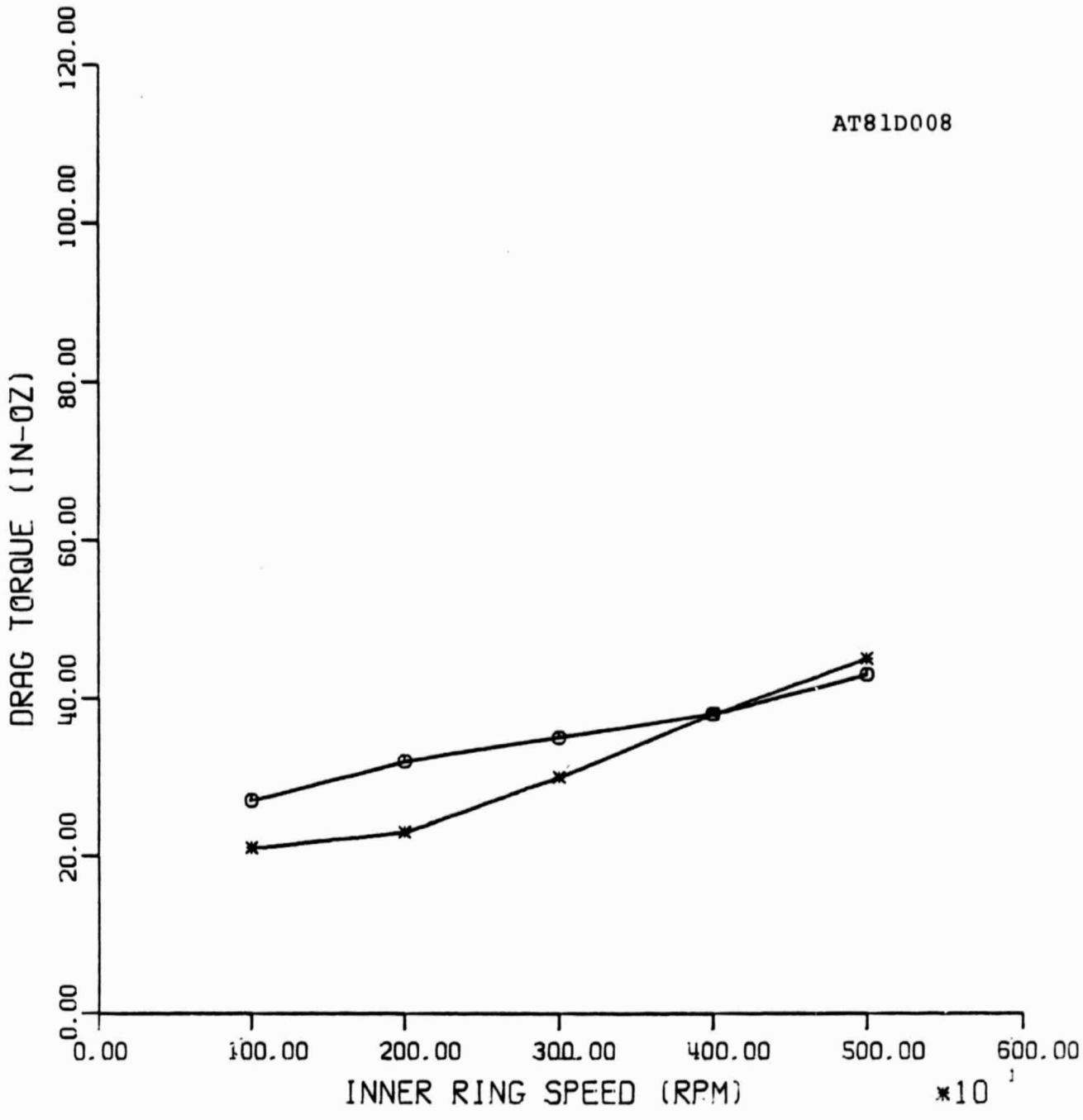

FIGURE 9:
COMPARISON OF PREDICTED AND MEASURED VALUES OF DRAG TORQUE UNDER PURE RADIAL LOAD (BRG. NO. 02).

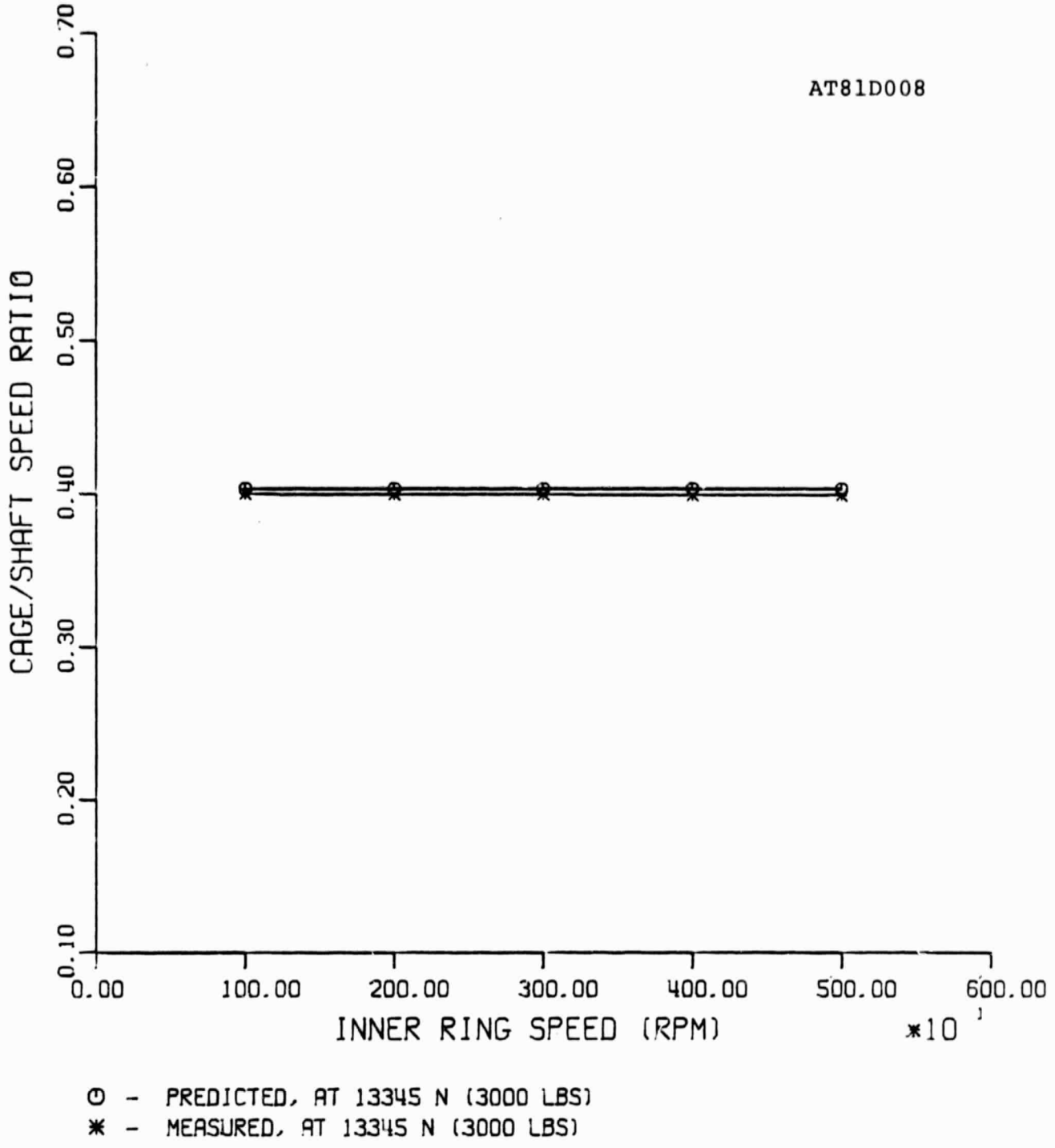

FIGURE 10:
COMPARISON OF PREDICTED AND MEASURED VALUES OF CAGE/SHAFT SPEED RATIO UNDER PURE RADIAL LOAD (BRG. NO. 02).

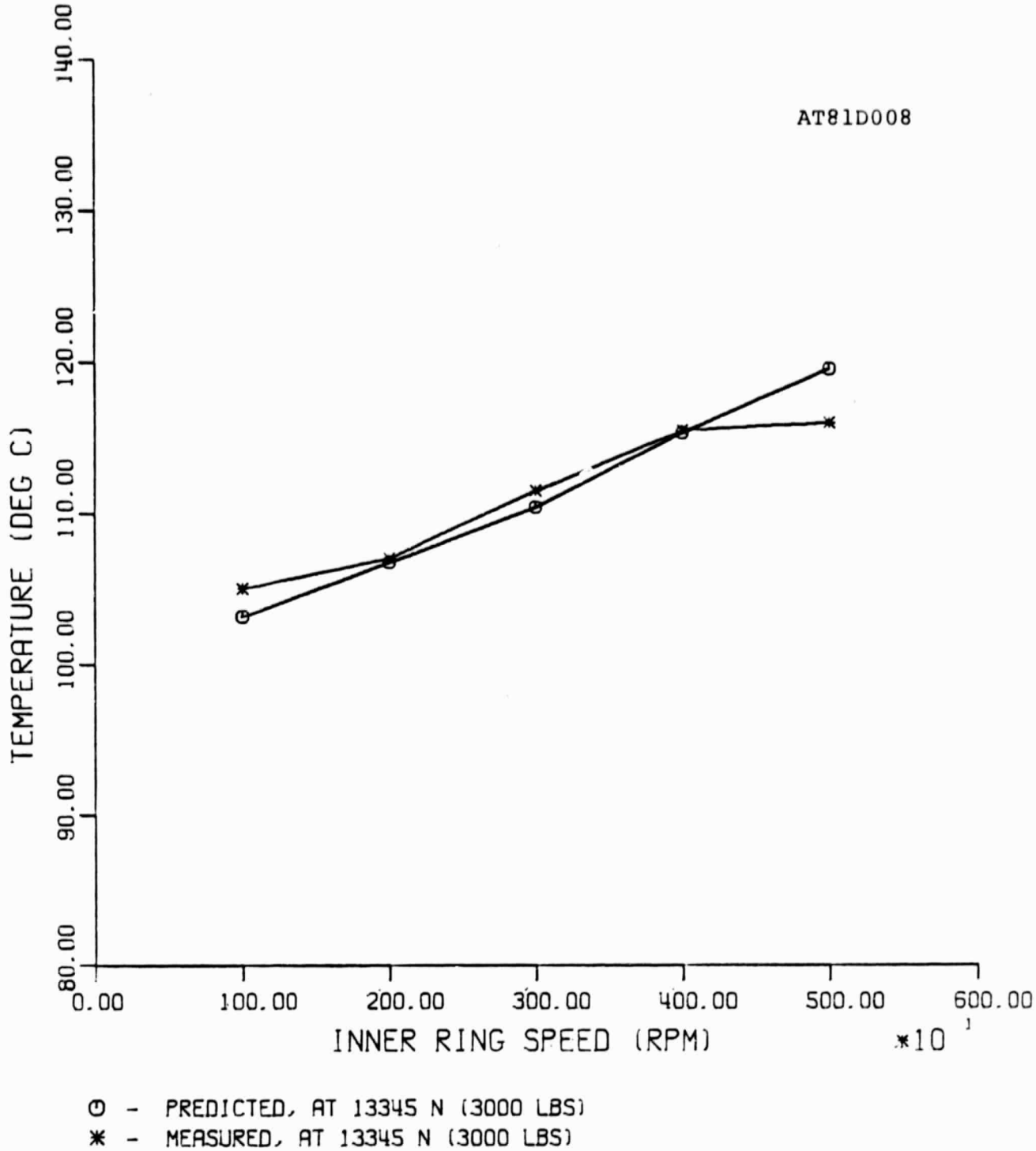

FIGURE 11:
COMPARISON OF PREDICTED AND MEASURED INNER RING TEMPERATURES UNDER PURE RADIAL LOAD (BRG. NO. 02).

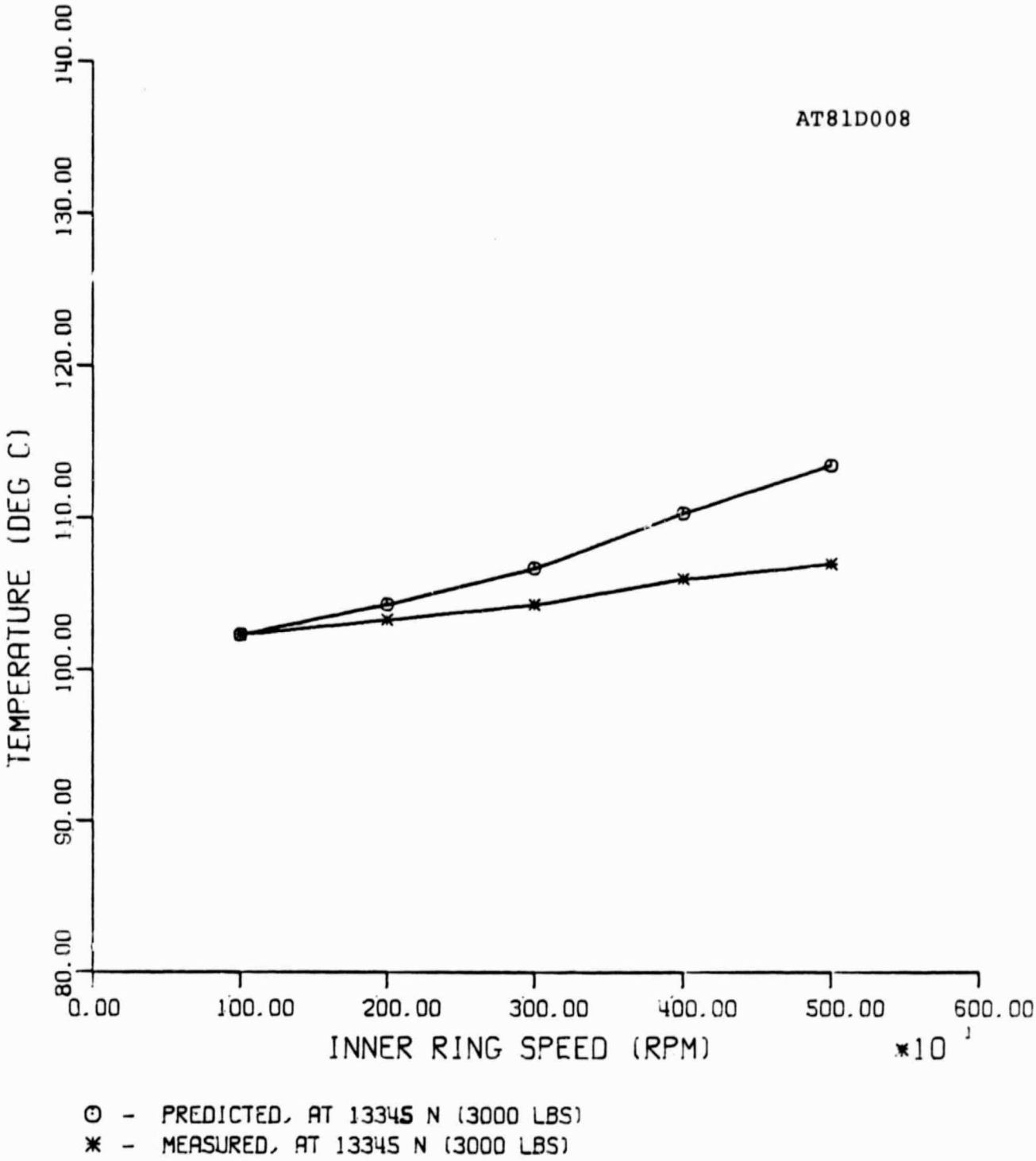

FIGURE 12:
COMPARISON OF PREDICTED AND MEASURED OUTER RING TEMPERATURES UNDER PURE RADIAL LOAD (BRG. NO. 02).

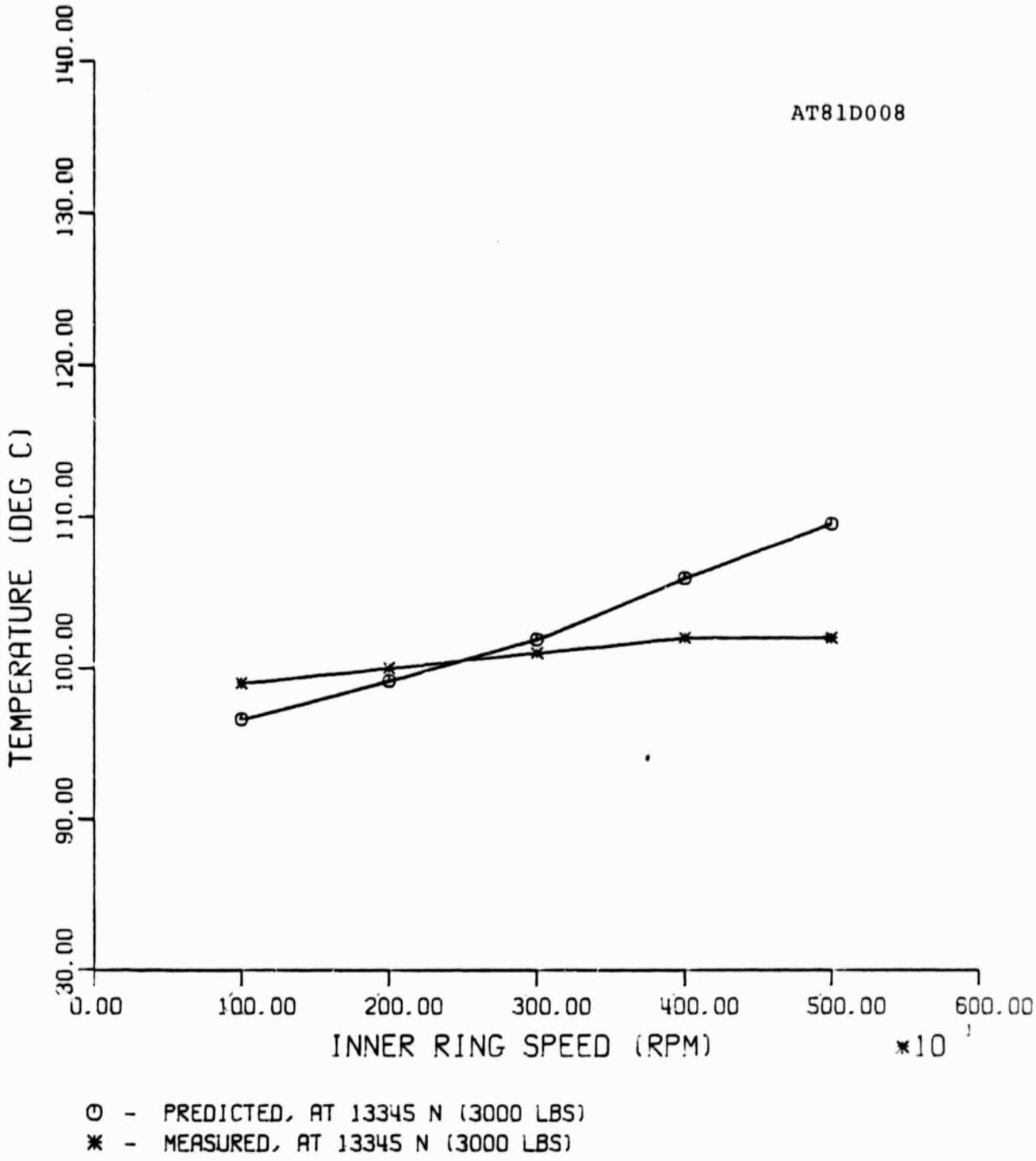

FIGURE 13:
COMPARISON OF PREDICTED AND MEASURED OUTLET LUBRICANT TEMPERATURES UNDER PURE RADIAL LOAD (BRG. NO. 02).

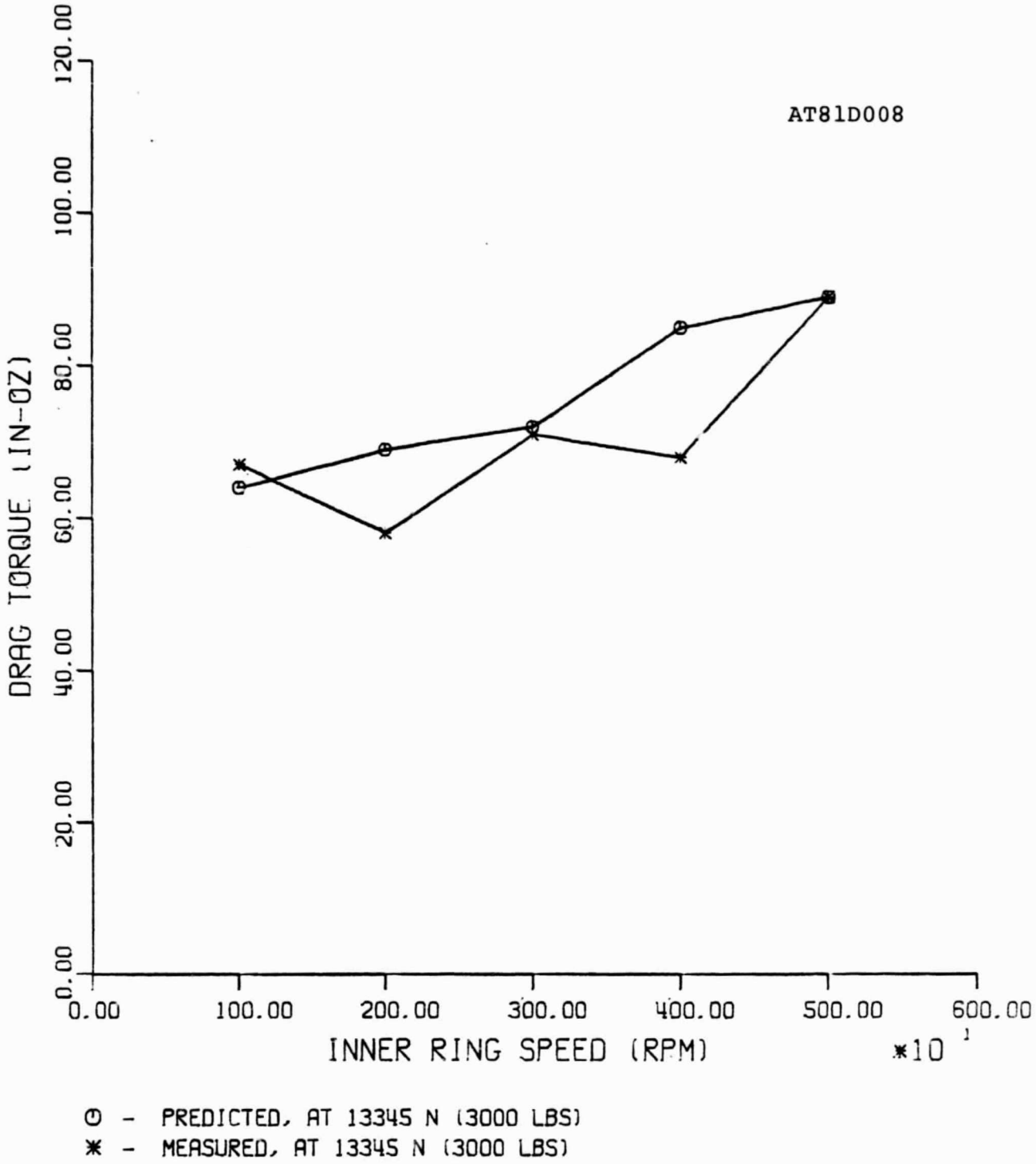

FIGURE 14:
COMPARISON OF PREDICTED AND MEASURED VALUES OF DRAG TORQUE UNDER PURE RADIAL LOAD (BRG. NO. 02).

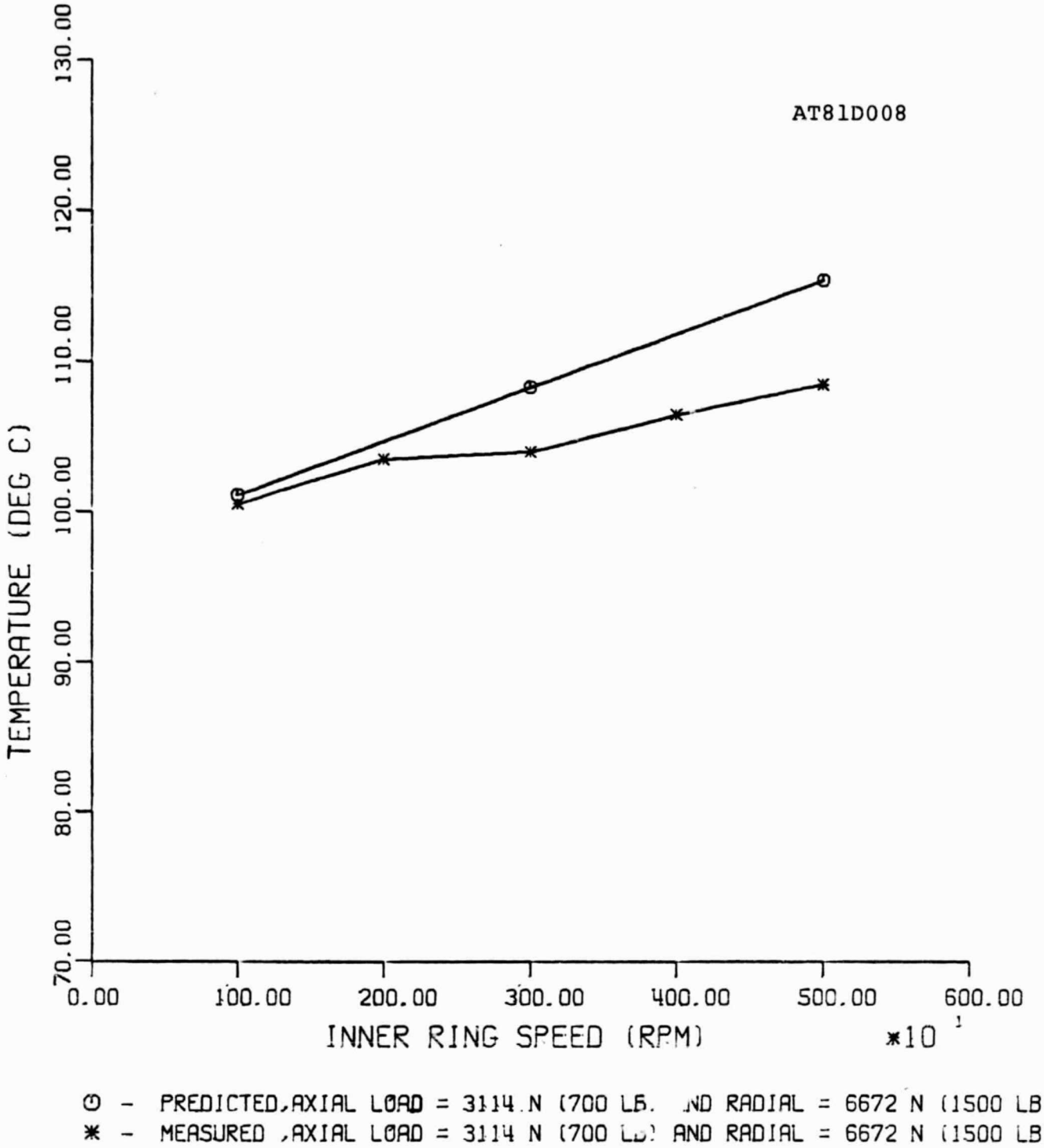

FIGURE 15:
COMPARISON OF PREDICTED AND MEASURED INNER RING TEMPERATURES UNDER COMBINED LOAD (BRG. NO. 02).

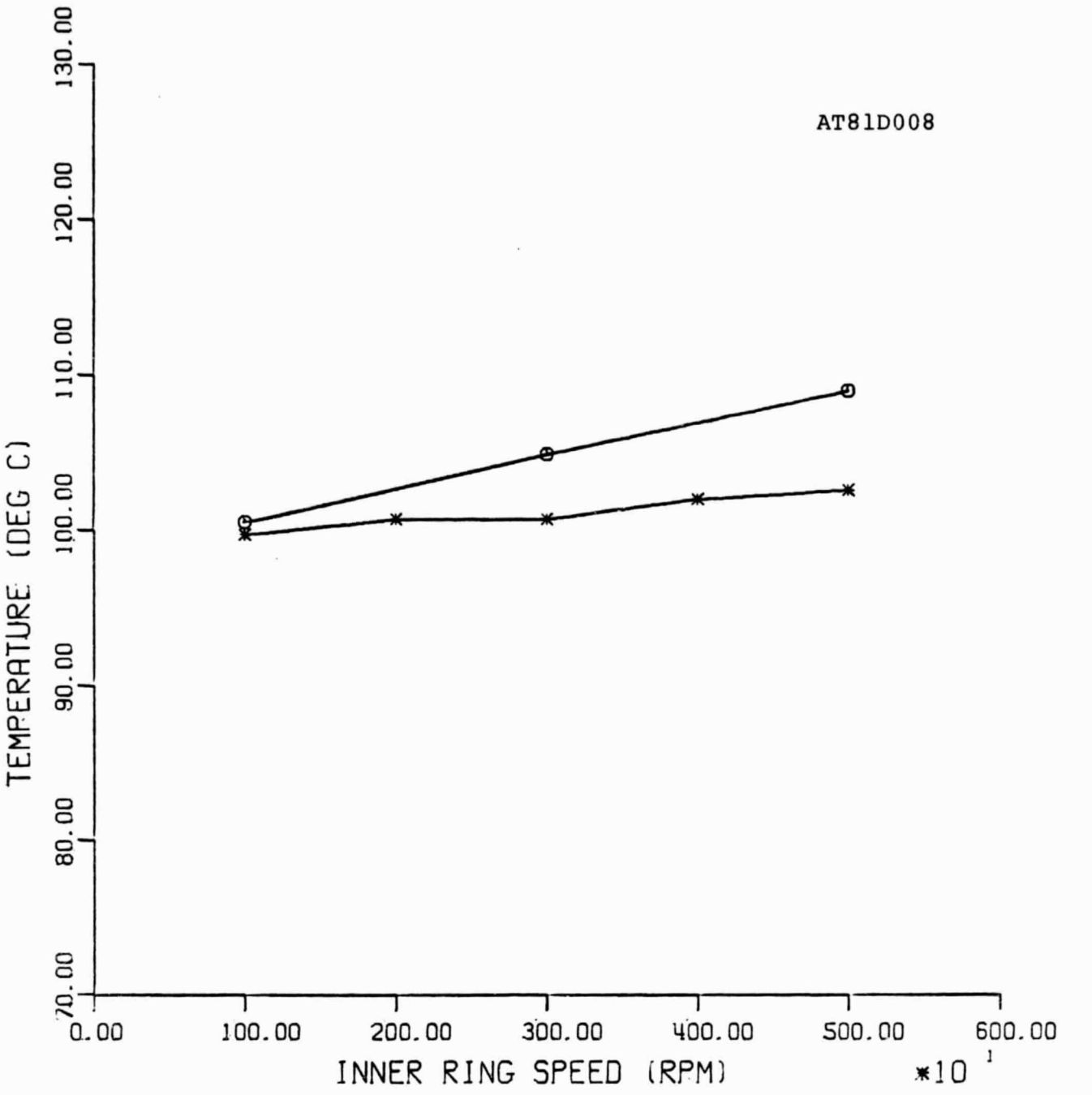

FIGURE 16:
COMPARISON OF PREDICTED AND MEASURED OUTER RING TEMPERATURES UNDER COMBINED LOAD (BRG. NO. 02).

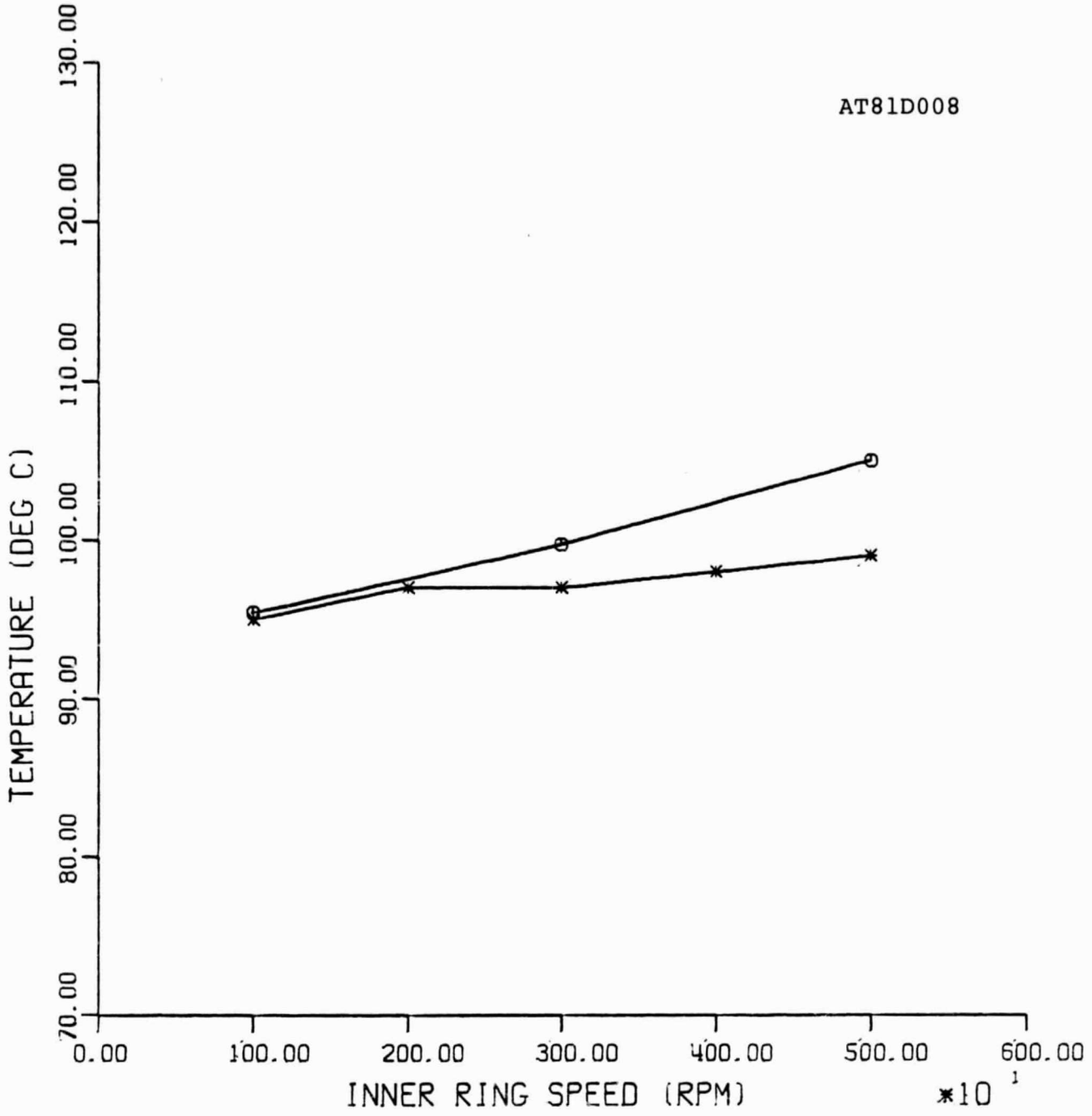

FIGURE 17:
COMPARISON OF PREDICTED AND MEASURED OUTLET LUBRICANT TEMPERATURES UNDER COMBINED LOAD (BRG. NO. 02).

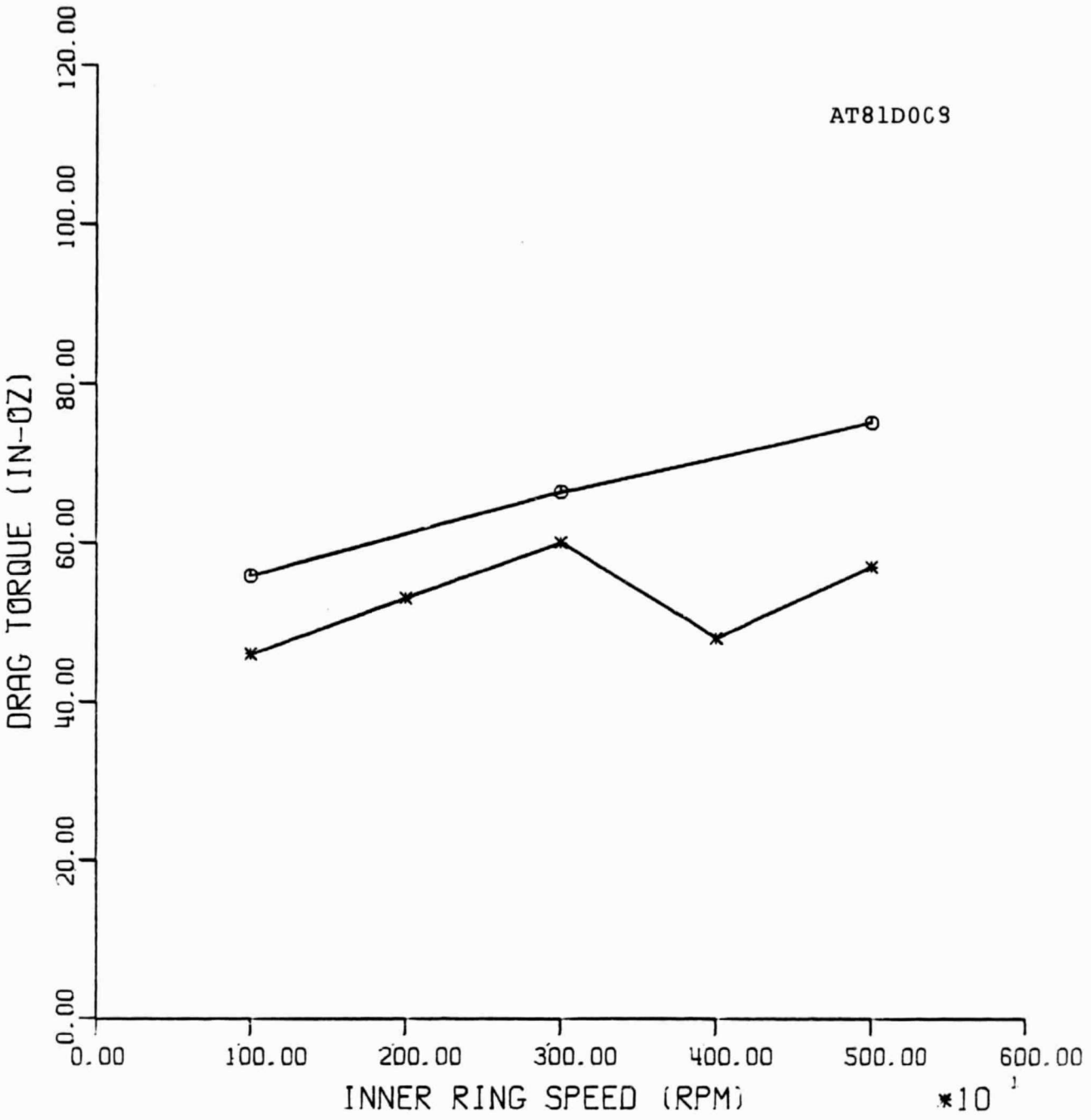

FIGURE 18:
COMPARISON OF PREDICTED AND MEASURED VALUES OF DRAG TORQUE UNDER COMBINED LOAD (BRG. NO. 02).

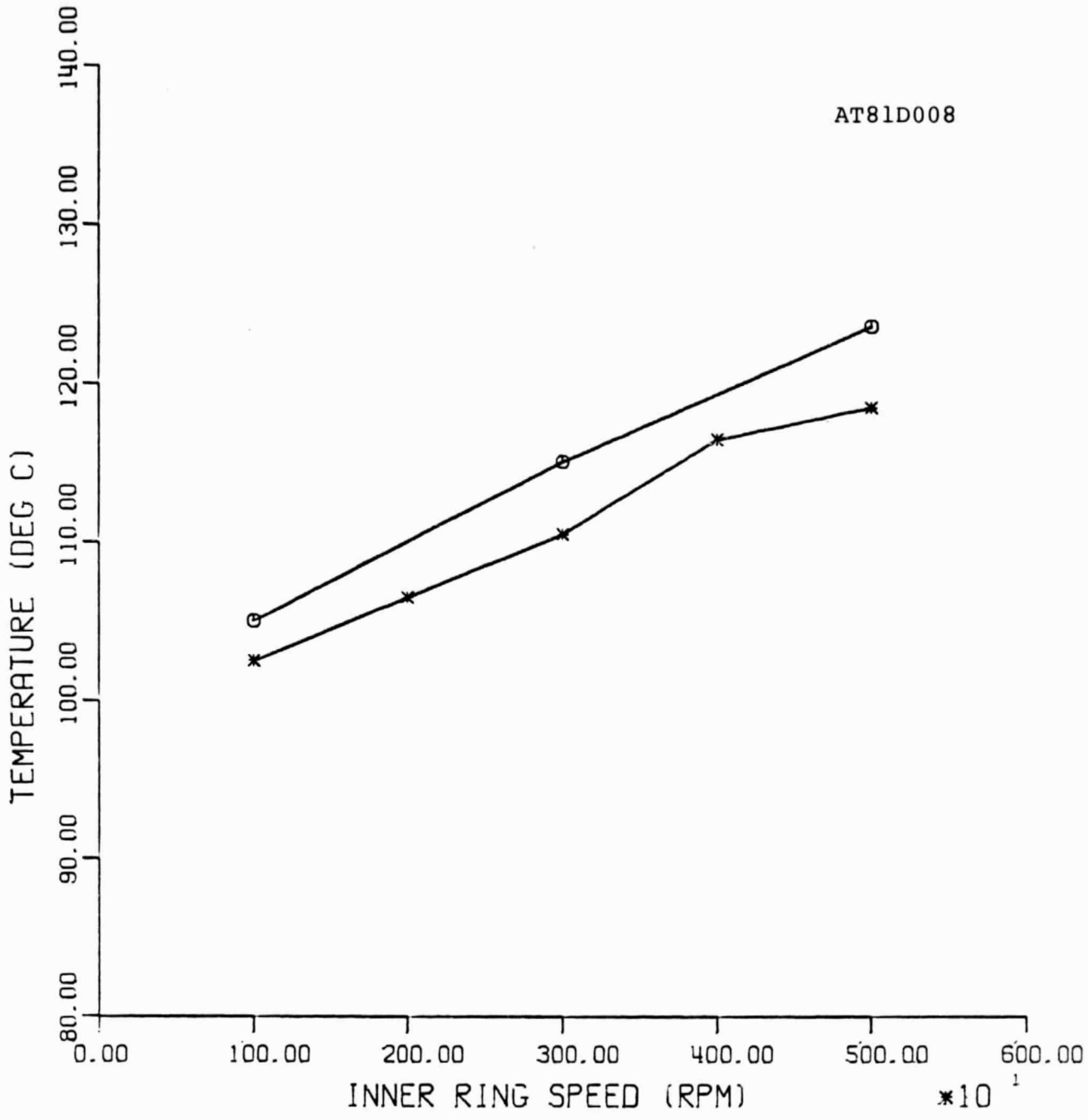

FIGURE 19:
COMPARISON OF PREDICTED AND MEASURED INNER RING TEMPERATURES UNDER COMBINED LOAD (BRG. NO. 02).

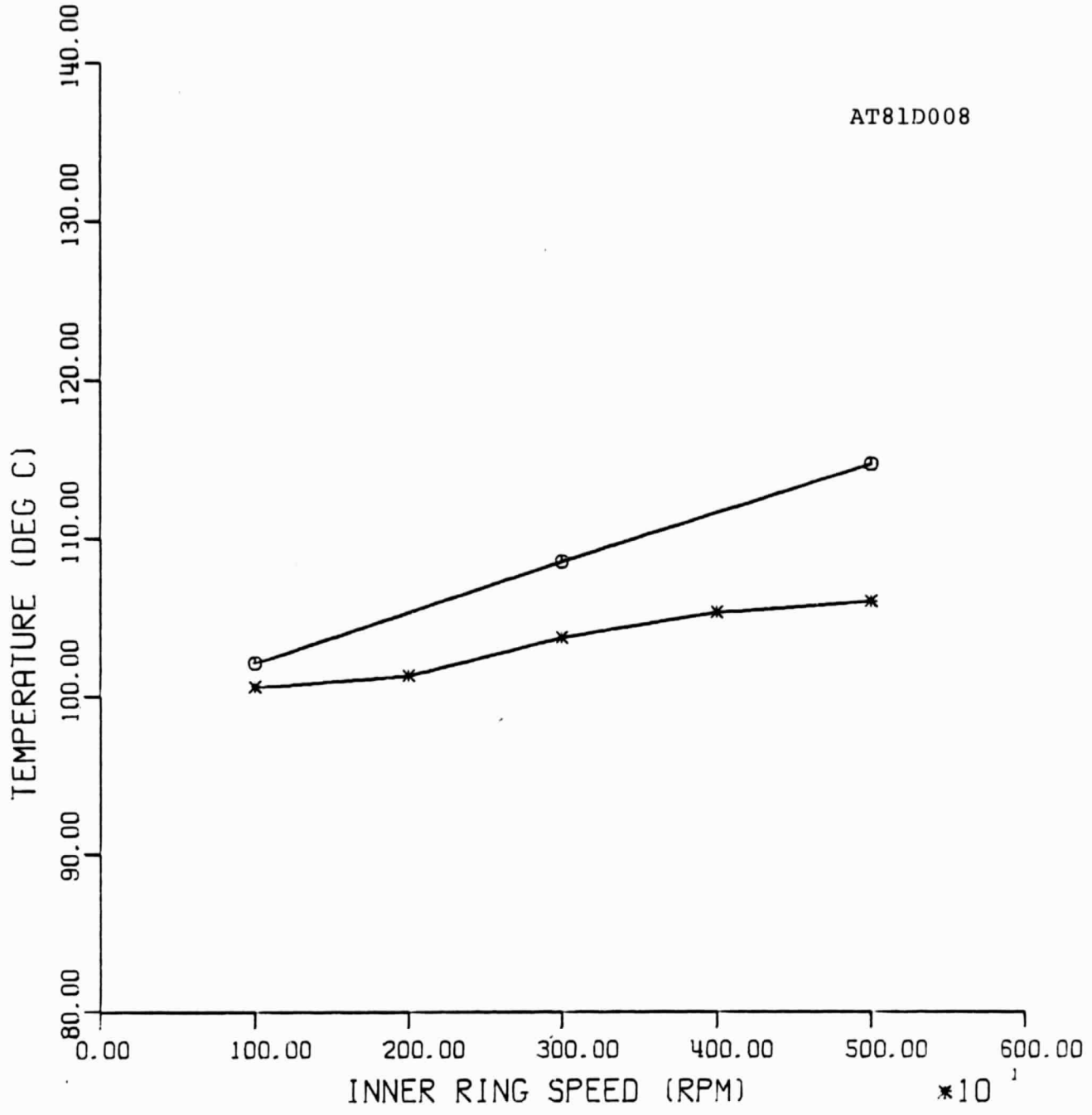

FIGURE 20:
COMPARISON OF PREDICTED AND MEASURED OUTER RING TEMPERATURES UNDER COMBINED LOAD (BRG. NO. 02).

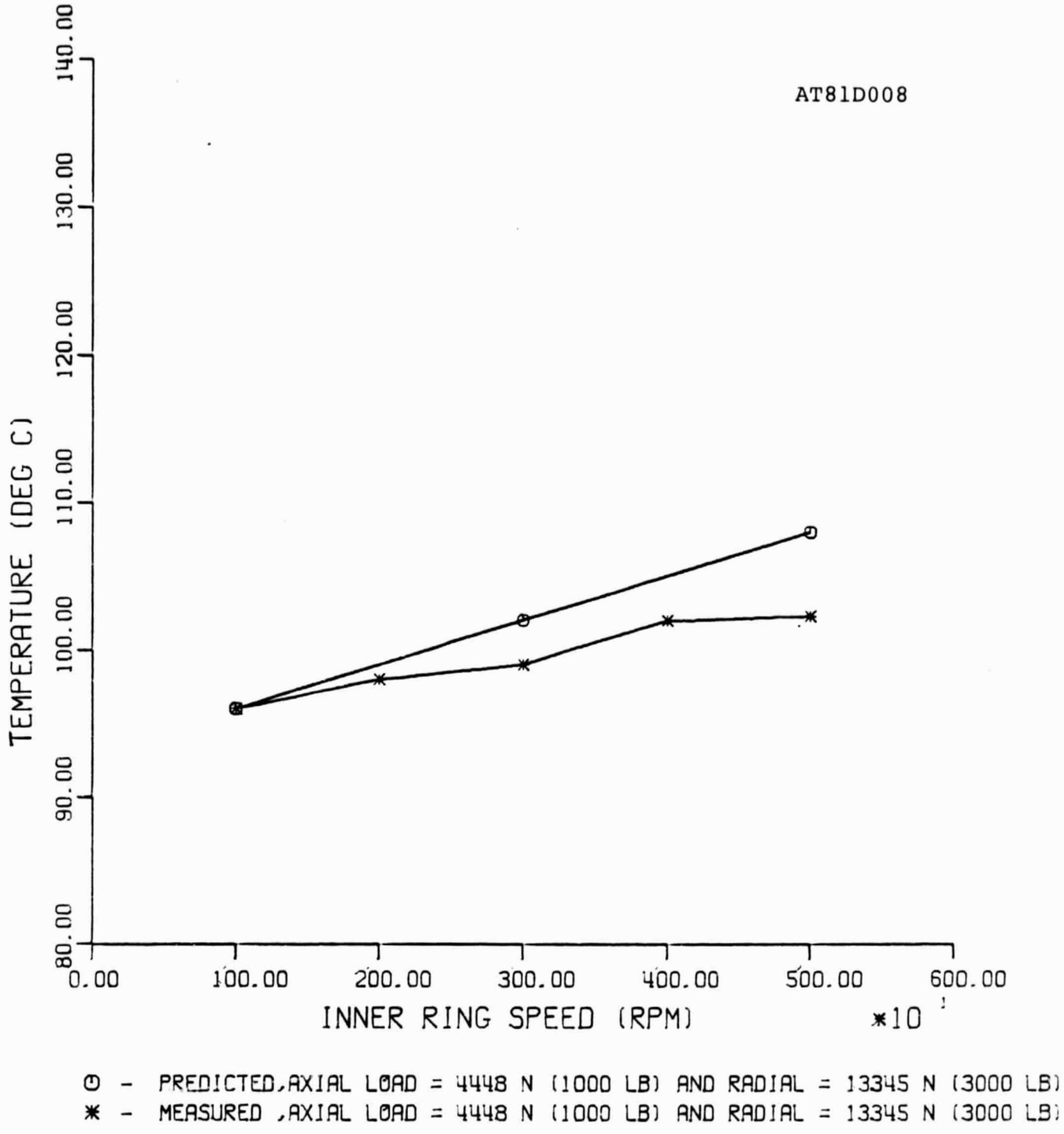

FIGURE 21:

COMPARISON OF PREDICTED AND MEASURED OUTLET LUBRICANT TEMPERATURES UNDER COMBINED LOAD (BRG. NO. 02).

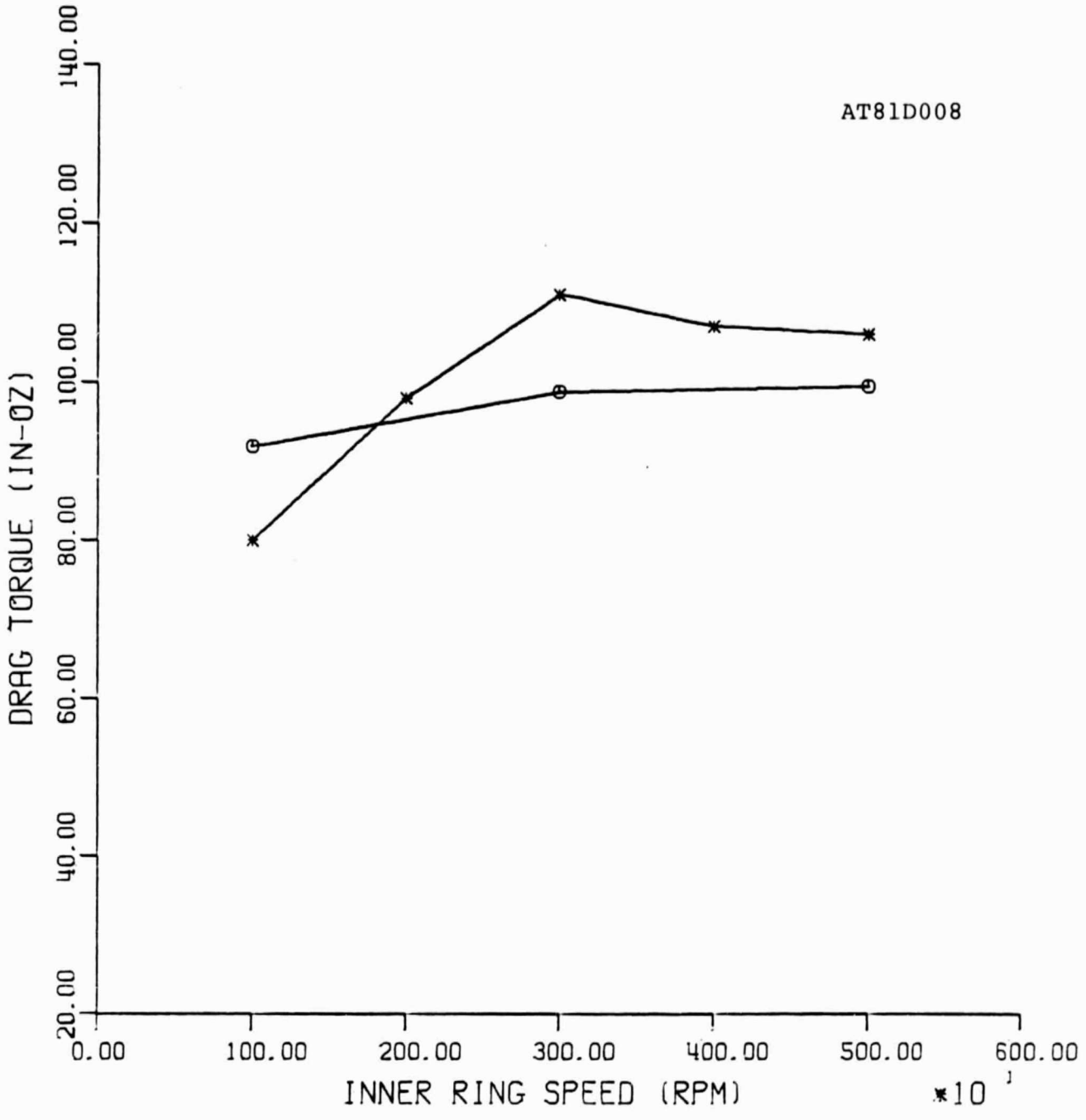

FIGURE 22:
COMPARISON OF PREDICTED AND MEASURED VALUES OF DRAG TORQUE UNDER COMBINED LOAD (BRG. NO. 02).

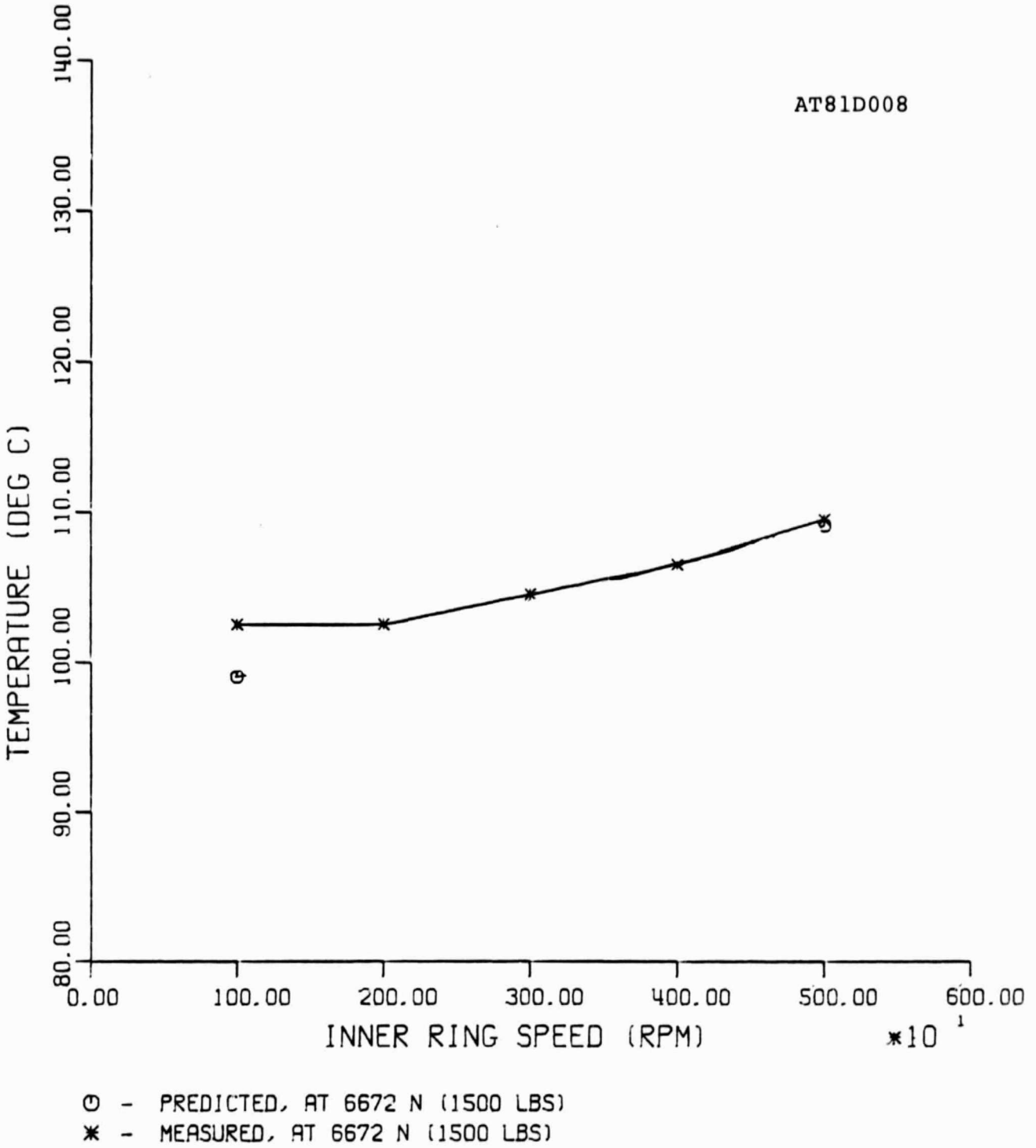

FIGURE 23:
COMPARISON OF PREDICTED AND MEASURED INNER RING TEMPERATURES UNDER PURE RADIAL LOAD (BRG. NO. 01).

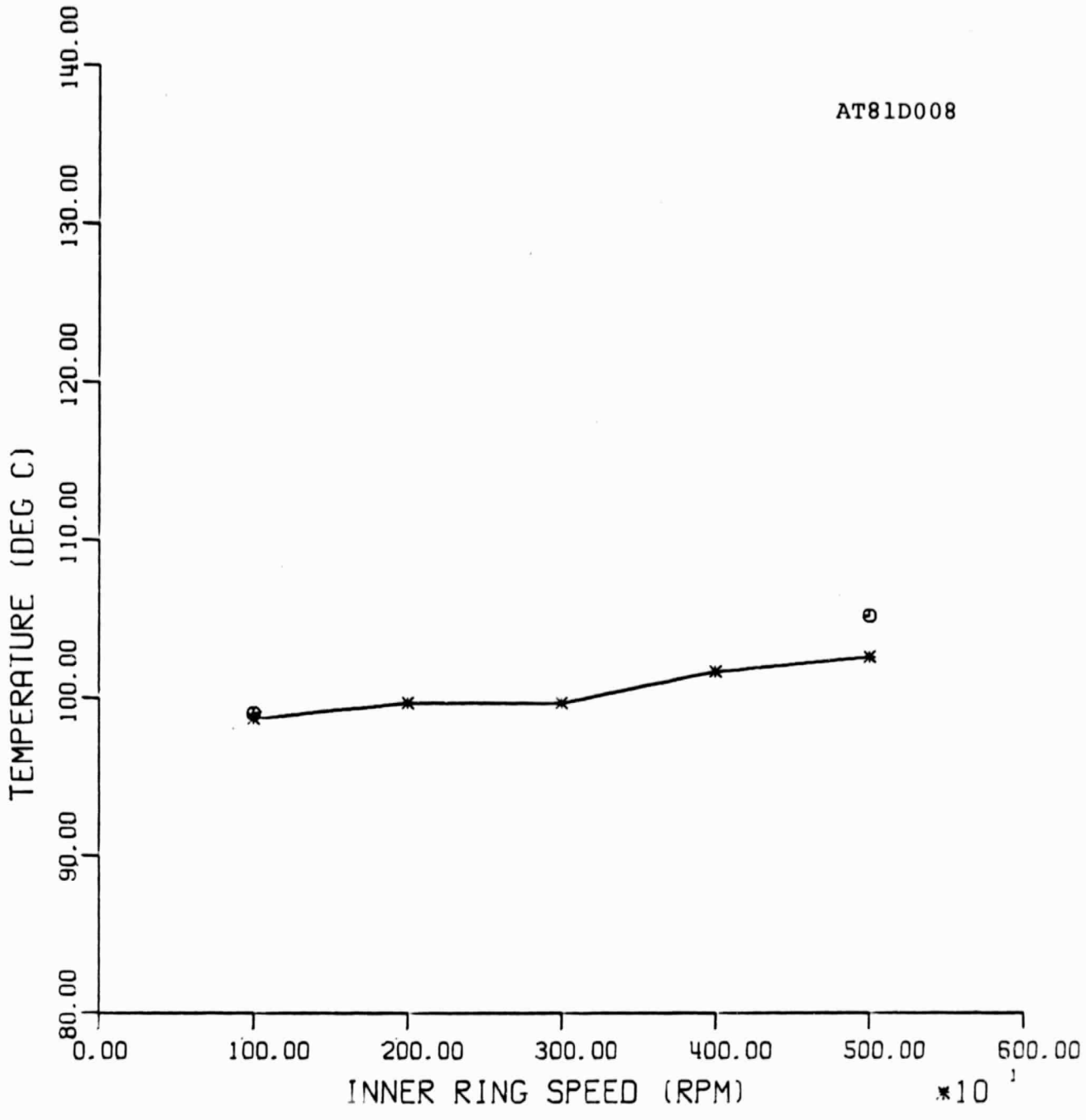

FIGURE 24:
COMPARISON OF PREDICTED AND MEASURED OUTER RING TEMPERATURES UNDER PURE RADIAL LOAD (BRG. NO. 01).

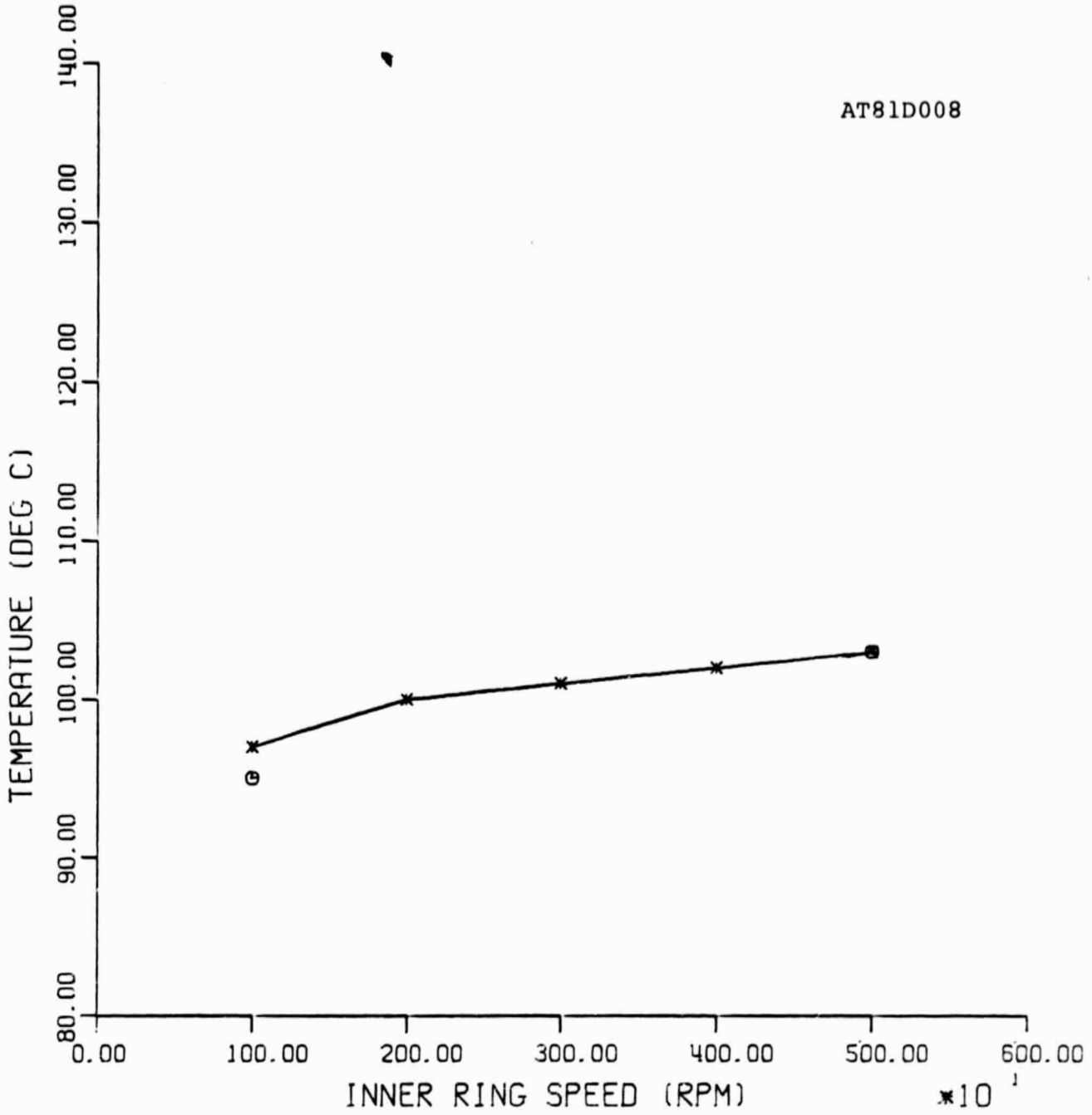

FIGURE 25:
COMPARISON OF PREDICTED AND MEASURED OUTLET LUBRICANT TEMPERATURES UNDER PURE RADIAL LOAD (BRG. NO. 01).

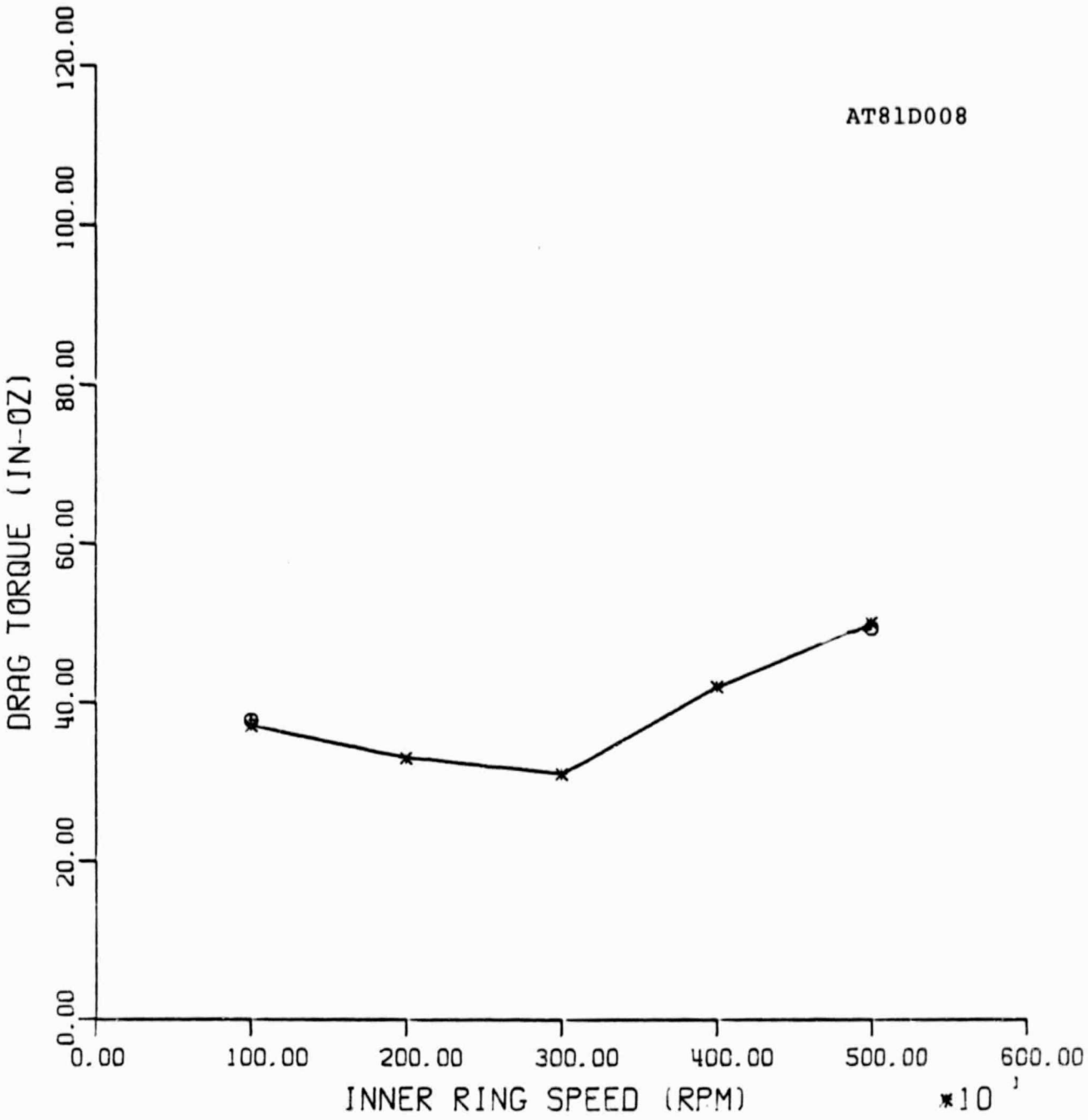

FIGURE 26:
COMPARISON OF PREDICTED AND MEASURED VALUES OF DRAG TORQUE UNDER PURE RADIAL LOAD (BRG. NO. 01).

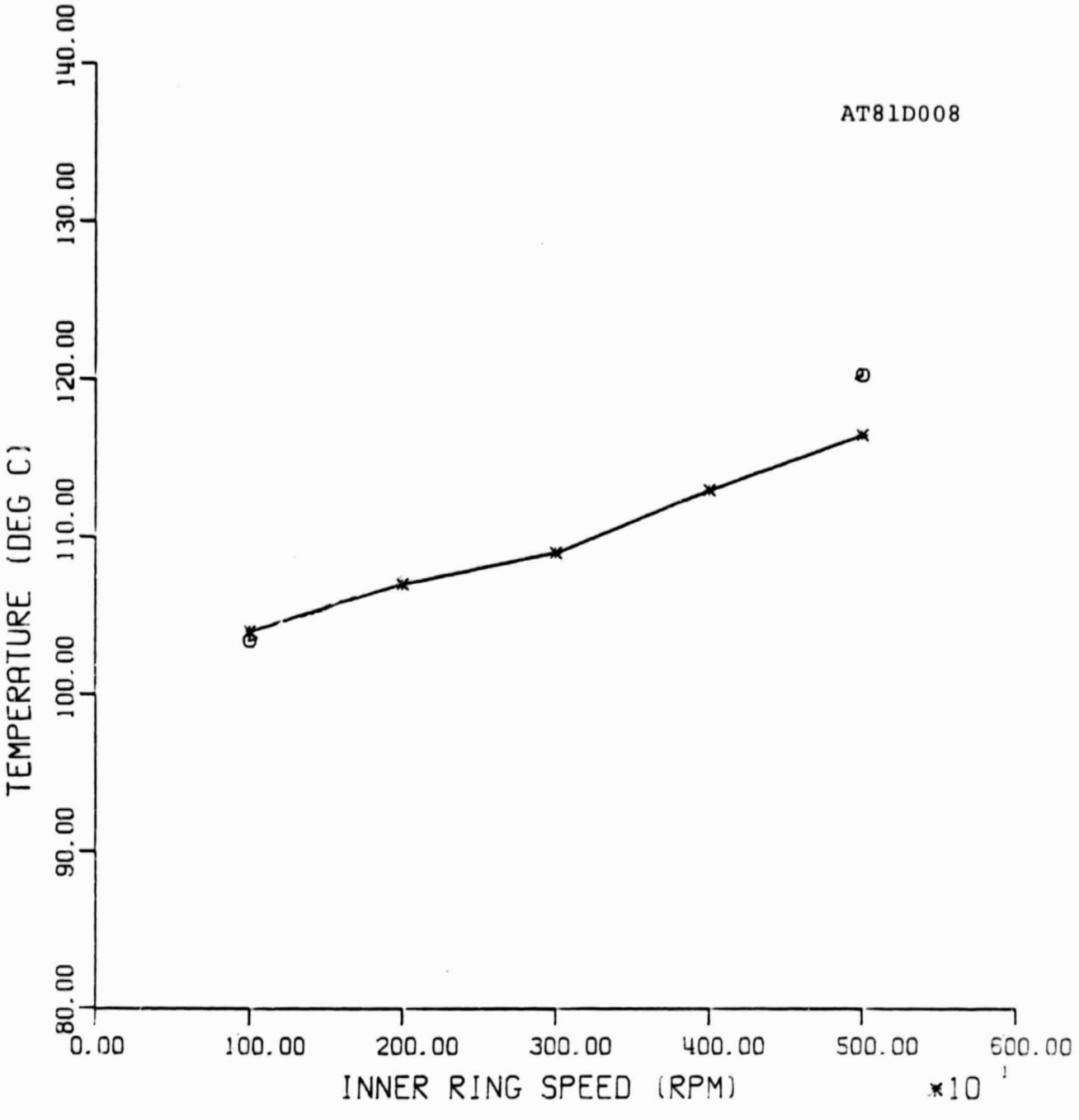

FIGURE 27:
COMPARISON OF PREDICTED AND MEASURED INNER RING TEMPERATURES UNDER PURE RADIAL LOAD (BRG. NO. 01).

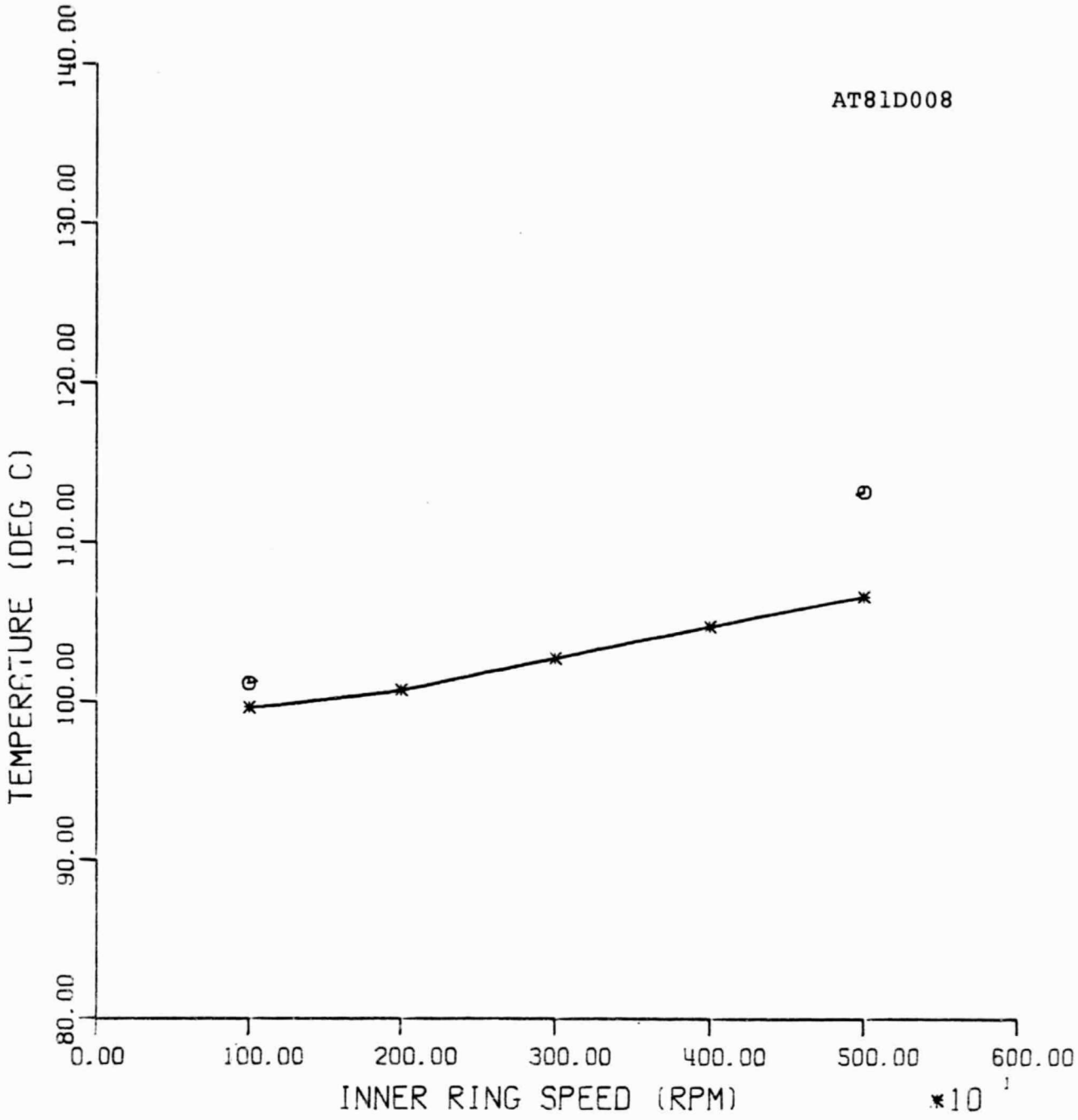

FIGURE 28:
COMPARISON OF PREDICTED AND MEASURED OUTER RING TEMPERATURES UNDER PURE RADIAL LOAD (BRG. NO. 01).

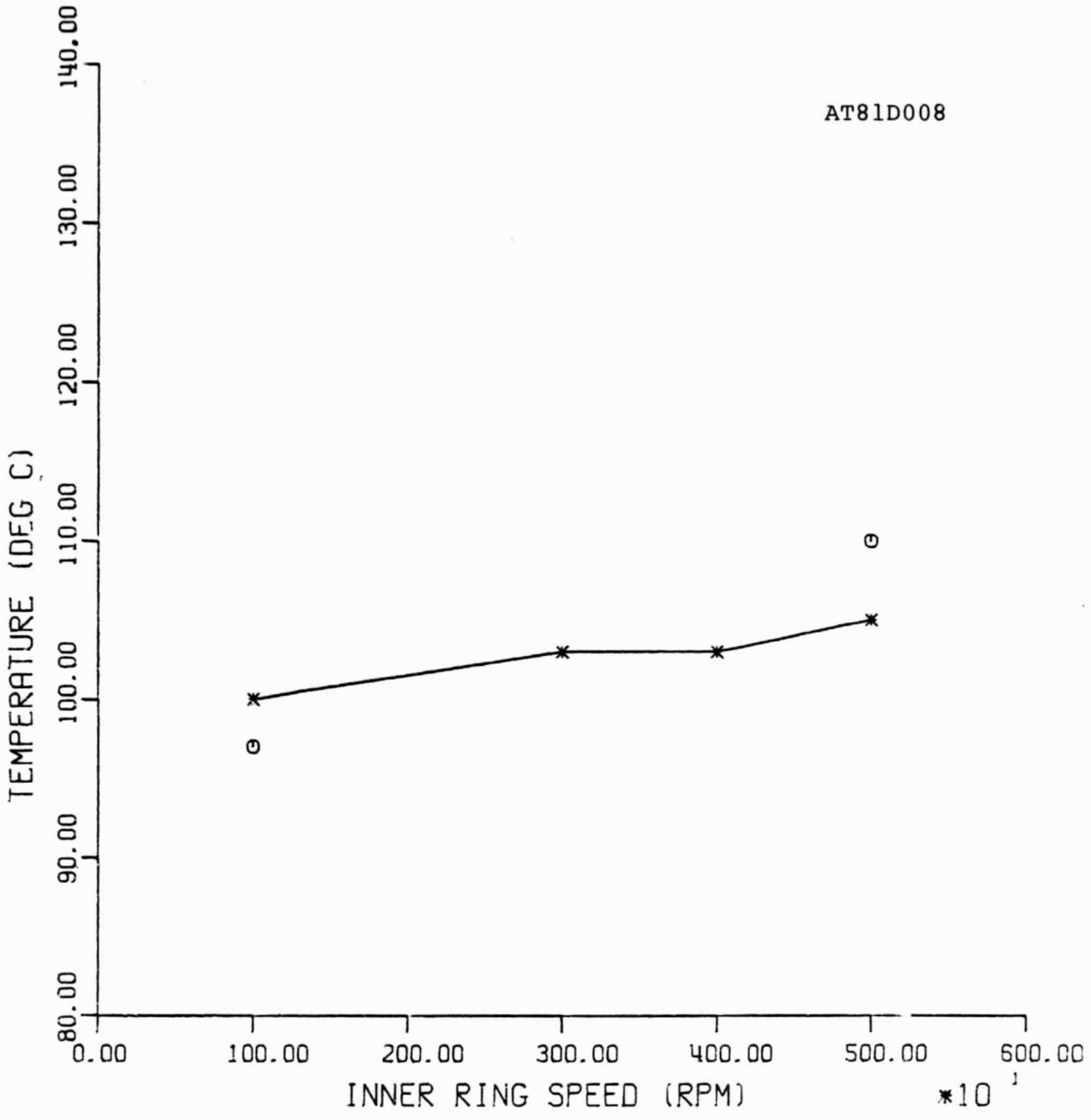

FIGURE 29:
COMPARISON OF PREDICTED AND MEASURED OUTLET LUBRICANT TEMPERATURES UNDER PURE RADIAL LOAD (BRG. NO. 01).

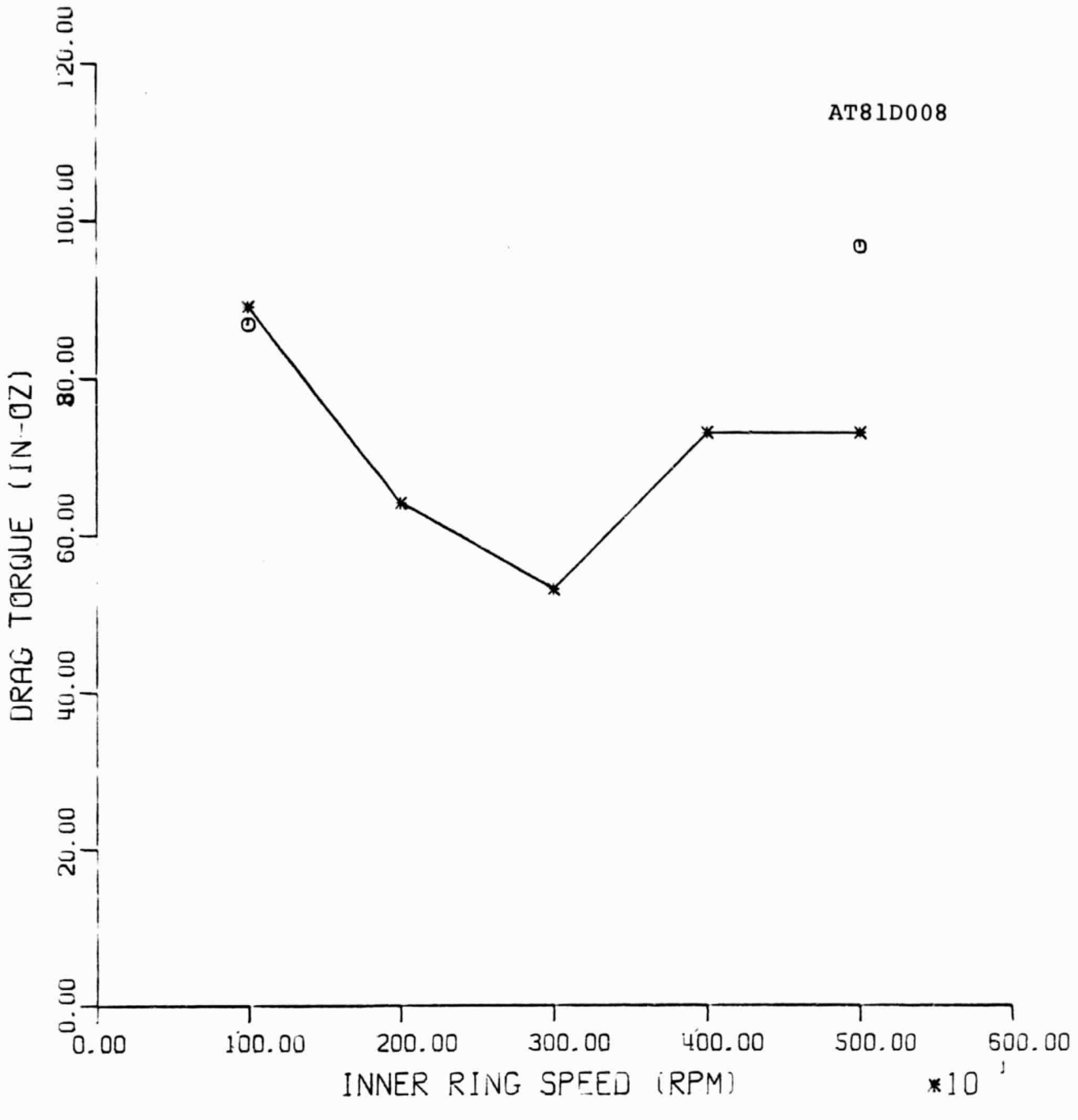

FIGURE 30:
COMPARISON OF PREDICTED AND MEASURED VALUES OF DRAG TORQUE UNDER PURE RADIAL LOAD (BRG. NO. 01).

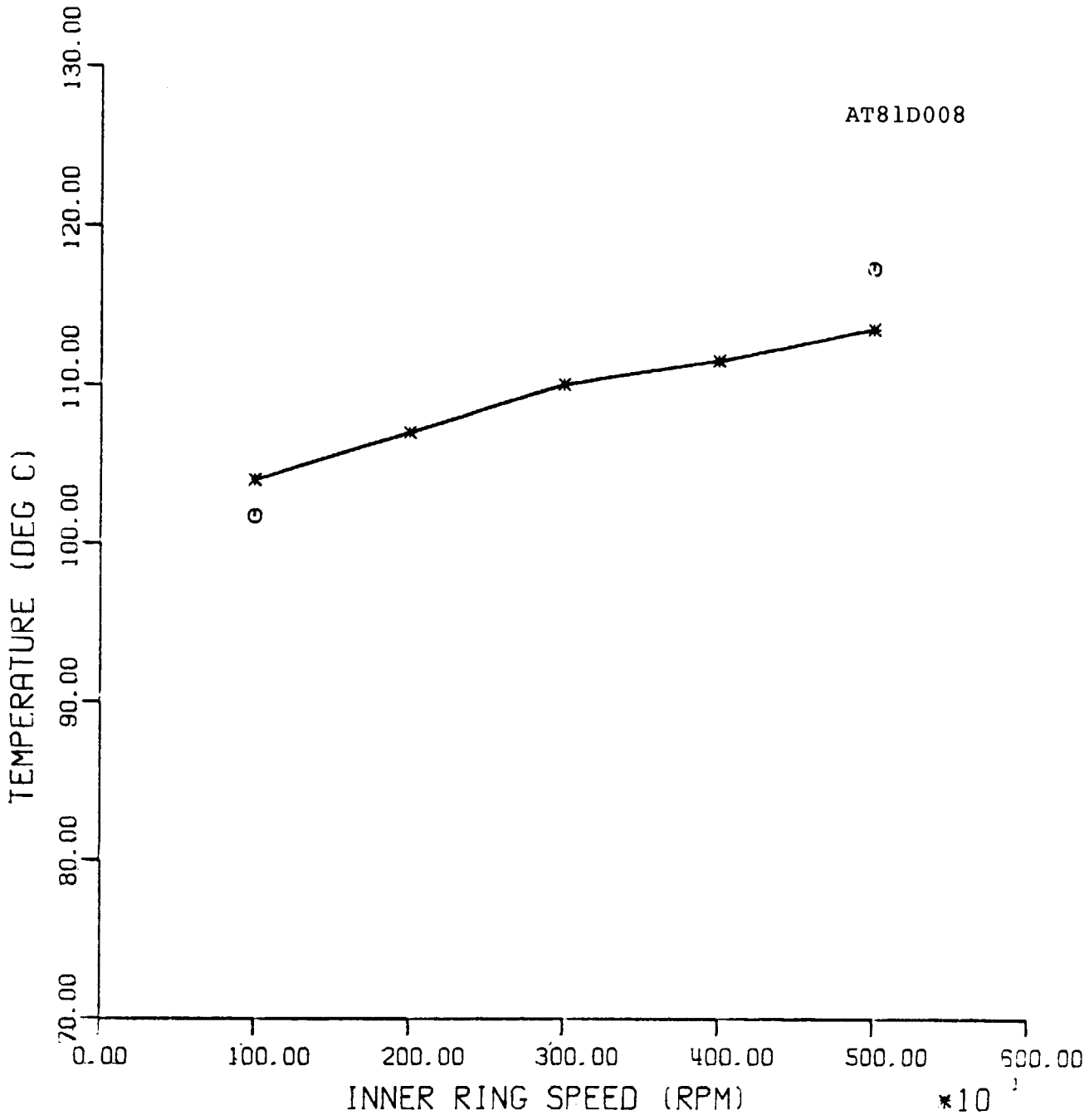

FIGURE 31:
COMPARISON OF PREDICTED AND MEASURED INNER RING TEMPERATURES UNDER COMBINED LOAD (BRG. NO. 01).

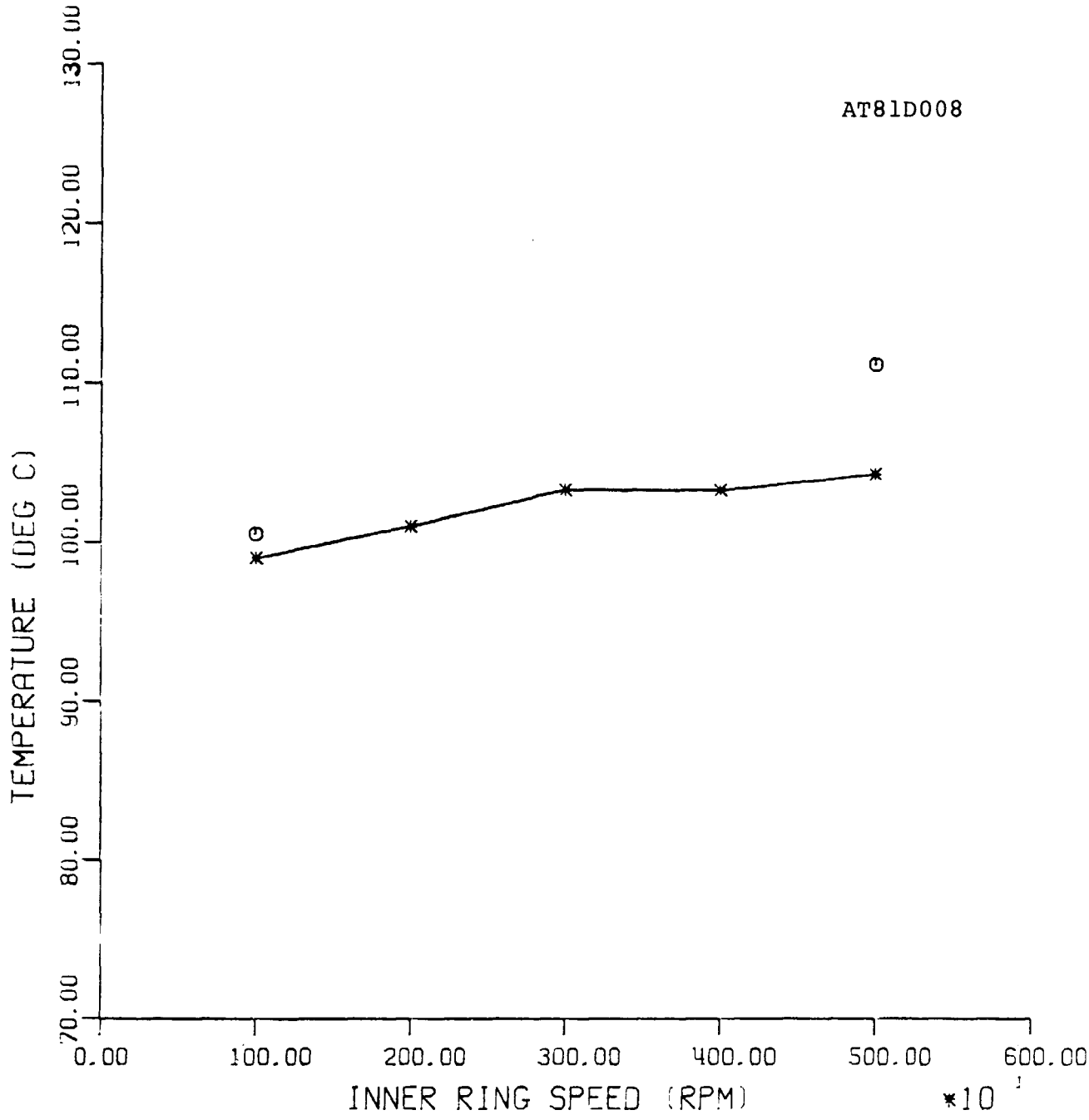

FIGURE 32:

COMPARISON OF PREDICTED AND MEASURED OUTER RING TEMPERATURES UNDER COMBINED LOAD (BRG. NO. 01).

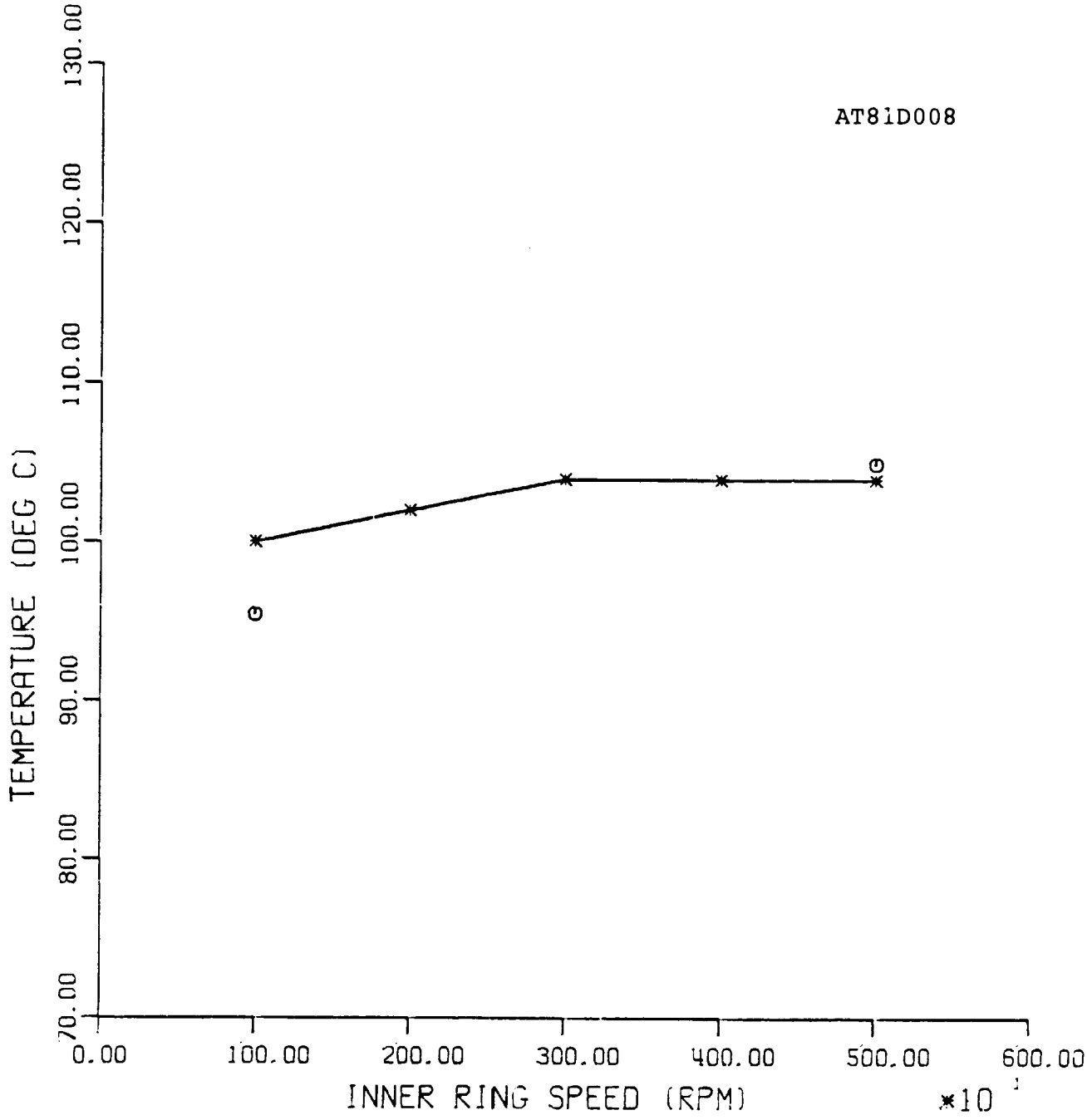

FIGURE 33:
COMPARISON OF PREDICTED AND MEASURED OUTLET LUBRICANT TEMPERATURES UNDER COMBINED LOAD (BRG. NO. 01).

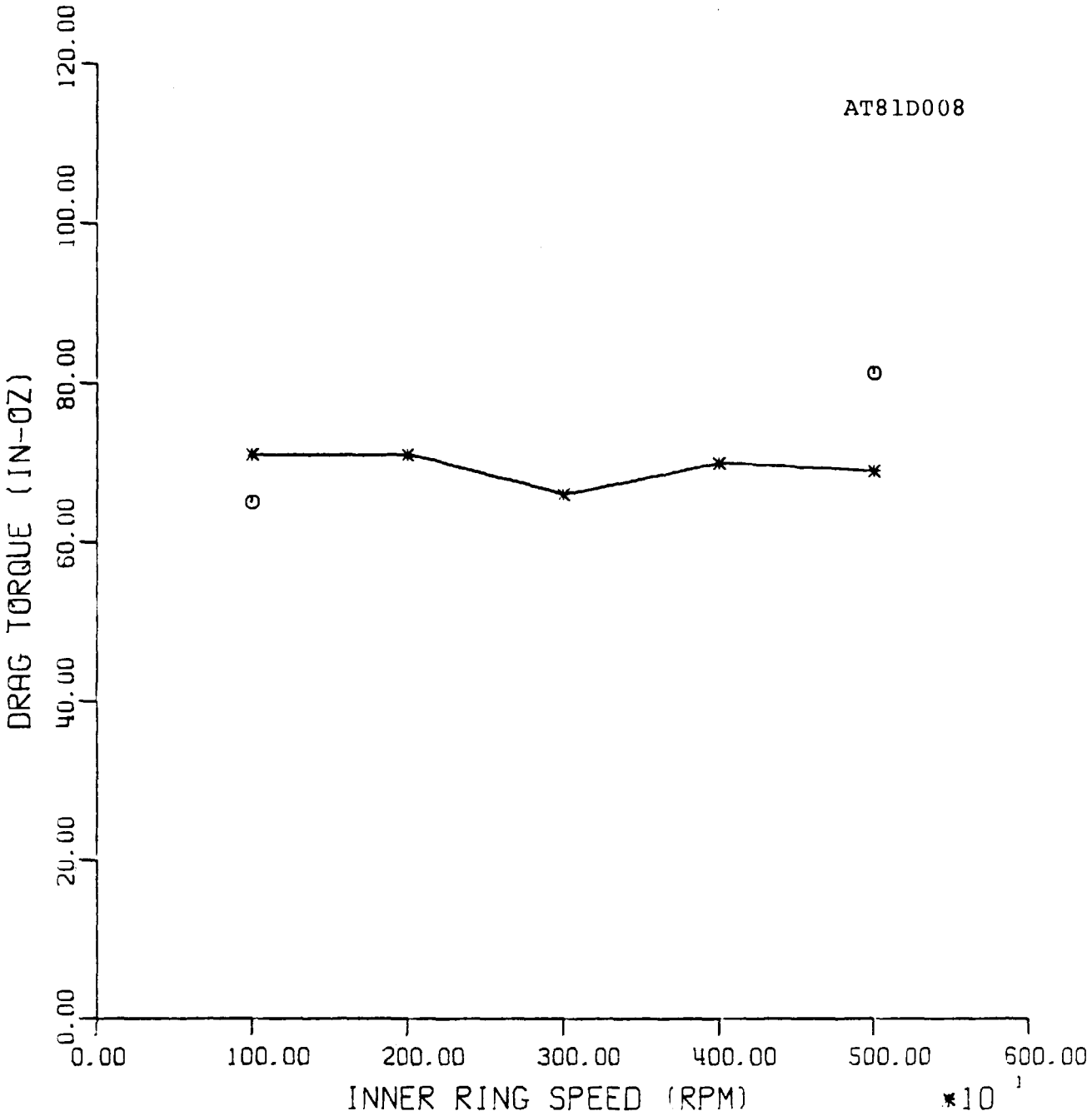

FIGURE 34:

COMPARISON OF PREDICTED AND MEASURED VALUES OF DRAG TORQUE UNDER COMBINED LOAD (BRG. NO. 01).

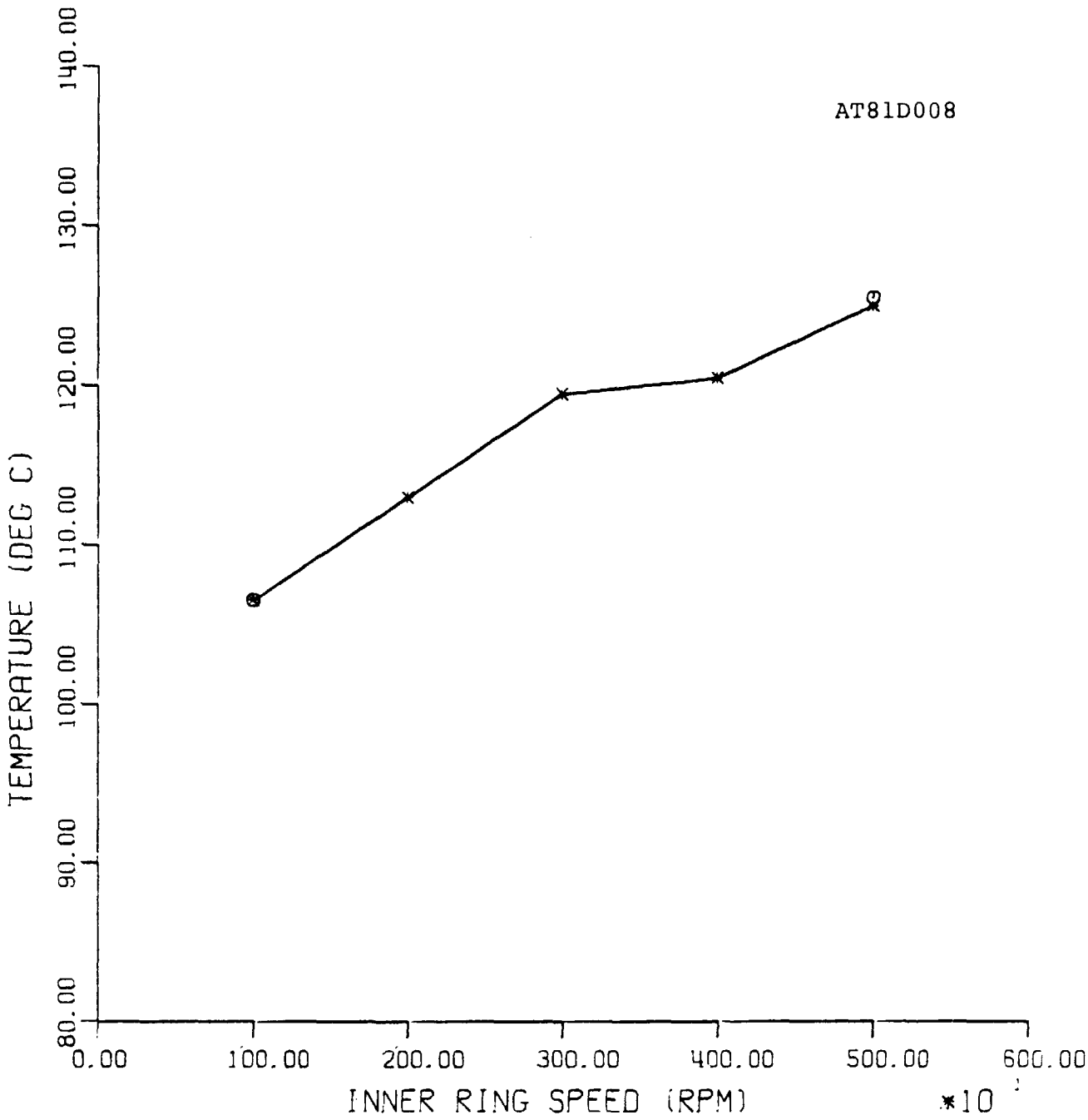

FIGURE 35:
COMPARISON OF PREDICTED AND MEASURED INNER RING TEMPERATURES UNDER COMBINED LOAD (BRG. NO. 01).

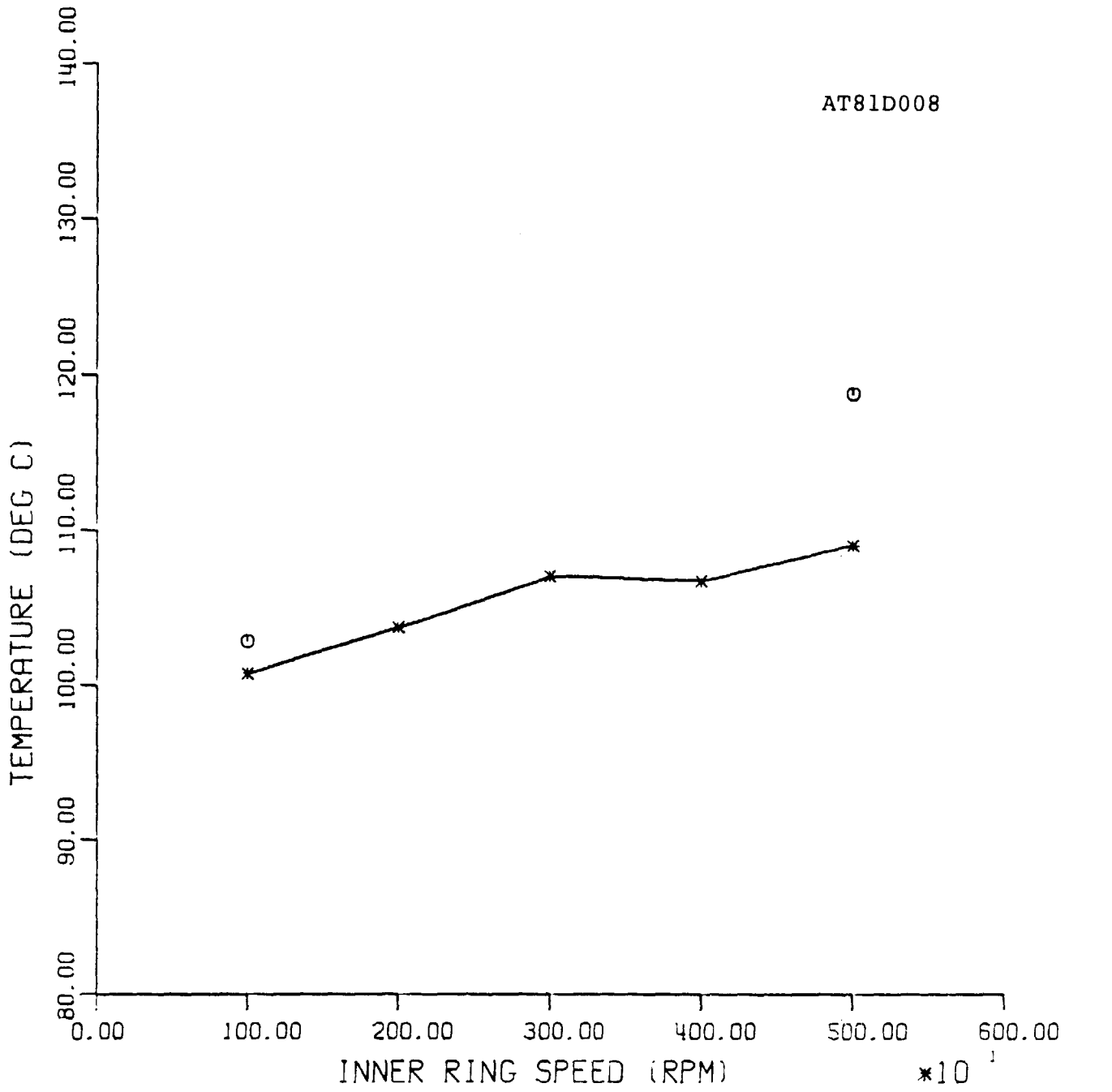

FIGURE 36:
COMPARISON OF PREDICTED AND MEASURED OUTER RING TEMPERATURES UNDER COMBINED LOAD (BRG. NO. 01).

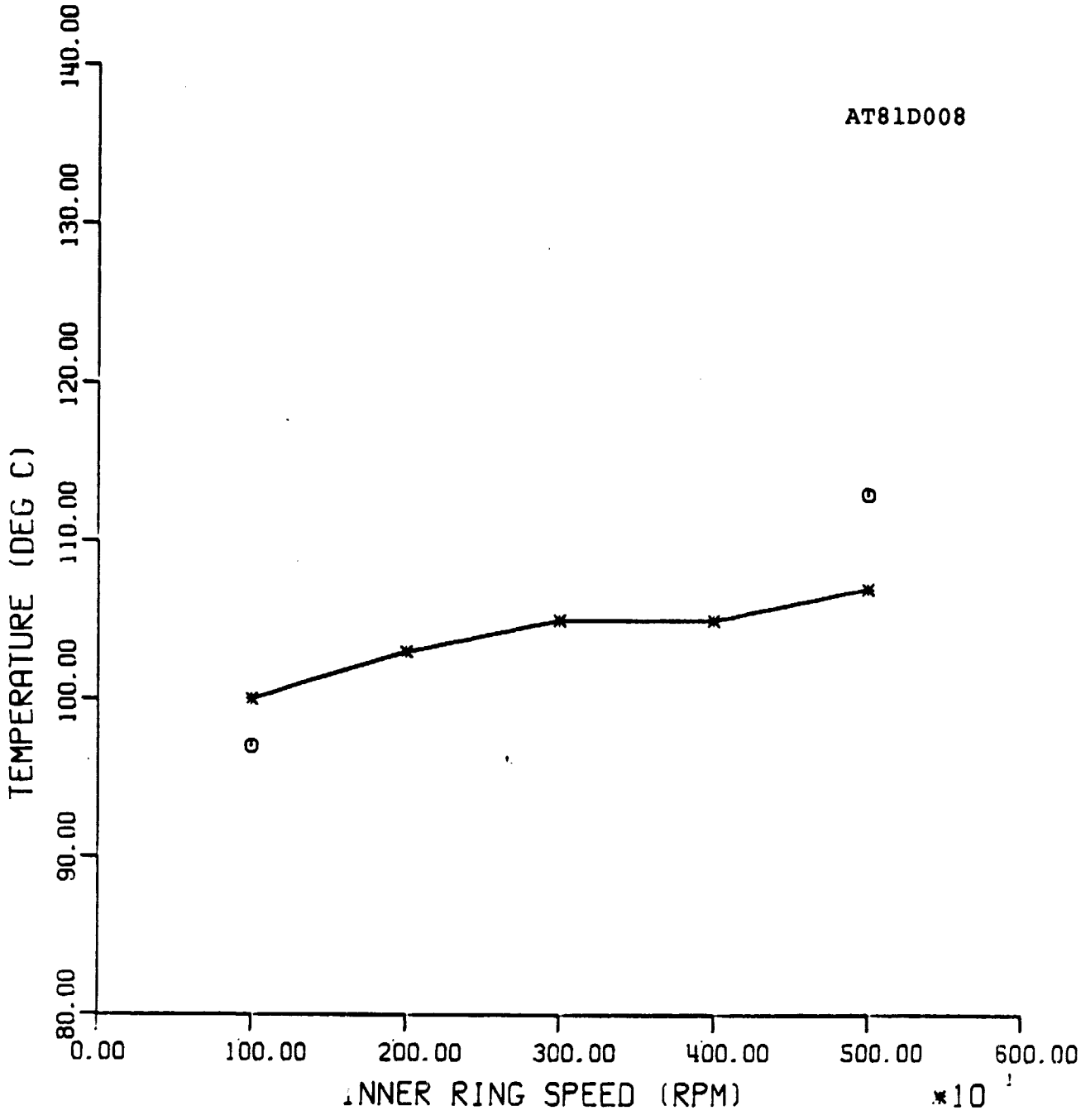

FIGURE 37:

COMPARISON OF PREDICTED AND MEASURED OUTLET LUBRICANT TEMPERATURES UNDER COMBINED LOAD (BRG. NO. 01).

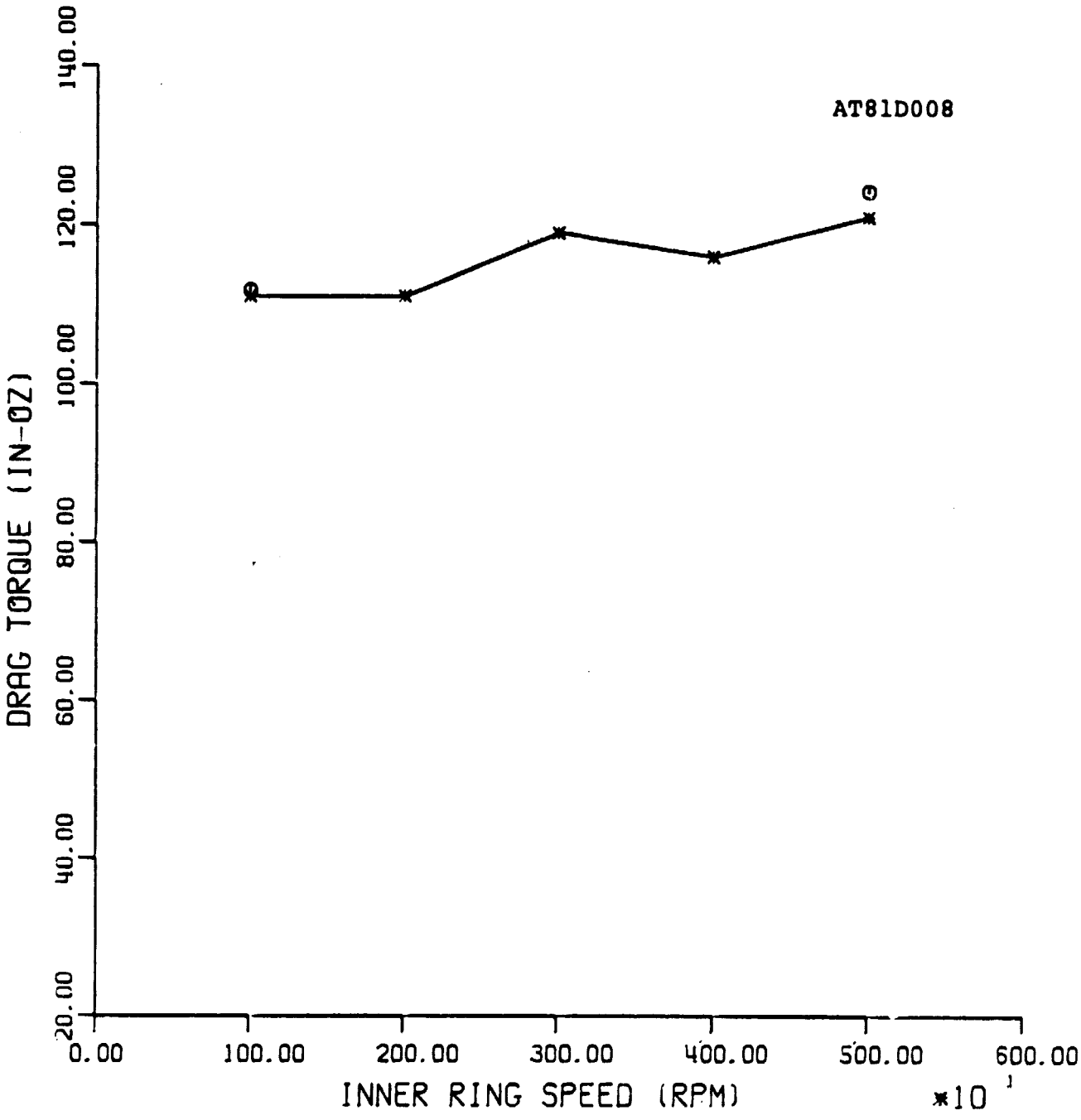

FIGURE 38:
COMPARISON OF PREDICTED AND MEASURED VALUES OF DRAG TORQUE UNDER COMBINED LOAD (BRG. NO. 01).

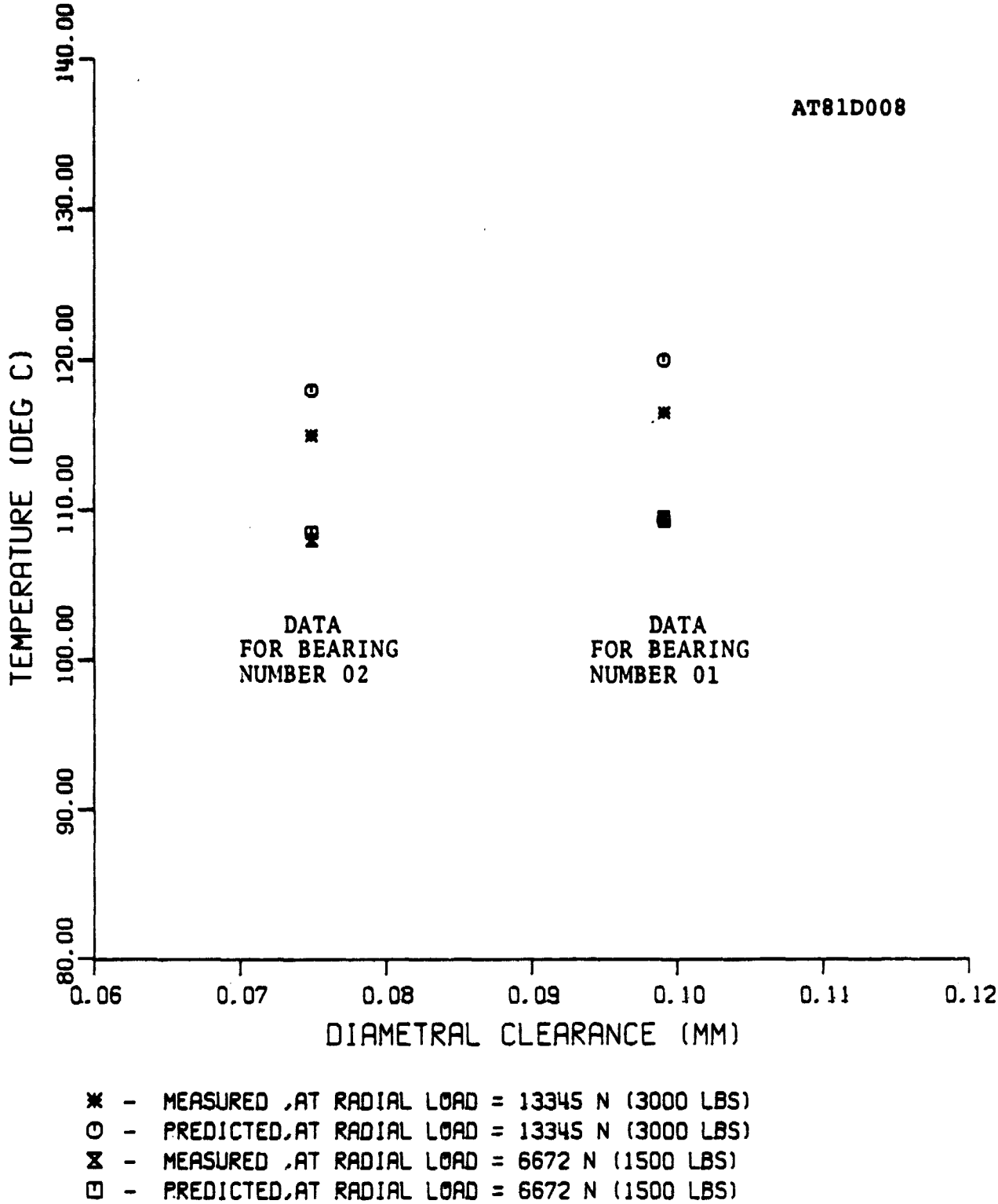

FIGURE 39:
COMPARISON OF INNER RING TEMPERATURES AS A FUNCTION OF DIAMETRAL CLEARANCE UNDER PURE RADIAL LOAD AT 5000 RPM.

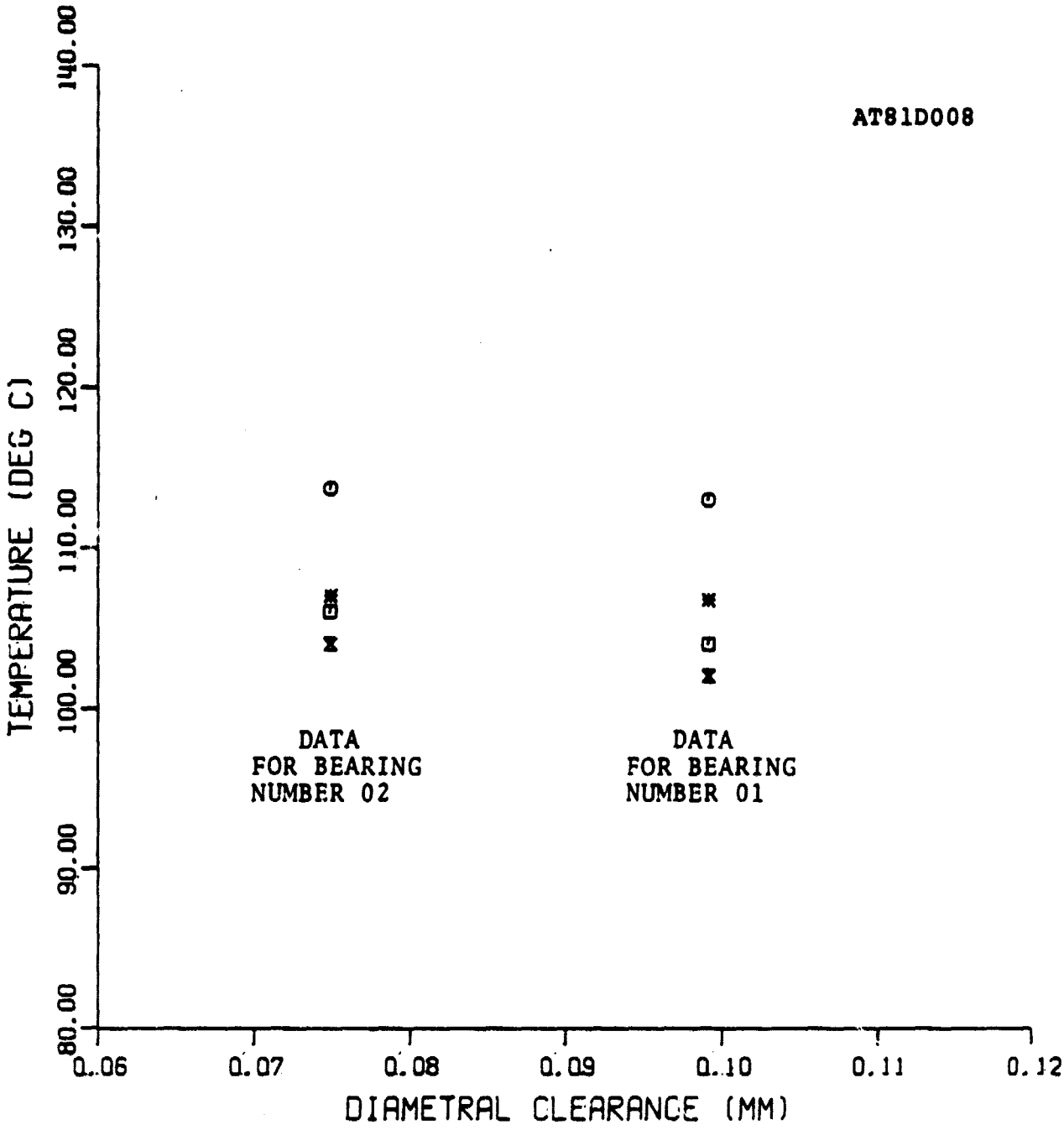

FIGURE 40:
COMPARISON OF OUTER RING TEMPERATURES AS A FUNCTION OF DIAMETRAL CLEARANCE UNDER PURE RADIAL LOAD AT 5000 RPM.

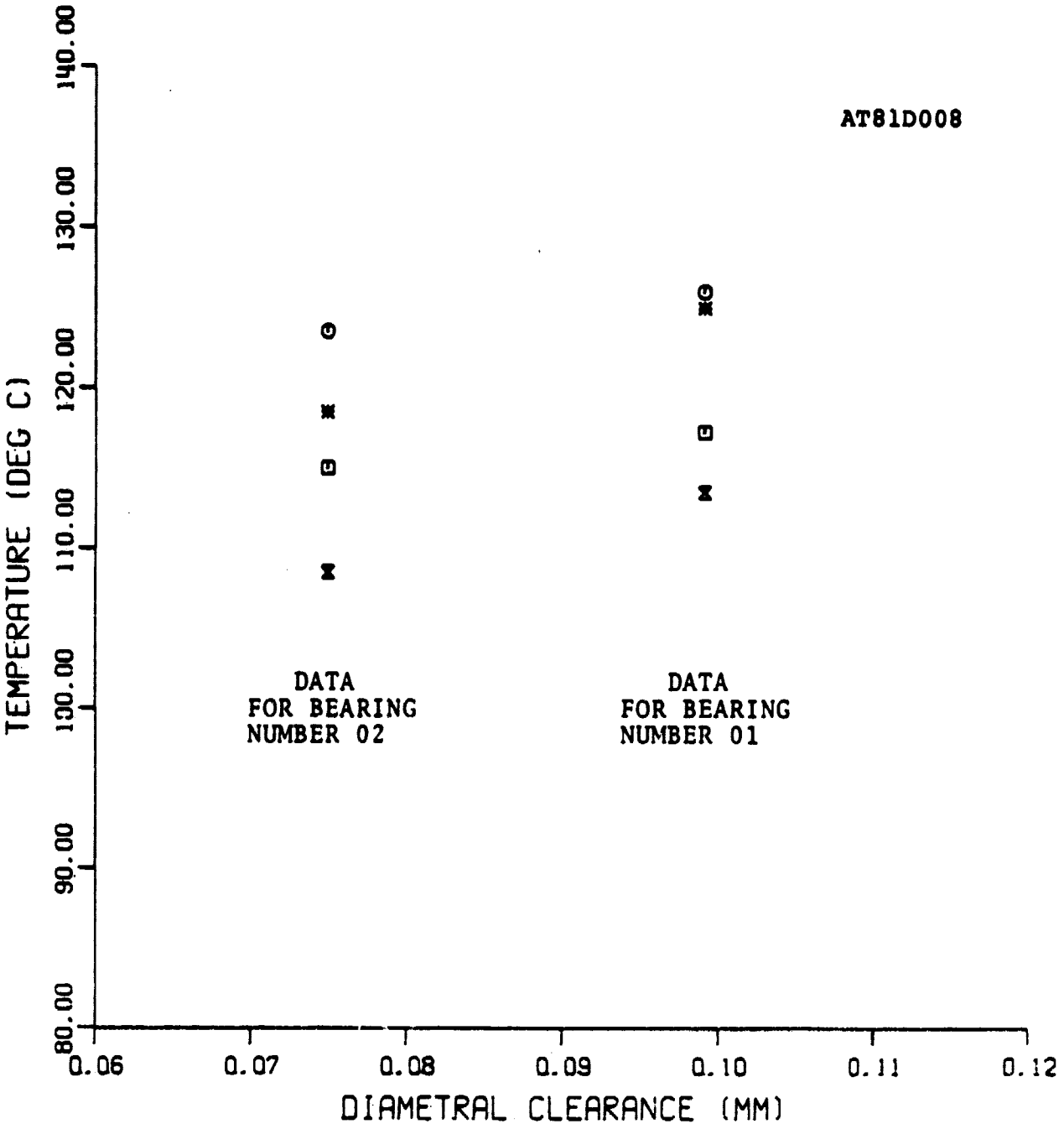

✱ - MEASURED ,AXIAL LOAD = 4448 N (1000 LB) AND RADIAL = 13345 N (3000 LB)
⊙ - PREDICTED,AXIAL LOAD = 4448 N (1000 LB) AND RADIAL = 13345 N (3000 LB)
⧗ - MEASURED ,AXIAL LOAD = 3114 N (700 LB) AND RADIAL = 6672 N (1500 LB)
⊡ - PREDICTED,AXIAL LOAD = 3114 N (700 LB) AND RADIAL = 6672 N (1500 LB)

FIGURE 41:
COMPARISON OF INNER RING TEMPERATURES AS A FUNCTION OF DIAMETRAL CLEARANCE UNDER COMBINED LOAD AT 5000 RPM.

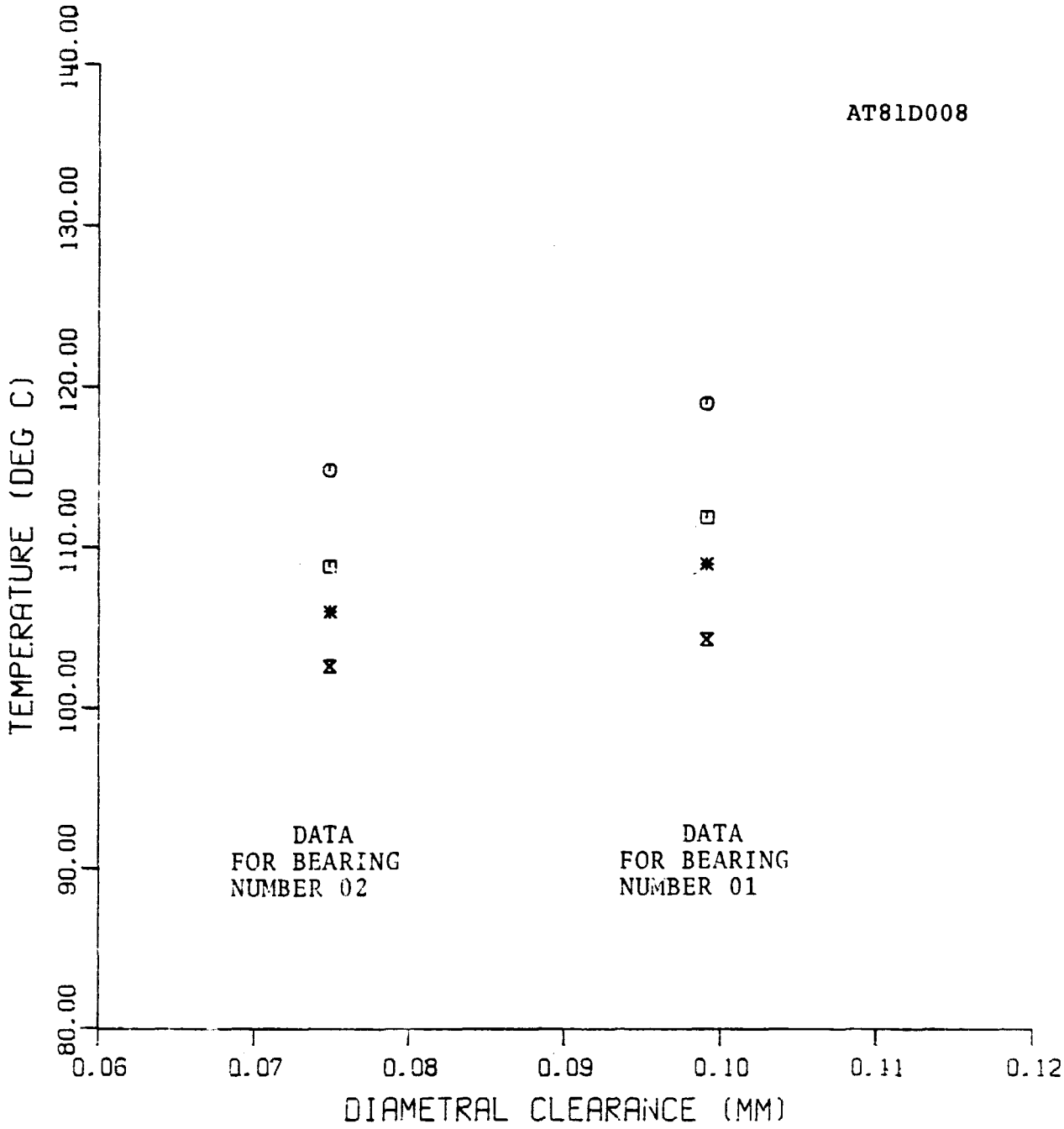

✱ - MEASURED ,AXIAL LOAD = 4448 N (1000 LB) AND RADIAL = 13345 N (3000 LB)
⊙ - PREDICTED,AXIAL LOAD = 4448 N (1000 LB) AND RADIAL = 13345 N (3000 LB)
⧗ - MEASURED ,AXIAL LOAD = 3114 N (700 LB) AND RADIAL = 6672 N (1500 LB)
⊡ - PREDICTED,AXIAL LOAD = 3114 N (700 LB) AND RADIAL = 6672 N (1500 LB)

FIGURE 42:
COMPARISON OF OUTER RING TEMPERATURES AS A FUNCTION OF DIAMETRAL CLEARANCE UNDER COMBINED LOAD AT 5000 RPM.

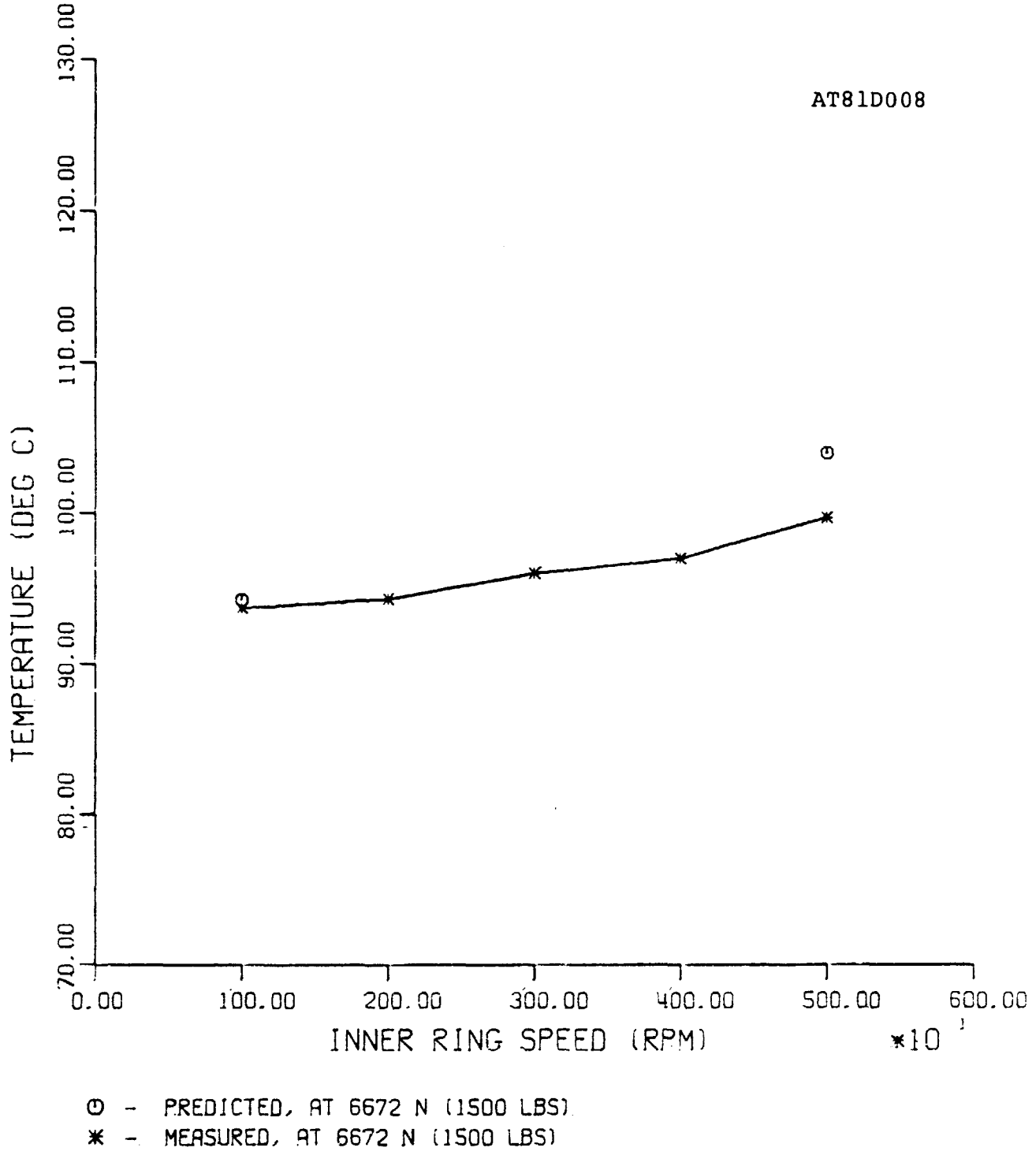

FIGURE 43:
COMPARISON OF PREDICTED AND MEASURED INNER RING TEMPERATURES UNDER PURE RADIAL LOAD (BRG. NO. 03).

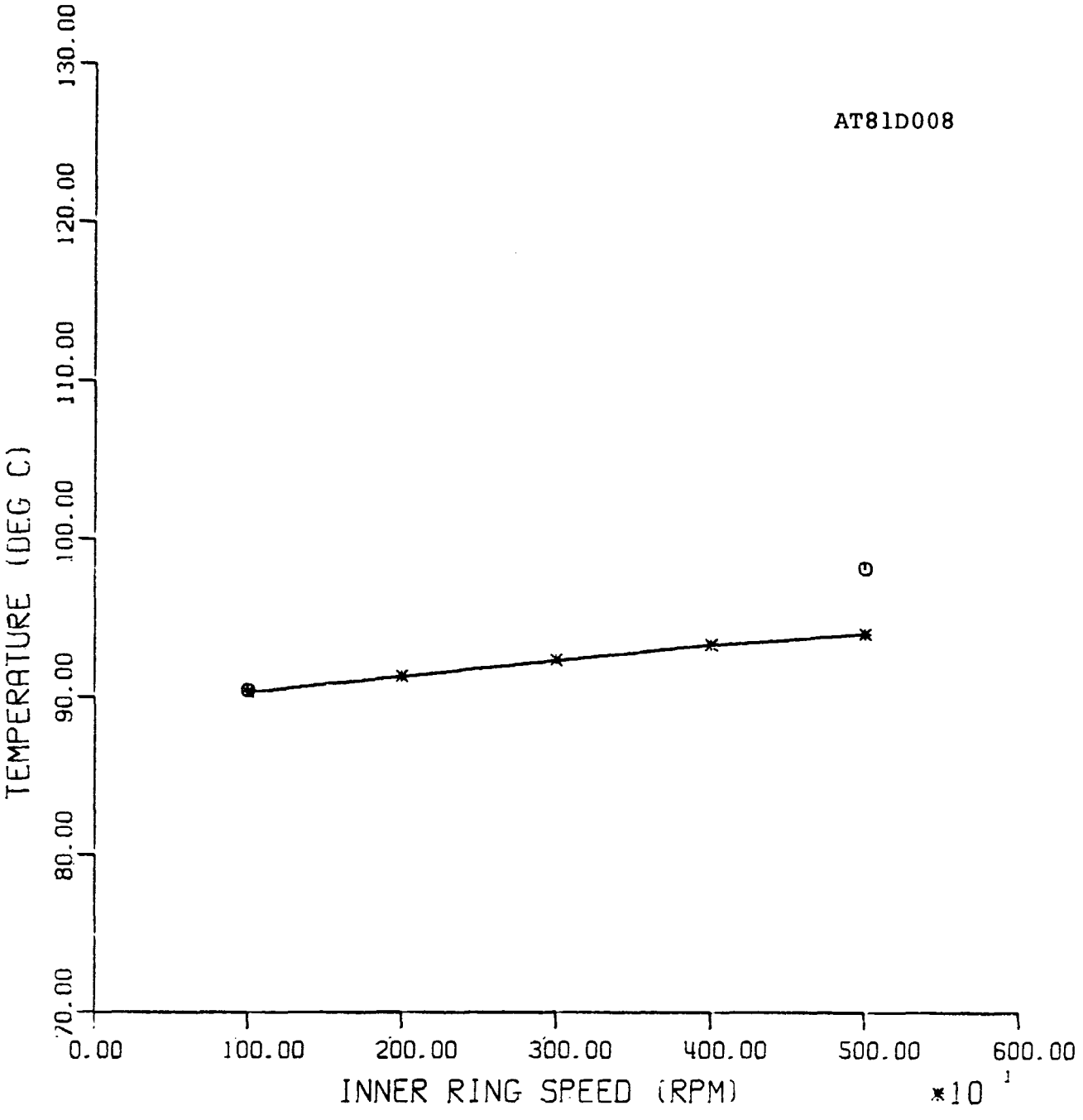

FIGURE 44:
COMPARISON OF PREDICTED AND MEASURED OUTER RING TEMPERATURES UNDER PURE RADIAL LOAD (BRG. NO. 03).

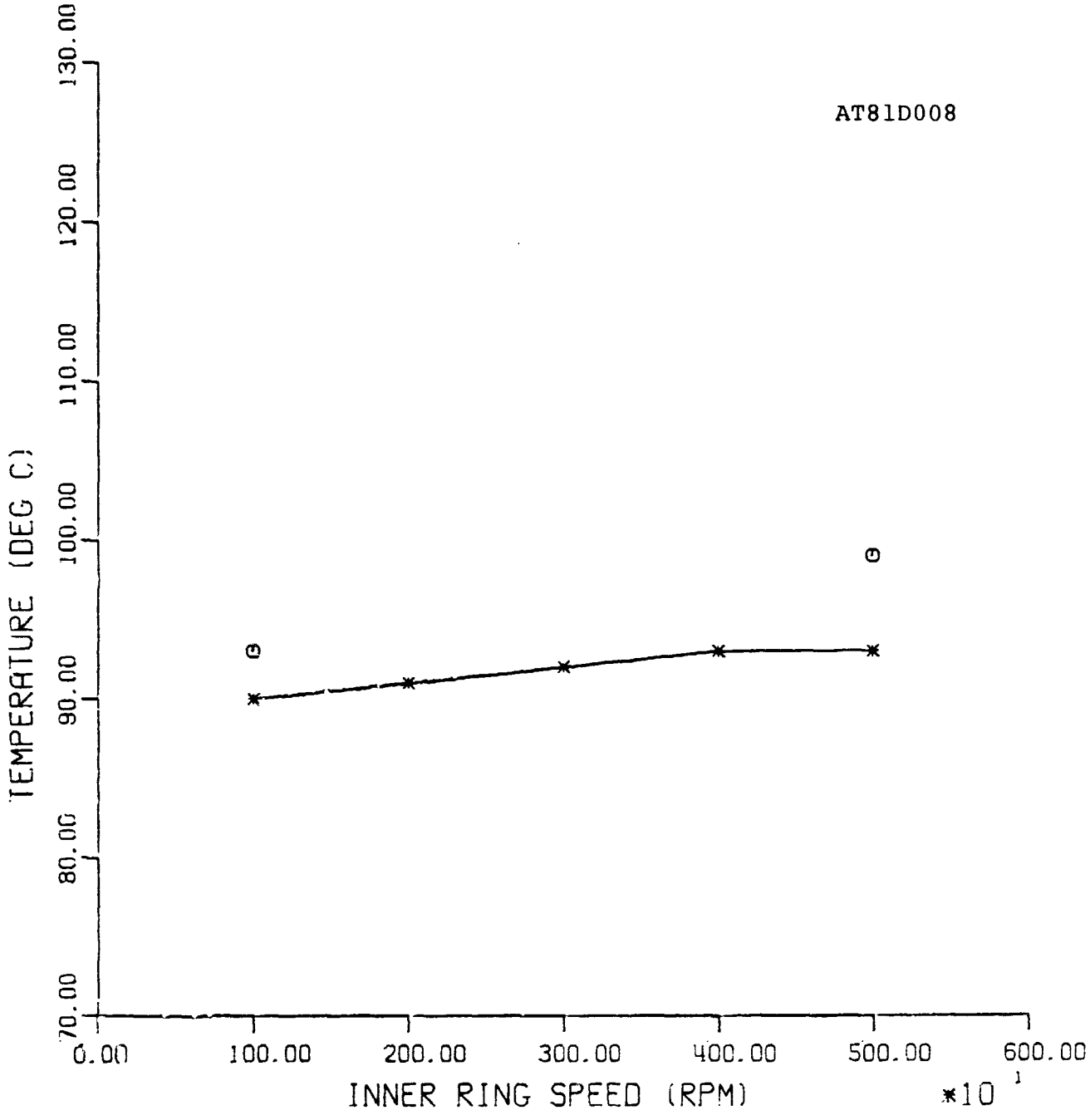

FIGURE 45:
COMPARISON OF PREDICTED AND MEASURED OUTLET LUBRICANT TEMPERATURES UNDER PURE RADIAL LOAD (BRG. NO. 03).

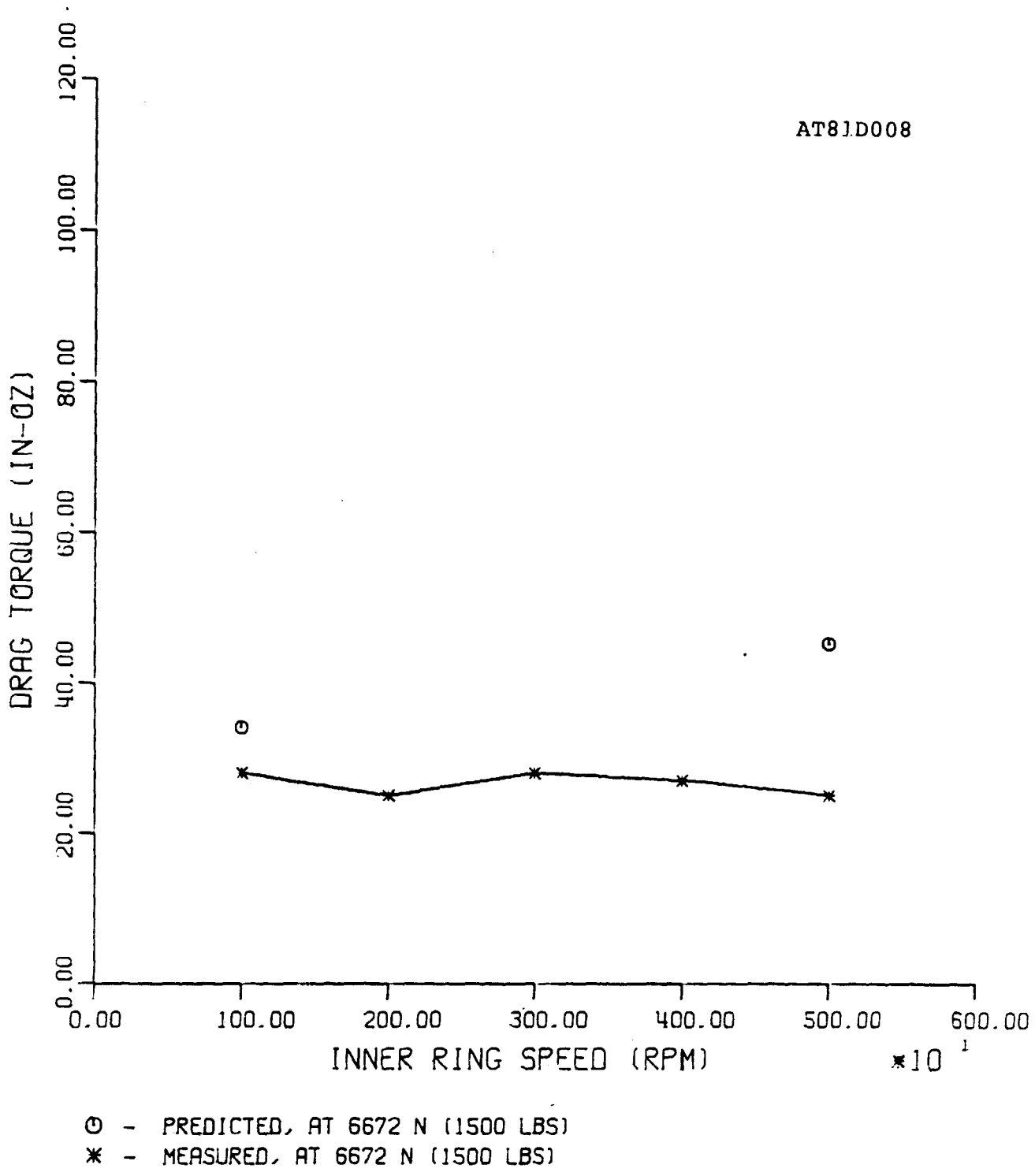

FIGURE 46:
COMPARISON OF PREDICTED AND MEASURED VALUES OF DRAG TORQUE UNDER PURE RADIAL LOAD (BRG. NO. 03).

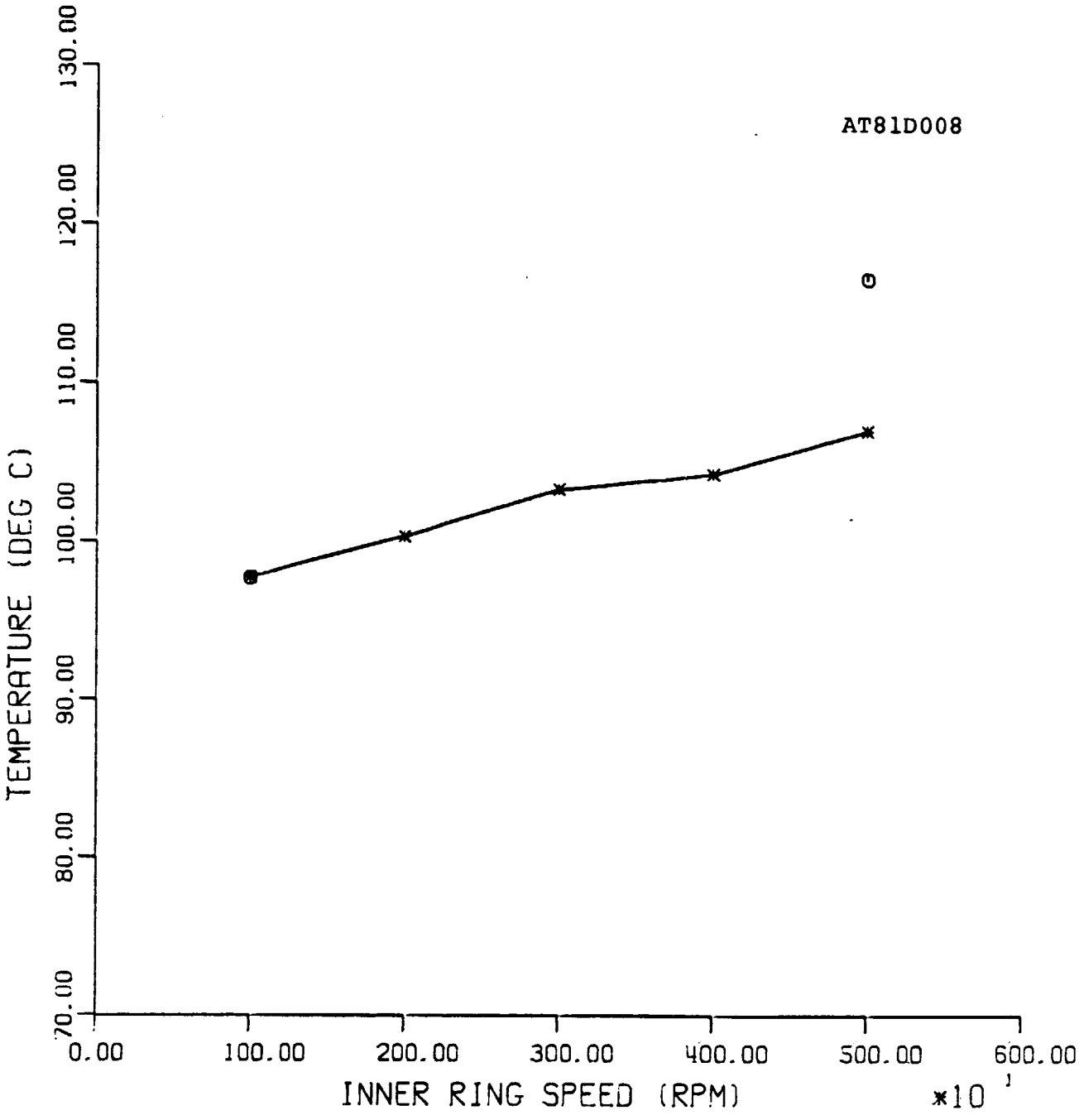

FIGURE 47:
COMPARISON OF PREDICTED AND MEASURED INNER RING TEMPERATURES UNDER PURE RADIAL LOAD (BRG. NO. 03).

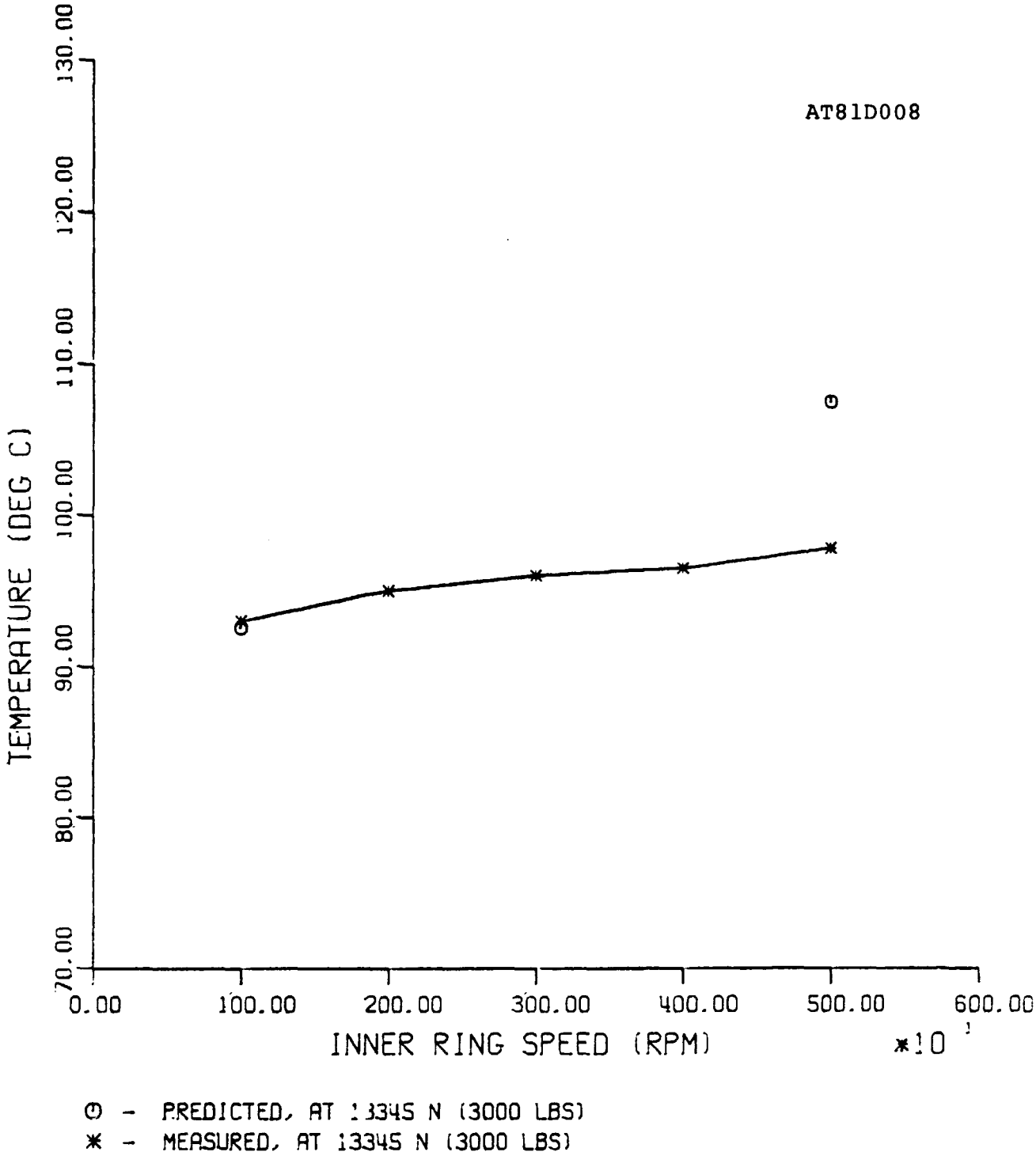

FIGURE 48:
COMPARISON OF PREDICTED AND MEASURED OUTER RING TEMPERATURES UNDER PURE RADIAL LOAD (BRG. NO. 03).

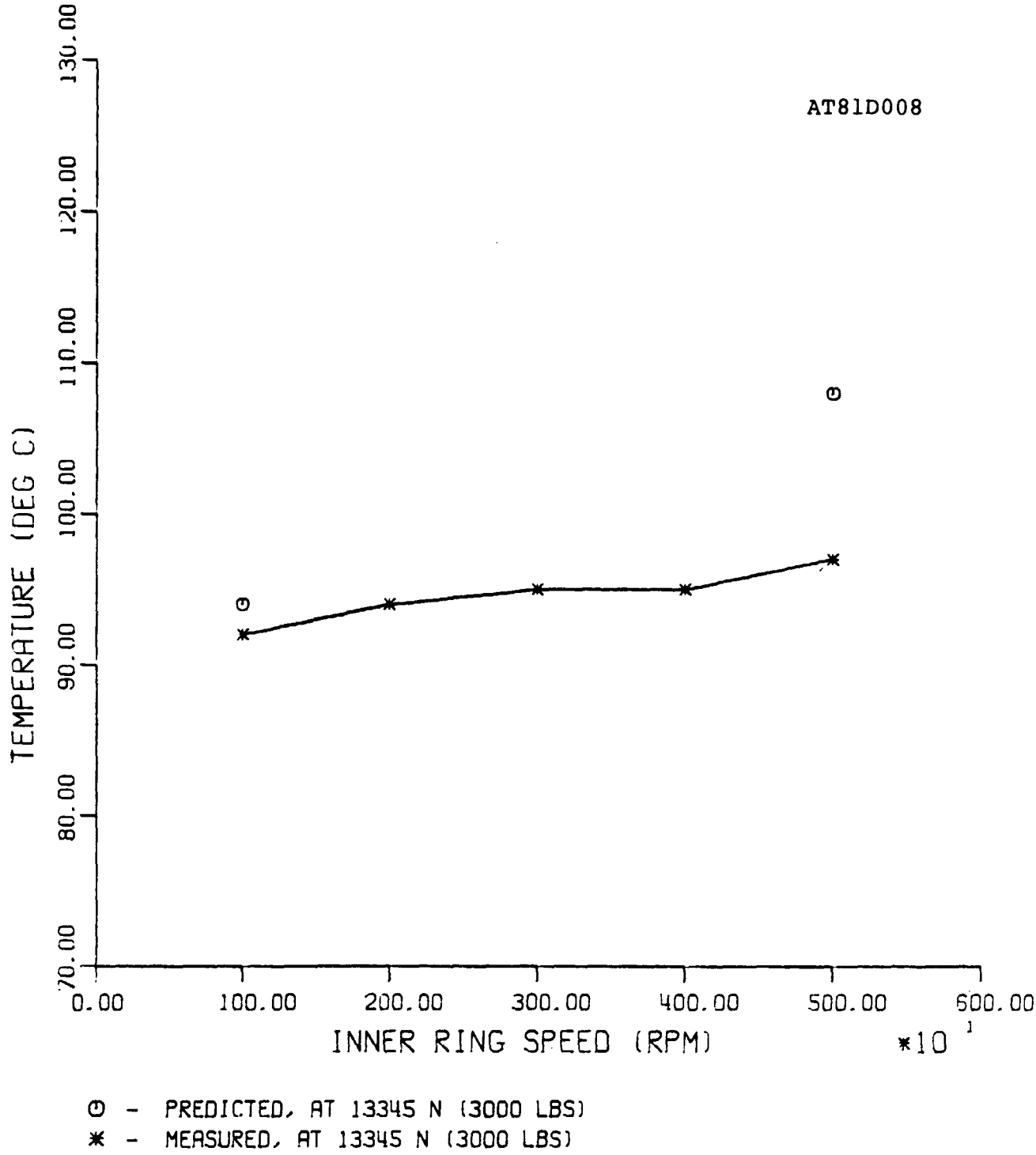

FIGURE 49:
COMPARISON OF PREDICTED AND MEASURED OUTLET LUBRICANT TEMPERATURES UNDER PURE RADIAL LOAD (BRG. NO. 03).

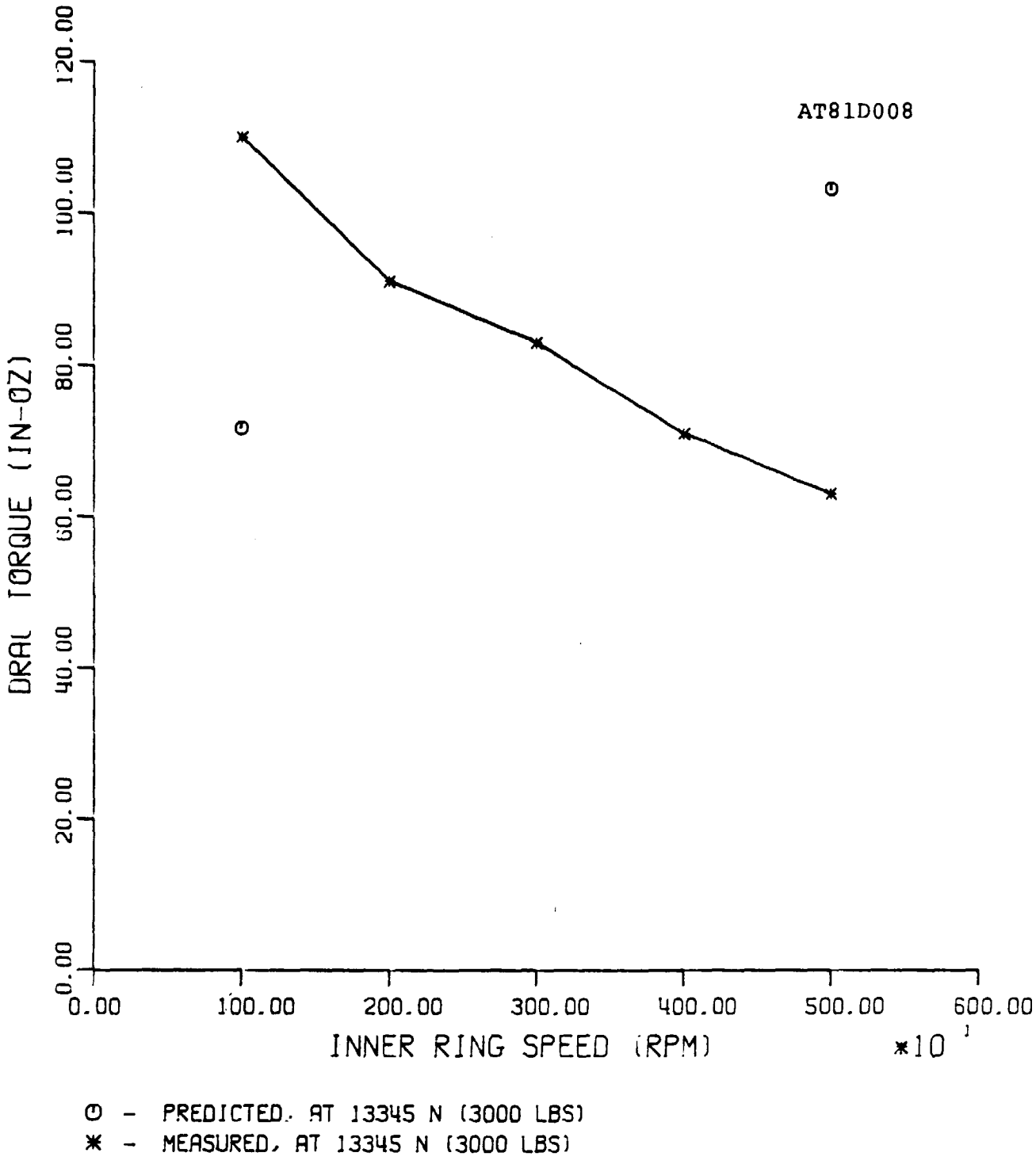

FIGURE 50:
COMPARISON OF PREDICTED AND MEASURED VALUES OF DRAG TORQUE UNDER PURE RADIAL LOAD (BRG. NO. 03).

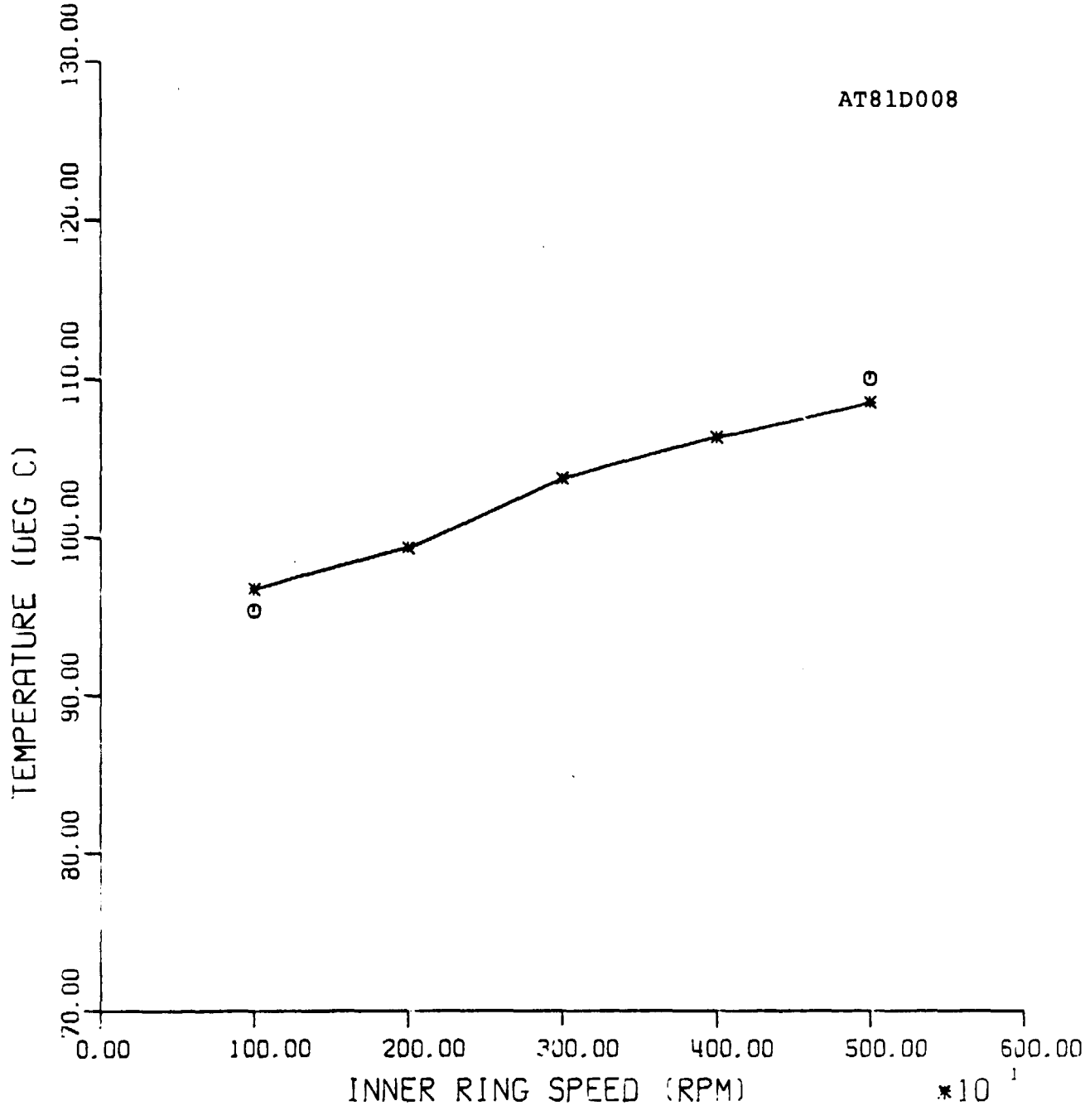

⊙ - PREDICTED,AXIAL LOAD = 3114 N (700 LB) AND RADIAL = 6672 N (1500 LB)
* - MEASURED ,AXIAL LOAD = 3114 N (700 LB) AND RADIAL = 6672 N (1500 LB)

FIGURE 51:
COMPARISON OF PREDICTED AND MEASURED INNER RING TEMPERATURES UNDER COMBINED LOAD (BRG. NO. 03).

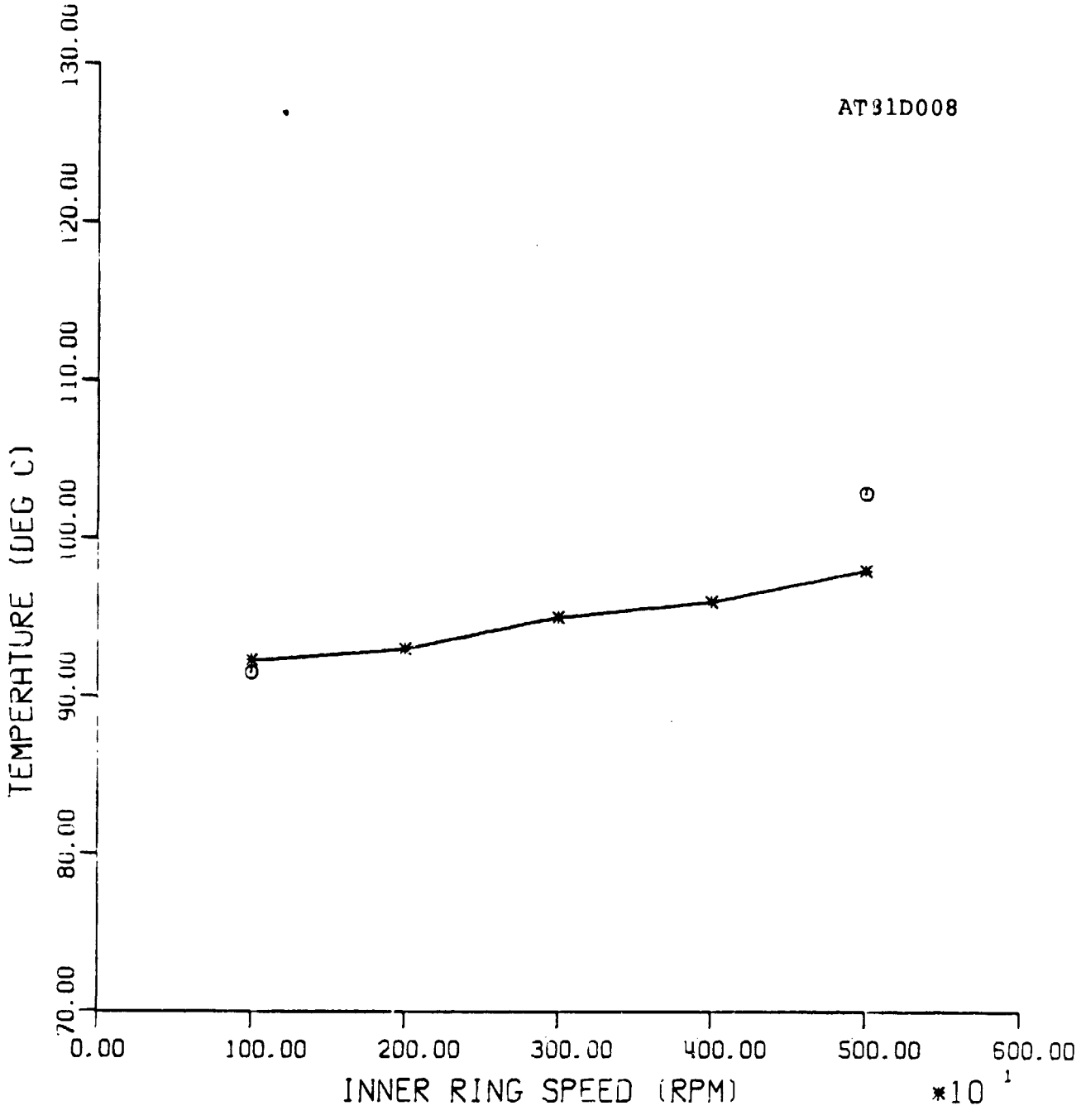

FIGURE 52:

COMPARISON OF PREDICTED AND MEASURED OUTER RING TEMPERATURES UNDER COMBINED LOAD (BRG. NO. 03).

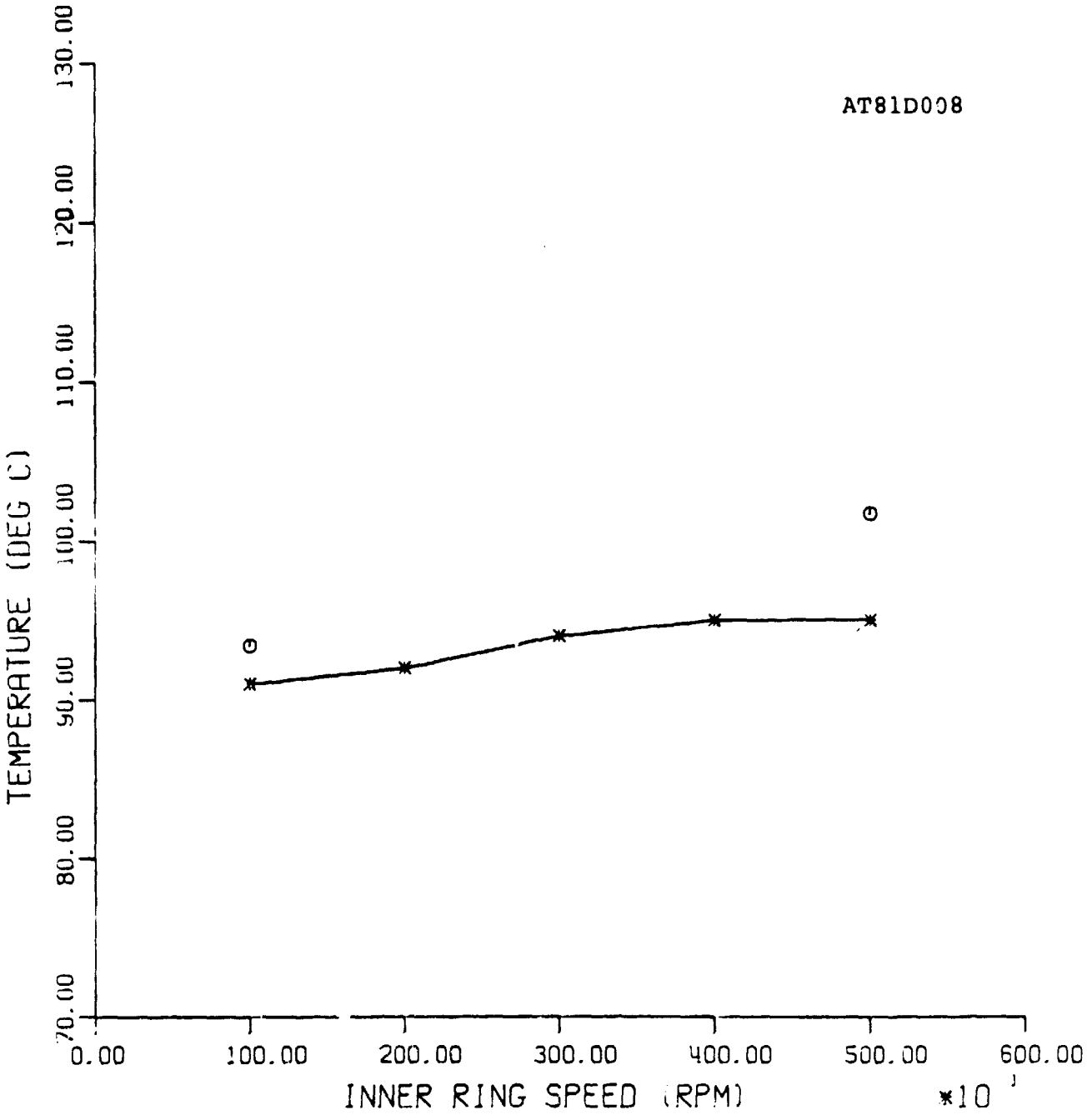

FIGURE 53:
COMPARISON OF PREDICTED AND MEASURED OUTLET LUBRICANT TEMPERATURES UNDER COMBINED LOAD (BRG. NO. 03).

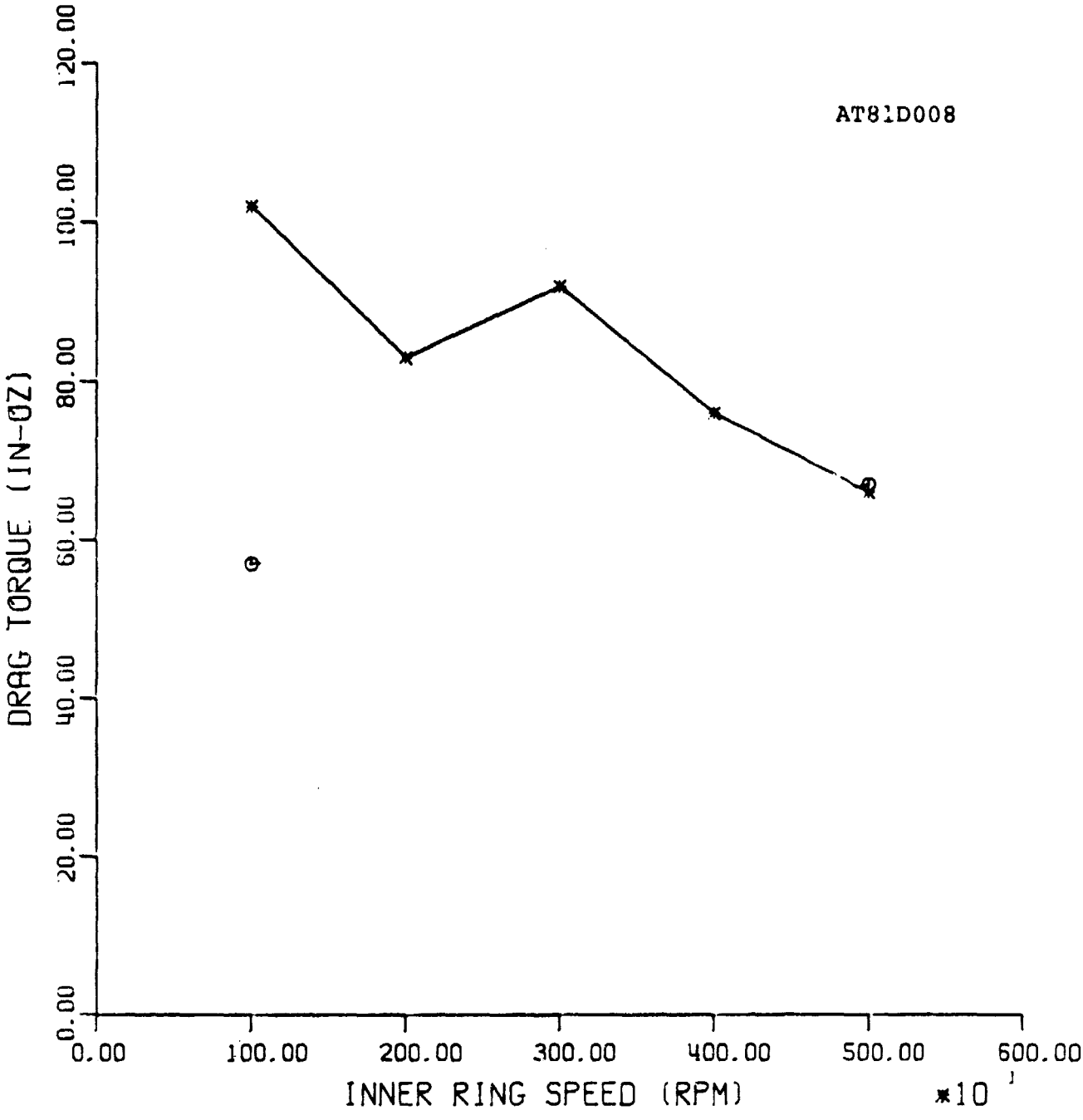

FIGURE 54:
COMPARISON OF PREDICTED AND MEASURED VALUES OF DRAG TORQUE UNDER COMBINED LOAD (BRG. NO. 03).

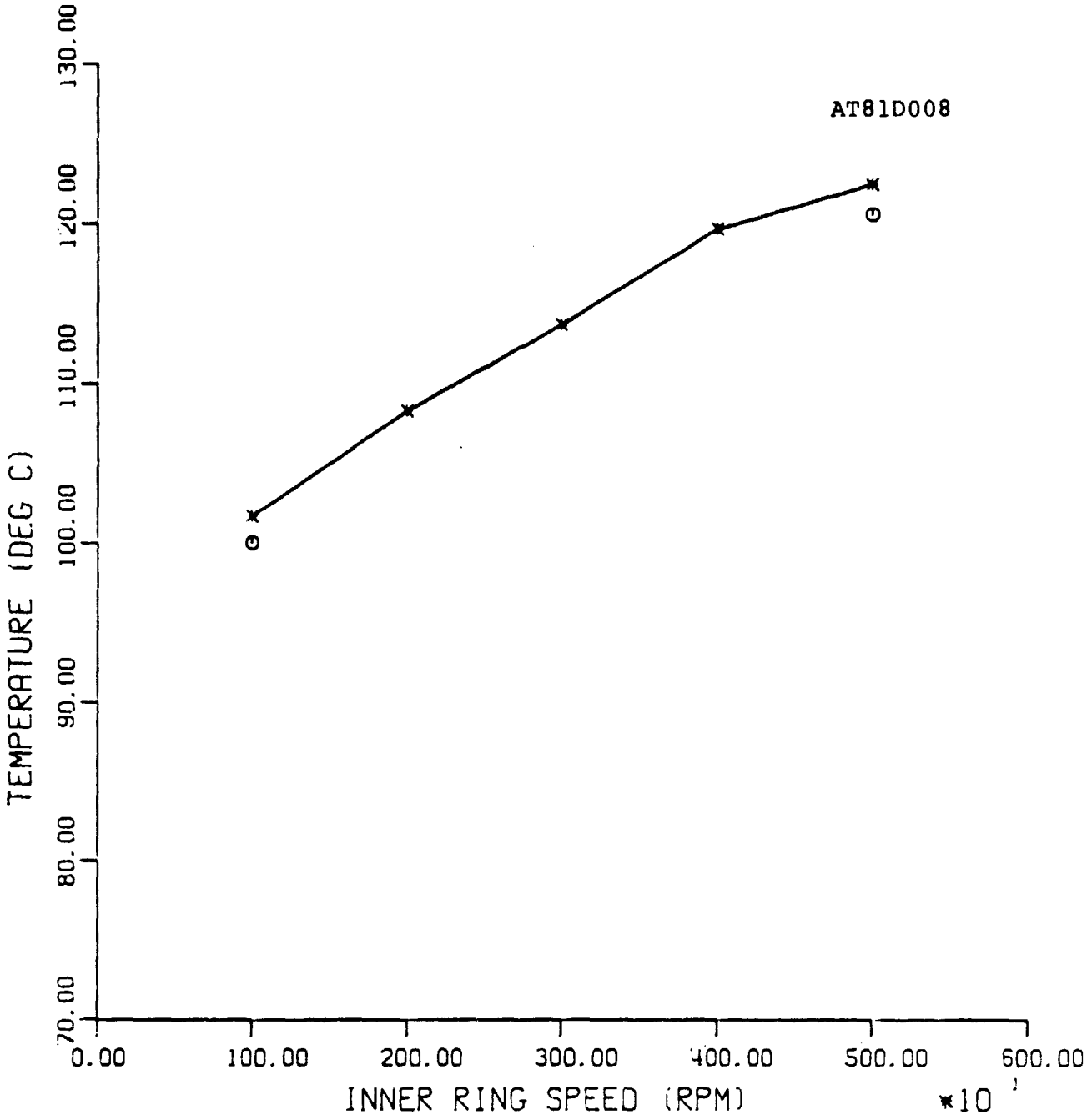

FIGURE 55:
COMPARISON OF PREDICTED AND MEASURED INNER RING TEMPERATURES UNDER COMBINED LOAD (BRG. NO. 03).

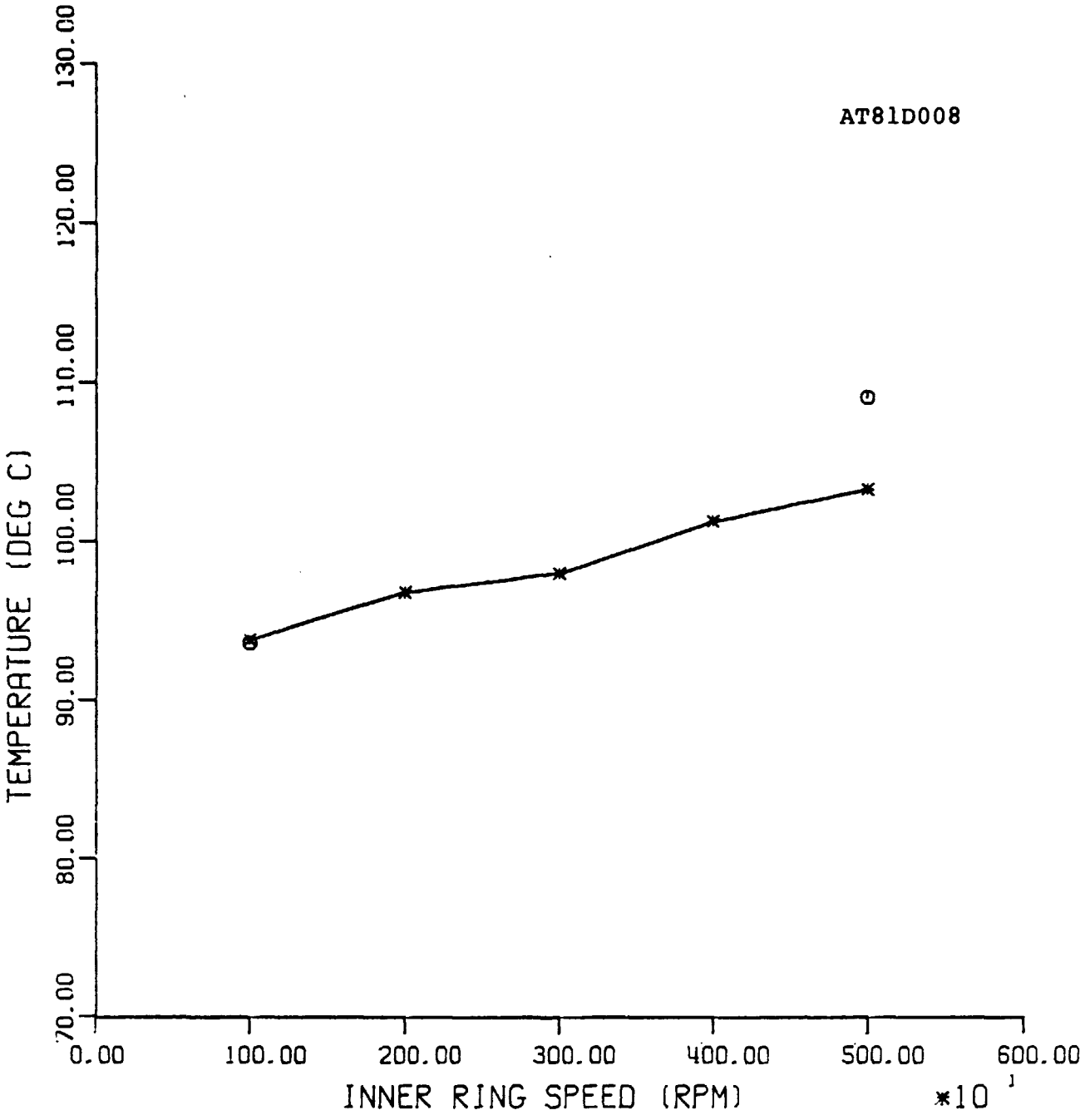

FIGURE 56:
COMPARISON OF PREDICTED AND MEASURED OUTER RING TEMPERATURES UNDER COMBINED LOAD (BRG. NO. 03).

C-2

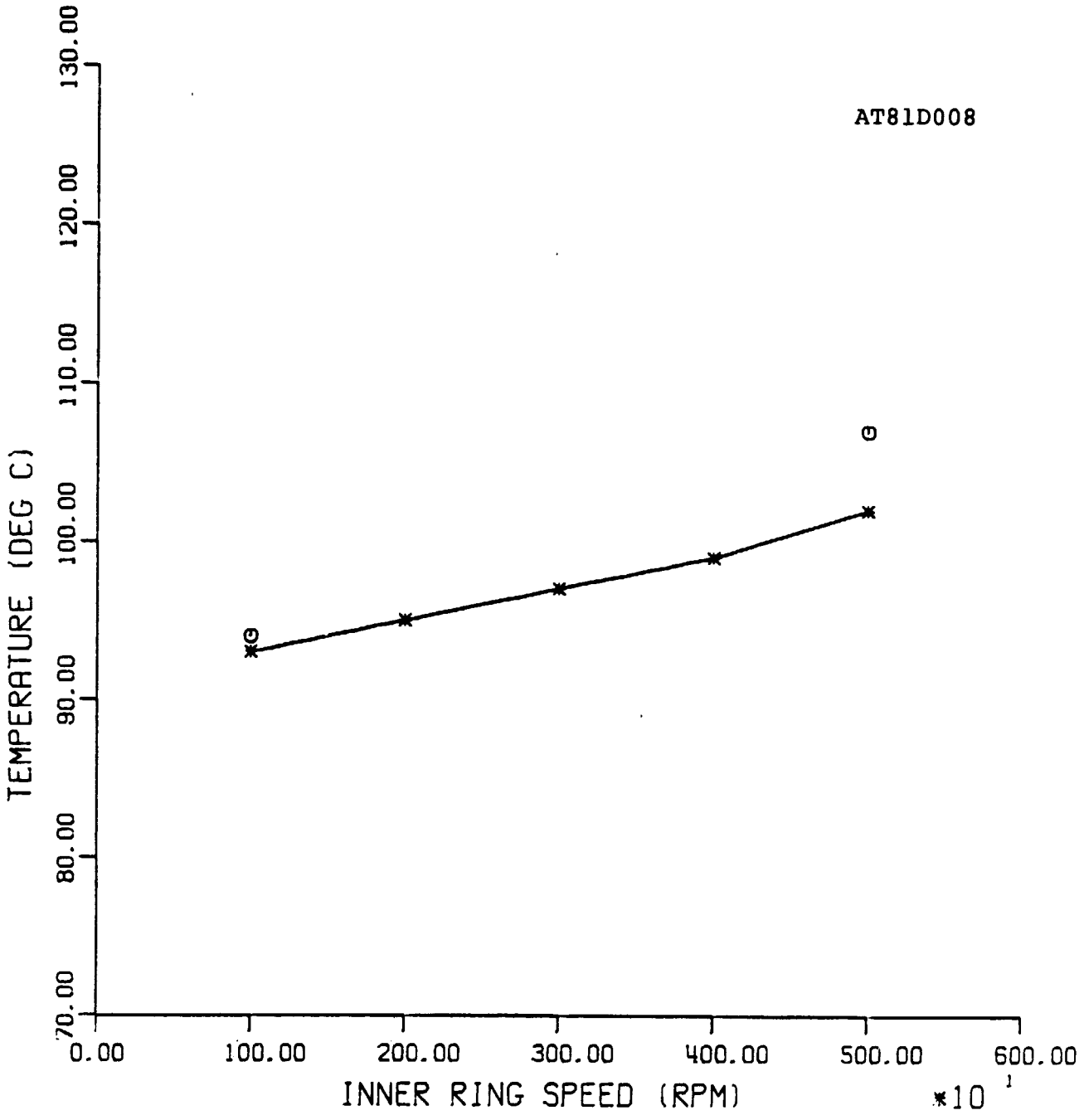

FIGURE 57:
COMPARISON OF PREDICTED AND MEASURED OUTLET LUBRICANT TEMPERATURES UNDER COMBINED LOAD (BRG. NO. 03).

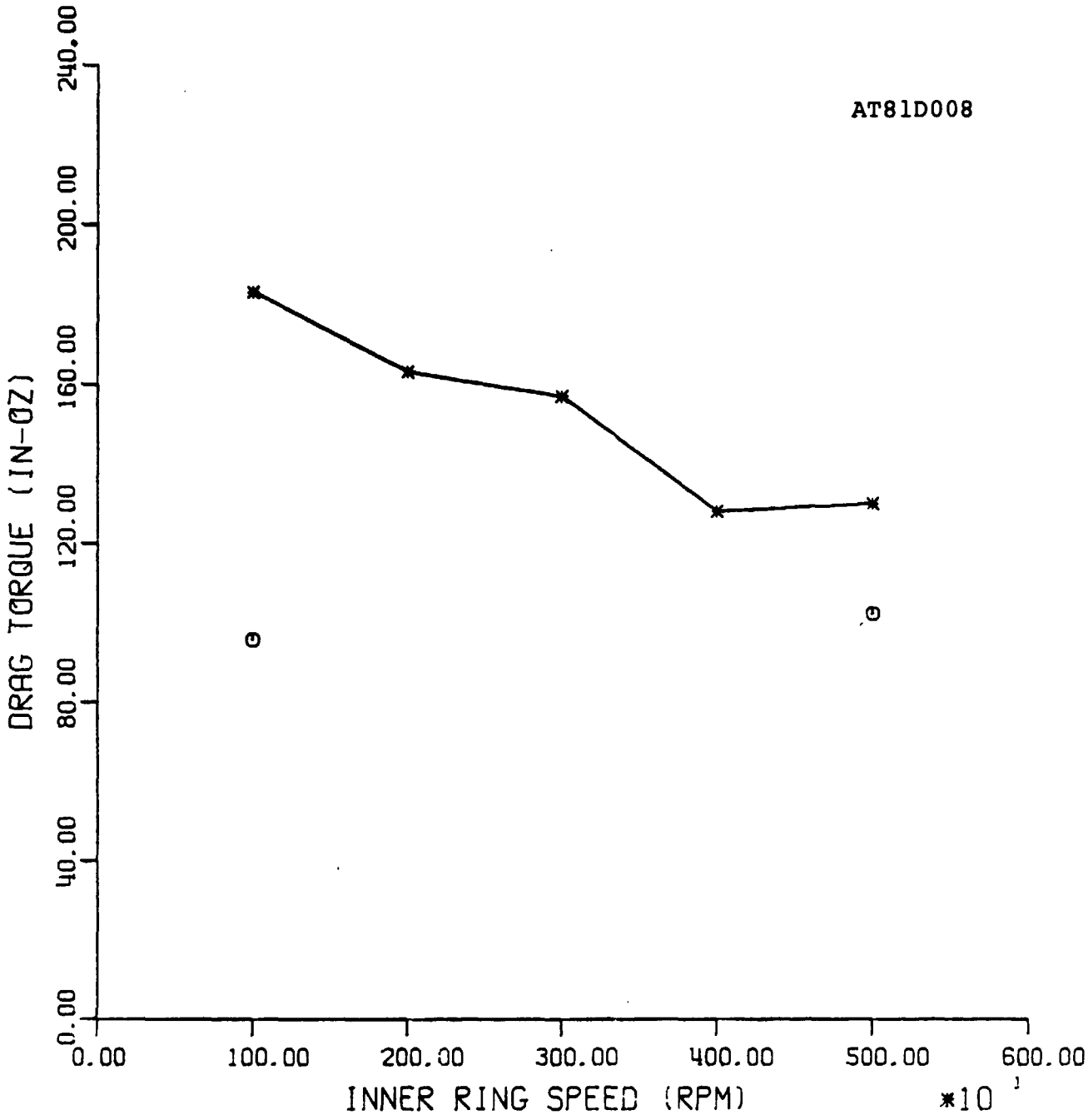

⊙ - PREDICTED,AXIAL LOAD = 4448 N (1000 LB) AND RADIAL = 13345 N (3000 LB)
✱ - MEASURED ,AXIAL LOAD = 4448 N (1000 LB) AND RADIAL = 13345 N (3000 LB)

FIGURE 58:
COMPARISON OF PREDICTED AND MEASURED VALUES OF DRAG TORQUE UNDER COMBINED LOAD (BRG. NO. 03).

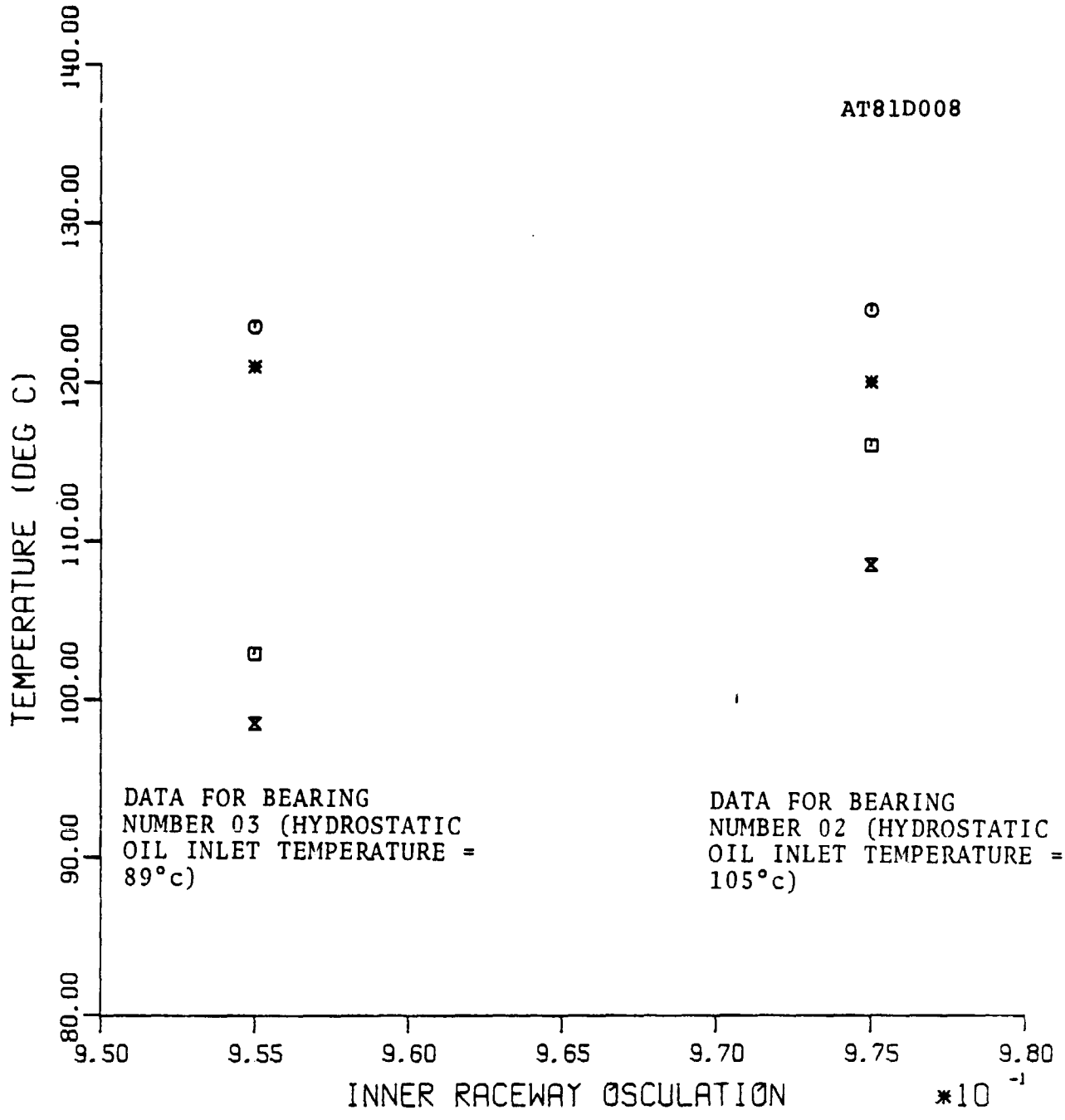

FIGURE 59:
COMPARISON OF INNER RING TEMPERATURES OF BEARING NUMBERS 02 AND 03 UNDER COMBINED LOAD AT 5000 RPM.

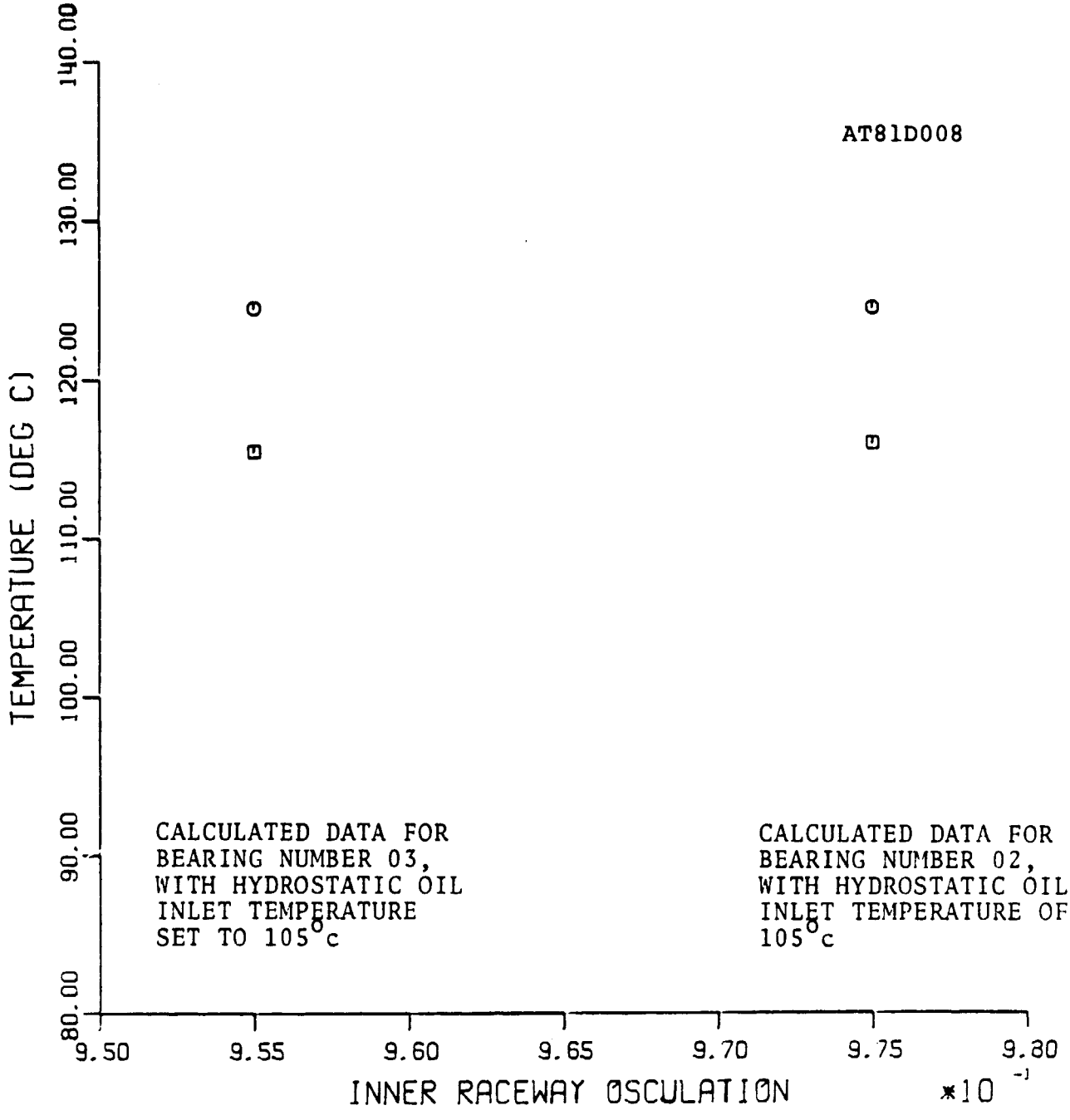

FIGURE 60:
COMPARISON OF CALCULATED INNER RING TEMPERATURES OF BEARING NOS. 02 AND 03 UNDER COMBINED LOAD AT 5000 RPM.

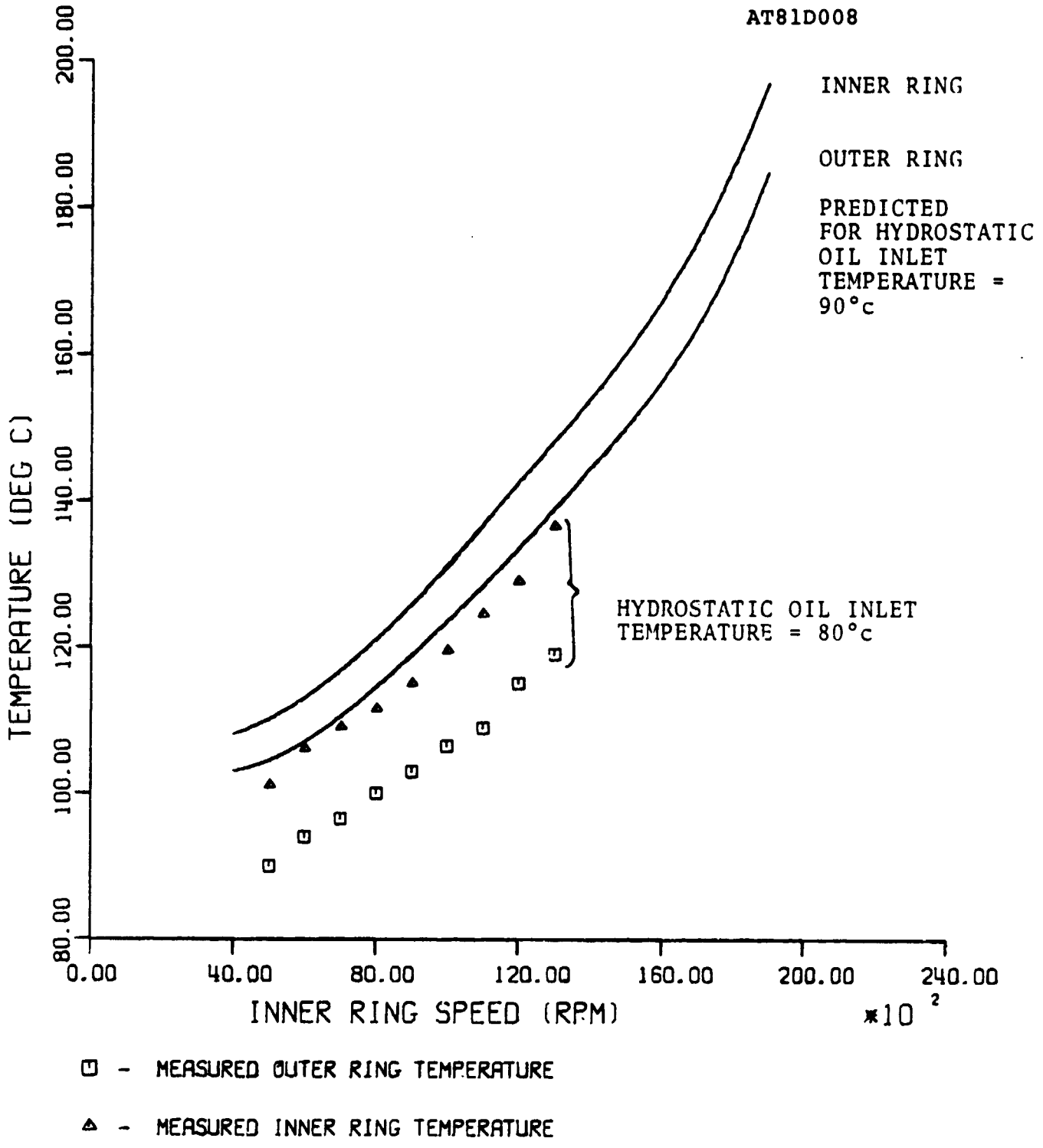

FIGURE 61:
RING TEMPERATURE AS A FUNCTION OF SPEED FOR BEARING NUMBER 06 UNDER PURE AXIAL LOAD OF 4448 N (1000 LB).

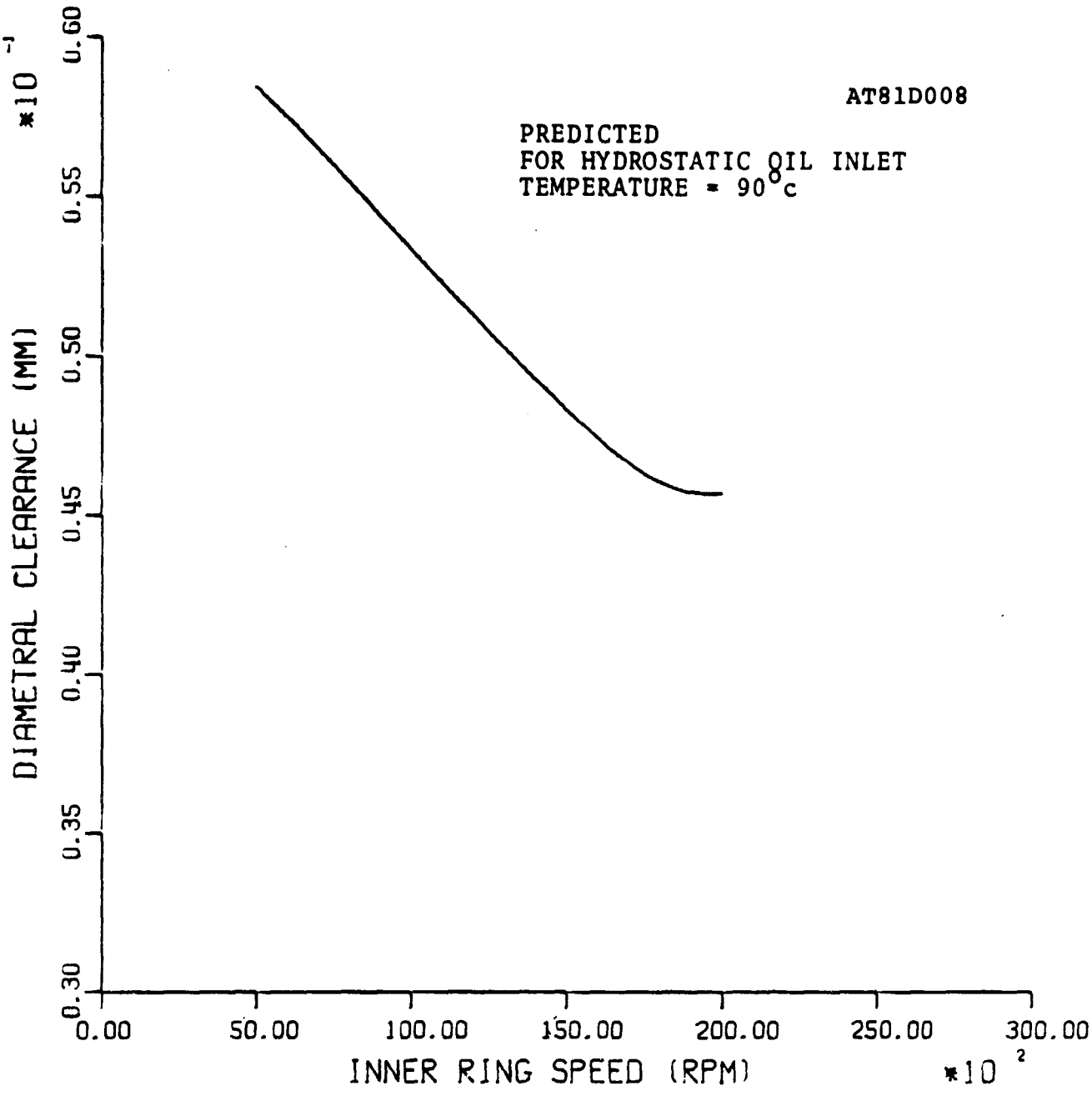

FIGURE 62:
DIAMETRAL CLEARANCE AS A FUNCTION OF SPEED FOR BEARING NUMBER 06, AXIAL LOAD OF 4448 N (1000 LB).

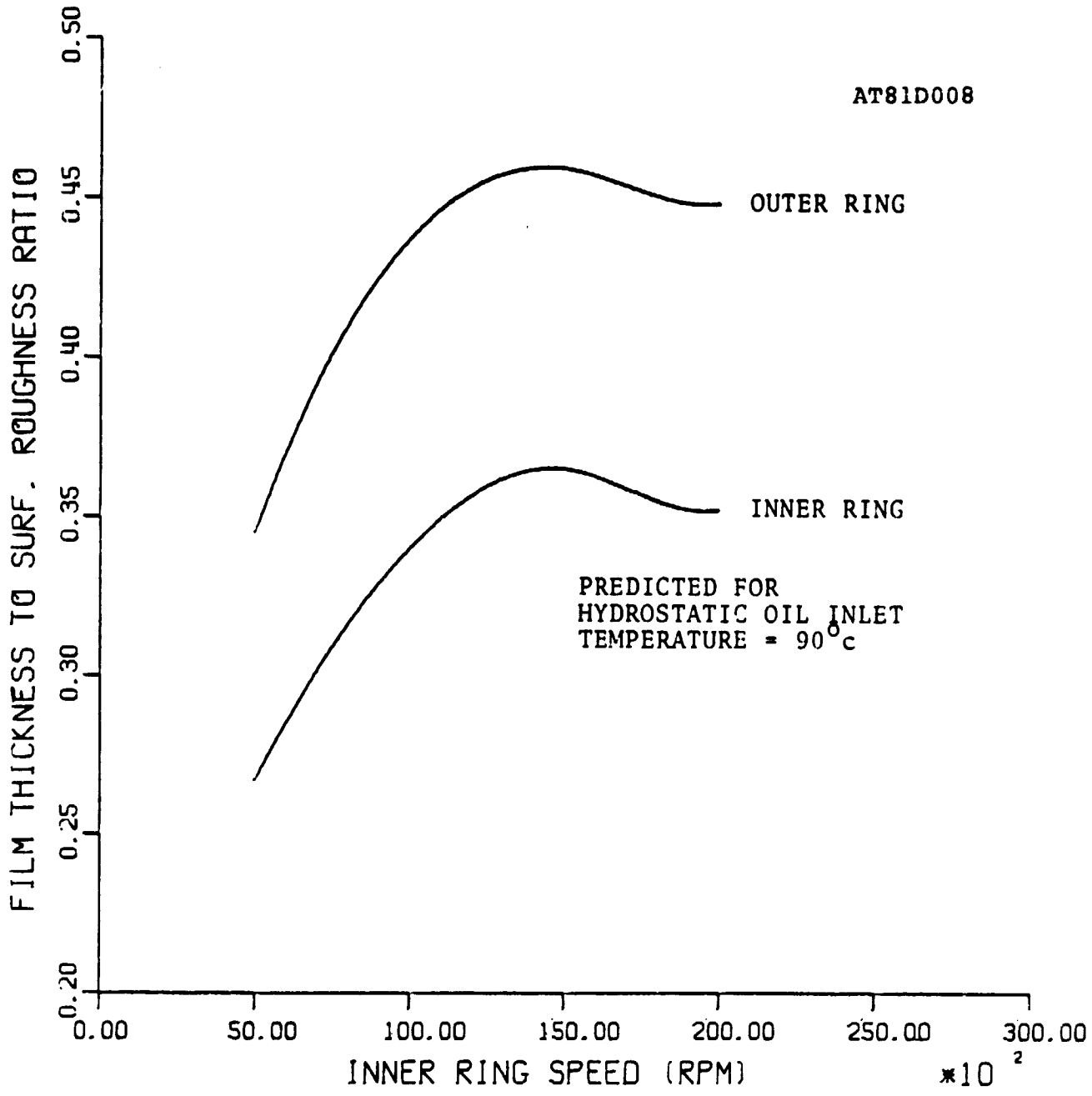

FIGURE 63:

FILM THICKNESS TO SURFACE ROUGHNESS RATIO AS A FUNCTION OF SPEED FOR BEARING NUMBER 06, AXIAL LOAD OF 4448 N.

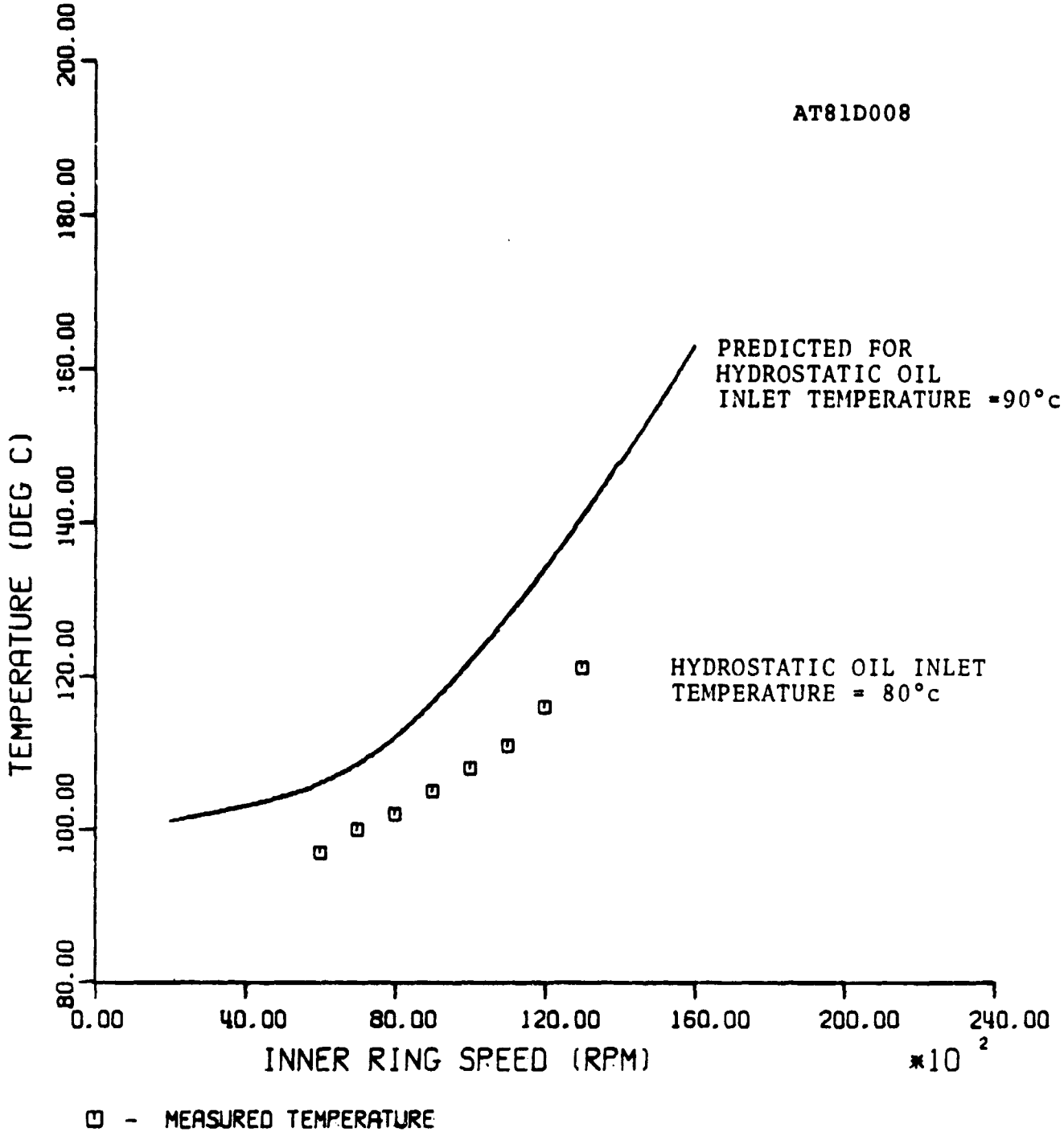

FIGURE 64:

OUTLET LUBRICANT TEMPERATURE AS A FUNCTION OF SPEED FOR BEARING NO. 06 UNDER AXIAL LOAD OF 4448 N (1000 LB).

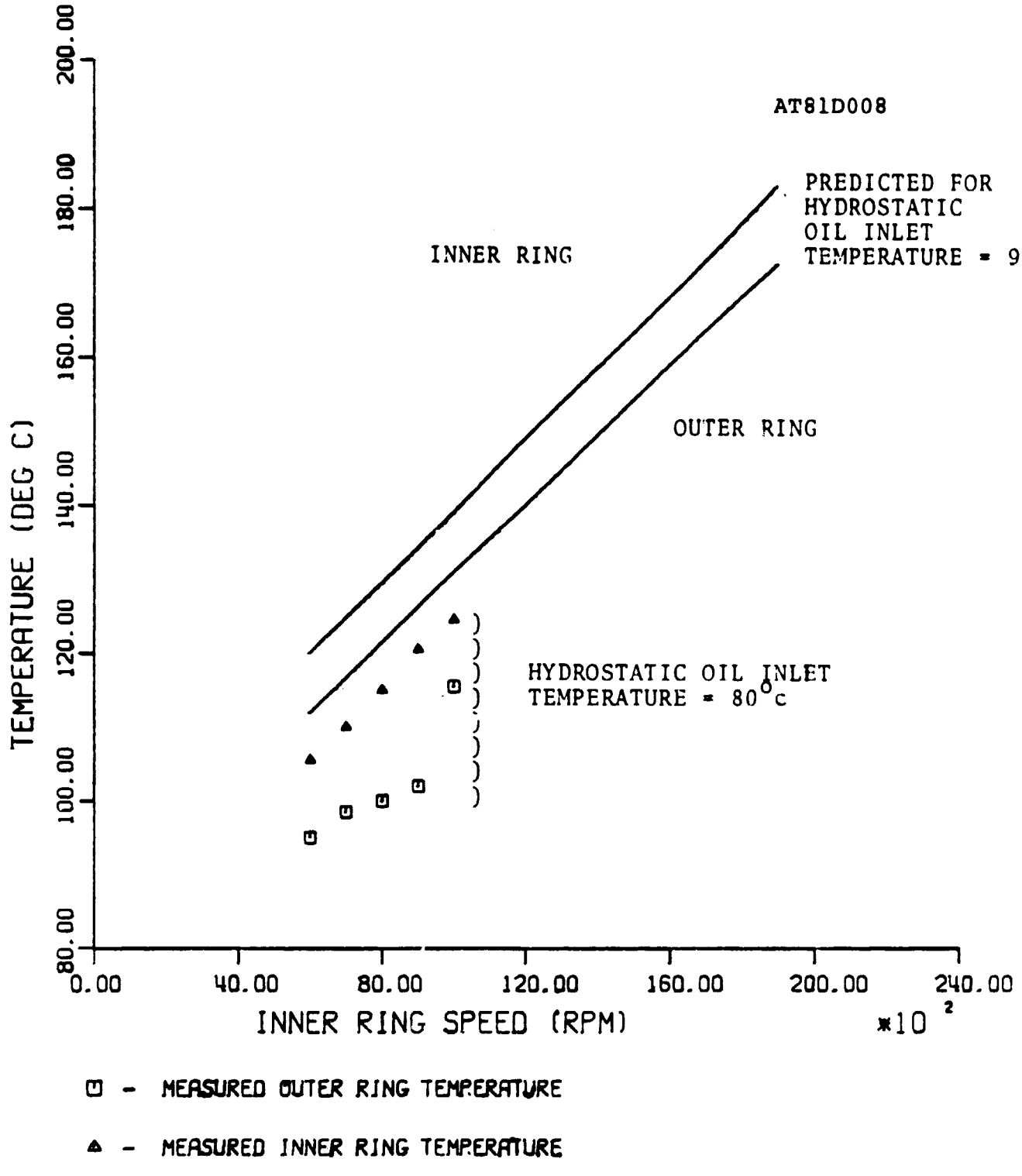

FIGURE 65:
INNER AND OUTER RING TEMPERATURES OF BEARING NO. 6 AS A FUNCTION OF SPEED UNDER 13345 N (3000 LB) RADIAL LOAD.

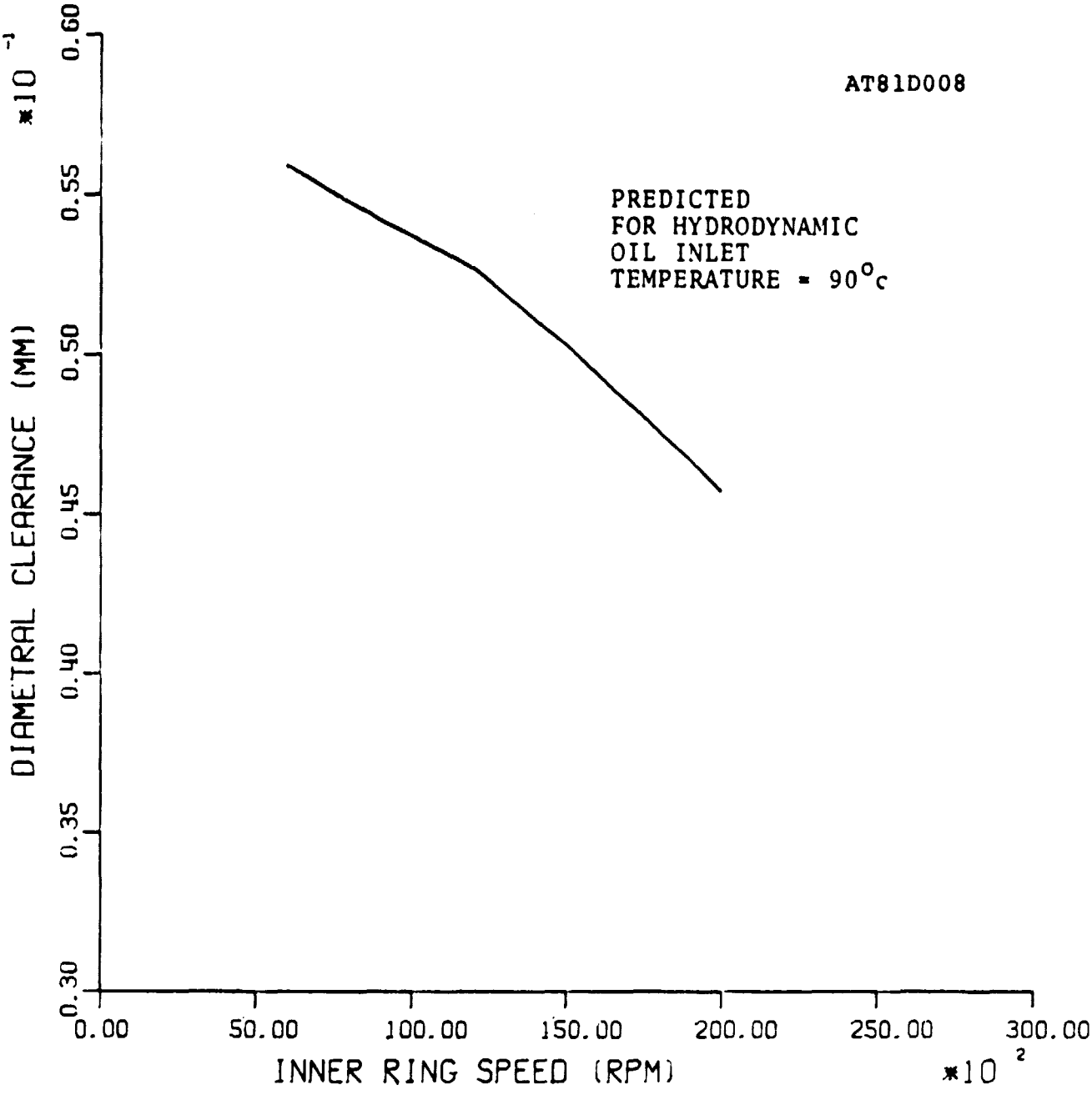

FIGURE 66:

DIAMETRAL CLEARANCE AS A FUNCTION OF SPEED FOR BEARING NUMBER 06 UNDER 13345 N (3000 LB) RADIAL LOAD.

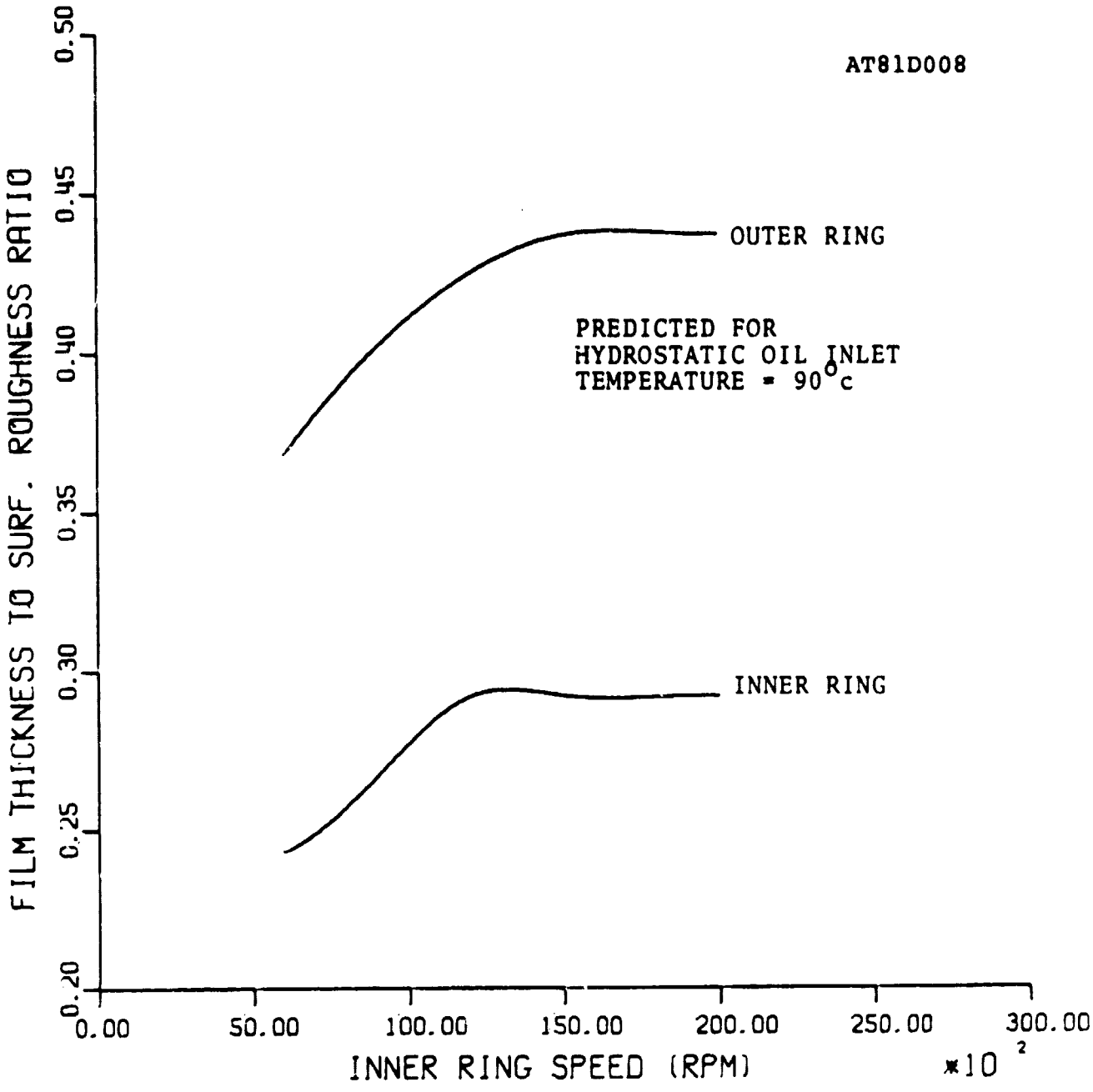

FIGURE 67:

FILM THICKNESS TO SURFACE ROUGHNESS RATIO, BEARING NUMBER 06, RADIAL LOAD OF 13345 N (3000 LB).

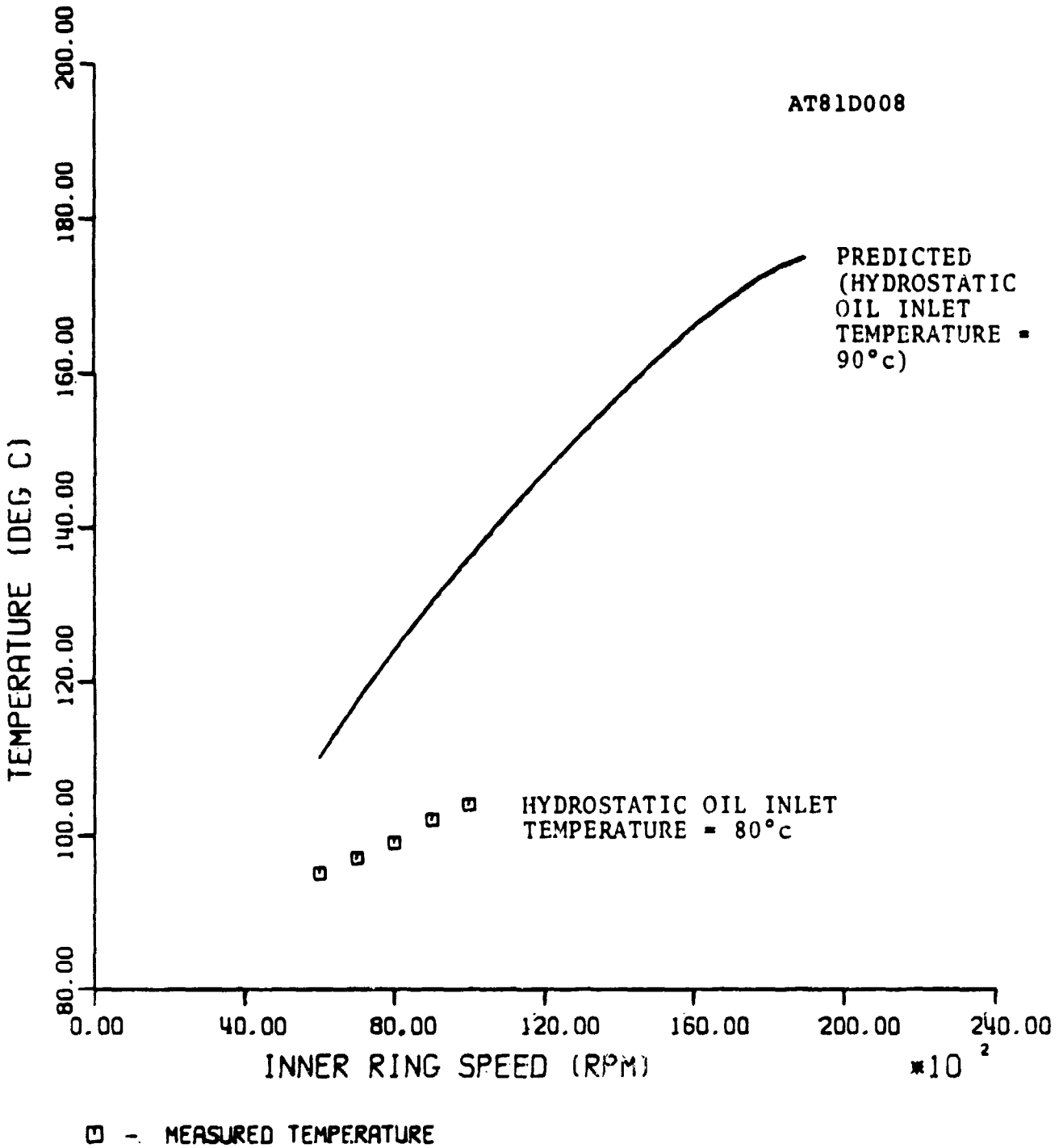

FIGURE 68:

OUTLET LUBRICANT TEMPERATURE AS A FUNCTION OF SPEED FOR BEARING NO. 06 UNDER RADIAL LOAD OF 13345 N(3000 LB).

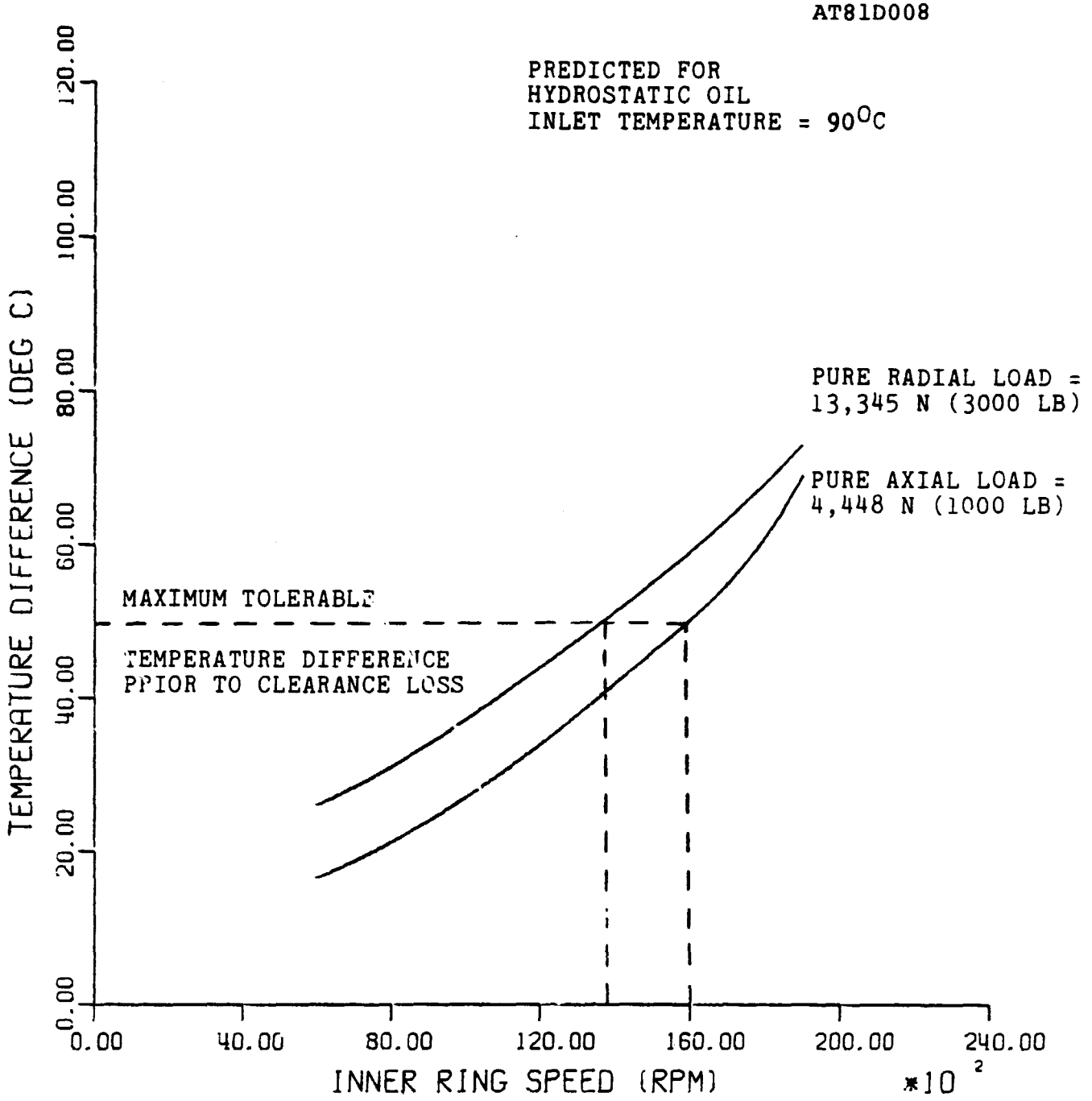

FIGURE 69:
CALCULATED TEMPERATURE DIFFERENCE BETWEEN INNER AND OUTER RINGS OF RADIAL HYDROSTATIC BRG. AS A FUNCTION OF SPEED.

APPENDIX A:

FULL SCALE BEARING TESTS

Contributor:

J.W. Rosenlieb

1.0 INTRODUCTION

Spherical roller bearings generally have an outer raceway which is ground to the shape of a spherical segment. Each roller has a curved generatrix in the direction transverse to rotation, which conforms closely to the inner and outer raceways (high osculation values). This results in a high load-carrying capacity. Because of the high osculation between the rollers and raceways, spherical roller bearings have inherently greater friction than cylindrical roller bearings. This is due to the degree of sliding which occurs in the roller-raceway contacts. They are, therefore, not generally considered suited for high speed operation. The bearings can carry a pure radial, pure thrust, or a combined radial and thrust load; they cannot support moment loading.

1.1 Test Objectives

The testing performed on this program had three goals:

1) Evaluation, at normal operating speeds, of the performance characteristics of three spherical roller bearings which incorporate minor differences in internal geometry. This information is needed to provide test data to compare with a computerized analytical model output developed on this program, and thus establish credibility for the model.

2) Establish an upper speed limit of the spherical test bearing under the imposed conditions.

3) Conduct high speed functional tests under various load conditions to establish performance characteristics.

2.0 MATERIALS TESTED

2.1 Spherical Test Bearing

The test bearing selected for this program is a double row, 40mm bore spherical with 12 symmetrical rollers per row. Figure A1 shows a photograph of an assembled and disassembled bearing. The 52100 steel rings and rollers are assembled with a roller riding, one piece, machined brass cage. A circumferential groove and three equally spaced radial holes are machined in the outer ring for lubricant access. The basic load rating (C) is 20,800 lbs, and the static load rating (C_o) is 15,300 lbs. The catalog listed speed limit is 4500 rpm when moderate loads are applied and oil bath lubrication is used.

Five different bearings of the same basic design were used during this program. Table A1 lists the bearing number, osculation, and radial looseness used in each test with a basic description of the test.

The following measurements were made on each bearing. A record of the values obtained are presented in Appendix B.

1) Radial looseness
2) Radius of inner ring roller paths
3) Radius of outer ring roller path
4) Surface roughness of inner ring roller paths
5) Surface roughness of outer ring roller path

6) Roller surface roughness - three rollers

7) Finished roller end radius - three rollers

8) Roller axial radius - three rollers

9) Roller diameter - three rollers

10) Roller length - three rollers.

For the purpose of obtaining autorotation data in test F-1, two rollers in bearing 02 were magnetized. One roller was magnetized along the rolling axis and one along an axis transverse to the rolling axis. These rollers were located diametrically opposite each other on the stamped side of the bearing.

The one piece cage of bearing 02 was replaced by a two piece cage during test H. The two piece cage was identical to the one piece cage with the exception that it was split in a plane transverse to the rolling axis at the center of the cage. The split cage was machined from two cages to retain the desired width.

2.2 Lubricant

The lubricant used in all testing was a type II ester (Mobil Jet II) which meets MIL-L-23699 specifications. The oil is composed of polyesters and antioxidant, antiwear, corrosion inhibitor, and defoamant additives. The physical properties are presented in the following table:

Viscosity, cs	
at 210°F	5.1
at 100°F	27.9
at -40°F	10,500
Flash Point, °F	485
Fire Point, °F	545
Specific Gravity at 77°F	1.003
Specific Heat, BTU/lb/°F	
at 100°F	0.536
at 300°F	0.561
at 450°F	0.651
Thermal Conductivity, BTU/hr/ft/°F x 10^3	
at 200°F	85.9

3.0 TEST FACILITY

All testing was performed on a test rig designed to accommodate detailed evaluation testing of spherical roller bearings operating at speeds from 0 to 20,000 rpm. The basic test equipment is shown diagrammatically in Figure A2 and consists of the following components:

Test Rig
Lubricating Oil System
High Pressure Oil System
Instrumentation

3.1 Test Rig

The test rig (layout drawing shown in Figure A3) consists of a hollow rectangular rig housing to accommodate the solid shaft, support bearings and lubrication rings which direct the recirculating oil into one side of each support bearing at three equally spaced locations.

The shaft is supported by three bearings, one 7215 ball bearing and two NU312 cylindrical roller bearings. The shaft extends from both ends of the housing through labyrinth seals. The test bearing (double row spherical roller bearing) is mounted on one end of the shaft extension. The other end is attached to a semi-flexible quill.

The quill doubles as a coupling and rig protection device by accommodating some misalignment and decoupling when the drag torque greatly increases. The quill is attached to either

a jack shaft for low speed operation or a gear box for high speed operation. The jack shaft or gear box is driven through a belt and pully arrangement by a variable speed AC motor.

The test bearing is mounted on the shaft with an interference fit and the inner ring is clamped between a shoulder on the shaft and an end cap which is attached to the shaft with four mounting screws. The shaft section located under the test bearing is hollow to accommodate the wiring and resistor circuit for the resistance temperature detectors (RTD's) mounted in slots on the shaft surface. The RTD's are mounted in silicone rubber which thermally isolates them from the shaft and physically presses them against the bore of the bearing.

The outer ring of the test bearing is mounted in a housing which also serves as the inner ring of a radial hydrostatic bearing. The outer ring of the radial hydrostatic bearing slips over the inner ring and contains the oil supply holes, restrictors, and pads of the bearing. The bottom of the hydrostatic bearing outer ring is attached by a pin and stirrup assembly to a hydraulic ram. The ram, attached to the base plate, applies the radial load through the center of the test bearing.

The test bearing is enclosed by a face plate on the inboard side which is bolt mounted to the housing and forms a

labyrinth seal around the shaft. On the outboard side, the enclosure is formed by a spherical segment which doubles as the face plate for the axial hydrostatic bearing. The axial hydrostatic block, containing the oil supply holes, restrictors and pads, has a matching contour. The axial load is applied through the axial hydrostatic bearing by a hydraulic ram located in an angle bracket bolted to the face plate.

3.2 Test and Rig Bearings Recirculating Lubrication System

Oil circulation to the test and rig bearings is provided by a gear pump through a filter unit, flowmeters and flow control valves, Figure A2. The oil is recovered through drain holes in the test rig and returned to the storage tank by a scavenge pump. The oil supplied to the test bearing enters the bearing housing and passes through three radial holes located in the outer ring. A by-pass line is incorporated downstream of the pump to permit the excess flow to be pumped directly back into the supply tank. The filter unit accepts fiberglass elements having a specific pore size of 20 microns and deliberately has excess flow capacity in order to secure low pressure drops and long life. The oil in the storage tank is circulated through two thermostatically controlled electric immersion heaters capable of maintaining the supply oil at the desired temperature.

3.3 High Pressure Oil System

The high pressure oil system, capable of supplying 1000 psi

pressure, provides oil to the loading rams and the hydrostatic bearings. The oil, leaving the high pressure pump, flows through a combined filter and heat exchanger before entering the control panel. At the control panel, the oil separates with the oil supplied to the hydrostatic bearings passing through flow control valves and the oil supplied to the hydraulic rams passing through pressure regulators. The oil flowing through the hydrostatic bearings is captured in a drain pan and returned to the supply tank by a scavenge pump.

3.4 Instrumentation

The test rig is instrumented to measure the following properties:

1) Test bearing oil-in and oil-out temperatures
2) Test bearing inner and outer ring temperatures
3) Shaft speed
4) Cage or roller orbiting speed
5) Rotational speed of the rollers about their own axis (autorotation speed).
6) Test bearing torque
7) Shaft to housing relative position
8) Oil flow rate to test bearing
9) Various other oil and bearing temperatures.

The test bearing oil-in and oil-out temperatures are sensed by shielded J type thermocouples located in the supply

and drain lines just prior to entering and just after leaving the test bearing housing.

The test bearing outer ring temperature is sensed in four locations, as shown in Figure A4, by J type thermocouples. The tips of the thermocouples are potted into holes in the bearing housing with silicone rubber. The rubber thermally insulates the tips from the housing while holding it with a positive force against the outer ring.

All thermocouples are recorded on an Esterline Angus, Speed Servo II, 24 point recorder. In addition to those discussed above, this includes outer ring temperature of the rig, jack shaft, and gear box bearings and the hydrostatic bearings oil inlet temperature.

The test bearing inner ring temperature is sensed by RTDs. The RTDs, with their resistance bridge circuit, are potted into the shaft with silicone rubber. The rubber provides structural strength to the bridges and thermally insulates the RTDs from the shaft while providing a positive pressure to force the sensors against the bore of the inner ring. The output from the bridge circuits pass through a connector located in the end of the shaft to a S. Himmelstein MCRT3-80(8L) rotary transformer. The temperatures are digitally displayed on a S. Himmelstein Model 6-201 transducer amplifier unit.

The shaft and cage speeds are sensed by proximity probes

and presented on a Hewlett Packard, 5214L preset counter.

To obtain the roller autorotational speed and its variation during one orbit or cage cycle, one roller is magnetized along an axis transverse to the rolling axis. The flux from the magnetized roller cuts a "search" or sensing coil located in proximity to the roller path. Thus, a varying voltage is generated as the roller spins about its own axis. The search coil signal is amplified and presented on a Nicolet Scientific Corp., 444A Mini-Ubiquitous FFT computing spectrum analyzer. A hard copy of the signal is also recorded by a Nicolet Scientific Corp., Model 136A digital plotter.

The bearing drag torque is sensed by a flexible strain gaged beam attached to the outer ring of the radial hydrostatic bearing. The beam reacts against a pin mounted in the test bearing housing which is otherwise free to rotate due to the radial and axial hydrostatic bearing. The output from the strain-gage bridge is recorded on a Hewlett Packard Model 7702B strip chart recorder.

The shaft to housing relative position is sensed by nine Bently Nevada proximity probes. Three probes are located on the inboard side of the test bearing and send the relative radial position of the shaft. Six proximity probes are located on the outboard side of the test bearing, three sensing radial and three sensing axial relative position. The sensers are mounted

in probe holders fastened rigidly to the test bearing housing. A schematic showing the azimuth locations of the probes are shown in Figures A5-A6. The output from the probes are presented on a digital multi-volt meter.

The oil flow rate supplied to the test bearing is controlled by a needle valve and measured by a Schutte and Koerting Co. rotometer which is calibrated for oil temperatures of 93 and 65°C.

4.0 TESTING

A total of eight test series (A-H) were performed. Series A-D were run at speeds of 1000 to 5000 rpm, considered to be normal or within the recommended operating range of the test bearing. These series were performed to establish the operating characteristics of the bearings and to provide data to compare with the computerized analytical model output.

Test series E was performed at speeds from 5000 to 19,400 rpm. The purpose of this test series was to establish the upper speed limit of the test bearing under the imposed conditions.

Test series F-H were performed at speeds above the normal or recommended operating range but at values established to be feasible under the applied conditions in series E. The speeds ranged from 5000 to 17,500 rpm in incremental steps of 2500 rpm or from 200,000 to 700,000dn. The purpose of these test series was to obtain the operating characteristics of the test bearing at the elevated speeds.

Test Series A - D

The first testing on the program was conducted at what is considered to be the normal operating range for the spherical roller test bearing. Each test series was conducted in an increased speed progression from 1000 to 5000 rpm in 1000 rpm

increments. At each speed, a set of combined radial and thrust loads and/or radial loads were applied to the test bearing. The load sets were:

RADIAL ONLY	COMBINED RADIAL AND THRUST	
1500 lbs	1500 lbs	700 lbs
2000 lbs	2000 lbs	700 lbs
2500 lbs	2500 lbs	830 lbs
3000 lbs	3000 lbs	1000 lbs

All tests in series A - D were performed with the MIL-L-23699 lubricating oil supplied to the test bearing at a temperature of $93 \pm 2^{o}C$ and at a rate of 0.125 gallons per minute through the three radial holes in the outer ring. At each set of test conditions the rig was operated until temperature stability of the test bearing was obtained before the data was recorded and a new set of conditions imposed.

Prior to initiating the rig operation, the low pressure or lubricating oil and the high pressure or hydrostatic oil systems were started. These systems were operated, with oil passing through the rig, until the desired lubrication oil temperature was obtained and stabilized. During this period, the unbalanced torque applied to the test bearing housing, by the attached flexible oil inlet and drain lines and instrumentation wires, was determined. This check was performed to verify proper operation of the hydrostatic bearings in the unloaded

condition and to obtain the correction value to be incorporated with the bearing torque readings recorded during testing. The rig was then started with a radial load of 4450N (1000 lbs) applied to minimize skidding of the rollers. The desired speed and load were then applied. This procedure was carried out at the beginning of every test performed.

In test series A and B test bearing No. 02, designated as the baseline bearing, was used. The bearing radial looseness and osculation values are listed in Table A1. Test Series A was performed using the radial load set. The test data are presented in Table A2. Test series B was performed with the combined load set. These test data are presented in Table A3.

Test series C incorporated test bearing 01 which had essentially the same osculation as the baseline bearing (02), but with a radial looseness of 99μm (o.0039"). In this series both the radial load and combined load sets were applied. The test data are presented in Table A4.

Test Series D was performed with test bearing 03, which had the same radial looseness and same osculation on the outer ring as the baseline bearing, but an appreciably lower osculation on the inner ring roller paths. The data from series D testing are presented in Table A5.

A review of the data from series A - D shows that specific trends occur, which are similar, in all the test series with the applied increases in speed and load. In general these trends are as expected. This is especially true with respect to inner and outer ring temperatures and cage to shaft speed ratios. Although the bearing drag torque values generally follow an expected trend, there are some anomalies that occur which are not readily explainable.

The temperatures of both the inner and outer rings increased with both load and speed. The change is greater on the inner ring which is better thermally insulated than the outer ring. The data also shows that the higher the speed the greater the temperature change per a given load change. This condition would be expected as the temperature is a gauge of the energy dissipated in the bearing. These trends are illustrated in Figure A7 which presents plots of the inner ring temperatures from test series A and B which are typical of all four series.

A review of the cage to shaft speed ratios show that the values vary approximately one percent over the full range of conditions. A close examination of the data taken when a radial load only was applied show two definite trends:

1) The ratio increases with load, which would

indicate a decrease in roller slippage as would be expected since the traction would be expected to increase with load.

2) The ratio decreased with speed, which indicates that slippage increases as speed increases.

These two trends are illustrated in Figures A8-A9, where data from Test Series A is plotted.

Both of these trends are in the direction that would be expected. In addition, it is noted that the ratio values are higher when a combined load is applied. This would be expected since all the rollers on one side of the bearing are constantly loaded. This loading condition results in lower inertial forces being generated than when in a pure radial loaded bearing, the unloaded rollers enter the load zone and are suddenly accelerated to speed. Such inertial forces would be transmitted through the cage to the loaded rollers and thus slow the cage resulting in roller slippage. It is also noted that the two trends observed under pure radial load essentially hold for combined load, but the results are somewhat complicated since the ratio of thrust to radial load is not always the same.

A review of the proximity probe measurements made to evaluate the shaft to housing relative approach indicate that the effect of speed, up to 5000 rpm, was minor and the approach measured was in the direction expected.

As discussed in the instrumentation section (3.4), there were three sets of three probes each used to measure the relative approach of the shaft to the housing. Set I, consisting of probes 1, 2 & 3, was used to measure the radial approach on the outboard side and set II, probes 7, 8, and 9 on the inboard side. Set III, consisting of probes 4, 5, and 6 on the inboard measure the axial approach between the shaft face and the housing. The azimuth location of the probes are shown in Figures A5 and A6. Each probe was calibrated before assembly and had gage factors near the rated value of 0.2 volts per 0.001 inch change in the proximity of the measured surface. A digital rms volt meter was used to record the position, thus compensating for any runout on the shaft. By noting the fluctuation in voltage while running at a given set of conditions, the accuracy of the readout was determined to be approximately $\pm$ 0.0001 inch.

To evaluate the repeatability of the changes in relative positions that took place at the specified speeds and loads, the data from test series A was plotted, Figures A10 - A12. The graphs were made by considering that the position measured by each probe with a 1500 lbs radial load applied was the zero position and all other positions located relative to zero as the load was changed.

These graphs show that changes in displacement did occur with load. In addition, with the exception of the values measured at a

speed of 1000 rpm, the displacement pattern produced with load change at all speeds was essentially the same. Thus, the results indicated that little or no relative motion effect resulted from speed changes up to 5000 rpm. No explanation could be established for why the pattern and position were somewhat different at 1000 rpm.

To evaluate whether the measured change in the relative position is in the direction expected, the expected change has to be analyzed. The relative change would be expected to occur in the following manner. With a radial load applied downward through the housing onto the test bearing along a vertical line, the bearing will compress, and the shaft will also bend forming a curved path from the support bearing in the rig housing to the test bearing. From the test bearing to the end of the shaft, the shaft will remain straight but tilted, with respect to a horizontal plane, at an angle produced by the bending. Since a spherical bearing is self-aligning, i.e., the inner ring and roller sets can tilt at an angle with respect to the axis of the outer ring without applying a moment to the outer ring, the bending of the shaft will not alter the transverse plane of the outer ring. Thus, the vertical planes formed by each of the three sets of probes will not change with applied load. Therefore, the measured changes in relative position result from the compression of the bearing and the bending of the shaft.

The bearing compression would occur along the line of the applied force or vertical line causing a decrease in the displacement between the housing and the top of the shaft on both the inboard and outboard side of the bearing. This motion would be sensed by the radial proximity probe sets. The bending of the shaft would position the top of this shaft farther away and the bottom of the shaft closer to the radial sensing probes on the outboard side of the bearing. The opposite would occur on the inboard side of the bearing. The bending would also cause the face of the shaft to tilt with respect to the housing face causing the top of the shaft face to be closer and the bottom to be farther away from the axial measuring proximity probes.

A summary of the effect of increased load on the direction of relative approach between the housing at the top and bottom of the shaft per the above analysis is presented in the following table:

	Outboard Side of Brg. Radial Change		Inboard Side of Brg. Radial Change		Outboard Side of Brg. Axial Chg.	
	Top(3)	Bottom(2)	Top(7)	Bottom(9)	Top(6)	Bottom(5)
Compression	Closer	Away	Closer	Away	None	None
Bending	Away	Closer	Closer	Away	Closer	Away
Comp.& Bend.	Closer & Away	Away & Closer	Closer &Closer	Away &Away	Closer	Away

The table shows that in two locations, inboard radial and outboard axial, the direction of relative motion is definite. In the third location, outboard radial, the direction of motion depends on whether the effect of compression or bending is the largest. Also shown in the table in parentheses are the numbers of the probes against which these expected directions of motion can be compared. The results of a comparison show that the measured directions of relative motion agree with the analysis where the combined effect is firm. In the third case, outboard radial, the comparison shows that the effect of bending is greater than that of compression as would be expected. Thus, it can be concluded that the relative motion measured is in agreement with what would be expected.

Bearing drag torque values were recorded at all load and speed conditions in each of the test series A-D. During a preliminary test run to check out the performance of the rig, it was noted that vibrations in the torque signal sensed by the strain gaged moment arm made the mean torque value difficult to establish. Therefore, the method of measuring the necessary resisting force to counter balance the drag torque was changed to using a gram spring scale at a fixed radial distance from the center of the test bearing.

Two readings of the required balancing force were made at each condition: the force applied when the stop pin moved

slightly off the retaining force transducer, and again when the pin made initial contact with the transducer. In none of the measurements was the difference more than 10 gr. The average of these two values was then used to establish the dry torque. This reading was corrected by an unbalanced torque on the bearing housing due to instrumentation wires, and flexible lubrication lines. This correction was determined prior to and following the test series with no load applied to the test bearing, but with all oil flows at the testing conditions.

A measurement of the change in the unbalanced torque between the beginning and the end of the test indicated that an error of $\pm$ 3 inch -ounces could exist from this effect alone.

Plots of the drag torque data measured while evaluating the baseline bearing 02 during test series A&B are presented in Figures A13 and A14 respectively. From these plots it is seen that the drag torque increases as the load is increased but it did not always increase with increases in speed.

To permit an evaluation of the effect of the changes in the internal geometry of the test bearings, Table A6 lists all drag torque measurements made during test series A-D.

The following observations are noted from this table:

1) With each of the three bearings tested, the drag torque always increased with load. The addition of the thrust to the radial load also produced an increase in the drag torque in all

cases.

2) Testing with a pure radial load applied to test bearing 01, having a 0.001 inch greater radial clearance than the baseline bearing 02, resulted in drag torque values approximately the same as those obtained with bearing 02, except at 1000rpm where the values were much higher. With a combined load, the drag torque values showed a trend of being greater at all speeds and loads.

3) Testing of bearing 03, which had an appreciable decrease in the osculation of the inner ring roller paths compared to bearings 01 and 02, resulted in appreciably higher drag torque values at the lower speed and essentially all loads. The torque values then decreased with speed increases. With a radial load only, the torque values decreased to a value below that measured with the other two bearings at a speed of 5000 rpm. With a combined load, the torque value decreased until they approximated those obtained with the other two bearings at the operating speed of 5000 rpm.

Test Series E

The purpose of the series E tests was to establish the upper speed limit of the spherical test bearing under the specified conditions imposed in test series A-D with the addition of a pure thrust load. The results were then used

to establish the maximum speed applied in test series F-H.

The test series was performed with test runs made at three different load conditions:

1) radial load of 3000 lbs
2) thrust loads of 1000 lbs
3) combined loads of 3000 lbs radial and 1000 lbs thrust.

Prior to performing the tests, two criteria were established to be used as indicators of a malfunction in the bearing: (1) abnormal increase in bearing drag torque for a given incremental speed change. (2) Abnormal increase in either the inner or outer ring temperatures. In addition, a test would be terminated if the difference in temperature between the test bearing housing and the inner ring approached 80°C. Hand calculation indicated that this temperature differential represented a conservative upper bound at which the bearing's radial looseness would be lost.

A total of six preliminary, rig checkout tests were performed, two at each of the three maximum load conditions. Test bearing 06 was used in all testing with the lubricating oil supplied at approximately 93°C at a rate of 0.125 to 0.15 gpm through the outer ring. Each test was performed by applying the desired load condition and increasing the speed in incremental steps after temperature stabilization was obtained.

The data recorded during the testing included the bearing inner and outer ring temperatures, the lubricating oil inlet and outlet temperature and flow rate, the hydrostatic oil inlet temperature, and the bearing drag torque.

During the first three tests, one at each load condition, a maximum speed of approximately 12,000 rpm was obtained. Following these runs the test bearing was inspected and found to be in excellent condition. Therefore, the second set of tests were performed where speeds as high as 19,400 rpm were obtained. The temperature data from these tests are presented in Tables A7 through A9.

In test E-4, radial load only, and test E-6, combined load, the testing was terminated at 18,000 rpm and 19,000 rpm respectively, due to the differential temperature approaching 80°C. Test E-5 was terminated only after the maximum speed of 19,400 rpm was obtained. Inspection of the bearing after each run showed it to be in excellent condition.

In none of the tests was there any indication of a malfunction of the test bearing as noted by an abnormal increase in torque or temperature. However, torque measurement could not be made at speeds above approximately 12,000 rpm due to thermal expansion binding the radial hydrostatic bearing.

As a result of test series E, an upper speed limit of 17,500 rpm (dn = 700,000) was established for test series F-H.

Test Series F - H

All tests in series F-H were performed with the baseline bearing 02. The tests were initiated at a speed of 5000 rpm (200,000dn) and progressed in incremental steps of 2500 rpm (100,000 dn) to a maximum speed of 17,500 (700,000dn). At each speed the following six load conditions were applied before advancing to the next speed.

Applied Loads

Radial (lbs)	Thrust (lbs)
1500	50
3000	50
50	750
50	1000
1500	750
3000	1000

Data was recorded at each speed and load condition after temperature stabilization had been obtained. In addition to the higher speed, the following changes were made in the high speed test procedure, which differed from Series A-D:

1) A minor axial or thrust load was applied when the major load was radial. This load was applied to minimize axial vibration.

2) A major thrust load was applied with only a very minor accompanying radial load.

3) The lubricating oil flow rate was increased slightly from 0.125 to 0.15 gallons per minute.

Test series F consisted of two tests with one being essentially a repeat of the other. In the first test (F-1), autorotation data was recorded. In the second test (F-2) the proximity probe data was recorded. Both types of data could not be obtained in a single test since the instrumentation was not compatible with the available space.

Test F-1 was performed to obtain the autorotation data in addition to obtaining the temperature and torque data. This information was not obtained in any other test. From this information, the change in the roller rotational velocity about its own axis could be evaluated as the roller set orbits about the shaft.

The autorotation data was generated in the form of a voltage in a "search" coil. The search coil had a pitch diameter of 2.5 inches that approximated the pitch diameter of the roller set. The coil was constructed of 700 wraps of 34 gage high temperature magnet wire and mounted to the bearing housing to position the coil as close to the roller set as possible. By magnetizing one roller in a plane transverse to the roller rotating axis, the magnetic flux cut by the coil as the roller rotated about its own axis results in a signal whose frequency was equal to the roller autorotation

frequency.

During test F-1, the output from the search coil was plotted on a Nicolet Scientific Corp. Model 136A digital plotter. The plots were then analyzed and the results presented with the other data in Table A10.

A typical plot of the autorotation signal is presented in Figure A15. These data were recorded during the first run when a radial load of 1500 lbs and a thrust load of 50 lbs were applied. The shaft speed was 5000 rpm. Figure A15 shows the roller frequency per roller cycle and the average frequency per cage cycle. Also presented on the plot are the cage and shaft periods as established from the counted frequencies. The autorotation data, presented in Table A10, shows the following trends:

1) The maximum change in the autorotation frequency, per cage cycle, occurs at the lowest speed with the lowest radial load. With either an increase in load or speed, the difference decreases.

2) With an essentially pure thrust load applied, no appreciable change occurred.

3) With a combined load, the autorotation frequency change is also greatest at the lowest speeds. The change is directly proportional to the ratio of radial to thrust load.

Figures A16 and A17 present the respective inner and outer ring

temperature plots and how they changed with speed and load condition. The offset between speeds of 10,000 and 12,500 rpm resulted from a change in the oil in temperature to the hydrostatic bearing.

Figure A18 shows the percent slip at the various load and speed conditions. The slip was determined from the measured cage to shaft speed ratio which was then compared to the theoretical no slip ratio of 0.4030. The plot shows that the greatest slip occurs with the essentially pure radial loads. The second largest slip resulted from the combined loads. In both cases, slip increased with speed. The least slip occurred with the essentially pure thrust load applied.

The test data from series F-2 are presented in Table A11. This series, as previously described, was similar to series F-1, with the exception that proximity probe data was recorded instead of the autorotation data. A plot of the torque data recorded in series F-1 and F-2 is presented in Figure A19. The purpose of this plot is to determine the spread in drag torque values that could be expected with repeated tests of the same bearing. The results of the analysis show that a spread as great as 14% can occur, but in the majority of the cases the spread is less than 10%.

An inspection of the test bearing following series F

testing showed the bearing to be in excellent condition and, as the data indicate, no malfunction of the bearing occurred.

Test series G was performed with the same bearing (02) and the same lubricating oil flow rate as series F but with an oil inlet temperature of 65°C (150°F) instead of 93°C (200°F). The hydrostatic bearing oil inlet temperature was also reduced to approximately 65°C.

The data recorded during the tests are presented in Table A12. Plots of the inner and outer ring temperatures are shown in Figures A20 and A21. These plots show essentially the same slopes as series F data, but at a lower temperature as would be expected. A plot of the percent slip is shown in Figure A22. The test bearing was in excellent condition following the test.

Test series H was also performed with test bearing 02. However, the one piece machined brass cage was replaced with a two piece cage. The two piece cage was identical to the one piece cage except it was split in the center along a plane transverse to the rotating axis. The test was performed in the same manner as series F with the lubricating oil flow rate and inlet temperature, and the hydrostatic bearing oil inlet temperature being essentially identical to that used in test series F.

The test data from series H are presented in Table A13. Plots of the inner and outer ring temperature are presented in

Figures A23 and A24. A plot of the percent slip is shown in Figure A25.

The split cage did not present any particular problem in its operation. However, as might be expected, major slip did occur on the unloaded side (inboard side where the cage speed was always measured) of the bearing when an essentially pure thrust load was applied. This occurred primarily at the lowest shaft speed evaluated (5000 rpm). At speeds of 7500 and 17,500 rpm, there was also a slippage of approximately 1% higher than normal with the minimum thrust load applied. The inner and outer ring temperatures were abnormally high when the high slippage occurred. These results indicate that the slippage would also be expected at speeds lower than 5000 rpm under the thrust and combined load conditions with the split cage design.

Inspection of the bearing following the test showed no indication of damage to any of the elements Photographs of the tested bearing and its component parts are shown in Figures A26 and A27.

These high speed performance tests have shown that, with proper lubrication, the bearing tested can perform under the imposed conditions at four times the catalog listed maximum speed, without any malfunction.

AT81D008

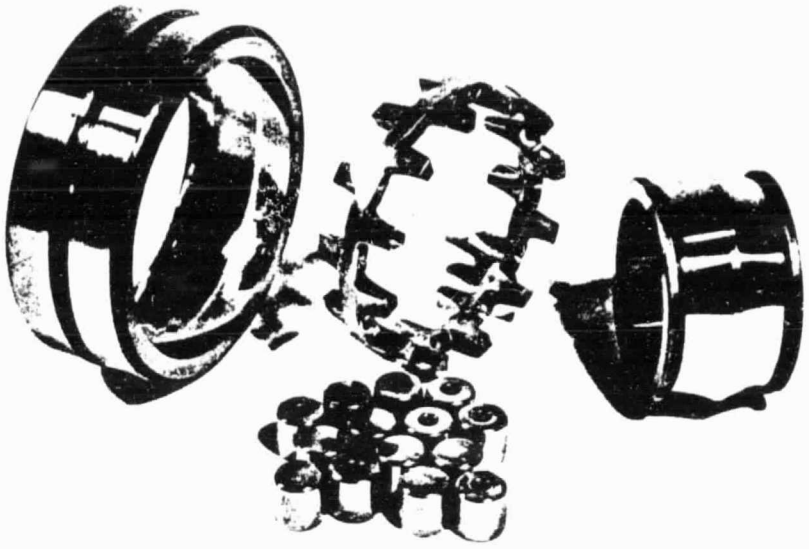

Disassembled 452308 M2/W502 Spherical
Roller Bearing

Assembled Test Bearing

FIGURE A1

FIGURE A2

HIGH PRESSURE OIL SYSTEM

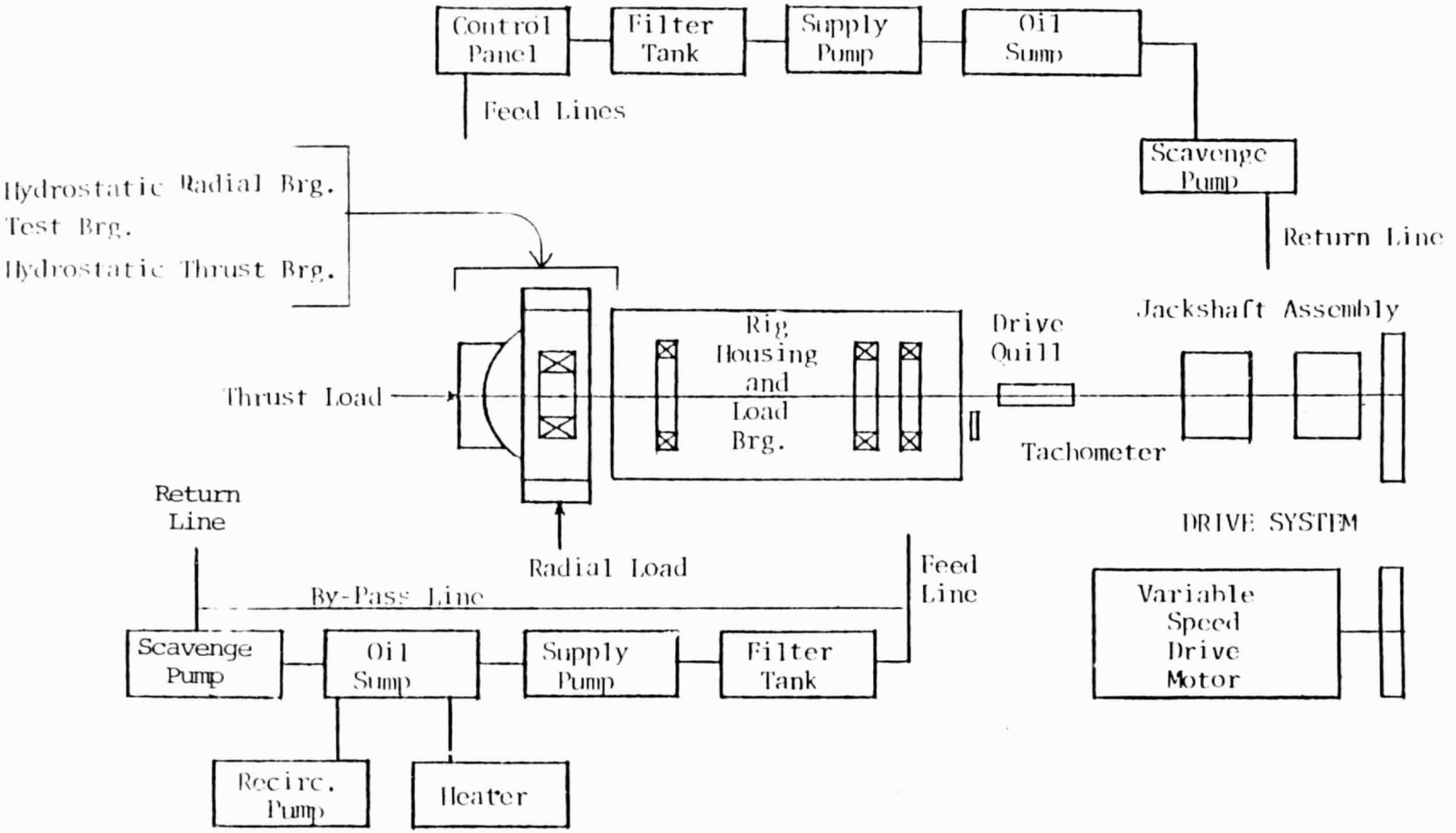

SCHEMATIC OF TEST EQUIPMENT

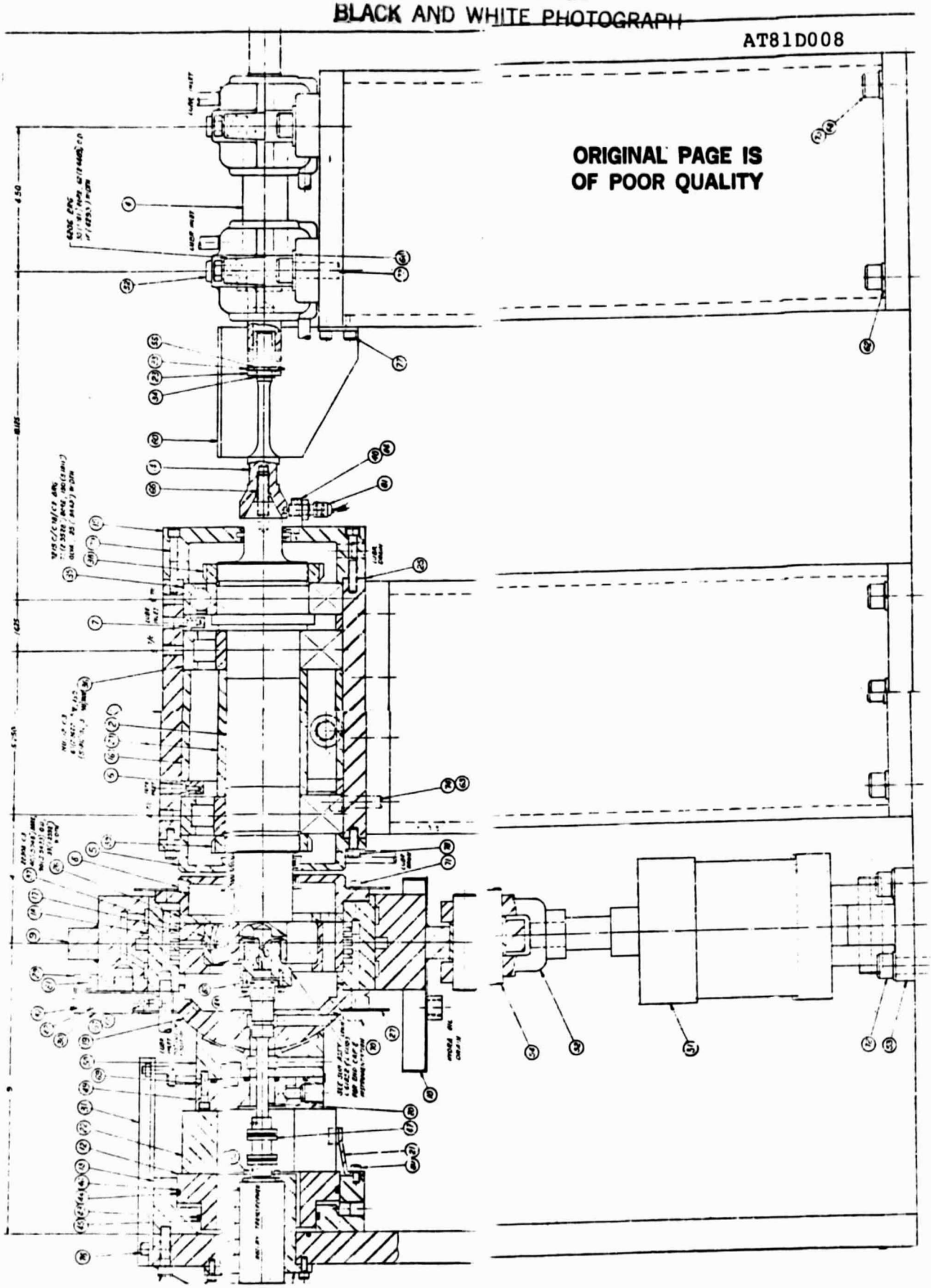

Layout Drawing of Test Rig

FIGURE A3

F-4185C-1-R100

AT81D008

Test Bearing Housing Sleeve
Showing Location of Outer
Ring Temperature Sensing Thermocouples

FIGURE A4

FIGURE A5

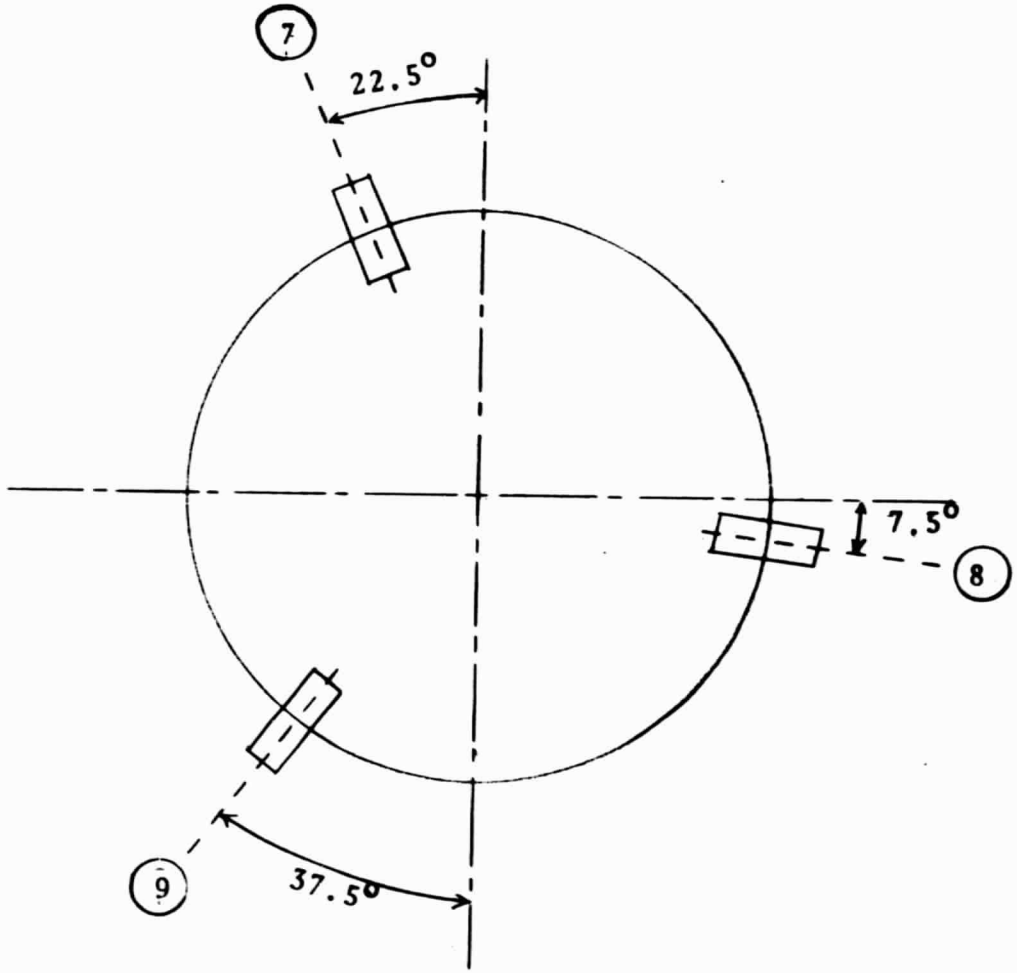

PROXIMITY PROBE AZIMUTH POSITIONS -
INBOARD SIDE

FIGURE A6

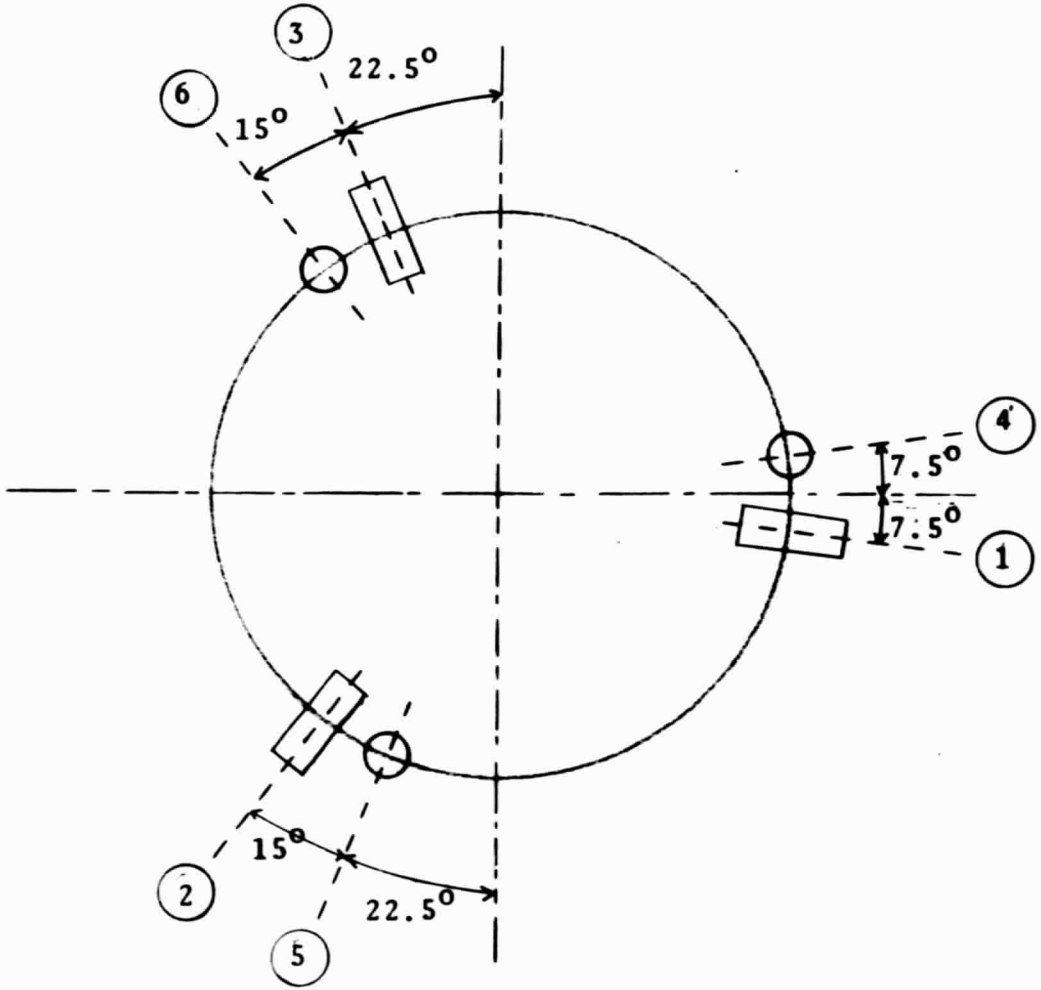

PROXIMITY PROBE AZIMUTH POSITIONS

OUTBOARD SIDE

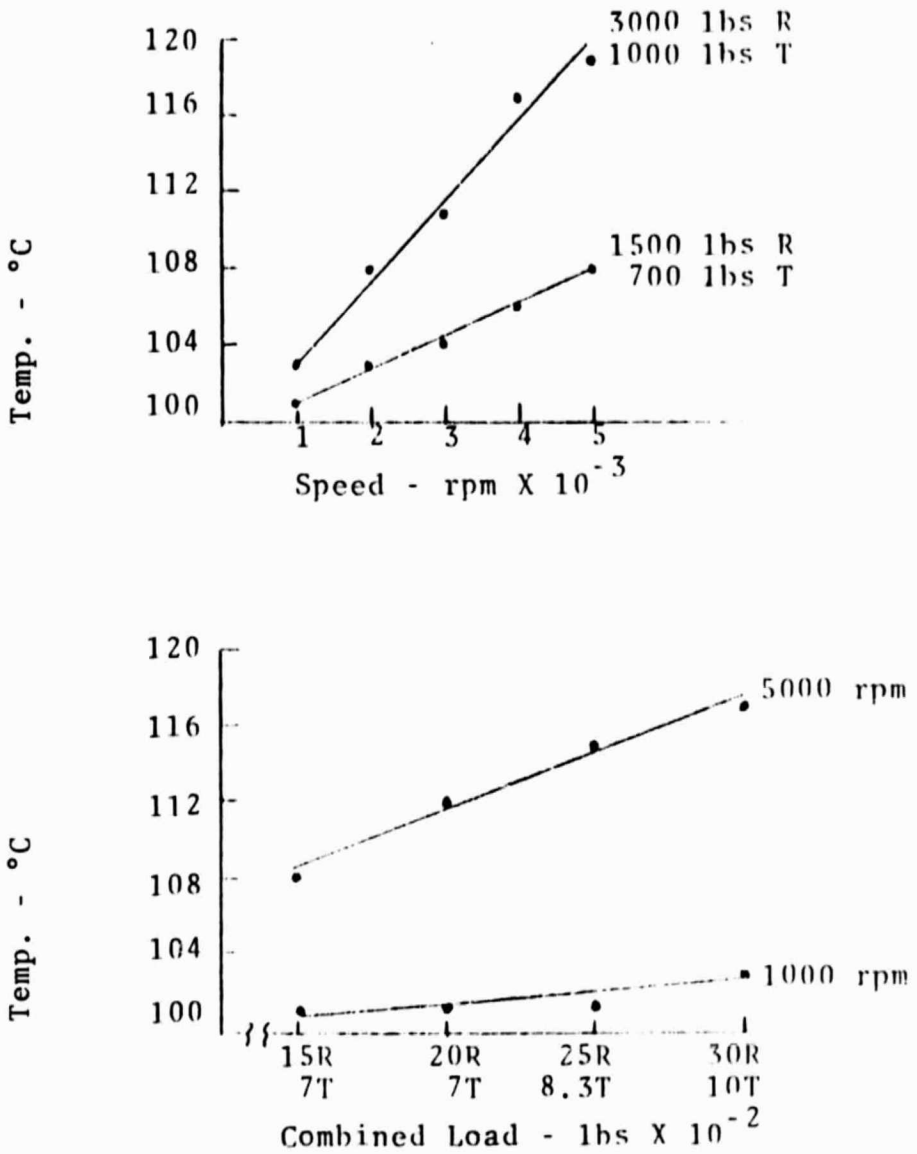

Graphs Showing Changes in Inner Ring Temperature
With Speed Changes and Load Changes
Data from Test Series A & B

FIGURE A7

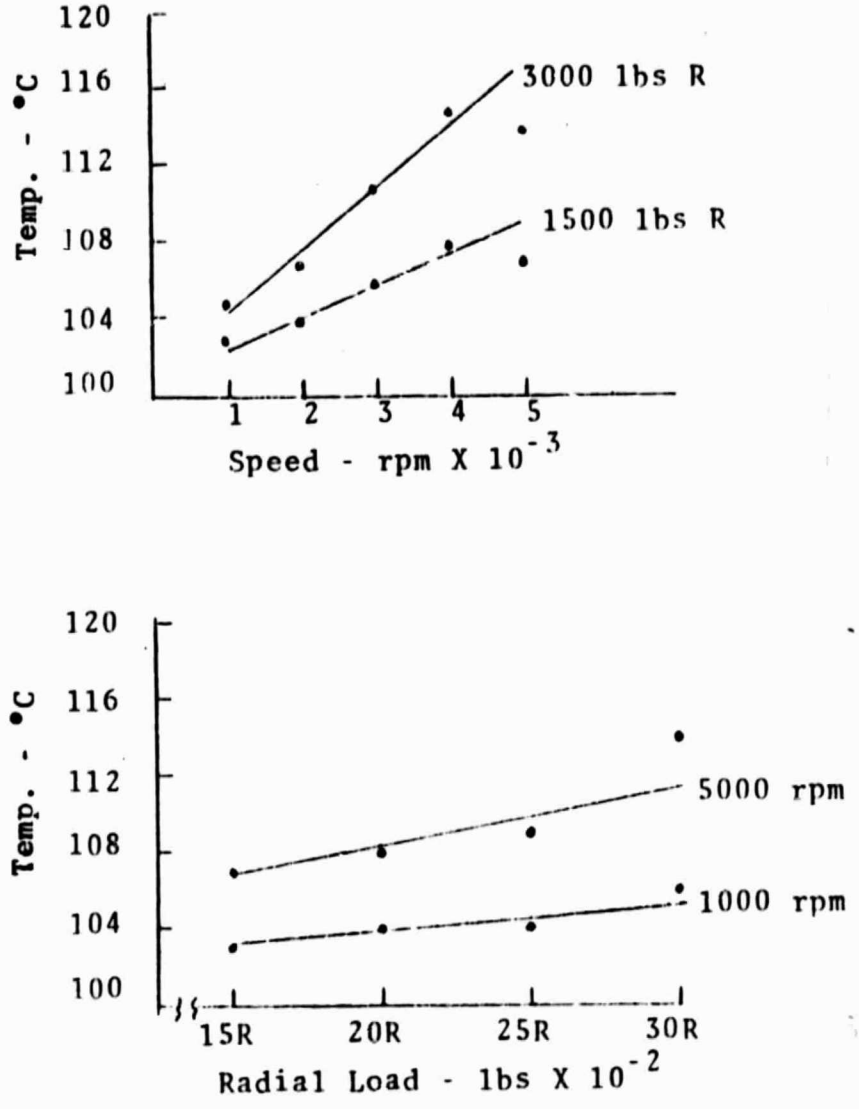

Graphs Showing Changes in Inner Ring Temperature
With Speed Changes and Load Changes
Data from Test Series A & B

FIGURE A7 (CONTINUED)

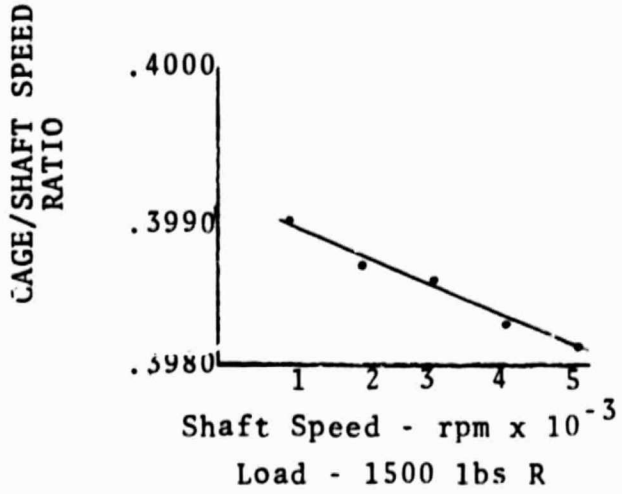

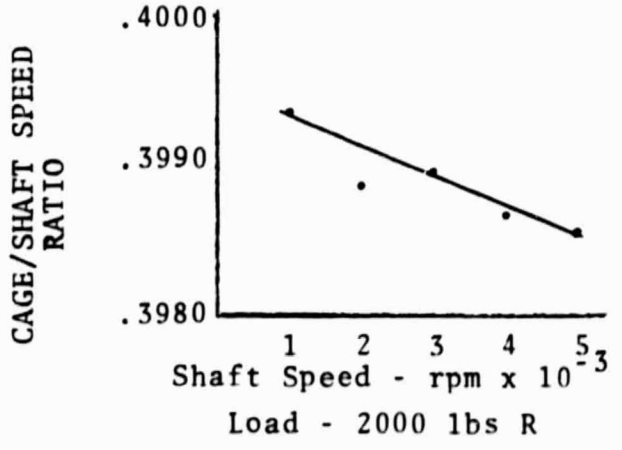

CAGE TO SHAFT SPEED RATIO VS. SHAFT SPEED - TEST A

FIGURE A8

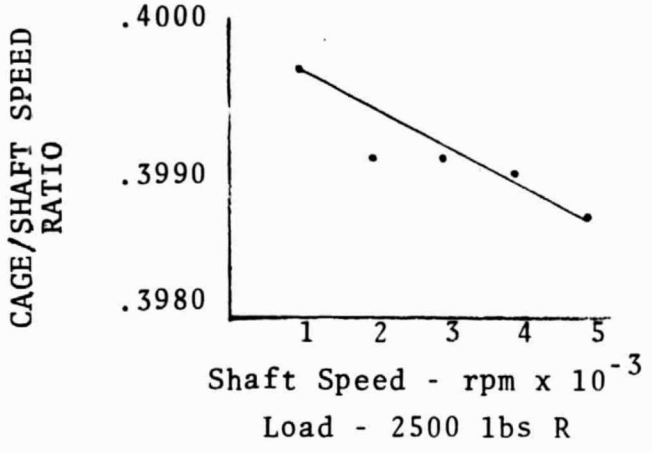

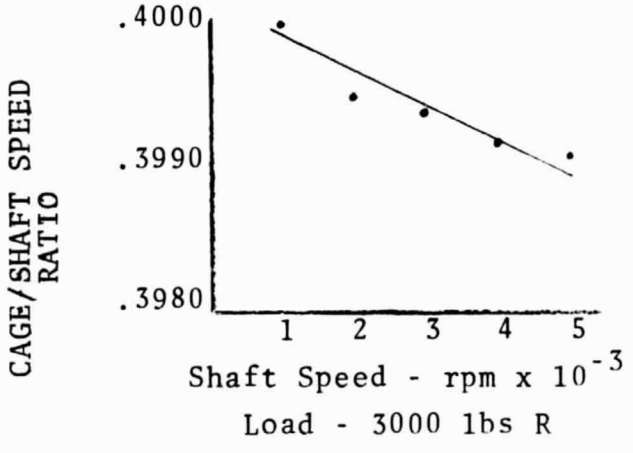

CAGE TO SHAFT SPEED RATIO VS. SHAFT SPEED - TEST A

FIGURE A8 (CONTINUED)

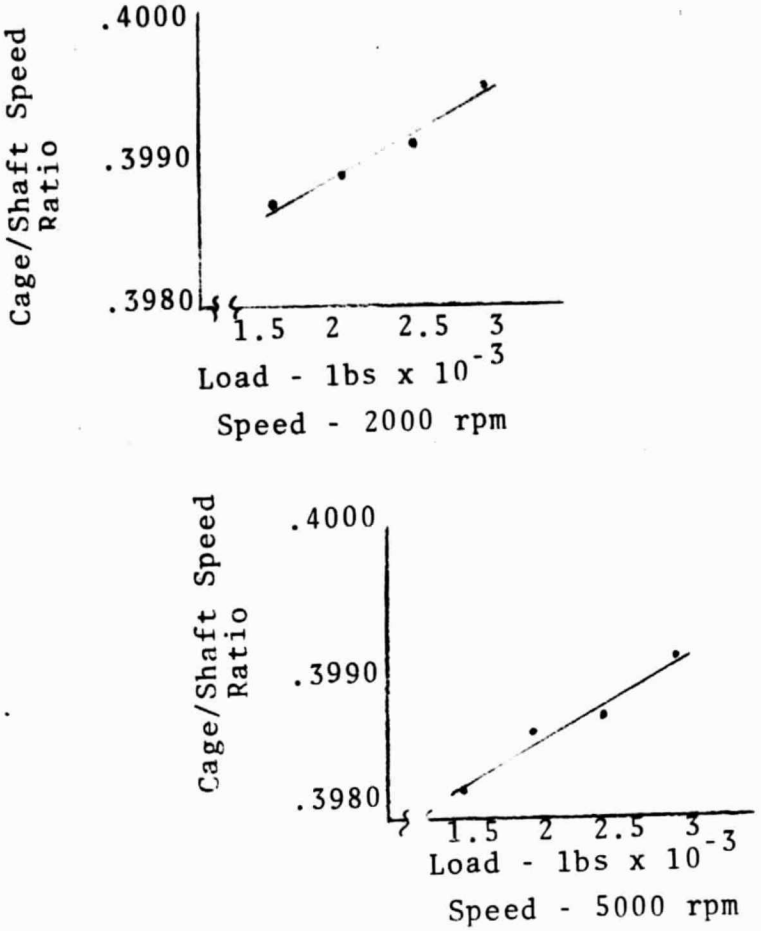

CAGE TO SHAFT SPEED RATIO VS. RADIAL LOAD - TEST A

FIGURE A9

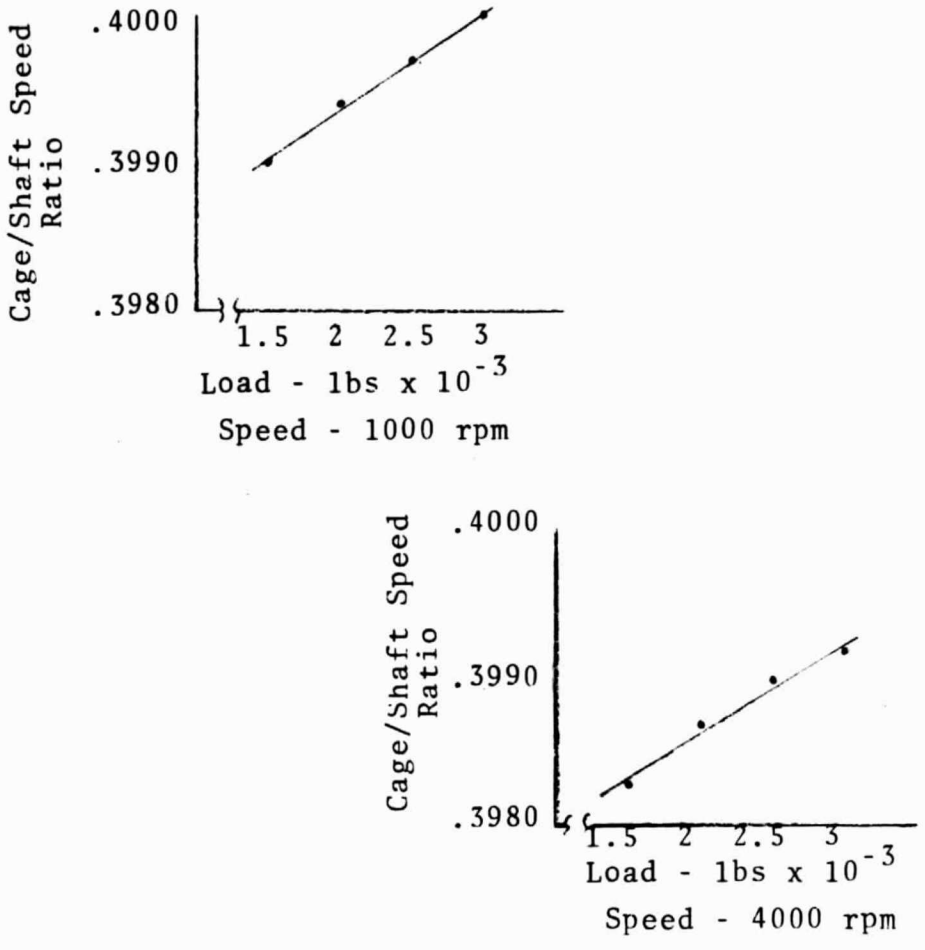

CAGE TO SHAFT SPEED RATIO VS. RADIAL LOAD - TEST A

FIGURE A9 (CONTINUED)

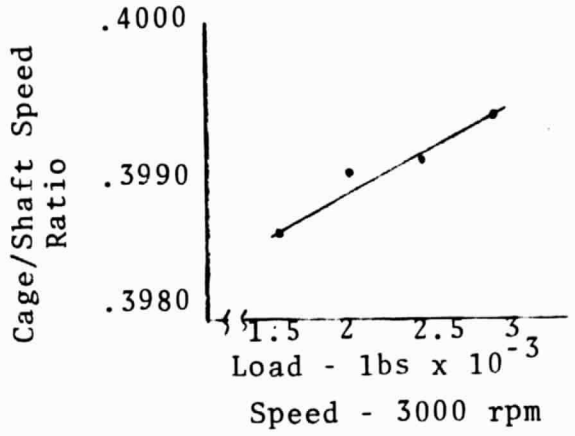

CAGE TO SHAFT SPEED RATIO VS. RADIAL LOAD - TEST A

FIGURE A9 (CONTINUED)

FIGURE A10

PLOT OF RADIAL DISPLACEMENT MEASURED BY OUTBOARD

PROBE SET I VERSUS LOAD AT DIFFERENT SPEEDS (TEST A)

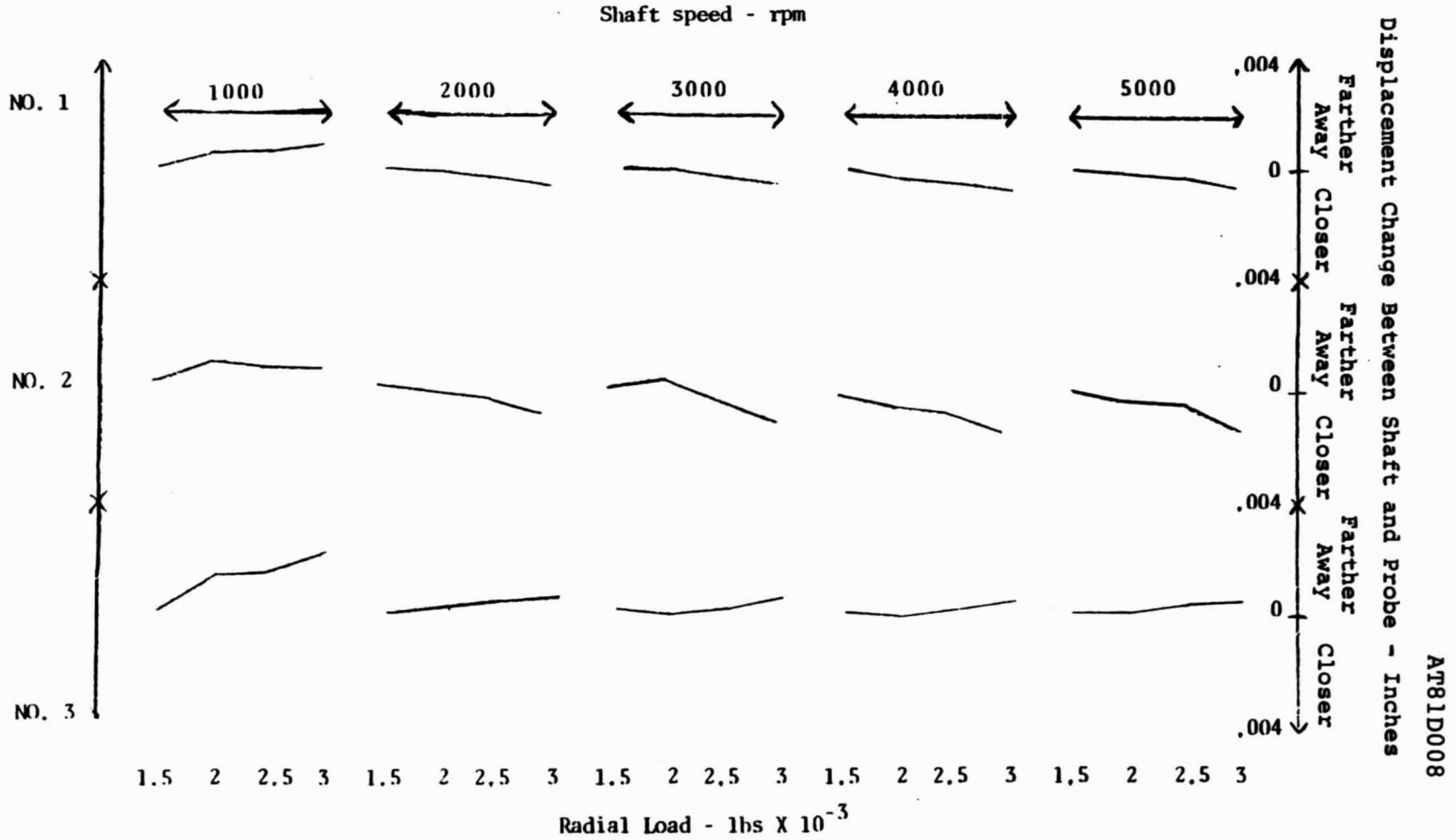

FIGURE A11

PLOT OF RADIAL DISPLACEMENT MEASURED BY INBOARD

PROBE SET II VERSUS LOAD AT DIFFERENT SPEEDS (TEST A)

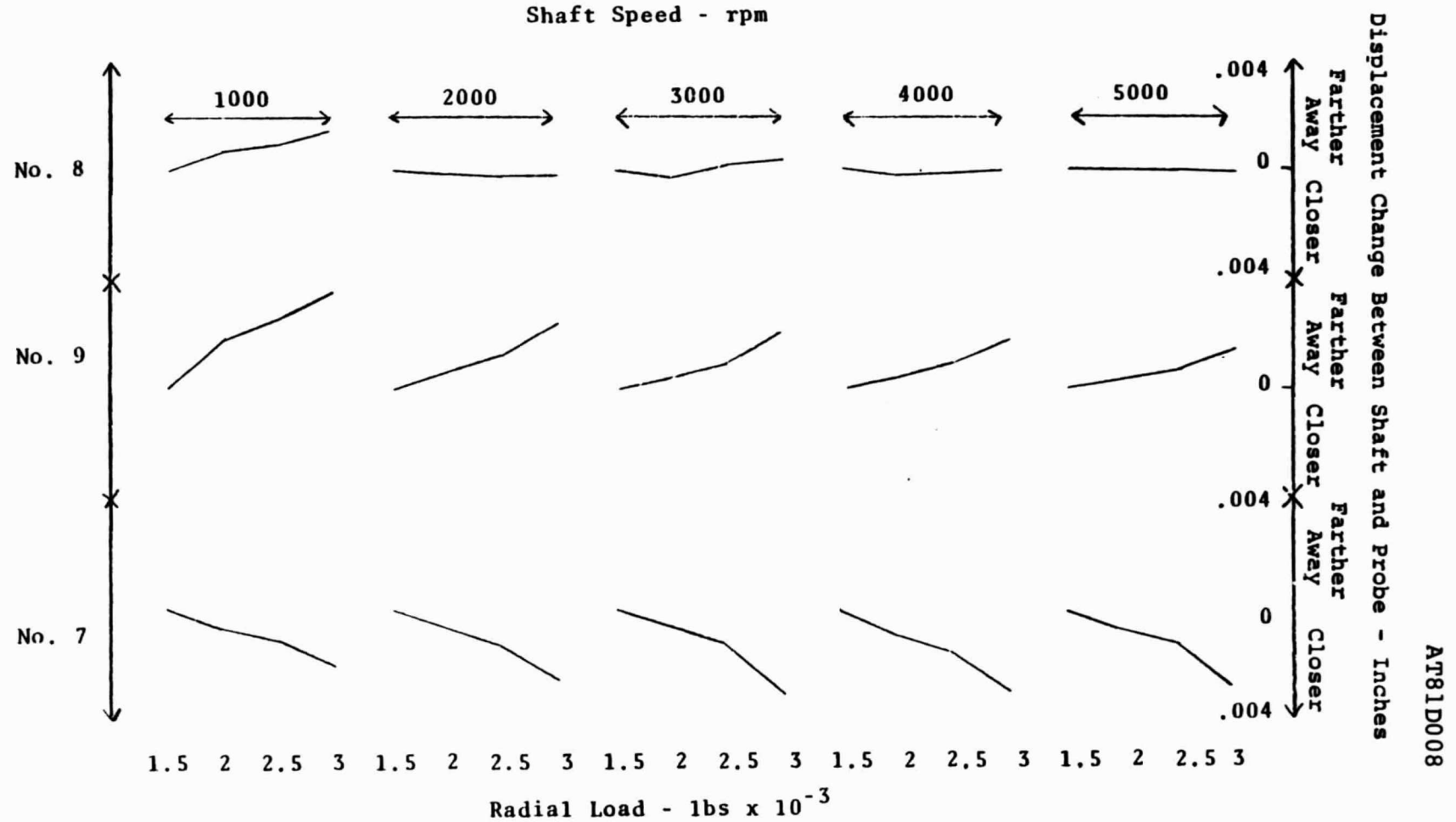

FIGURE A12

PLOT OF AXIAL DISPLACEMENT MEASURED BY OUTBOARD

PROBE SET III VERSUS LOAD AT DIFFERENT SPEEDS (TEST A)

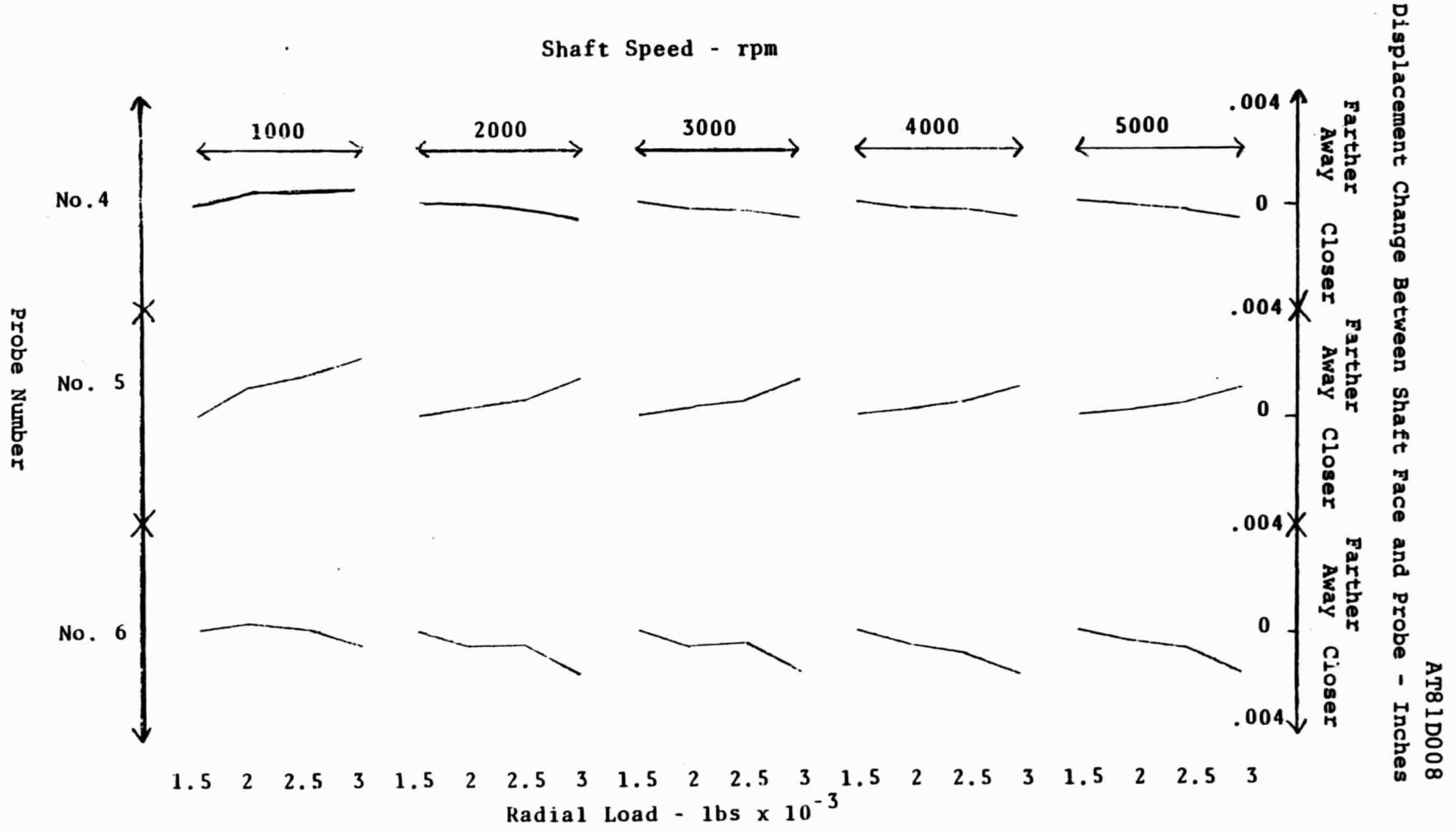

PLOT OF BEARING DRAG TORQUE
VERSUS RADIAL LOAD AT VARIOUS SPEEDS
(TEST SERIES A)

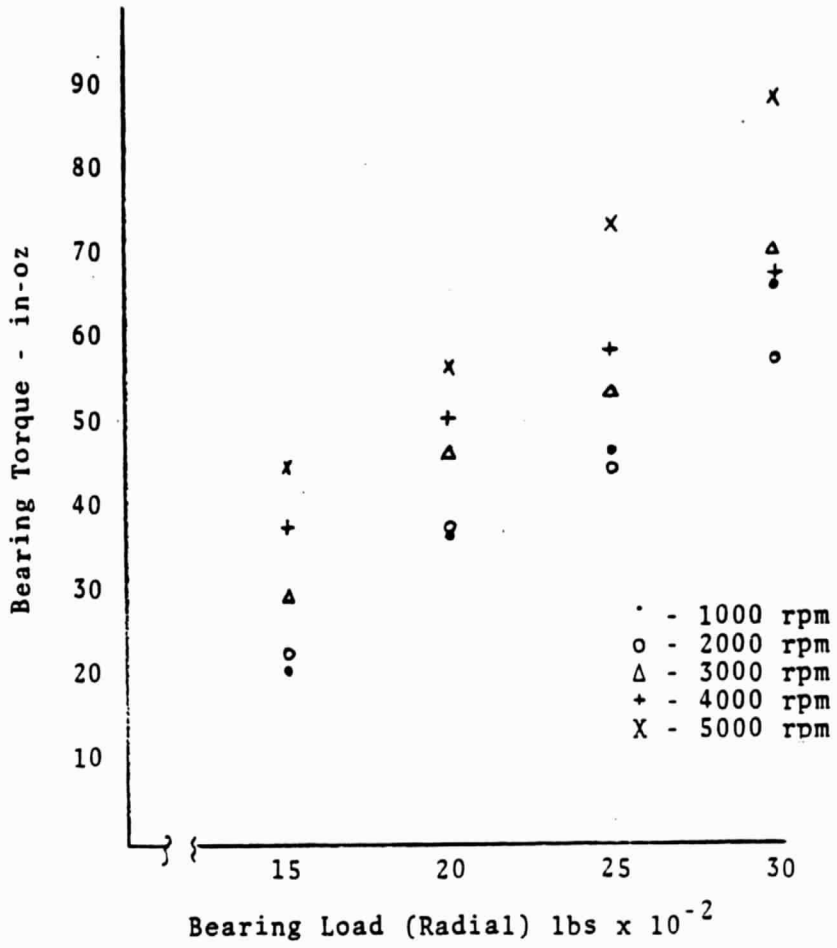

FIGURE A13

PLOT OF BEARING DRAG TORQUE
VERSUS COMBINED LOAD AT VARIOUS SPEEDS
(TEST SERIES B)

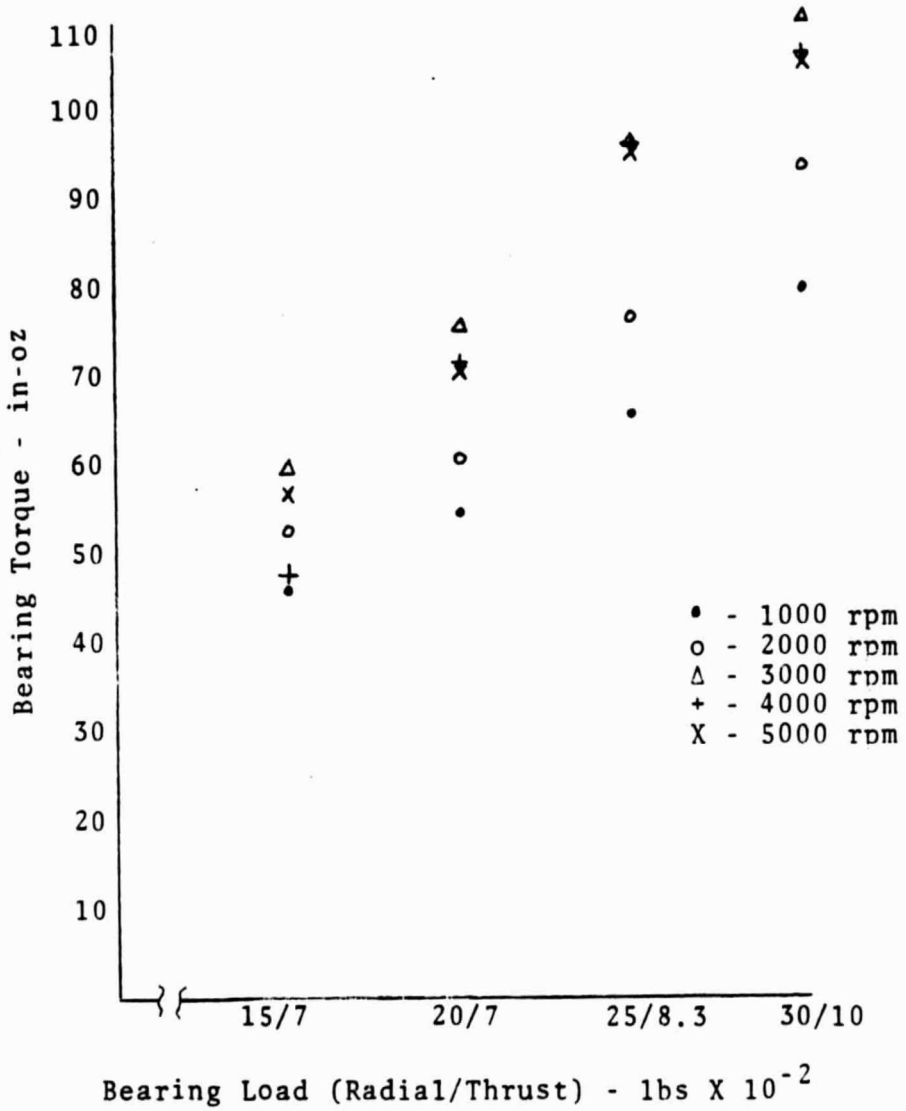

FIGURE A14

FIGURE A15

PLOT OF AUTOROTATION FREQUENCY, TEST SERIES F-1, RUN 1

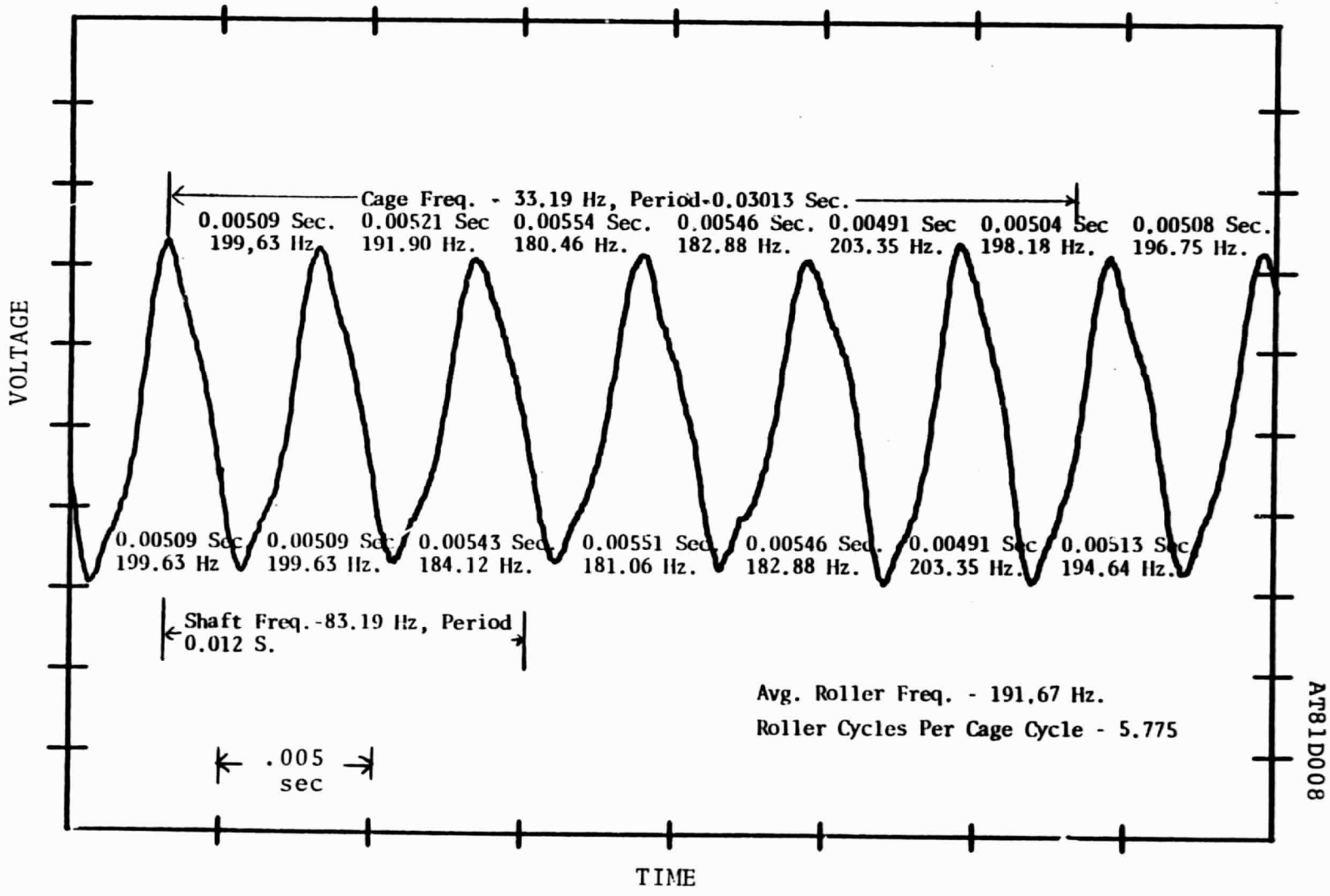

FIGURE A16

INNER RING TEMPERATURE VS. SHAFT SPEED & LOAD CONDITIONS

TEST SERIES F-1

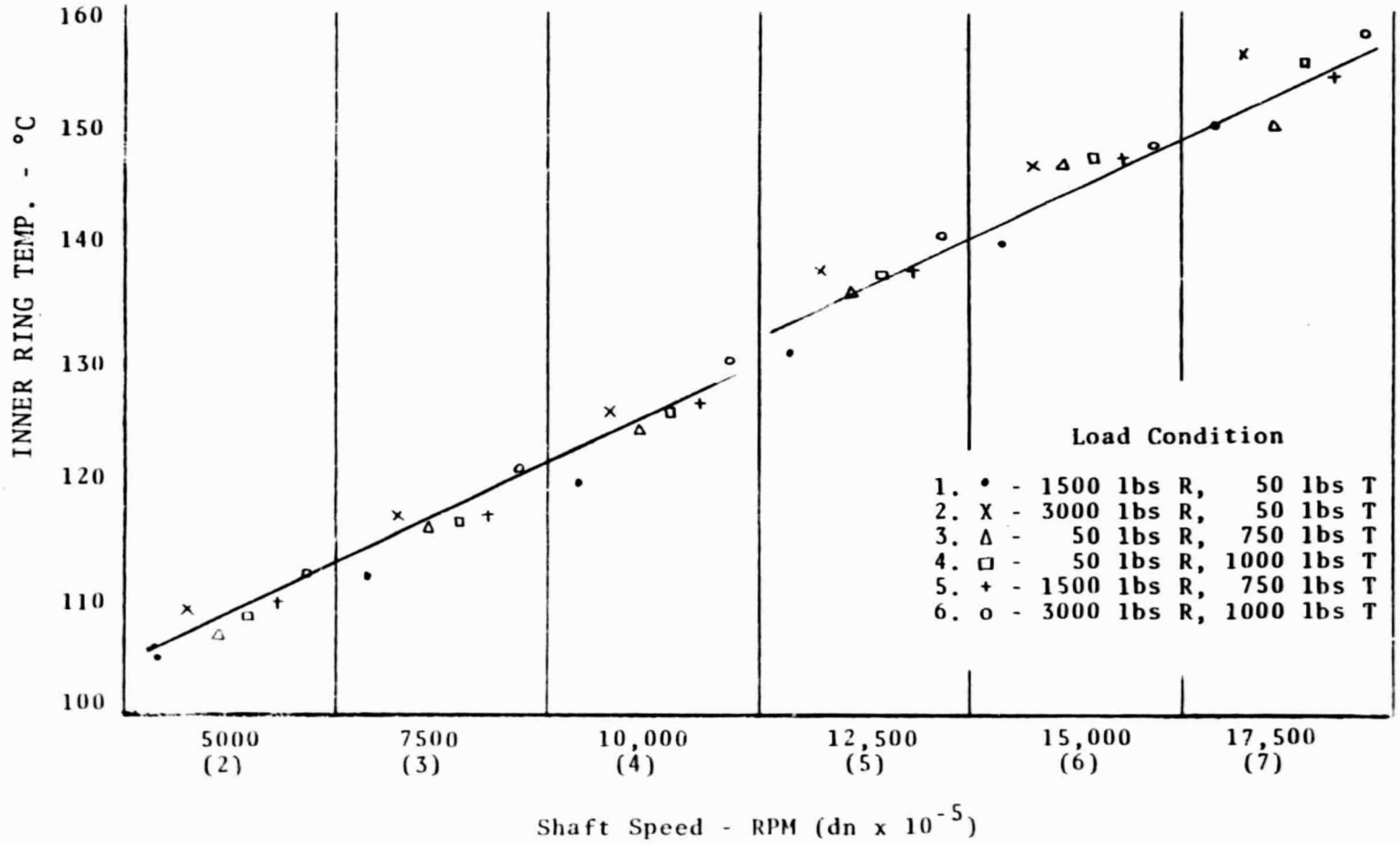

AT81D008

FIGURE A17

OUTER RING TEMPERATURE VS. SHAFT SPEED & LOAD CONDITIONS

TEST SERIES F-1

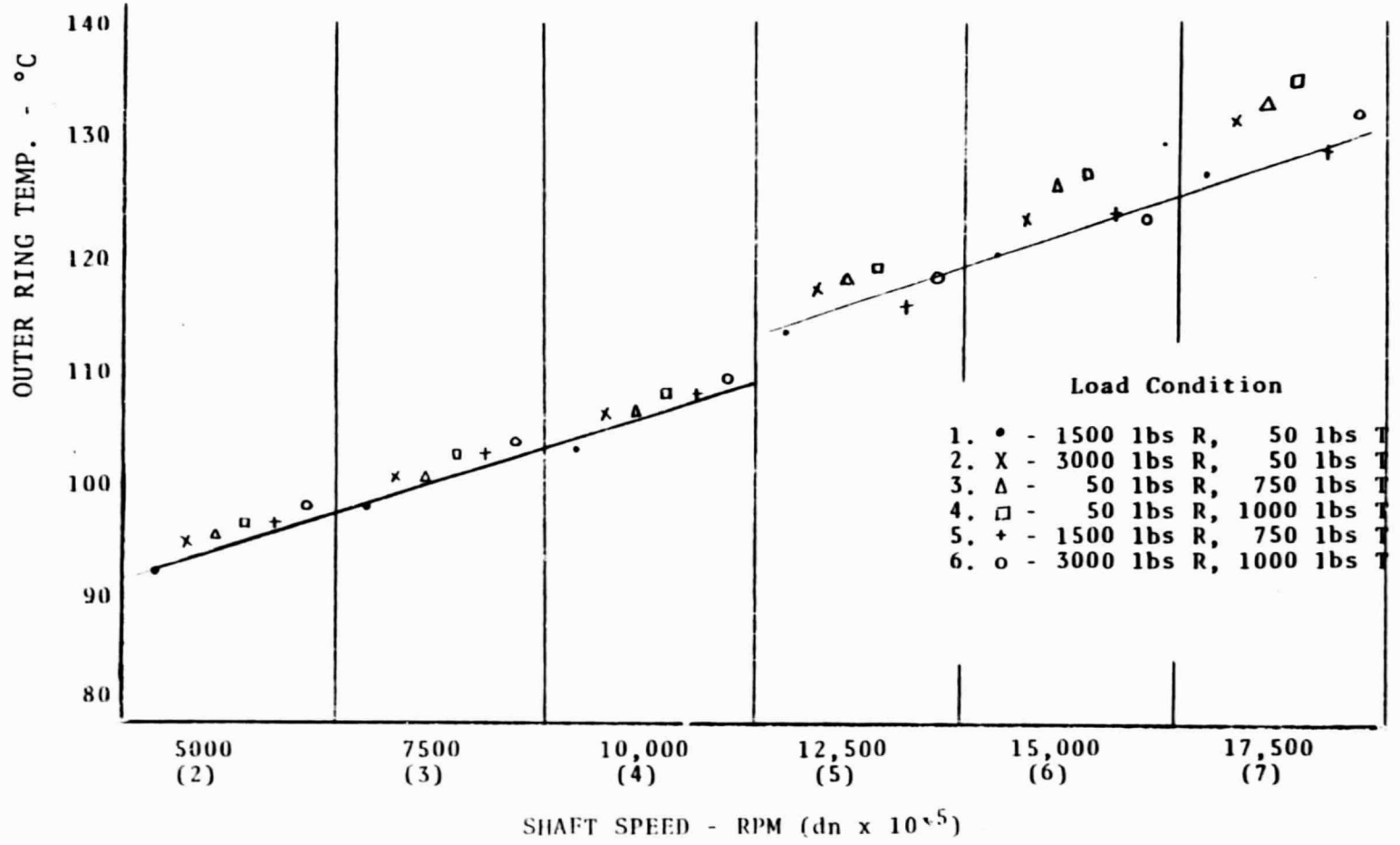

FIGURE A18

Test Series F-1

PERCENT SLIP DETERMINED FROM MEASURED CAGE TO SHAFT SPEED RATIO AND COMPARED TO THE THEORETICAL ZERO SLIP RATIO OF 0.4030

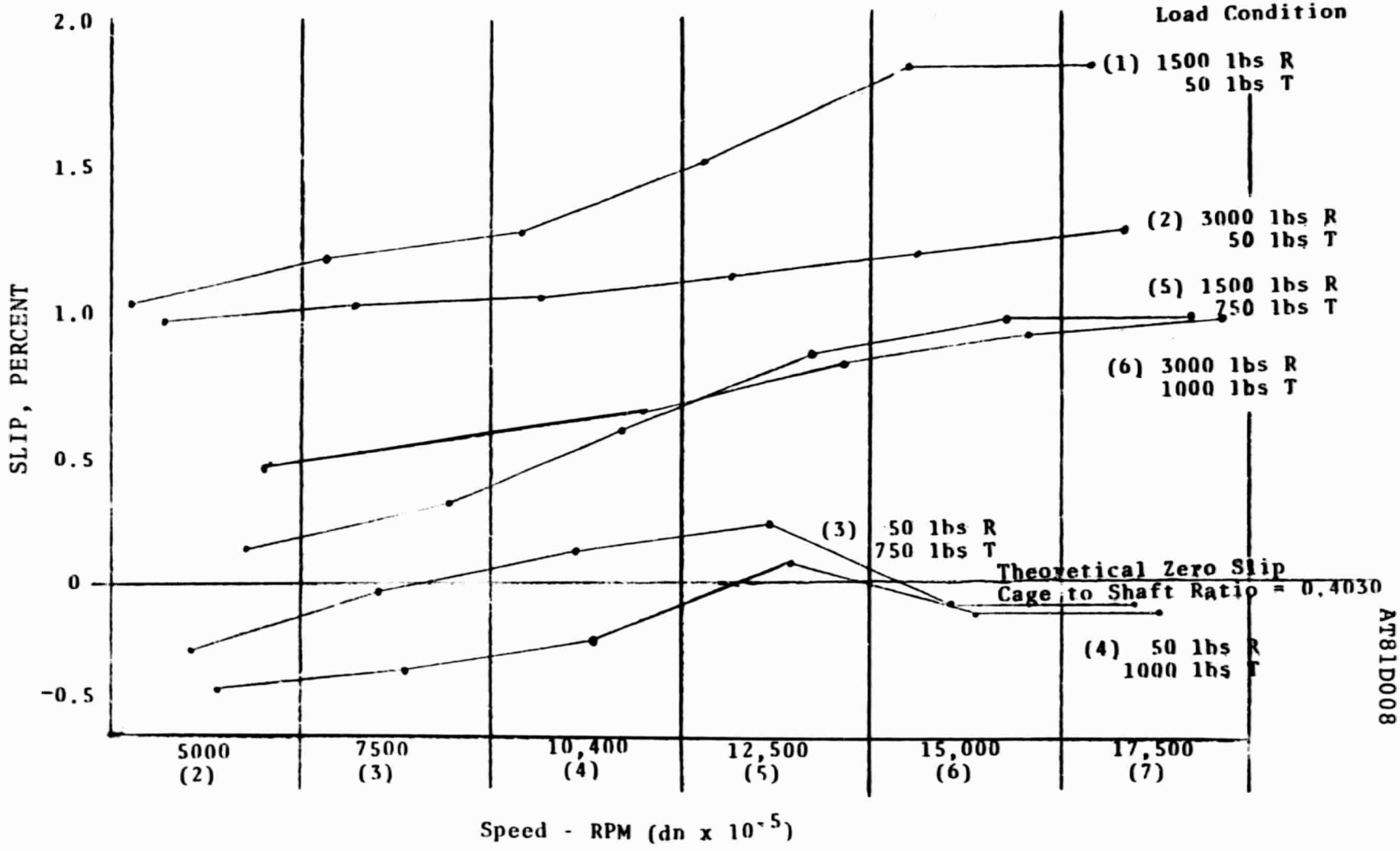

FIGURE A19

PLOT OF BEARING DRAG TORQUE FROM SERIES F1 & F2 SHOWING MEASURED DIFFERENCES UNDER SAME OPERATING CONDITIONS AND TEST BEARING

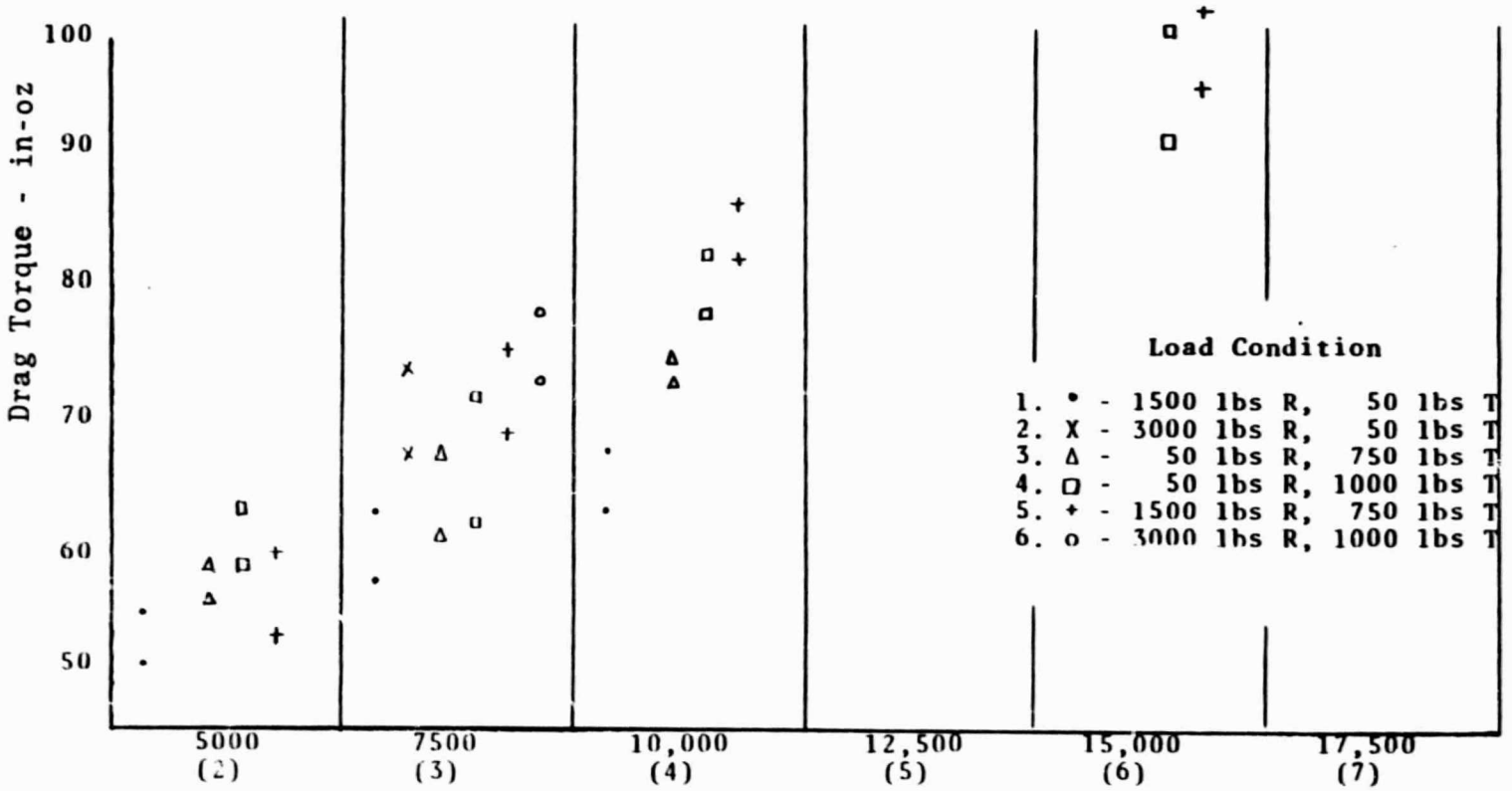

AT81D008

FIGURE A20

INNER RING TEMPERATURE VS. SHAFT SPEED & LOAD CONDITIONS

TEST SERIES G

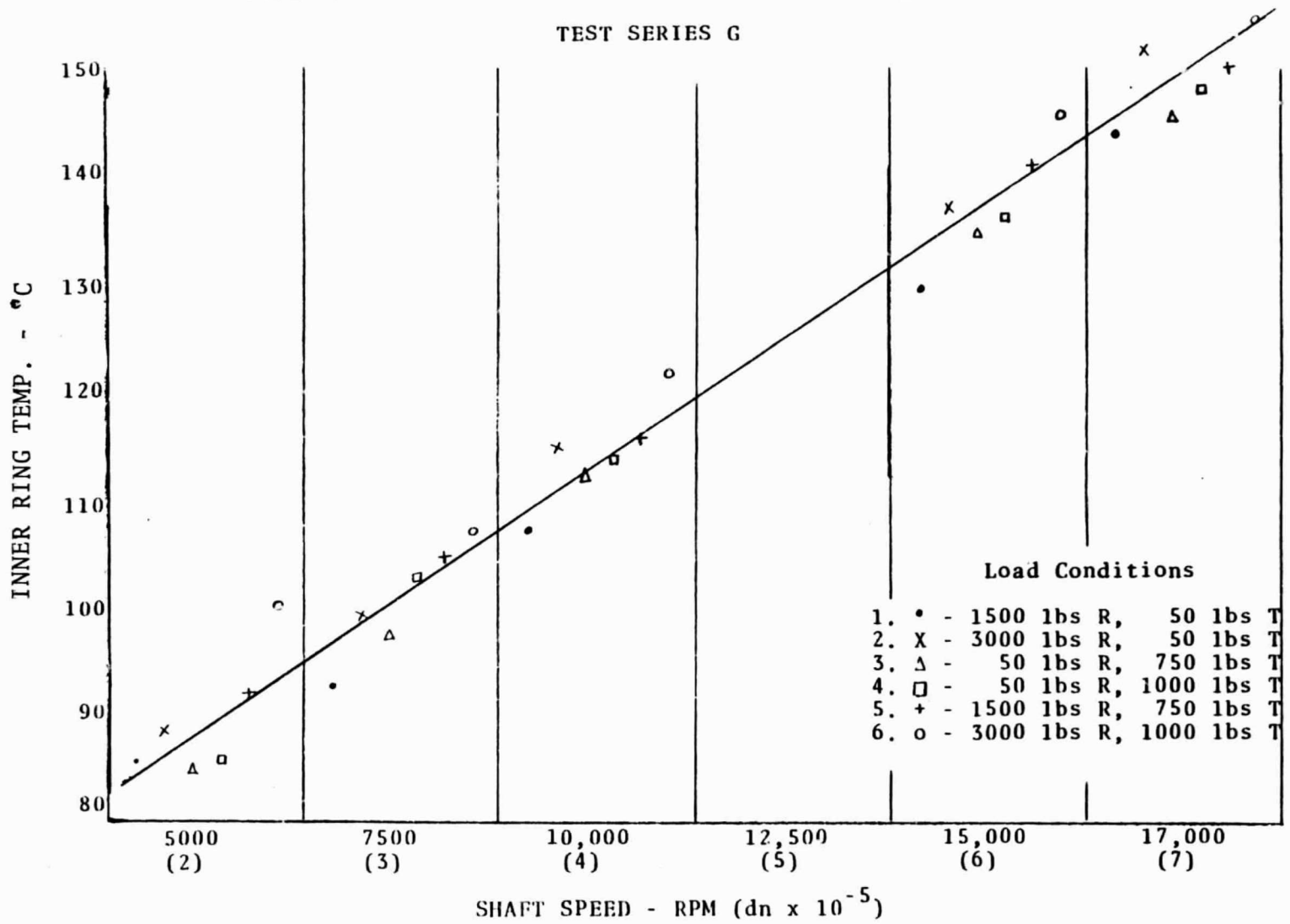

AT81D008

FIGURE A21

OUTER RING TEMPERATURE VS. SHAFT SPEED & LOAD CONDITIONS

TEST SERIES G

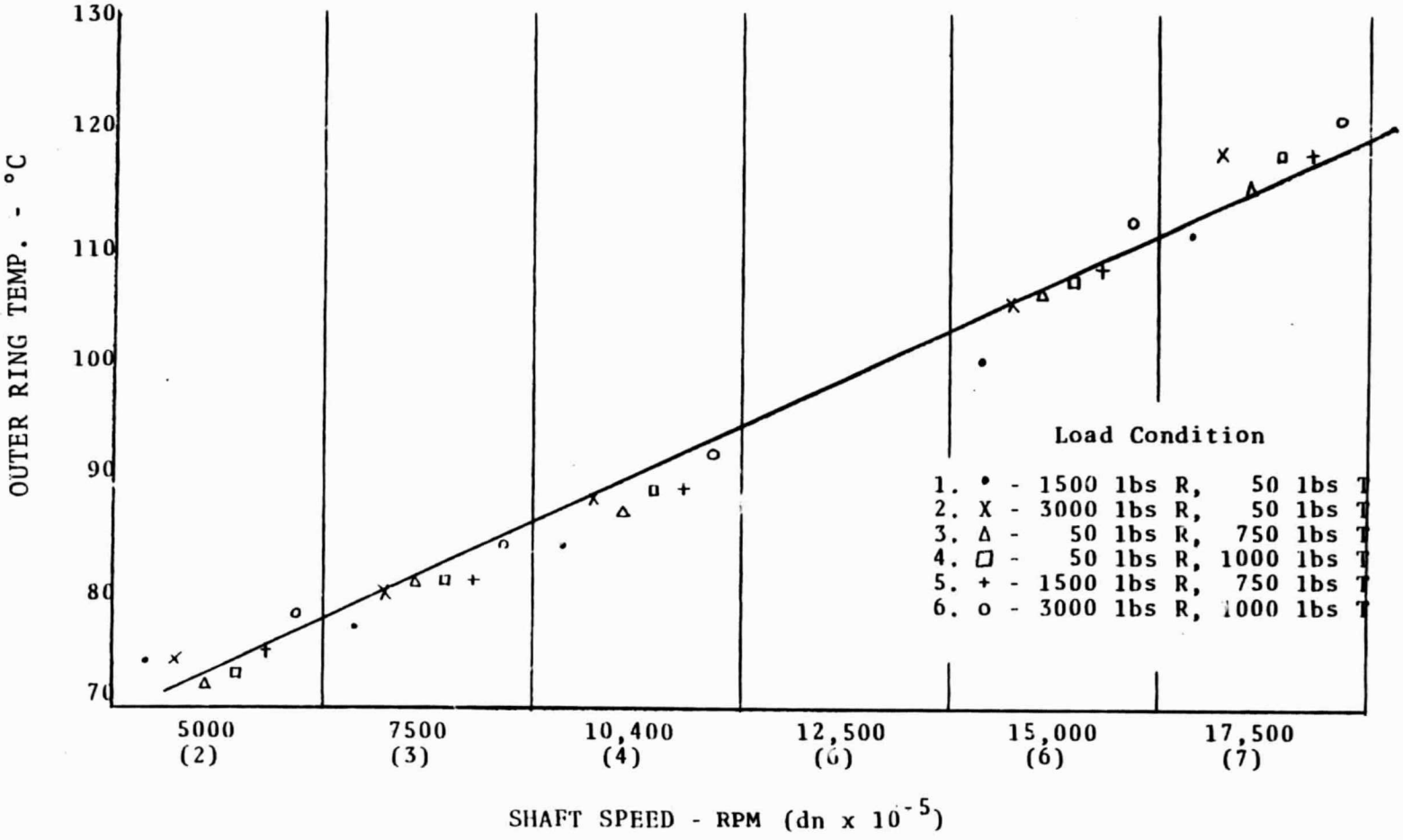

AT81D008

FIGURE A22

Test Series G

PERCENT SLIP DETERMINED FROM MEASURED CAGE TO SHAFT SPEED RATIO AND COMPARED TO THE THEORETICAL ZERO SLIP RATIO OF 0.4030

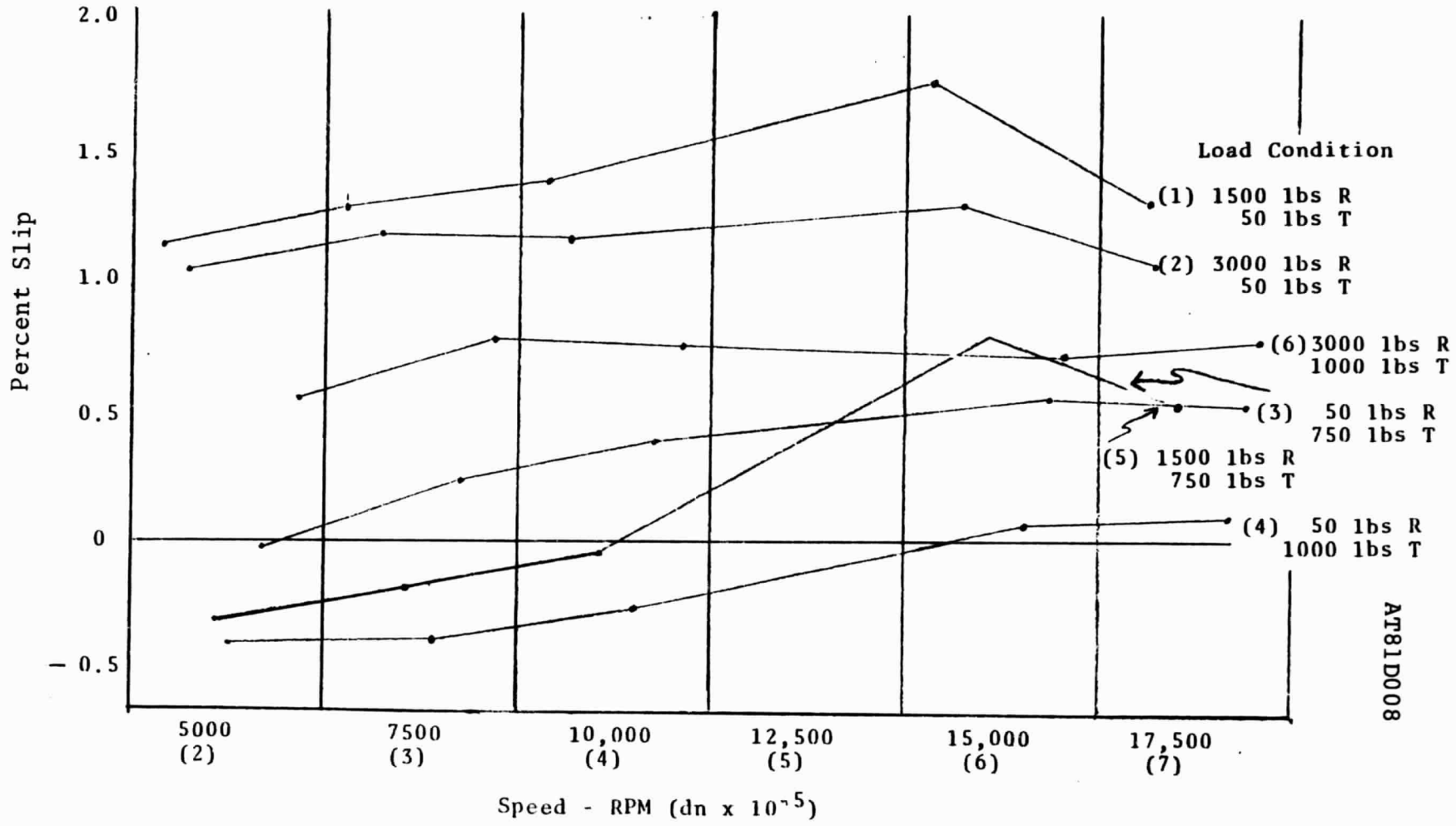

FIGURE A23

INNER RING TEMPERATURE VS. SHAFT SPEED & LOAD CONDITIONS

TEST SERIES H

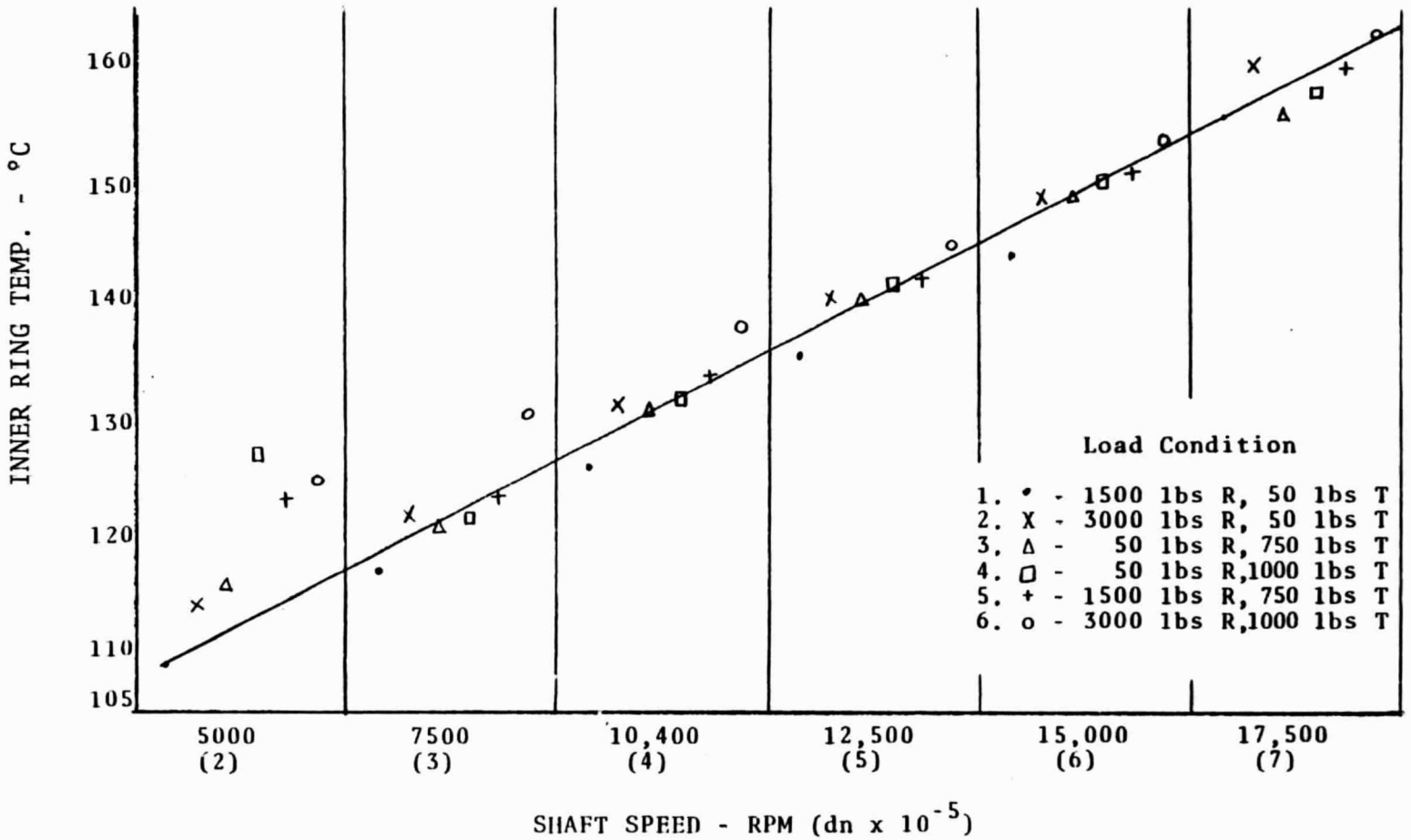

AT81D008

FIGURE A24

OUTER RING TEMPERATURE VS. SHAFT SPEED & LOAD CONDITIONS

TEST SERIES H

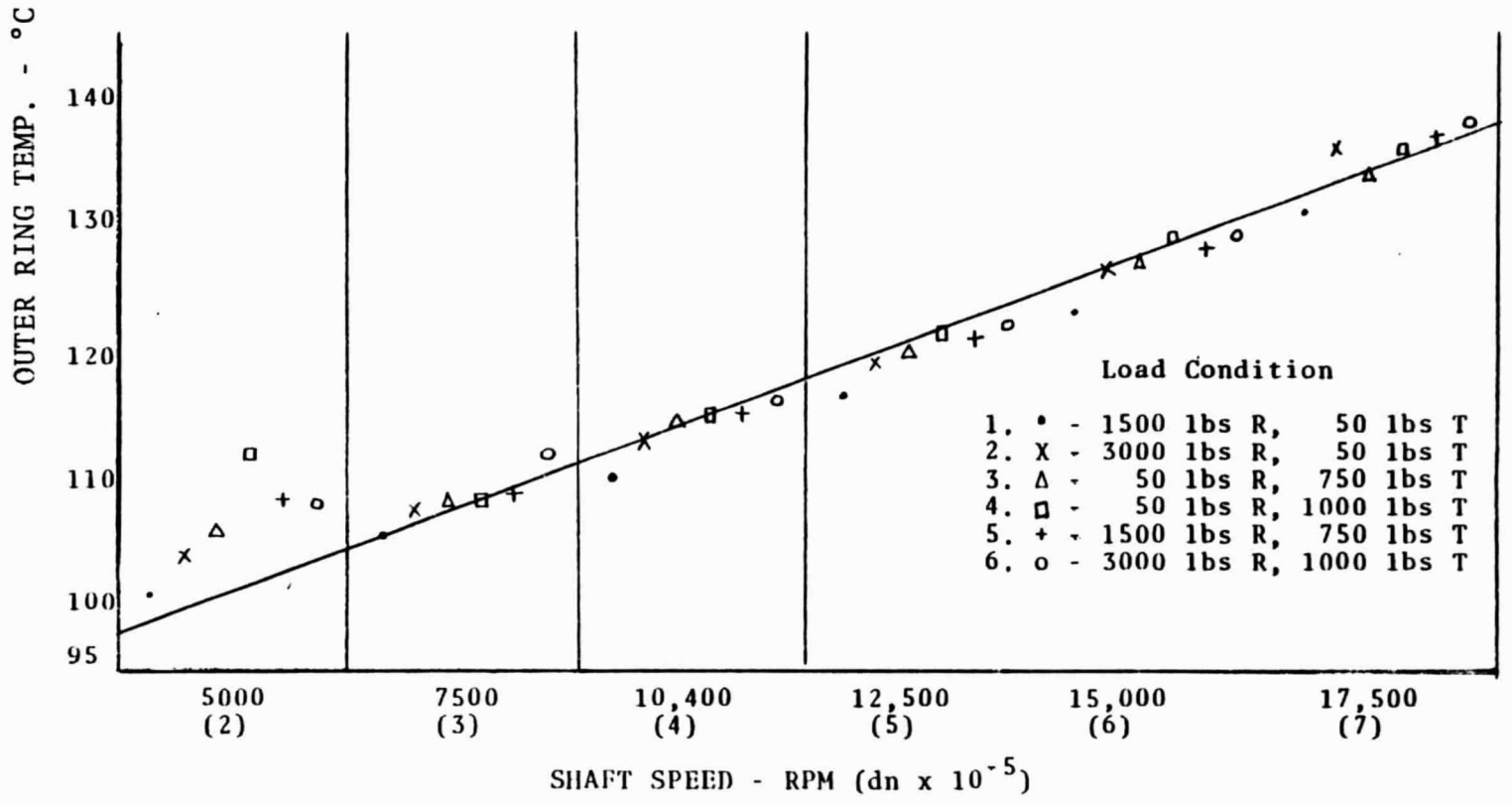

AT81D008

FIGURE A25

PERCENT SLIP DETERMINED FROM MEASURED CAGE TO SHAFT SPEED RATIO AND COMPARED TO THE THEORETICAL ZERO SLIP RATIO OF 0.4030

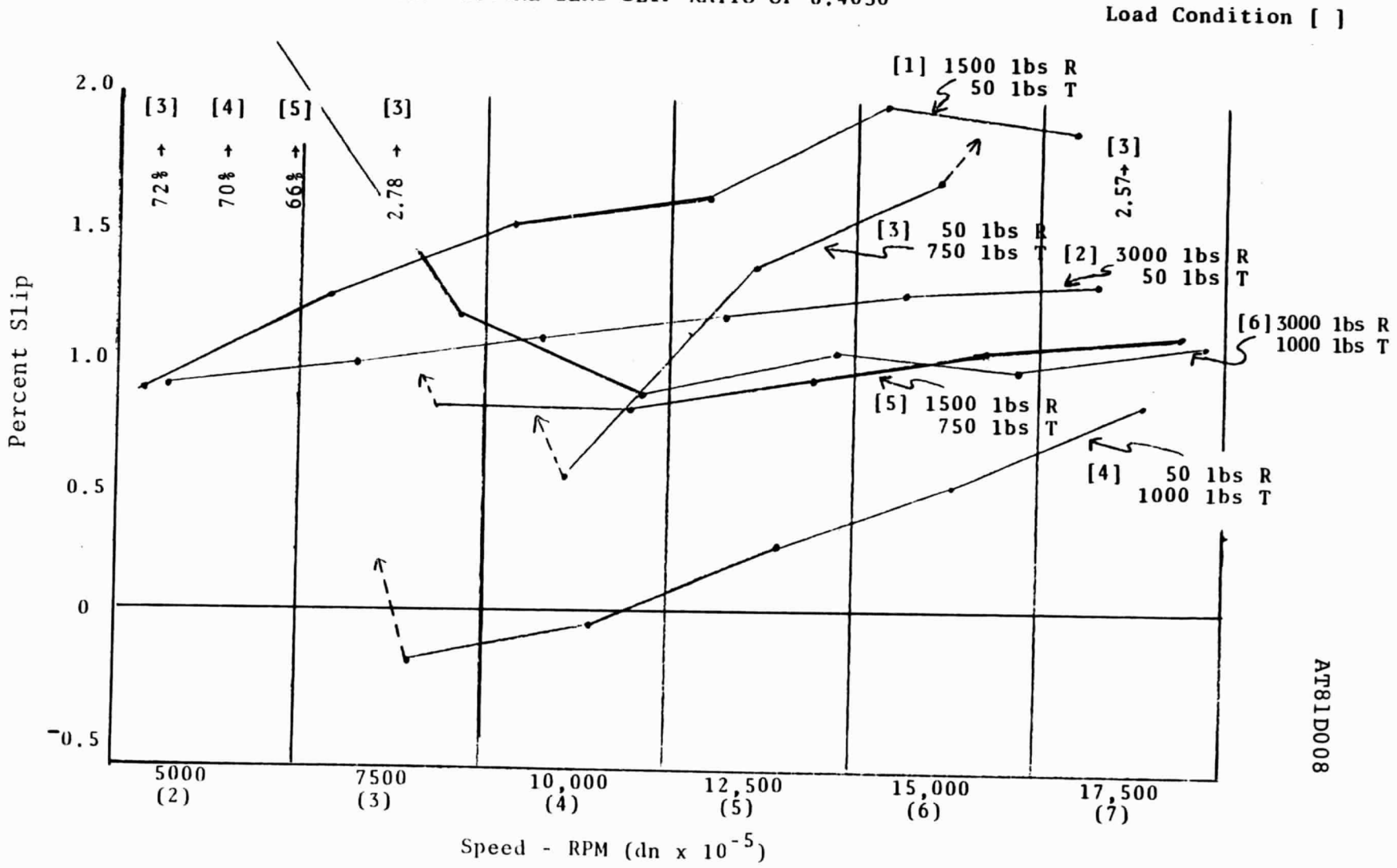

AT81D008

Test Bearing 02
with Split Cage Following
Series H Testing

FIGURE A26

ORIGINAL PAGE
BLACK AND WHITE PHOTOGRAPH

AT81D008

Outer Ring and Portion of Rollers

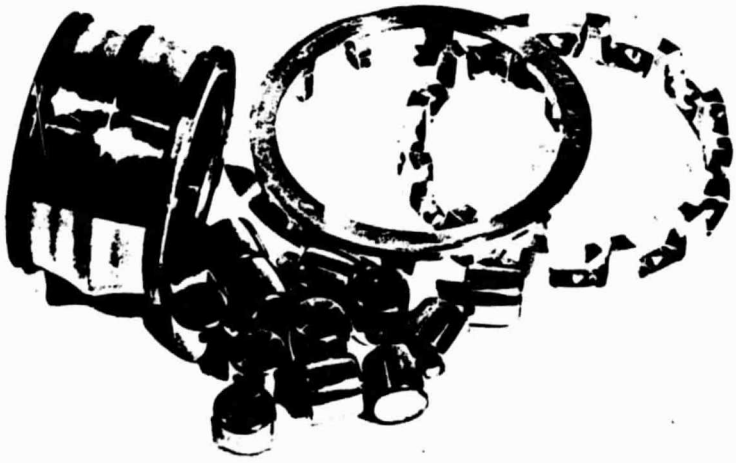

Inner Ring, Split Cage and Portion of Rollers
Component Parts of
Bearing 02 Following Test Series H

FIGURE A27

TABLE A1

MEASURED OSCULATION AND RADIAL LOOSENESS OF TEST BEARINGS

TEST	BASIC TEST DESCRIPTION	BRG. NO.	OSCULATION OUTER	OSCULATION INNER *(SS)	OSCULATION INNER *(PS)	RADIAL LOOSENESS μm/in x 10^3
A	Normal Speed Baseline (Radial Load)	02	0.964	0.980	0.970	75/2.95
B	Normal Speed Baseline (Combined Load)	02	0.964	0.980	0.970	75/2.95
C	Normal Speed Increased Radial Looseness (Radial & Combined Load)	01	0.967	0.987	0.976	99/3.90
D	Normal Speed Inner Ring Osculation Change (Radial & Combined Load)	03	0.965	0.955	0.955	75/2.95
E	Speed Limitation (Radial, Thrust, and Combined Load)	06	0.980	0.956	0.961	75/2.95
F-1	High Speed Autorotation Measurement (Radial, Thrust & Combined Load)	02	0.964	0.980	0.970	75/2.95

TABLE A1
(continued)

MEASURED OSCULATION AND RADIAL LOOSENESS OF TEST BEARINGS

TEST	BASIC TEST DESCRIPTION	BRG. NO.	OSCULATION OUTER	OSCULATION INNER *(SS)	OSCULATION INNER *(PS)	RADIAL LOOSENESS $\mu m/in \times 10^3$
F-2	High Speed Shaft-housing Relative Position (Radial, Thrust & Combined Load)	02	0.964	0.980	0.970	75/2.95
G	High Speed 150°F Oil Inlet Temp. (Radial, Thrust, & Combined Load)	02	0.964	0.980	0.970	75/2.95
H	High Speed Split Cage (Radial, Thrust & Combined Load)	02	0.964	0.980	0.970	75/2.95

* SS stands for stamped side of bearing and was always located outboard on the rig.
PS stands for plain side of bearing.

TABLE A2

Test Series A Data (Brg. No. 02)

Temperature Record

TEST & RUN NO.	OPERATING CONDITION SHAFT SPEED (rpm)	RADIAL LOAD (lb)	THRUST LOAD (lb)	INNER RING TEMP. RTD. NO. 1 (^{o}C)	2 (^{o}C)	3 (^{o}C)	4 (^{o}C)	OUTER RING TEMP. THERMOCOUPLE NO. 1 (^{o}C)	2 (^{o}C)	3 (^{o}C)	4 (^{o}C)	LUBE OIL Temp. In (^{o}C)	Out (^{o}C)	Flow Rate (gpm)	HYDROSTATIC OIL IN TEMP. (^{o}C)
A-1	1000	1500	0	103	-	103	-	104	101	-	102	93	98	0.125	108
A-2	1000	2000	0	104	-	104	-	103	102	-	102	94	99	0.125	108
A-3	1000	2500	0	104	-	104	-	103	101	-	102	93	99	0.125	107
A-4	1000	3000	0	105	-	105	-	103	102	-	102	92	99	0.125	107
A-5	2000	1500	0	104	-	105	-	103	101	-	102	93	99	0.125	108
A-6	2000	2000	0	105	-	105	-	104	102	-	102	93	100	0.125	108
A-7	2000	2500	0	106	-	107	-	104	103	-	103	94	100	0.125	108
A-8	2000	3000	0	107	-	107	-	104	103	-	103	93	100	0.125	108
A-9	3000	1500	0	106	-	106	-	104	102	-	102	93	100	0.125	108
A-10	3000	2000	0	108	-	108	-	104	102	-	103	94	100	0.125	107
A-11	3000	2500	0	107	-	108	-	104	103	-	103	93	100	0.125	107
A-12	3000	3000	0	111	-	112	-	104	105	-	104	93	101	0.125	107
A-13	4000	1500	0	108	-	109	-	104	103	-	103	93	100	0.125	107
A-14	4000	2000	0	109	-	110	-	105	104	-	104	93	100	0.125	107
A-15	4000	2500	0	110	-	111	-	104	104	-	104	93	100	0.125	107
A-16	4000	3000	0	115	-	116	-	105	107	-	106	93	102	0.125	107
A-17	5000	1500	0	107	-	109	-	104	104	-	104	93	100	0.125	107
A-18	5000	2000	0	108	-	110	-	105	105	-	105	93	101	0.125	107
A-19	5000	2500	0	109	-	112	-	105	106	-	106	94	101	0.125	107
A-20	5000	3000	0	114	-	116	-	106	108	-	107	93	102	0.125	107

TABLE A2 (CONTINUED)

Proximity Probe Measurements

TEST & RUN NO.	OPERATING CONDITION SHAFT SPEED / RADIAL LOAD / THRUST LOAD	PROBE NO.	RMS DISTANCE FROM PROBE TO MEASURED SURFACE 1 In.	2 In.	3 In.	4 In.	5 In.	6 In.	7 In.	8 In.	9 In.
0	0 / 0 / 0 At operating temp.		.03015	.03375	.03790	.01406	.01017	.01812	.02769	.03048	.03487
A-1	1000 / 1500 / 0		.03075	.03398	.03707	.01818	.01522	.02140	.02228	.03231	.04023
A-2	1000 / 2000 / 0		.03101	.03434	.03768	.01834	.01578	.02151	.02200	.03268	.04117
A-3	1000 / 2500 / 0		.03101	.03422	.03777	.01839	.01596	.02142	.02174	.03279	.04148
A-4	1000 / 3000 / 0		.03106	.03423	.03811	.01845	.01633	.02118	.02122	.03310	.04199
A-5	2000 / 1500 / 0		.03123	.03447	.03765	.01864	.01572	.02171	.02234	.03319	.04090
A-6	2000 / 2000 / 0		.03119	.03438	.03773	.01857	.01587	.02154	.02203	.03316	.04123
A-7	2000 / 2500 / 0		.03108	.03425	.03786	.01846	.01605	.02137	.02170	.03309	.04154
A-8	2000 / 3000 / 0		.03093	.03398	.03804	.01836	.01638	.02101	.02102	.03309	.04210
A-9	3000 / 1500 / 0		.03063	.03351	.03809	.01813	.01593	.02083	.02128	.03266	.04124
A-10	3000 / 2000 / 0		.03069	.03369	.03801	.01817	.01609	.02052	.02093	.03252	.04144
A-11	3000 / 2500 / 0		.03055	.03334	.03815	.01809	.01623	.02057	.02067	.03279	.04170
A-12	3000 / 3000 / 0		.03040	.03295	.03838	.01799	.01669	.02008	.01978	.03284	.04234
A-13	4000 / 1500 / 0		.03062	.03349	.03797	.01819	.01601	.02090	.02135	.03269	.04117
A-14	4000 / 2000 / 0		.03047	.03327	.03791	.01806	.01611	.02067	.02089	.03261	.04136
A-15	4000 / 2500 / 0		.03045	.03317	.03800	.01803	.01624	.02054	.02061	.03265	.04162
A-16	4000 / 3000 / 0		.03026	.03278	.03818	.01793	.01657	.02012	.01986	.03269	.04206
A-17	5000 / 1500 / 0		.03025	.03227	.03920	.01819	.01715	.01973	.01940	.03292	.04249
A-18	5000 / 2000 / 0		.03019	.03209	.03921	.01811	.01727	.01953	.01906	.03288	.04266
A-19	5000 / 2500 / 0		.03018	.03202	.03928	.01808	.01740	.01942	.01882	.03290	.04287
A-20	5000 / 3000 / 0		.02995	.03157	.03937	.01793	.01769	.01895	.01799	.03288	.04328

TABLE A2 (CONTINUED)

Bearing Drag Torque And Cage/Shaft Speed Ratio Measurements

TEST & RUN NO.	OPERATING CONDITION SHAFT SPEED rpm	RADIAL LOAD lbs	THRUST LOAD lbs	DRAG TORQUE in - oz	SPEED RATIO
A-1	1000	1500	0	21	0.3990
A-2	1000	2000	0	37	0.3994
A-3	1000	2500	0	47	0.3997
A-4	1000	3000	0	67	0.4000
A-5	2000	1500	0	23	0.3987
A-6	2000	2000	0	38	0.3989
A-7	2000	2500	0	45	0.3991
A-8	2000	3000	0	58	0.3995
A-9	3000	1500	0	30	0.3986
A-10	3000	2000	0	47	0.3990
A-11	3000	2500	0	54	0.3991
A-12	3000	3000	0	71	0.3994
A-13	4000	1500	0	38	0.3983
A-14	4000	2000	0	51	0.3987
A-15	4000	2500	0	59	0.3990
A-16	4000	3000	0	68	0.3992
A-17	5000	1500	0	45	0.3982
A-18	5000	2000	0	57	0.3986
A-19	5000	2500	0	74	0.3987
A-20	5000	3000	0	89	0.3991

TABLE A3

Test Series B Data (Brg. No. 02)

Temperature Record

TEST & RUN NO.	OPERATING CONDITION SHAFT SPEED (rpm)	RADIAL LOAD (lb)	THRUST LOAD (lb)	INNER RING TEMP. RTD. NO. 1 (^{o}C)	2 (^{o}C)	3 (^{o}C)	4 (^{o}C)	OUTER RING TEMP. THERMOCOUPLE NO. 1 (^{o}C)	2 (^{o}C)	3 (^{o}C)	4 (^{o}C)	LUBE OIL Temp. In (^{o}C)	Out (^{o}C)	Flow Rate (gpm)	HYDROSTATIC OIL IN TEMP. (^{o}C)
B-1	1000	1500	700	101	-	100	-	100	99	-	99	93	95	0.125	103
B-2	1000	2000	700	101	-	101	-	100	99	-	100	93	95	0.125	103
B-3	1000	2500	830	101	-	100	-	100	99	-	100	93	95	0.125	103
B-4	1000	3000	1000	103	-	102	-	101	100	-	101	93	96	0.125	103
B-5	2000	1500	700	103	-	104	-	101	100	-	101	93	97	0.125	104
B-6	2000	2000	700	104	-	105	-	101	101	-	102	94	97	0.125	104
B-7	2000	2500	830	105	-	104	-	101	100	-	100	92	97	0.125	103
B-8	2000	3000	1000	108	-	105	-	101	101	-	102	93	98	0.125	103
B-9	3000	1500	700	104	-	104	-	101	100	-	101	92	97	0.125	103
B-10	3000	2000	700	107	-	107	-	101	101	-	102	93	98	0.125	104
B-11	3000	2500	830	110	-	109	-	102	102	-	103	93	98	0.125	104
B-12	3000	3000	1000	111	-	110	-	103	104	-	104	93	99	0.125	104
B-13	4000	1500	700	106	-	107	-	102	102	-	102	91	98	0.125	104
B-14	4000	2000	700	107	-	107	-	102	102	-	103	91	98	0.125	104
B-15	4000	2500	830	113	-	112	-	103	104	-	104	92	99	0.125	104
B-16	4000	3000	1000	117	-	116	-	104	106	-	106	92	102	0.125	104
B-17	5000	1500	700	108	-	109	-	102	102	-	103	92	99	0.125	104
B-18	5000	2000	700	112	-	112	-	102	104	-	104	94	99	0.125	104
B-19	5000	2500	830	117	-	116	-	103	106	-	106	93	101	0.125	104
B-20	5000	3000	1000	119	-	118	-	104	107	-	107	94	102	0.125	104

TABLE A3 (CONTINUED)

Proximity Probe Measurements

TEST & RUN NO.	OPERATING CONDITION SHAFT SPEED	RADIAL LOAD	THRUST LOAD	PROBE NO.	RMS DISTANCE FROM PROBE TO MEASURED SURFACE 1	2	3	4	5	6	7	8	9
	rpm	lbs	lbs		In.	In.	In.	In.	In.	In.	In.	In.	In.
0	0	/ 0	/ 0		.02976	.03166	.03950	.01847	.01733	.01965	.01980	.03007	.04275
B-1	1000	/ 1500	/ 700		.03083	.03283	.04092	.01528	.01459	.01659	.01944	.03304	.04239
B-2	1000	/ 2000	/ 700		.03071	.03264	.04048	.01686	.01650	.01815	.01871	.03343	.04339
B-3	1000	/ 2500	/ 830		.03053	.03240	.04047	.01675	.01662	.01784	.01826	.03343	.04359
B-4	1000	/ 3000	/ 1000		.03041	.03297	.04070	.01726	.01694	.01725	.01727	.03360	.04429
B-5	2000	/ 1500	/ 700		.03030	.03170	.04094	.01341	.01285	.01486	.01969	.03273	.04187
B-6	2000	/ 2000	/ 700		.03036	.03219	.04025	.01607	.01576	.01738	.01879	.03315	.04302
B-7	2000	/ 2500	/ 830		.03035	.03214	.04027	.01621	.01600	.01732	.01837	.03321	.04328
B-8	2000	/ 3000	/ 1000		.03016	.03176	.04029	.01621	.01635	.01708	.01767	.03324	.04369
B-9	3000	/ 1500	/ 700										
B-10	3000	/ 2000	/ 700		.03049	.03217	.04052	.00972	.01275	.01548	.02013	.03281	.04175
B-11	3000	/ 2500	/ 830		.03035	.03217	.04009	.01490	.01408	.01649	.01949	.03294	.04231
B-12	3000	/ 3000	/ 1000		.03031	.03217	.03986	.01570	.01509	.01711	.01881	.03308	.04293
B-13	4000	/ 1500	/ 700		.03035	.03183	.04066	.01248	.01138	.01443	.02068	.03249	.04105
B-14	4000	/ 2000	/ 700		.03026	.03191	.04033	.01290	.01266	.01544	.02009	.03262	.04162
B-15	4000	/ 2500	/ 830		.03031	.03191	.03995	.01453	.01367	.01623	.01957	.03276	.04205
B-16	4000	/ 3000	/ 1000		.03000	.03183	.03958	.01589	.01546	.01724	.01843	.03294	.04288
B-17	5000	/ 1500	/ 700		.03026	.03174	.04052	.01243	.01133	.01443	.02068	.03231	.04092
B-18	5000	/ 2000	/ 700		.03017	.03183	.04009	.01393	.01298	.01575	.02000	.03253	.04162
B-19	5000	/ 2500	/ 830		.03009	.03183	.03972	.01509	.01431	.01671	.01940	.03271	.04218
B-20	5000	/ 3000	/ 1000		.03000	.03178	.03953	.01561	.01505	.01715	.01881	.03281	.04258

TABLE A3 (CONTINUED)

Bearing Drag Torque and Cage/Shaft Speed Ratio Measurements

TEST & RUN NO.	OPERATING CONDITION SHAFT SPEED	RADIAL LOAD	THRUST LOAD	DRAG TORQUE	SPEED RATIO
	rpm	lbs	lbs	in-oz	
B-1	1000	1500	700	46	0.4026
B-2	1000	2000	700	55	0.4003
B-3	1000	2500	830	66	0.4000
B-4	1000	3000	1000	80	0.4005
B-5	2000	1500	700	53	0.4015
B-6	2000	2000	700	61	0.4006
B-7	2000	2500	830	77	0.4007
B-8	2000	3000	1000	94	0.4001
B-9	3000	1500	700	60	0.4010
B-10	3000	2000	700	76	0.4009
B-11	3000	2500	830	97	0.4009
B-12	3000	3000	1000	111	0.4004
B-13	4000	1500	700	48	0.4006
B-14	4000	2000	700	72	0.4008
B-15	4000	2500	830	97	0.4009
B-16	4000	3000	1000	107	0.4002
B-17	5000	1500	700	57	0.4002
B-18	5000	2000	700	71	0.4004
B-19	5000	2500	830	96	0.4005
B-20	5000	3000	1000	106	0.4003

TABLE A4

Test Series C Data (Brg. No. 01)

Temperature Record

TEST & RUN NO.	OPERATING CONDITION SHAFT SPEED (rpm)	RADIAL LOAD (lb)	THRUST LOAD (lb)	INNER RING TEMP. RTD. NO. 1 (°C)	2 (°C)	3 (°C)	4 (°C)	OUTER RING TEMP. THERMOCOUPLE NO. 1 (°C)	2 (°C)	3 (°C)	4 (°C)	LUBE OIL Temp. In (°C)	Out (°C)	Flow Rate (gpm)	HYDROSTATIC OIL IN TEMP. (°C)
C-1	1000	1500	0	102	103	-	-	98	98	-	100	93	97	0.125	103
C-2	1000	2000	0	103	104	-	-	99	98	-	100	93	99	0.125	103
C-3	1000	2500	0	103	103	-	-	99	99	-	100	93	100	0.125	103
C-4	1000	3000	0	104	104	-	-	99	99	-	101	93	100	0.125	103
C-5	2000	1500	0	102	103	-	-	99	99	-	100	94	100	0.125	103
C-6	2000	2000	0	104	104	-	-	99	99	-	100	93	100	0.125	103
C-7	2000	2500	0	106	106	-	-	101	100	-	101	94	101	0.125	103
C-8	2000	3000	0	107	107	-	-	101	100	-	101	93	-	0.125	103
C-9	3000	1500	0	104	105	-	-	99	99	-	100	93	101	0.125	103
C-10	3000	2000	0	106	106	-	-	101	101	-	101	93	102	0.125	103
C-11	3000	2500	0	107	108	-	-	101	101	-	102	93	102	0.125	103
C-12	3000	3000	0	109	109	-	-	103	102	-	103	94	103	0.125	103
C-13	4000	1500	0	106	107	-	-	101	101	-	102	93	102	0.125	103
C-14	4000	2000	0	109	109	-	-	102	102	-	103	94	103	0.125	104
C-15	4000	2500	0	110	110	-	-	103	102	-	103	94	103	0.125	104
C-16	4000	3000	0	113	113	-	-	105	104	-	105	94	103	0.125	104
C-17	5000	1500	0	109	110	-	-	102	102	-	103	93	103	0.125	104
C-18	5000	2000	0	111	111	-	-	104	103	-	104	93	103	0.125	104
C-19	5000	2500	0	114	113	-	-	105	105	-	105	93	104	0.125	104
C-20	5000	3000	0	117	116	-	-	107	106	-	106	93	105	0.125	105
C-21	1000	1500	700	104	104	-	-	99	98	-	100	94	100	0.125	102
C-22	1000	2000	700	105	104	-	-	99	98	-	100	92	100	0.125	102
C-23	1000	2500	830	105	105	-	-	100	99	-	101	94	100	0.125	103
C-24	1000	3000	1000	107	106	-	-	101	100	-	101	93	100	0.125	103
C-25	2000	1500	700	107	107	-	-	101	100	-	102	93	102	0.125	103
C-26	2000	2000	700	108	108	-	-	102	101	-	102	93	103	0.125	103
C-27	2000	2500	830	111	110	-	-	103	102	-	104	93	103	0.125	104
C-28	2000	3000	1000	113	113	-	-	105	102	-	104	93	103	0.125	104

TABLE A4
(continued)

Test Series C Data (Brg. No. 01)

Temperature Record

TEST & RUN NO.	OPERATING CONDITION SHAFT SPEED (rpm)	RADIAL LOAD (lb)	THRUST LOAD (lb)	INNER RING TEMP. RTD. NO. 1 (^{o}C)	2 (^{o}C)	3 (^{o}C)	4 (^{o}C)	OUTER RING TEMP. THERMOCOUPLE NO. 1 (^{o}C)	2 (^{o}C)	3 (^{o}C)	4 (^{o}C)	LUBE OIL Temp. In (^{o}C)	Out (^{o}C)	Flow Rate (gpm)	HYDROSTATIC OIL IN TEMP. (^{o}C)
C-29	3000	/ 1500	/ 700	111	110	-	-	104	102	-	104	93	104	0.125	104
C-30	3000	/ 2000	/ 700	111	110	-	-	104	101	-	103	93	103	0.125	104
C-31	3000	/ 2500	/ 830	115	114	-	-	106	103	-	104	94	104	0.125	104
C-32	3000	/ 3000	/ 1000	120	119	-	-	109	105	-	107	95	105	0.125	104
C-33	4000	/ 1500	/ 700	112	111	-	-	104	102	-	104	93	104	0.125	104
C-34	4000	/ 2000	/ 700	114	114	-	-	105	103	-	105	94	104	0.125	104
C-35	4000	/ 2500	/ 830	118	117	-	-	108	104	-	106	94	105	0.125	104
C-36	4000	/ 3000	/ 1000	121	120	-	-	109	105	-	106	93	105	0.125	104
C-37	5000	/ 1500	/ 700	114	113	-	-	105	103	-	105	93	104	0.125	104
C-38	5000	/ 2000	/ 700	117	117	-	-	107	105	-	106	94	105	0.125	104
C-39	5000	/ 2500	/ 830	122	122	-	-	110	105	-	107	92	105	0.125	104
C-40	5000	/ 3000	/ 1000	126	124	-	-	112	107	-	108	93	107	0.125	103

TABLE A4
(continued)

Proximity Probe Measurements

TEST & RUN NO.	OPERATING CONDITION SHAFT SPEED (rpm)	RADIAL LOAD (lbs)	THRUST LOAD (lbs)	PROBE NO.	RMS DISTANCE FROM PPOBE TO MEASURED SURFACE 1 In.	2 In.	3 In.	4 In.	5 In.	6 In.	7 In.	8 In.	9 In.
C-1	1000	1500	0		.03323	.02870	.03792	.01280	.01826	.01882	.02255	.02891	.04550
C-2	1000	2000	0		.03327	.02866	.03811	.01280	.01844	.01868	.02230	.02900	.04585
C-3	1000	2500	0		.03332	.02866	.03840	.01285	.01867	.01860	.02196	.02919	.04633
C-4	1000	3000	0		.03336	.02870	.03863	.01290	.01890	.01851	.02166	.02937	.04672
C-5	2000	1500	0		.03354	.02887	.03830	.01290	.01844	.01899	.02277	.02905	.04594
C-6	2000	2000	0		.03358	.02887	.03844	.01290	.01862	.01890	.02243	.02923	.04638
C-7	2000	2500	0		.03358	.02887	.03863	.01299	.01885	.01886	.02209	.02946	.04672
C-8	2000	3000	0		.03358	.02887	.03877	.01303	.01904	.01868	.02183	.02959	.04699
C-9	3000	1500	0		.03394	.02922	.03863	.01322	.01880	.01943	.02289	.02946	.04659
C-10	3000	2000	0		.03385	.02913	.03873	.01322	.01894	.01921	.02251	.02959	.04681
C-11	3000	2500	0		.03381	.02905	.03887	.01318	.01904	.01906	.02221	.02968	.04703
C-12	3000	3000	0		.03367	.02896	.03892	.01327	.01913	.01882	.02183	.02986	.04716
C-13	4000	1500	0		.03398	.02930	.03873	.01336	.01885	.01952	.02302	.02950	.04659
C-14	4000	2000	0		.03385	.02913	.03882	.01332	.01904	.01912	.02251	.02964	.04685
C-15	4000	2500	0		.03385	.02905	.03887	.01332	.01917	.01917	.02230	.02968	.04707
C-16	4000	3000	0		.03376	.02883	.03896	.01322	.01927	.01886	.02183	.02977	.04725
C-17	5000	1500	0		.03403	.02926	.03872	.01336	.01894	.01956	.02302	.02946	.04659
C-18	5000	2000	0		.03389	.02913	.03877	.01327	.01904	.01934	.02264	.02973	.04677
C-19	5000	2500	0		.03381	.02900	.03887	.01332	.01917	.01917	.02230	.02977	.04699
C-20	5000	3000	0		.03376	.02883	.03892	.01332	.01931	.01895	.02179	.02986	.04721
C-21	1000	1500	70		.03332	.02913	.04071	.00874	.01138	.01241	.02387	.02973	.04432
C-22	1000	2000	70		.03327	.02922	.04042	.00780	.01280	.01346	.02315	.02982	.04493
C-23	1000	2500	83.3		.03336	.02961	.04009	.00981	.01468	.01496	.02222	.03027	.04585
C-24	1000	3000	100		.03305	.02961	.04005	.01065	.01546	.01522	.02151	.03068	.04611
C-25	2000	1500	70		.03301	.02900	.04080	.00617	.01115	.01202	.02370	.02982	.04415
C-26	2000	2000	70		.03296	.02900	.04080	.00673	.01170	.01219	.02324	.03000	.04458
C-27	2000	2500	83.3		.03283	.02900	.04085	.00724	.01220	.01232	.02273	.03027	.04494
C-28	2000	3000	100		.03261	.02900	.04061	.00841	.01312	.01289	.02206	.03054	.04524

TABLE A4
(continued)

Proximity Probe Measurements

TEST & RUN NO.	OPERATING CONDITION SHAFT SPEED rpm	RADIAL LOAD lbs	THRUST LOAD lbs	PROBE NO.	RMS DISTANCE FROM PPOBE TO MEASURED SURFACE 1 In.	2 In.	3 In.	4 In.	5 In.	6 In.	7 In.	8 In.	9 In.
C-29	3000	1500	70		.03345	.02891	.04052	.00607	.01151	.01254	.02387	.02941	.04454
C-30	3000	2000	70		.03332	.02887	.04042	.00692	.01225	.01289	.02315	.02959	.04489
C-31	3000	2500	83.3		.03301	.02874	.04028	.00762	.01284	.01316	.02222	.02977	.04511
C-32	3000	3000	100		.03265	.02865	.04014	.00850	.01362	.01342	.02151	.03014	.04537
C-33	4000	1500	70		.03319	.02848	.04009	.00589	.01147	.01254	.02370	.02891	.04424
C-34	4000	2000	70		.03314	.02848	.03995	.00678	.01225	.01303	.02324	.02905	.04463
C-35	4000	2500	83.3		.03279	.02830	.03962	.00776	.01312	.01351	.02273	.02923	.04480
C-36	4000	3000	100		.03257	.02830	.03958	.00841	.01367	.01368	.02206	.02950	.04511
C-37	5000	1500	70		.03327	.02826	.03986	.00561	.01147	.01268	.02399	.02851	.04415
C-38	5000	2000	70		.03310	.02826	.03976	.00673	.01234	.01311	.02336	.02878	.04450
C-39	5000	2500	83.3		.03279	.02813	.03943	.00780	.01326	.01368	.02269	.02896	.04472
C-40	5000	3000	100		.03252	.02800	.03939	.00822	.01362	.01368	.02193	.02914	.04493

TABLE A4
(continued)

Bearing Drag Torque and Cage/Shaft Speed Ratio Measurements

TEST & RUN NO.	OPERATING CONDITION SHAFT SPEED (rpm)	RADIAL LOAD (lbs)	THRUST LOAD (lbs)	DRAG TORQUE (IN-OZ)	SPEED RATIO
C-1	1000	1500	0	37	0.4005
C-2	1000	2000	0	46	0.4007
C-3	1000	2500	0	57	0.4008
C-4	1000	3000	0	89	0.4013
C-5	2000	1500	0	33	0.4006
C-6	2000	2000	0	42	0.4011
C-7	2000	2500	0	53	0.4015
C-8	2000	3000	0	64	0.4017
C-9	3000	1500	0	31	0.4002
C-10	3000	2000	0	42	0.4008
C-11	3000	2500	0	53	0.4012
C-12	3000	3000	0	53	0.4015
C-13	4000	1500	0	42	0.3998
C-14	4000	2000	0	53	0.4005
C-15	4000	2500	0	60	0.4007
C-16	4000	3000	0	73	0.4012
C-17	5000	1500	0	50	0.3995
C-18	5000	2000	0	57	0.4000
C-19	5000	2500	0	64	0.4004
C-20	5000	3000	0	73	0.4007
C-21	1000	1500	700	71	0.4035
C-22	1000	2000	700	76	0.4027
C-23	1000	2500	830	90	0.4024
C-24	1000	3000	1000	111	0.4022
C-25	2000	1500	700	71	0.4029
C-26	2000	2000	700	78	0.4028
C-27	2000	2500	830	95	0.4028
C-28	2000	3000	1000	111	0.4028

TABLE A4
(continued)

TEST & RUN NO.	OPERATING CONDITION SHAFT SPEED (rpm)	RADIAL LOAD (lbs)	THRUST LOAD (lbs)	DRAG TORQUE (IN-OZ)	SPEED RATIO
C-29	3000	1500	700	66	0.4025
C-30	3000	2000	700	85	0.4027
C-31	3000	2500	830	93	0.4030
C-32	3000	3000	1000	119	0.4031
C-33	4000	1500	700	70	0.4021
C-34	4000	2000	700	76	0.4026
C-35	4000	2500	830	90	0.4029
C-36	4000	3000	1000	116	0.4029
C-37	5000	1500	700	69	0.4016
C-38	5000	2000	700	88	0.4021
C-39	5000	2500	830	95	0.4026
C-40	5000	3000	1000	121	0.4026

TABLE A5

Test Series D Data (Brg. No. 03)

Temperature Record

TEST & RUN NO.	OPERATING CONDITION SHAFT SPEED (rpm)	RADIAL LOAD (lb)	THRUST LOAD (lb)	INNER RING TEMP. RTD. NO. 1 (°C)	2 (°C)	3 (°C)	4 (°C)	OUTER RING TEMP. THERMOCOUPLE NO. 1 (°C)	2 (°C)	3 (°C)	4 (°C)	LUBE OIL Temp. In (°C)	Out (°C)	Flow Rate (gpm)	HYDROSTATIC OIL IN TEMP. (°C)
D-1	1000	1500	0	93	94	-	93	91	90	89	91	91	90	0.125	88
D-2	1000	2000	0	94	95	-	95	92	92	91	92	94	91	0.125	89
D-3	1000	2500	0	95	96	-	95	93	92	91	92	94	91	0.125	89
D-4	1000	3000	0	97	98	-	97	93	93	92	93	93	92	0.125	89
D-5	2000	1500	0	94	95	-	94	92	91	90	92	92	91	0.125	89
D-6	2000	2000	0	97	98	-	97	92	93	92	94	94	93	0.125	89
D-7	2000	2500	0	98	99	-	98	94	94	93	94	93	93	0.125	89
D-8	2000	3000	0	100	101	-	100	96	95	93	95	94	94	0.125	89
D-9	3000	1500	0	95	97	-	96	93	92	91	93	93	92	0.125	89
D-10	3000	2000	0	98	99	-	98	98	94	93	92	94	93	0.125	89
D-11	3000	2500	0	100	102	-	101	96	95	94	95	94	94	0.125	90
D-12	3000	3000	0	103	104	-	103	97	96	95	96	92	95	0.125	90
D-13	4000	1500	0	96	98	-	97	94	93	92	94	93	93	0.125	90
D-14	4000	2000	0	99	100	-	99	95	94	93	95	92	93	0.125	90
D-15	4000	2500	0	100	102	-	101	96	95	94	95	92	94	0.125	90
D-16	4000	3000	0	104	105	-	104	97	97	95	97	92	95	0.125	90
D-17	5000	1500	0	99	101	-	99	94	94	93	95	92	93	0.125	89
D-18	5000	2000	0	101	103	-	102	96	95	94	96	93	94	0.125	89
D-19	5000	2500	0	104	105	-	104	97	96	95	97	93	95	0.125	89
D-20	5000	3000	0	106	108	-	107	99	98	96	98	93	97	0.125	89
D-21	1000	1500	700	96	97	-	96	93	91	92	93	93	91	0.125	89
D-22	1000	2000	700	98	99	-	98	93	91	92	93	93	91	0.125	89
D-23	1000	2500	830	100	100	-	100	95	92	93	93	95	92	0.125	89
D-24	1000	3000	1000	101	102	-	101	96	92	93	94	93	93	0.125	89
D-25	2000	1500	700	99	100	-	99	94	92	93	93	92	92	0.125	89
D-26	2000	2000	700	100	101	-	101	95	92	93	93	92	92	0.125	89
D-27	2000	2500	830	104	105	-	104	97	93	95	95	94	94	0.125	89
D-28	2000	3000	1000	108	109	-	108	99	95	97	96	94	95	0.125	89

TABLE A5
(continued)

Temperature Record

TEST & RUN NO.	OPERATING CONDITION SHAFT SPEED (rpm)	RADIAL LOAD (lb)	THRUST LOAD (lb)	INNER RING TEMP. RTD. NO. 1 (°C)	2 (°C)	3 (°C)	4 (°C)	OUTER RING TEMP. THERMOCOUPLE NO. 1 (°C)	2 (°C)	3 (°C)	4 (°C)	LUBE OIL Temp. In (°C)	Out (°C)	Flow Rate (gpm)	HYDROSTATIC OIL IN TEMP. (°C)
D-29	3000	1500	700	103	104	-	104	97	93	95	95	93	94	0.125	89
D-30	3000	2000	700	105	106	-	106	97	94	96	96	94	95	0.125	89
D-31	3000	2500	830	109	109	-	109	99	95	97	96	94	95	0.125	89
D-32	3000	3000	1000	113	114	-	114	102	96	97	97	93	97	0.125	89
D-33	4000	1500	700	106	107	-	106	98	94	96	96	93	95	0.125	89
D-34	4000	2000	700	109	110	-	110	100	95	98	97	94	95	0.125	89
D-35	4000	2500	830	113	113	-	113	101	96	99	98	93	97	0.125	89
D-36	4000	3000	1000	119	118	-	122	105	98	102	100	93	99	0.125	89
D-37	5000	1500	700	108	109	-	-	99	97	98	98	93	95	0.125	89
D-38	5000	2000	700	110	110	-	-	100	96	98	98	93	96	0.125	89
D-39	5000	2500	830	115	115	-	-	103	97	100	99	93	98	0.125	89
D-40	5000	3000	1000	123	122	-	-	108	100	103	102	93	102	0.125	89

TABLE A5
(continued)

Proximity Probe Measurements

TEST & RUN NO.	OPERATING CONDITION SHAFT SPEED (rpm)	RADIAL LOAD (lbs)	THRUST LOAD (lbs)	PROBE NO.	RMS DISTANCE FROM PROBE TO MEASURED SURFACE 1 In.	2 In.	3 In.	4 In.	5 In.	6 In.	7 In.	8 In.	9 In.
D-1	1000	1500	0		.03513	.03296	.03127	.02061	.02560	.03877	.02588	.02655	.04314
D-2	1000	2000	0		.03637	.03296	.03137	.02056	.02569	.03860	.02524	.02674	.04354
D-3	1000	2500	0		.03624	.03283	.03151	.02056	.02583	.03842	.02496	.02683	.04389
D-4	1000	3000	0		.03619	.03265	.03186	.02093	.02606	.03833	.02462	.02697	.04410
D-5	2000	1500	0		.03646	.03296	.03132	.02061	.02560	.03873	.02571	.02498	.04336
D-6	2000	2000	0		.03624	.03283	.03137	.02061	.02560	.03855	.02538	.02679	.04354
D-7	2000	2500	0		.03602	.03256	.03137	.02047	.02560	.03829	.02500	.02670	.04362
D-8	2000	3000	0		.03588	.03239	.03137	.02047	.02583	.03811	.02462	.02674	.04380
D-9	3000	1500	0		.03624	.03278	.03118	.02061	.02550	.03873	.02567	.02665	.04314
D-10	3000	2000	0		.03611	.03270	.03127	.02061	.02560	.03851	.02534	.02665	.04341
D-11	3000	2500	0		.03597	.03252	.03137	.02047	.02578	.03833	.02500	.02674	.04384
D-12	3000	3000	0		.03584	.03235	.03146	.02047	.02587	.03811	.02466	.02679	.04384
D-13	4000	1500	0		.03637	.03287	.03123	.02070	.02564	.03886	.02584	.02670	.04314
D-14	4000	2000	0		.03624	.03278	.03137	.02070	.02578	.03868	.02542	.02674	.04349
D-15	4000	2500	0		.03628	.03283	.03142	.02070	.02596	.03851	.02504	.02683	.04384
D-16	4000	3000	0		.03593	.03243	.03146	.02051	.02596	.03811	.02471	.02679	.04367
D-17	5000	1500	0		.03619	.03278	.03118	.02070	.02560	.03877	.02584	.02656	.04297
D-18	5000	2000	0		.03602	.03257	.03118	.02056	.02560	.03846	.02538	.02652	.04314
D-19	5000	2500	0		.03593	.03252	.03132	.02051	.02573	.03829	.02504	.02656	.04336
D-20	5000	3000	0		.03575	.03230	.03137	.02047	.02578	.03803	.02462	.02665	.04354
D-21	1000	1500	700		.03593	.03087	.03481	.00804	.01330	.02759	.02819	.02520	.04066
D-22	1000	2000	700		.03597	.03096	.03462	.00893	.01436	.02846	.02756	.02539	.04118
D-23	1000	2500	830		.03588	.03091	.03458	.00944	.01500	.02860	.02697	.02552	.04162
D-24	1000	3000	1000		.03580	.03078	.03472	.00921	.01491	.02811	.02668	.02561	.04183
D-25	2000	1500	700		.03611	.03096	.03486	.00808	.01339	.02772	.02824	.02516	.04079
D-26	2000	2000	700		.03575	.03074	.03434	.00921	.01459	.02846	.02731	.02525	.04122
D-27	2000	2500	830		.03562	.03061	.03434	.00939	.01491	.02842	.02693	.02529	.04140
D-28	2000	3000	1000		.03527	.03039	.03396	.01009	.01578	.02899	.02626	.02529	.04166

TABLE A5
(continued)

Proximity Probe Measurements

TEST & RUN NO.	OPERATING CONDITION SHAFT SPEED (rpm)	RADIAL LOAD (lbs)	THRUST LOAD (lbs)	PROBE NO.	RMS DISTANCE FROM PROBE TO MEASURED SURFACE 1 In.	2 In.	3 In.	4 In.	5 In.	6 In.	7 In.	8 In.	9 In.
D-29	3000	1500	700		.03535	.03026	.03425	.00813	.01335	.02754	.02790	.02480	.04022
D-30	3000	2000	700		.03527	.03017	.03420	.00850	.01390	.02768	.02739	.02498	.04053
D-31	3000	2500	830		.03513	.03009	.03406	.00911	.01463	.02798	.02681	.02502	.04100
D-32	3000	3000	1000		.03504	.02991	.03401	.00939	.01518	.02811	.02630	.02511	.04140
D-33	4000	1500	700		.03527	.03013	.03406	.00822	.01344	.02759	.02786	.02471	.04009
D-34	4000	2000	700		.03522	.03009	.03406	.00869	.01404	.02781	.02739	.02484	.04052
D-35	4000	2500	830		.03509	.03000	.03401	.00911	.01454	.02794	.02702	.02493	.04079
D-36	4000	3000	1000		.03496	.02987	.03401	.00953	.01514	.02811	.02651	.02507	.04122
D-37	5000	1500	700		.03539	.03029	.03416	.00846	.01365	.02780	.02797	.02479	.04018
D-38	5000	2000	700		.03548	.03033	.03421	.00892	.01434	.02795	.02761	.02498	.04067
D-39	5000	2500	830		.03522	.03011	.03404	.00952	.01497	.02842	.02697	.02508	.04100
D-40	5000	3000	1000		.03492	.02997	.03364	.01095	.01660	.02940	.02612	.02533	.04173

TABLE A5
(continued)

Bearing Drag Torque and Cage/Shaft Speed Ratio Measurements

TEST & RUN NO.	OPERATING CONDITION SHAFT SPEED (rpm)	RADIAL LOAD (lbs)	THRUST LOAD (lbs)	DRAG TORQUE (IN-OZ)	SPEED RATIO
D-1	1000	1500	0	28	0.4030
D-2	1000	2000	0	59	0.4032
D-3	1000	2500	0	82	0.4035
D-4	1000	3000	0	110	0.4034
D-5	2000	1500	0	25	0.4015
D-6	2000	2000	0	43	0.4023
D-7	2000	2500	0	67	0.4024
D-8	2000	3000	0	91	0.4029
D-9	3000	1500	0	28	0.4007
D-10	3000	2000	0	44	0.4014
D-11	3000	2500	0	65	0.4020
D-12	3000	3000	0	83	0.4023
D-13	4000	1500	0	27	0.3997
D-14	4000	2000	0	37	0.4004
D-15	4000	2500	0	61	0.4006
D-16	4000	3000	0	71	0.4017
D-17	5000	1500	0	25	0.3994
D-18	5000	2000	0	33	0.3997
D-19	5000	2500	0	50	0.4004
D-20	5000	3000	0	63	0.4007
D-21	1000	1500	700	102	0.4049
D-22	1000	2000	700	112	0.4022
D-23	1000	2500	830	142	0.4020
D-24	1000	3000	1000	183	0.4025
D-25	2000	1500	700	83	0.4034
D-26	2000	2000	700	90	0.4019
D-27	2000	2500	830	125	0.4016
D-28	2000	3000	1000	163	0.4019

TABLE A5
(continued)

TEST & RUN NO.	OPERATING CONDITION SHAFT SPEED (rpm) / RADIAL LOAD (lbs) / THRUST LOAD (lbs)	DRAG TORQUE (IN-OZ)	SPEED RATIO
D-29	3000 / 1500 / 700	92	0.4032
D-30	3000 / 2000 / 700	102	0.4021
D-31	3000 / 2500 / 830	122	0.4018
D-32	3000 / 3000 / 1000	157	0.4018
D-33	4000 / 1500 / 700	76	0.4033
D-34	4000 / 2000 / 700	89	0.4019
D-35	4000 / 2500 / 830	108	0.4016
D-36	4000 / 3000 / 1000	128	0.4015
D-37	5000 / 1500 / 700	66	0.4025
D-38	5000 / 2000 / 700	76	0.4012
D-39	5000 / 2500 / 830	93	0.4005
D-40	5000 / 3000 / 1000	130	0.4006

TABLE A6

MEASURED DRAG TORQUE VALUES FOR TEST SERIES A-D

TEST BEARING DRAG TORQUE

SHAFT SPEED	RADIAL LOAD	TEST SERIES / BRG. NO.			COMBINED LOAD	TEST SERIES BRG. NO.		
		A/02	C/01	D/03	Radial/Thrust	B/02	C/01	D/03
(rpm)	(lb)	(in-oz)	(in-oz)	(in-oz)	(lb)	(in-oz)	(in-oz)	(in-oz)
1000	1500	21	37	28	1500/700	46	71	102
	2000	37	46	59	2000/700	55	76	112
	2500	47	57	82	2500/830	66	90	142
	3000	67	89	110	3000/1000	80	111	183
2000	1500	23	33	25	1500/700	53	71	83
	2000	38	42	43	2000/700	61	78	90
	2500	45	53	67	2500/830	77	95	125
	3000	58	64	91	3000/1000	94	111	163
3000	1500	30	31	28	1500/700	60	66	92
	2000	47	42	44	2000/700	76	85	102
	2500	54	53	65	2500/830	97	93	122
	3000	71	53	83	3000/1000	111	119	157
4000	1500	38	42	27	1500/700	48	70	76
	2000	51	53	37	2000/700	72	76	89
	2500	59	60	61	2500/830	97	90	108
	3000	68	73	71	3000/1000	107	116	128
5000	1500	45	50	25	1500/700	57	69	66
	2000	57	57	33	2000/700	71	88	76
	2500	74	64	50	2500/830	96	95	93
	3000	89	73	63	3000/1000	106	121	130

TABLE A7

TEST SERIES E-4 DATA

(BEARING 06)

TEST & RUN NO.	SHAFT SPEED (rpm)	BRG. RADIAL (lbs.)	LOAD THRUST (lbs.)	INNER RING TEMP. RTD. PROBE NO. 1 (°C)	INNER RING TEMP. RTD. PROBE NO. 3 (°C)	INNER RING TEMP. RTD. PROBE NO. 4 (°C)	OUTER RING TEMP. THERMOCOUPLE NUMBER 1 (°C)	OUTER RING TEMP. THERMOCOUPLE NUMBER 2 (°C)	OUTER RING TEMP. THERMOCOUPLE NUMBER 3 (°C)	OUTER RING TEMP. THERMOCOUPLE NUMBER 4 (°C)	OIL FLOW RATE (gpm)	OIL IN TEMP. (°C)	OIL OUT TEMP. (°C)	HYDRO. OIL TEMP. (°C)
0	0	1500	50	89.2	91.4	90.4	81	82	82	82	.125	93	88	82
1	5000	1500	50	99.9	101.4	99.5	92	92	92	92	.125	93	94	82
2	6000	1500	50	102.9	104.5	103.3	94.5	94	94	94	.125	93	97	82
3	7000	3000	50	109.7	111.3	110.2	99	98	98	98	.125	94	102	82
4	8000	3000	50	113.4	115.7	-	100.5	100	100	100	.125	93	104	83
5	9000	3000	50	120.1	121.7	-	101.5	102	102	102	.125	92	106	83
6	10000	3000	50	123.0	124.7	-	105	105	105	105	.125	92	108	84
7	11000	3000	50	126.9	128.6	-	108.5	108	108	108	.125	93	112	84
8	12000	3000	50	131.3	132.9	-	111.5	111	111	111	.125	93	115	84
9	13000	3000	50	135.3	137.0	-	116	114	114	114	.125	93	117	84
10	14000	3000	50	138.9	140.8	-	119	118	118	118	.125	92	119	84
11	15000	3000	50	142.4	144.2	-	123	122	121	121	.125	92	121	84
12	16000	3000	50	144	147.0	148.4	127	126	125	125	.125	93	-	84
13	17000	3000	50	150.6	152.0	153.2	131	130	129	129	.125	93	126	84
14	18000	3000	50	156.1	157.5	159.2	137	136	135	134	.125	93	132	84

TABLE A8

TEST SERIES E-5 DATA

(BEARING 06)

TEST & RUN NO.	SHAFT SPEED (rpm)	BRG. RADIAL (lbs.)	LOAD THRUST (lbs.)	INNER RING TEMP. RTD. PROBE NO. 1 (^{o}C)	INNER RING TEMP. RTD. PROBE NO. 2 (^{o}C)	INNER RING TEMP. RTD. PROBE NO. 4 (^{o}C)	OUTER RING TEMP. THERMOCOUPLE NUMBER 1 (^{o}C)	OUTER RING TEMP. THERMOCOUPLE NUMBER 2 (^{o}C)	OUTER RING TEMP. THERMOCOUPLE NUMBER 3 (^{o}C)	OUTER RING TEMP. THERMOCOUPLE NUMBER 4 (^{o}C)	OIL FLOW RATE (gpm)	OIL IN TEMP. (^{o}C)	OIL OUT TEMP. (^{o}C)	HYDRO. OIL TEMP. (^{o}C)
1	5000	70	1000	106	108	105	95	93	95	94	.125	94	99	81
2	7000	70	1000	114	116	-	99	98	101	99	.125	95	106	82
3	9000	70	1000	121	124	-	105	102	106	105	.125	94	111	82
4	11000	70	1000	131	133	-	112	111	113	114	.125	95	118	83
5	12000	70	1000	131	134	-	112	111	114	114	.15	93	118	84
6	13000	70	1000	136	138	-	116	116	118	119	.15	93	122	84
7	14000	70	1000	139	141	-	118	116	120	120	.15	95	122	85
8	15000	70	1000	141	143	-	120	117	121	121	.15	93	122	86
9	16000	70	1000	143	145	-	121	1 6	122	120	.15	90	122	87
10	17000	70	1000	146	149	-	124	119	126	123	.15	93	125	87
11	18000	70	1000	150	152	-	127	122	129	126	.15	94	127	86
12	19000	70	1000	155	156	-	131	126	133	130	.15	93	130	86
13	19400	70	1000	157	158	155	133	128	135	132	.15	94	131	86

TABLE A9

TEST SERIES E-6 DATA

(BEARING 06)

TEST & RUN NO.	SHAFT SPEED (rpm)	BRG. LOAD RADIAL (lbs.)	THRUST (lbs.)	INNER RING TEMP. RTD. PROBE NO. 1 (°C)	2 (°C)	4 (°C)	OUTER RING TEMP. THERMOCOUPLE NUMBER 1 (°C)	2 (°C)	3 (°C)	4 (°C)	OIL FLOW RATE (gpm)	OIL IN TEMP. (°C)	OIL OUT TEMP. (°C)	HYDRO. OIL TEMP. (°C)
1	5000	3000	1000	111	113	110	92	92	95	94	.15	93	101	81
2	7000	3000	1000	115	117	-	99	95	98	95	.15	93	104	81
3	9000	3000	1000	121	124	-	103	99	102	100	.15	92	107	81
4	10000	3000	1000	124	127	-	106	102	105	103	.15	92	109	82
5	11000	3000	1000	128	129	-	109	104	108	106	.15	93	112	83
6	12000	3000	1000	132	134	-	112	108	111	109	.15	94	114	83
7	13000	3000	1000	135	138	-	116	111	114	112	.15	94	119	84
8	14000	3000	1000	140	142	-	119	114	117	114	.15	94	119	84
9	15000	3000	1000	142	145	-	123	117	120	118	.15	94	121	84
10	16000	3000	1000	145	147	144	126	120	124	121	.15	94	124	84
11	17000	3000	1000	149	151	148	130	124	127	125	.15	94	127	85
12	18000	3000	1000	155	157	154	135	129	133	129	.15	94	130	85
13	19000	3000	1000	160	162	159	139	134	138	134	.15	94	132	85

TABLE A10

Temperature Record

TEST & RUN NO.	OPERATING CONDITION SHAFT SPEED (rpm)	RADIAL LOAD (lb)	THRUST LOAD (lb)	INNER RING TEMP. RTD. NO. 1 (°C)	2 (°C)	3 (°C)	4 (°C)	OUTER RING TEMP. THERMOCOUPLE NO. 1 (°C)	2 (°C)	3 (°C)	4 (°C)	LUBE OIL Temp. In (°C)	Out (°C)	Flow Rate (gpm)	HYDROSTATIC OIL IN TEMP. (°C)
F-1-1	5000	1500	50	-	105	-	103	-	93	93	94	93	98	0.15	85
F-1-2	5000	3000	50	-	109	-	108	-	96	96	96	93	100	0.15	85
F-1-3	5000	50	750	-	107	-	106	-	94	96	95	93	100	0.15	85
F-1-4	5000	50	1000	-	109	-	108	-	95	97	95	93	101	0.15	86
F-1-5	5000	1500	750	-	110	-	108	-	95	97	96	93	101	0.15	86
F-1-6	5000	3000	1000	-	112	-	111	-	95	99	97	92	103	0.15	87
F-1-7	7500	1500	50	-	112	-	110	-	98	99	99	93	104	0.15	87
F-1-8	7500	3000	50	-	117	-	115	-	100	101	101	93	107	0.15	87
F-1-9	7500	50	750	-	116	-	114	-	99	101	100	93	106	0.15	87
F-1-10	7500	50	1000	-	117	-	115	-	99	103	101	93	107	0.15	87
F-1-11	7500	1500	750	-	118	-	116	-	100	103	101	94	108	0.15	87
F-1-12	7500	3000	1000	-	121	-	119	-	100	104	102	92	109	0.15	88
F-1-13	10000	1500	50	-	120	-	118	-	102	104	103	93	109	0.15	88
F-1-14	10000	3000	50	-	126	-	125	-	105	107	106	92	112	0.15	88
F-1-15	10000	50	750	-	125	-	123	-	103	107	105	92	112	0.15	88
F-1-16	10000	50	1000	-	126	-	124	-	103	108	106	92	113	0.15	88
F-1-17	10000	1500	750	-	127	-	125	-	103	108	106	93	113	0.15	88
F-1-18	10000	3000	1000	-	130	-	129	-	104	110	107	92	114	0.15	88
F-1-19	12500	1500	50	-	131	-	-	-	113	114	113	93	117	0.15	96
F-1-20	12500	3000	50	-	138	-	-	-	117	117	117	94	118	0.15	96
F-1-21	12500	50	750	-	136	-	-	-	113	118	116	93	120	0.15	96
F-1-22	12500	50	1000	-	138	-	-	-	114	119	117	93	120	0.15	95
F-1-23	12500	1500	750	-	138	-	139	-	111	116	110	93	120	0.15	93
F-1-24	12500	3000	1000	-	141	-	142	-	112	118	114	92	121	0.15	94
F-1-25	15000	1500	50	-	140	-	142	-	118	120	-	94	122	0.15	96
F-1-26	15000	3000	50	-	147	-	148	-	122	123	-	93	126	0.15	95
F-1-27	15000	50	750	-	147	-	-	-	120	126	-	94	124	0.15	95
F-1-28	15000	50	1000	-	148	-	-	-	120	127	-	93	125	0.15	94
F-1-29	15000	1500	750	-	148	-	148	-	118	124	-	94	124	0.15	94
F-1-30	15000	3000	1000	-	149	-	150	-	119	123	-	92	124	0.15	94

TABLE A10
(continued)

Temperature Record

TEST & RUN NO.	OPERATING CONDITION SHAFT SPEED (rpm)	RADIAL LOAD (lb)	THRUST LOAD (lb)	INNER RING TEMP. RTD. NO. 1 (°C)	2 (°C)	3 (°C)	4 (°C)	OUTER RING TEMP. THERMOCOUPLE NO. 1 (°C)	2 (°C)	3 (°C)	4 (°C)	LUBE OIL Temp. In (°C)	Out (°C)	Flow Rate (gpm)	HYDROSTATIC OIL IN TEMP. (°C)
F-1-31	17500	1500	50	-	150	-	152	-	123	127	-	93	129	0.15	95
F-1-32	17500	3000	50	-	156	-	158	-	130	132	-	94	134	0.15	95
F-1-33	17500	50	750	-	150	-	-	-	125	133	-	93	129	0.15	95
F-1-34	17500	50	1000	-	156	-	-	-	126	135	-	93	130	0.15	95
F-1-35	17500	1500	750	-	155	-	156	-	122	129	-	88	129	0.15	95
F-1-36	17500	3000	1000	-	158	-	161	-	-	132	-	93	132	0.15	95

TABLE A10
(continued)

Autorotation Data

TEST & RUN NO.	OPERATING CONDITION SHAFT SPEED (rpm)	RADIAL LOAD (lb)	THRUST LOAD (lb)	MAX. ROLLER SPEED (Hz)	MIN. ROLLER SPEED (Hz)	PERCENT CHANGE (%)	AVERAGE ROLLER SPEED * (Hz)	AVERAGE ROLLER SPEED † (Hz)	ROLLER CYCLES PER CAGE CYCLES
F-1-1	5000	1500	50	203.35	180.45	11.3	191.67	191.5	5.775
F-1-2	5000	3000	50	198.71	179.28	9.8	195.84	193.6	5.92
F-1-3	5000	50	750	201.85	201.85	0	201.78	201.85	6.0
F-1-4	5000	50	1000	201.85	201.85	0	201.95	201.85	6.0
F-1-5	5000	1500	750	203.4	194.63	4.3	199.68	199.81	5.971
F-1-6	5000	3000	1000	204.12	187.93	7.9	196.35	196.27	5.903
F-1-7	7500	1500	50	304.46	278.06	8.7	289.23	291.70	5.81
F-1-8	7500	3000	50	302.77	280.92	7.2	290.23	290.27	5.84
F-1-9	7500	50	750	302.77	302.77	0	302.45	302.77	6.0
F-1-10	7500	50	1000	302.77	302.77	0	303.17	302.77	6.0
F-1-11	7500	1500	750	304.46	294.59	3.2	298.56	299.03	5.95
F-1-12	7500	3000	1000	302.77	283.85	6.2	296.71	295.82	5.94
F-1-13	10000	1500	50	403.71	374.58	7.2	393.05	392.10	5.92
F-1-14	10000	3000	50	403.25	381.13	6.6	393.53	393.40	5.94
F-1-15	10000	50	750	403.72	403.72	0	403.00	403.72	6.0
F-1-16	10000	50	1000	402.97	402.97	0	404.21	402.97	6.0
F-1-17	10000	1500	750	403.72	392.10	2.9	397.21	399.65	5.95
F-1-18	10000	3000	1000	406.73	378.49	6.9	397.65	396.03	5.96
F-1-19	12500	1500	50	509.36	473.93	7.0	494.33	491.56	5.97
F-1-20	12500	3000	50	509.36	478.09	6.1	493.87	494.35	5.96
F-1-21	12500	50	750	500.00	495.47	0.9	501.70	498.67	5.98
F-1-22	12500	50	1000	506.99	504.65	0.5	506.85	505.62	6.03
F-1-23	12500	1500	750	506.99	482.31	4.9	498.52	498.51	5.99
F-1-24	12500	3000	1000	509.36	486.62	4.5	496.02	497.39	5.98
F-1-25	15000	1500	50	605.58	582.91	3.7	595.08	593.76	5.99
F-1-26	15000	3000	50	618.33	573.70	7.2	598.25	595.38	6.
F-1-27	15000	50	750	608.95	605.58	0.6	606.3	605.86	6.
F-1-28	15000	50	1000	605.58	605.58	0	606.3	605.58	6.
F-1-29	15000	750	750	605.51	589.14	2.7	597.57	598.58	5.98
F-1-30	15000	1000	1000	608.96	599.92	1.5	600.7	603.90	6.02

TABLE A10
(continued)

Autorotation Data

TEST & RUN NO.	OPERATING CONDITION SHAFT SPEED (rpm)	RADIAL LOAD (lb)	THRUST LOAD (lb)	MAX. ROLLER SPEED (Hz)	MIN. ROLLER SPEED (Hz)	PERCENT CHANGE (%)	AVERAGE ROLLER SPEED * (Hz)	AVERAGE ROLLER SPEED † (Hz)	ROLLER CYCLES PER CAGE CYCLES
F-1-31	17500	1500	50	702.25	672.86	4.2	691.69	693.93	6.
F-1-32	17500	3000	50	707.82	681.27	3.8	696.89	695.40	6.03
F-1-33	17500	50	750	698.74	698.74	0	704.90	698.74	5.98
F-1-34	17500	50	1000	707.81	707.81	0	708.31	707.81	6.
F-1-35	17500	1500	750	694.29	694.29	0	697.70	694.29	6.01
F-1-36	17500	3000	1000	693.09	693.09	0	696.58	693.09	6.

* Avg. roller speed per cage cycle established by multiplying the cage speed by roller cycles per cage cycle.

† Avg. roller speed determined from the measured values of each roller cycle.

TABLE A10
(continued)

BEARING DRAG TORQUE MEASURED CAGE AND SHAFT SPEED DATA

TEST & RUN NO.	OPERATING CONDITION SHAFT SPEED (rpm)	RADIAL LOAD (lb)	THRUST LOAD (lb)	CAGE SPEED (rpm)	SHAFT SPEED (rpm)	CAGE SPEED/SHAFT SPEED RATIO	PERCENT SLIP BASED ON NO SLIP RATIO OF 0.40300 (%)	DRAG TORQUE (in-oz)
F-1-1	5000 /	1500 /	50	1991.4	4991.4	0.39872	1.06	54
F-1-2	5000 /	3000 /	50	1984.9	4973.5	0.39909	0.97	-
F-1-3	5000 /	50 /	750	2017.7	4994.5	0.40399	-0.25	55
F-1-4	5000 /	50 /	1000	2019.5	4991.0	0.40464	-0.40	62
F-1-5	5000 /	1500 /	750	2006.5	4985.0	0.40250	0.12	59
F-1-6	5000 /	3000 /	1000	1995.8	4974.5	0.40120	0.44	-
F-1-7	7500 /	1500 /	50	2987.0	7503.0	0.39810	1.22	56
F-1-8	7500 /	3000 /	50	2981.9	7476.0	0.39885	1.03	66
F-1-9	7500 /	50 /	750	3024.8	7503.0	0.40315	-0.04	66
F-1-10	7500 /	50 /	1000	3031.7	7498.5	0.40431	-0.33	61
F-1-11	7500 /	1500 /	750	3010.8	7491.0	0.40192	0.27	68
F-1-12	7500 /	3000 /	1000	2998.6	7480.5	0.40086	0.53	72
F-1-13	10000 /	1500 /	50	3982.3	10014.0	0.39767	1.32	62
F-1-14	10000 /	3000 /	50	3978.4	9979.4	0.39866	1.07	-
F-1-15	10000 /	50 /	750	4029.9	10010.5	0.40257	0.11	72
F-1-16	10000 /	50 /	1000	4042.1	10008.5	0.40387	-0.21	77
F-1-17	10000 /	1500 /	750	4006.8	9999.5	0.40070	0.57	82
F-1-18	10000 /	3000 /	1000	4001.2	9993.0	0.40040	0.64	-
F-1-19	12500 /	1500 /	50	4965.9	12522	0.39657	1.60	74
F-1-20	12500 /	3000 /	50	4971.9	12481	0.39836	1.15	-
F-1-21	12500 /	50 /	750	5033.9	12518	0.40213	0.22	95
F-1-22	12500 /	50 /	1000	5043.3	12506	0.40327	0.07	96
F-1-23	12500 /	1500 /	750	4996.0	12504	0.39957	0.85	106
F-1-24	12500 /	3000 /	1000	4973.5	12443	0.39970	0.82	-
F-1-25	15000 /	1500 /	50	5961.8	15084.5	0.39522	1.93	-
F-1-26	15000 /	3000 /	50	5982.6	15029.5	0.39805	1.23	-
F-1-27	15000 /	50 /	750	6063.0	15032.5	0.40339	-0.09	-
F-1-28	15000 /	50 /	1000	6063.0	15027.0	0.40347	-0.12	100
F-1-29	15000 /	1500 /	750	5997.7	15029.5	0.39906	0.98	101
F-1-30	15000 /	3000 /	1000	5985.2	14990.0	0.39928	0.92	-

TABLE A10
(continued)

BEARING DRAG TORQUE MEASURED CAGE AND SHAFT SPEED DATA

TEST & RUN NO.	OPERATING CONDITION SHAFT SPEED (rpm)	RADIAL LOAD (lb)	THRUST LOAD (lb)	CAGE SPEED (rpm)	SHAFT SPEED (rpm)	CAGE SPEED/SHAFT SPEED RATIO	PERCENT SLIP BASED ON NO SLIP RATIO OF 0.40300 (%)	DRAG TORQUE (in-oz)
F-1-31	17500	1500	50	6916.9	17504	0.39516	1.95	-
F-1-32	17500	3000	50	6940.0	17454	0.39762	1.33	-
F-1-33	17500	50	750	7085.0	17564	0.40338	-0.09	-
F-1-34	17500	50	1000	7083.1	17554	0.40350	-0.12	-
F-1-35	17500	1500	750	6997.7	17534	0.39910	0.97	-
F-1-36	17500	3000	1000	6965.8	17456	0.39905	0.98	-

TABLE A11

Test Series F-2 Data (Bearing No. 02)

Temperature Record

TEST & RUN NO.	OPERATING CONDITION SHAFT SPEED (rpm)	RADIAL LOAD (lb)	THRUST LOAD (lb)	INNER RING TEMP. RTD. NO. 1 (°C)	2 (°C)	3 (°C)	4 (°C)	OUTER RING TEMP. THERMOCOUPLE NO. 1 (°C)	2 (°C)	3 (°C)	4 (°C)	LUBE OIL Temp. In (°C)	Out (°C)	Flow Rate (gpm)	HYDROSTATIC OIL IN TEMP. (°C)
F-2-1	5000	1500	50		111		111	101	99	101		94	103	0.15	97
F-2-2	5000	3000	50		116		116	104	102	103		95	105	0.15	97
F-2-3	5000	50	750		112		113	102	100	103		93	103	0.15	97
F-2-4	5000	50	1000		110		111	101	99	101		90	101	0.15	98
F-2-5	5000	1500	750		112		113	101	100	101		94	102	0.15	97
F-2-6	5000	3000	1000		118		119	105	102	104		95	106	0.15	97
F-2-7	7500	1500	50		118		119	106	106	106		96	108	0.15	98
F-2-8	7500	3000	50		126		126	110	109	109		96	112	0.15	98
F-2-9	7500	50	750		120		120	106	106	107		94	109	0.15	98
F-2-10	7500	50	1000		119		120	106	104	107		93	109	0.15	99
F-2-11	7500	1500	750		122		122	107	105	108		93	109	0.15	99
F-2-12	7500	3000	1000		128		129	111	107	109		93	110	0.15	99
F-2-13	10000	1500	50		125		126	109	109	109		91	111	0.15	98
F-2-14	10000	3000	50		134		135	113	113	113		91	115	0.15	98
F-2-15	10000	50	750		127		128	110	108	111		91	112	0.15	98
F-2-16	10000	50	1000		128		129	111	108	113		92	113	0.15	99
F-2-17	10000	1500	750		131		132	112	109	113		92	113	0.15	98
F-2-18	10000	3000	1000		138		140	116	111	114		92	115	0.15	98
F-2-19	12500	1500	50												
F-2-20	12500	3000	50												
F-2-21	12500	50	750												
F-2-22	12500	50	1000					NO DATA RECORDED							
F-2-23	12500	1500	750												
F-2-24	12500	3000	1000												
F-2-25	15000	1500	50		145		146	121	120	122		91	122	0.15	98
F-2-26	15000	3000	50		-		154	126	124	126		91	125	0.15	98
F-2-27	15000	50	750		-		-	121	118	124		92	122	0.15	99
F-2-28	15000	50	1000		-		-	124	119	126		92	124	0.15	99
F-2-29	15000	1500	750		-		-	125	120	126		93	124	0.15	99
F-2-30	15000	3000	1000		-		-	129	123	128		91	126	0.15	99

TABLE A11
(continued)

Temperature Record

TEST & RUN NO.	OPERATING CONDITION SHAFT SPEED	RADIAL LOAD	THRUST LOAD	INNER RING TEMP. RTD. NO. 1	2	3	4	OUTER RING TEMP. THERMOCOUPLE NO. 1	2	3	4	LUBE OIL Temp. In	Out	Flow Rate	HYDROSTATIC OIL IN TEMP.
	(rpm)	(lb)	(lb)	(^{o}C)	(^{o}C)	(^{o}C)	(^{o}C)	(^{o}C)	(^{o}C)	(^{o}C)	(^{o}C)	(^{o}C)	(^{o}C)	(gpm)	(^{o}C)
F-2-31	17500 /	1500 /	50		-		-	128	126	129		91	129	0.15	99
F-2-32	17500 /	3000 /	50		-			133	131	133		92	134	0.15	99
F-2-33	17500 /	50 /	750		-		-	-	-	-		-	-	-	-
F-2-34	17500 /	50 /	1000		-		-	-	-	-		-	-	-	-
F-2-35	17500 /	1500 /	750		-		-	-	-	-		-	-	-	-
F-2-36	17500 /	3000 /	1000		-		-	-	-	-		-	-	-	-

TABLE A11
(continued)

Proximity Probe Measurements

TEST & RUN NO.	OPERATING CONDITION SHAFT SPEED (rpm)	RADIAL LOAD (lbs)	THRUST LOAD (lbs)	PROBE NO.	RMS DISTANCE FROM PROBE TO MEASURED SURFACE 1 In.	2 In.	3 In.	4 In.	5 In.	6 In.	7 In.	8 In.	9 In.
F-2-1	5000	1500	50		.03500	.02543	.03873	.02949	.03812	.03618	.01950	.02032	.04769
F-2-2	5000	3000	50		.03447	.02496	.03887	.02930	.03835	.03544	.01819	.02059	.04821
F-2-3	5000	50	750		.03473	.02552	.03901	.02318	.03078	.03136	.02273	.01919	.04485
F-2-4	5000	50	1000		.03473	.02552	.03910	.02299	.03059	.03118	.02273	.01010	.04489
F-2-5	5000	1500	750		.03451	.02435	.03953	.02425	.03330	.03154	.02021	.01946	.04569
F-2-6	5000	3000	1000		.03434	.02457	.03896	.02654	.03583	.03316	.01845	.02009	.04773
F-2-7	7500	1500	50		.03478	.02530	.03863	.02935	.03789	.03605	.01962	.02018	.04747
F-2-8	7500	3000	50		.03412	.02478	.03882	.02921	.03794	.03509	.01815	.02068	.04773
F-2-9	7500	50	750		.03478	.02678	.03689	.02402	.0300	.03329	.02475	.01860	.04310
F-2-10	7500	50	1000		.03491	.02683	.03708	.02350	.02959	.03281	.02475	.01864	.04323
F-2-11	7500	1500	750		.03465	.02561	.03821	.02379	.03133	.03215	.02240	.01905	.04485
F-2-12	7500	3000	1000		.03425	.02587	.03759	.02710	.03454	.03454	.01996	.02018	.04616
F-2-13	10000	1500	50		.03460	.02643	.03684	.02944	.03638	.03680	.02109	.01986	.04559
F-2-14	10000	3000	50		.03354	.02565	.03769	.02949	.03674	.03535	.01869	.02072	.04607
F-2-15	10000	50	750		.03327	.02539	.03877	.02481	.03138	.03149	.02172	.02000	.04397
F-2-16	10000	50	1000		.03319	.02539	.03877	.02449	.03106	.03114	.02164	.01991	.04830
F-2-17	10000	1500	750		.03385	.02443	.03873	.02407	.03216	.03140	.02076	.01919	.04520
F-2-18	10000	3000	1000		.03363	.02461	.03792	.02664	.03505	.03329	.01861	.01995	.04642
F-2-25	15000	1500	50		.03341	.02504	.03703	.02883	.03615	.03548	.01975	.01959	.04515
F-2-26	15000	3000	50		.03265	.02452	.03726	.02925	.03647	.03456	.01815	.02023	.04572
F-2-27	15000	50	750		.03372	.02622	.03561	.02547	.03115	.03430	.02412	.01810	.04218
F-2-28	15000	50	1000		.03358	.02609	.03561	.02500	.03073	.03373	.02395	.01810	.04214
F-2-29	15000	1500	750		.03301	.02509	.03684	.02570	.03234	.03285	.02084	.01923	.04384
F-2-30	15000	3000	1000		.03270	.02496	.03675	.02743	.03436	.03360	.01903	.01982	.04502
F-2-31	17500	1500	50		.03283	.02548	.03608	.02907	.03541	.03561	.02008	.01946	.04370
F-2-32	17500	3000	50		.03221	.02496	.03632	.02921	.03578	.03465	.01853	.01986	.04441
F-2-33	17500	50	750										
F-2-34	17500	50	1000										
F-2-35	17500	1500	750										
F-2-36	17500	3000	1000										

TABLE A11
(continued)

BEARING DRAG TORQUE, MEASURED CAGE AND SHAFT SPEED DATA

TEST & RUN NO.	OPERATING CONDITION SHAFT SPEED (rpm)	RADIAL LOAD (lb)	THRUST LOAD (lb)	CAGE SPEED (rpm)	SHAFT SPEED (rpm)	CAGE SPEED/SHAFT SPEED RATIO	PERCENT SLIP BASED ON NO SLIP RATIO OF 0.40300 (%)	DRAG TORQUE (in-oz)
F-2-1	5000	1500	50	2003.1	5024.0	0.39870	1.07	50
F-2-2	5000	3000	50	1999.9	5010.0	0.39918	0.95	62
F-2-3	5000	50	750	2031.5	5025.0	0.40428	0.32	58
F-2-4	5000	50	1000	2032.1	5022.5	0.40460	0.40	62
F-2-5	5000	1500	750	2009.4	5020.0	0.40028	0.67	52
F-2-6	5000	3000	1000	2003.0	5009.0	0.39988	0.77	66
F-2-7	7500	1500	50	2989.0	7509.5	0.39802	1.23	62
F-2-8	7500	3000	50	2988.7	7491.0	0.39897	1.00	73
F-2-9	7500	50	750	3024.5	7520.5	0.40216	0.21	60
F-2-10	7500	50	1000	3032.2	7507.0	0.40392	-0.22	72
F-2-11	7500	1500	750	3006.4	7501.0	0.40080	0.55	74
F-2-12	7500	3000	1000	2994.6	7490.5	0.39979	0.80	77
F-2-13	10000	1500	50	3977.9	10010.5	0.39737	1.40	66
F-2-14	10000	3000	50	3982.1	9984.5	0.39882	1.04	83
F-2-15	10000	50	750	4016.5	10015.0	0.40105	0.48	74
F-2-16	10000	50	1000	4051.9	10008.5	0.40485	-0.46	82
F-2-17	10000	1500	750	4001.3	10003.0	0.40001	0.74	86
F-2-18	10000	3000	1000	3993.8	9993.0	0.39965	0.83	89
F-2-19	12500	1500	50					
F-2-20	12500	3000	50					
F-2-21	12500	50	750			NO DATA RECORDED		
F-2-22	12500	50	1000					
F-2-23	12500	1500	750					
F-2-24	12500	3000	1000					
F-2-25	15000	1500	50	5934.8	15003.5	0.39556	1.85	89
F-2-26	15000	3000	50	5958.4	14959.5	0.39842	1.14	96
F-2-27	15000	50	750	5934.5	15042.5	0.39451	2.10	-
F-2-28	15000	50	1000	6020.7	15011.0	0.40109	0.47	91
F-2-29	15000	1500	750	5984.9	14993.5	0.39917	0.95	95
F-2-30	15000	3000	1000	5982.6	14984.5	0.39925	0.93	-

TABLE A11
(continued)

BEARING DRAG TORQUE, MEASURED CAGE AND SHAFT SPEED DATA

TEST & RUN NO.	OPERATING CONDITION SHAFT SPEED (rpm)	RADIAL LOAD (lb)	THRUST LOAD (lb)	CAGE SPEED (rpm)	SHAFT SPEED (rpm)	CAGE SPEED/SHAFT SPEED RATIO	PERCENT SLIP BASED ON NO SLIP RATIO OF 0.403^2 (%)	DRAG TORQUE (in-oz)
F-2-31	17500	1500	50	6908.4	17513.0	0.39447	2.12	-
F-2-32	17500	3000	50	6945.9	17453.0	0.39797	1.25	-
F-2-33	17500	50	750	6854.3	17546.0	0.39065	3.06	-
F-2-34	17500	50	1000	-	-	-	-	-
F-2-35	17500	1500	750	-	-	-	-	-
F-2-36	17500	3000	1000	-	-	-	-	-

TABLE A12

Test Series Data (Brg. No. 02)

Temperature Record

TEST & RUN NO.	OPERATING CONDITION SHAFT SPEED (rpm)	RADIAL LOAD (lb)	THRUST LOAD (lb)	INNER RING TEMP. RTD. NO. 1 (°C)	2 (°C)	3 (°C)	4 (°C)	OUTER RING TEMP. THERMOCOUPLE NO. 1 (°C)	2 (°C)	3 (°C)	4 (°C)	LUBE OIL Temp. In (°C)	Out (°C)	Flow Rate (gpm)	HYDROSTATIC OIL IN TEMP. (°C)
G-1	5000	1500	50	87	86			75	74	74		66	76	0.15	68
G-2	5000	3000	50	90	89			76	74	74		66	76	0.15	63
G-3	5000	50	750	86	85			71	69	72		65	75	0.15	61
G-4	5000	50	1000	88	86			72	70	73		65	76	0.15	62
G-5	5000	1500	750	93	92			75	72	75		65	78	0.15	63
G-6	5000	3000	1000	101	100			81	75	78		65	83	0.15	63
G-7	7500	1500	50	95	93			77	76	77		65	80	0.15	64
G-8	7500	3000	50	101	99			82	80	80		66	84	0.15	65
G-9	7500	50	750	99	97			80	77	81		65	84	0.15	65
G-10	7500	50	1000	104	102			81	78	81		66	85	0.15	65
G-11	7500	1500	750	106	104			82	78	81		65	85	0.15	65
G-12	7500	3000	1000	108	107			86	80	84		66	87	0.15	65
G-13	10000	1500	50	109	107			84	82	84		66	86	0.1	65
G-14	10000	3000	50	116	115			90	88	88		65	91	0.15	65
G-15	10000	50	750	113	112			86	82	87		65	89	0.15	64
G-16	10000	50	1000	115	114			87	83	89		65	89	0.15	64
G-17	10000	1500	750	117	116			89	83	89		65	90	0.15	64
G-18	10000	3000	1000	123	122			93	86	92		65	91	0.15	64
G-19	12500	1500	50												
G-20	12500	3000	50												
G-21	12500	50	750												
G-22	12500	50	1000					NO DATA RECORDED							
G-23	12500	1500	750												
G-24	12500	3000	1000												
G-25	15000	1500	50	132	130			100	99	100		65	93	0.15	64
G-26	15000	3000	50	144	137			107	105	105		65	107	0.15	68
G-27	15000	50	750	142	135			104	99	106		67	105	0.15	69
G-28	15000	50	1000	145	136			105	101	107		67	107	0.15	69
G-29	15000	1500	750	150	141			108	102	108		68	107	0.15	69
G-30	15000	3000	1000	156	146			115	108	112		67	109	0.15	69

TABLE A12
(continued)

Temperature Record

TEST & RUN NO.	OPERATING CONDITION SHAFT SPEED (rpm)	RADIAL LOAD (lb)	THRUST LOAD (lb)	INNER RING TEMP. RTD. NO. 1 (^{o}C)	2 (^{o}C)	3 (^{o}C)	4 (^{o}C)	OUTER RING TEMP. THERMOCOUPLE NO. 1 (^{o}C)	2 (^{o}C)	3 (^{o}C)	4 (^{o}C)	LUBE OIL Temp. In (^{o}C)	Out (^{o}C)	Flow Rate (gpm)	HYDROSTATIC OIL IN TEMP. (^{o}C)
G-31	17500	1500	50	154	144			112	108	111		68	111	0.15	69
G-32	17500	3000	50	163	152			121	116	118		67	118	0.15	69
G-33	17500	50	750	157	145			113	108	115		68	113	0.15	69
G-34	17500	50	1000	159	148			115	110	118		68	116	0.15	69
G-35	17500	1500	750	163	150			118	112	118		67	115	0.15	70
G-36	17500	3000	1000	167	154			124	117	121		66	118	0.15	70

TABLE A12
(continued)

Proximity Probe Measurements

TEST & RUN NO.	OPERATING CONDITION SHAFT SPEED (rpm)	RADIAL LOAD (lbs)	THRUST LOAD (lbs)	PROBE NO.	RMS DISTANCE FROM PPOBE TO MEASURED SURFACE 1 In.	2 In.	3 In.	4 In.	5 In.	6 In.	7 In.	8 In.	9 In.
G-1	5000	1500	50		.03628	.03004	.03816	.03047	.03858	.03829	.02143	.03018	.04777
G-2	5000	3000	50		.03571	.02952	.03910	.03075	.03908	.03737	.01992	.02095	.04843
G-3	5000	50	750		.03637	.03048	.03802	.02467	.03133	.03435	.02576	.01878	.04419
G-4	5000	50	1000		.03628	.03039	.03802	.02430	.03101	.03425	.02576	.01864	.04419
G-5	5000	1500	750		.03553	.02887	.03976	.02514	.03312	.03294	.02202	.02018	.04607
G-6	5000	3000	1000		.03403	.02883	.04052	.02668	.03422	.03197	.01941	.02190	.04690
G-7	7500	1500	50		.03540	.03013	.03882	.03107	.03830	.03768	.02088	.02104	.04716
G-8	7500	3000	50		.03469	.02948	.03958	.03126	.03881	.03662	.01916	.02172	.04782
G-9	7500	50	750		.03593	.03022	.03764	.02533	.03183	.03500	.02542	.01878	.04393
G-10	7500	50	1000		.03584	.02995	.03774	.02495	.03161	.03452	.02525	.01878	.04406
G-11	7500	1500	750		.03571	.02874	.03906	.02528	.03339	.03368	.02244	.01937	.04616
G-12	7500	3000	1000		.03482	.02835	.03967	.02631	.03436	.03303	.02038	.02041	.04690
G-13	10000	1500	50		.03562	.02961	.03816	.03407	.03803	.03798	.02118	.02018	.04694
G-14	10000	3000	50		.03473	.02900	.03882	.03075	.03839	.03684	.01962	.02095	.04734
G-15	10000	50	750		.03496	.02987	.03764	.02617	.03197	.03487	.02492	.01946	.04314
G-16	10000	50	1000		.03460	.02978	.03741	.02617	.03174	.03434	.02487	.01941	.04310
G-17	10000	1500	750		.03496	.02826	.03844	.02584	.03353	.03390	.02197	.01919	.04555
G-18	10000	3000	1000		.03442	.02787	.03882	.02617	.03422	.03329	.02042	.01973	.04638
G-25	15000	1500	50		.03420	.02852	.03755	.03005	.03706	.03693	.02076	.01968	.04546
G-26	15000	3000	50		.03447	.03009	.03330	.03098	.03404	.03925	.02483	.01946	.04157
G-27	15000	50	750		.03447	.03057	.03302	.02804	.02973	.03803	.02887	.01842	.03869
G-28	15000	50	1000		.03434	.03039	.03311	.02762	.02940	.03750	.02866	.01846	.03873
G-29	15000	1500	750		.03425	.02939	.03387	.02789	.03087	.03693	.02592	.01905	.04066
G-30	15000	3000	1000		.03394	.02913	.03410	.02799	.03151	.03640	.02445	.01923	.04157
G-31	17500	1500	50		.03389	.02909	.03429	.02967	.03289	.03768	.02462	.01946	.04131
G-32	17500	3000	50		.03350	.02869	.03410	.02977	.03353	.03732	.02340	.01941	.04188
G-33	17500	50	750		.03389	.02930	.03358	.02832	.03092	.03754	.02714	.01846	.03935
G-34	17500	50	1000		.03341	.02952	.03396	.02836	.03050	.03684	.02689	.01905	.03917
G-35	17500	1500	750		.03283	.02883	.03509	.02916	.03206	.03588	.02366	.02027	.04105
G-36	17500	3000	1000		.03305	.02843	.03500	.02916	.03307	.03605	.02265	.01995	.04214

TABLE A12
(continued)

BEARING DRAG TORQUE, MEASURED CAGE AND SHAFT SPEED DATA

TEST & RUN NO.	OPERATING CONDITION SHAFT SPEED (rpm)	RADIAL LOAD (lb)	THRUST LOAD (lb)	CAGE SPEED (rpm)	SHAFT SPEED (rpm)	CAGE SPEED/SHAFT SPEED RATIO	PERCENT SLIP BASED ON NO SLIP RATIO OF 0.40300 (%)	DRAG TORQUE (in-oz)
G-1	5000	1500	50	1989.9	4994.0	0.39845	1.13	69
G-2	5000	3000	50	1987.5	4983.5	0.39881	1.04	92
G-3	5000	50	750	2017.4	4993.0	0.4045	-0.26	95
G-4	5000	50	1000	2018.1	4990.5	0.40439	-0.34	100
G-5	5000	1500	750	2003.9	4978.0	0.40296	0.01	107
G-6	5000	3000	1000	1990.3	4967.0	0.40069	0.57	127
G-7	7500	1500	50	2985.1	7503.0	0.39785	1.28	91
G-8	7500	3000	50	2985.8	7492.0	0.39853	1.11	110
G-9	7500	50	750	3026.0	7498.5	0.40355	-0.14	105
G-10	7500	50	1000	3030.6	7495.0	0.40434	-0.33	113
G-11	7500	1500	750	3009.2	7487.5	0.40189	0.26	114
G-12	7500	3000	1000	2990.9	7480.5	0.39982	0.79	118
G-13	10000	1500	50	3975.9	10004.0	0.39744	1.38	100
G-14	10000	3000	50	3979.8	9989.5	0.39839	1.14	115
G-15	10000	50	750	4032.2	10005.0	0.40301	0.00	112
G-16	10000	50	1000	4039.5	10001.0	0.40390	-0.22	116
G-17	10000	1500	750	4011.4	9994.5	0.40139	0.41	121
G-18	10000	3000	1000	3991.9	9982.5	0.39989	0.77	142
G-19	12500	1500	50					
G-20	12500	3000	50					
G-21	12500	50	750					
G-22	12500	50	1000			NO DATA RECORDED		
G-23	12500	1500	750					
G-24	12500	3000	1000					
G-25	15000	1500	50	5945.2	15015.0	0.39595	1.75	-
G-26	15000	3000	50	5958.3	14978.0	0.39780	1.29	-
G-27	15000	50	750	6003.2	15018.5	0.39972	0.81	112
G-28	15000	50	1000	6038.4	14998.0	0.40261	0.10	121
G-29	15000	1500	750	6006.5	14992.0	0.40065	0.58	-
G-30	15000	3000	1000	5992.4	14978.5	0.40006	0.73	-

TABLE A12
(continued)

BEARING DRAG TORQUE, MEASURED CAGE AND SHAFT SPEED DATA

TEST & RUN NO.	OPERATING CONDITION SHAFT SPEED (rpm)	RADIAL LOAD (lb)	THRUST LOAD (lb)	CAGE SPEED (rpm)	SHAFT SPEED (rpm)	CAGE SPEED/SHAFT SPEED RATIO	PERCENT SLIP BASED ON NO SLIP RATIO OF 0.40300 (%)	DRAG TORQUE (in-oz)
G-31	17500	1500	50	6968.2	17525.0	0.39761	1.34	-
G-32	17500	3000	50	6980.5	17510.0	0.39866	1.08	-
G-33	17500	50	750	7027.6	17538.0	0.40076	0.56	-
G-34	17500	50	1000	7049.0	17516.0	0.40243	0.14	-
G-35	17500	1500	750	7018.2	17513.0	0.40073	0.56	-
G-36	17500	3000	1000	6997.3	17503.5	0.39976	0.80	-

TABLE A13

Temperature Record

TEST & RUN NO.	OPERATING CONDITION SHAFT SPEED (rpm)	RADIAL LOAD (lb)	THRUST LOAD (lb)	INNER RING TEMP. RTD. NO. 1 (°C)	2 (°C)	3 (°C)	4 (°C)	OUTER RING TEMP. THERMOCOUPLE NO. 1 (°C)	2 (°C)	3 (°C)	4 (°C)	LUBE OIL Temp. In (°C)	Out (°C)	Flow Rate (gpm)	HYDROSTATIC OIL IN TEMP. (°C)
H-1	5000	1500	50		109	109			100	101		93	103	0.15	97
H-2	5000	3000	50		114	114			103	104		95	106	0.15	98
H-3	5000	50	750		116	115			102	106		94	104	0.15	98
H-4	5000	50	1000		127	127			105	112		94	108	0.15	98
H-5	5000	1500	750		123	124			103	109		94	106	0.15	98
H-6	5000	3000	1000		125	126			103	108		93	109	0.15	98
H-7	7500	1500	50		117	117			104	106		94	107	0.15	98
H-8	7500	3000	50		122	121			111	108		93	108	0.15	98
H-9	7500	50	750		121	120			-	108		93	110	0.15	98
H-10	7500	50	1000		122	122			-	109		93	110	0.15	98
H-11	7500	1500	750		123	123			-	109		93	110	0.15	98
H-12	7500	3000	1000		131	130			-	112		93	114	0.15	98
H-13	10000	1500	50		126	126				110		93	111	0.15	98
H-14	10000	3000	50		131	132				113		93	114	0.15	98
H-15	10000	50	750		131	131				114		94	114	0.15	98
H-16	10000	50	1000		132	131				115		94	118	0.15	98
H-17	10000	1500	750		134	134				115		93	115	0.15	98
H-18	10000	3000	1000		138	138				116		93	115	0.15	98
H-19	12500	1500	50		136	135				117		94	118	0.15	98
H-20	12500	3000	50		140	140				119		94	120	0.15	98
H-21	12500	50	750		140	140				120		94	120	0.15	98
H-22	12500	50	1000		142	141				122		95	123	0.15	98
H-23	12500	1500	750		142	142				121		94	123	0.15	98
H-24	12500	3000	1000		145	145				122		94	122	0.15	98
H-25	15000	1500	50		144	143				123		94	126	0.15	97
H-26	15000	3000	50		149	149				126		94	128	0.15	97
H-27	15000	50	750		149	148				127		94	129	0.15	98
H-28	15000	50	1000		151	150				129		94	130	0.15	97
H-29	15000	1500	750		151	151				128		94	130	0.15	97
H-30	15000	3000	1000		154	154				129		94	130	0.15	97

TABLE A13
(continued)

Temperature Record

TEST & RUN NO.	OPERATING CONDITION SHAFT SPEED (rpm)	RADIAL LOAD (lb)	THRUST LOAD (lb)	INNER RING TEMP. RTD. NO. 1 (^{o}C)	2 (^{o}C)	3 (^{o}C)	4 (^{o}C)	OUTER RING TEMP. THERMOCOUPLE NO. 1 (^{o}C)	2 (^{o}C)	3 (^{o}C)	4 (^{o}C)	LUBE OIL Temp. In (^{o}C)	Out (^{o}C)	Flow Rate (gpm)	HYDROSTATIC OIL IN TEMP. (^{o}C)
H-31	17500 /	1500 /	50		156	156				131		94	131	0.15	97
H-32	17500 /	3000 /	50		160	160				136		93	136	0.15	97
H-33	17500 /	50 /	750		156	155				134		94	133	0.15	97
H-34	17500 /	50 /	1000		158	157				136		93	135	0.15	97
H-35	17500 /	1500 /	750		160	159				137		93	136	0.15	97
H-36	17500 /	3000 /	1000		163	163				138		93	138	0.15	97

TABLE A13
(continued)

Proximity Probe Measurements

TEST & RUN NO.	OPERATING CONDITION SHAFT SPEED (rpm)	RADIAL LOAD (lb)	THRUST LOAD (lb)	PROBE NO.	RMS DISTANCE FROM PROBE TO MEASURED SURFACE 1 In.	2 In.	3 In.	4 In.	5 In.	6 In.	7 In.	8 In.	9 In.
H-1	5000	1500	50		.03349	.03248	.03249	.03313	.03353	.03943	.02651	.02199	.03908
H-2	5000	3000	50		.03345	.03217	.03434	.03322	.03422	.03899	.02462	.02235	.04026
H-3	5000	50	750		.03309	.03043	.03623	.02738	.02890	.03452	.027676	.02127	.03821
H-4	5000	50	1000		.03283	.03022	.03575	.02729	.02872	.03456	.02707	.02127	.03786
H-5	5000	1500	750		.03278	.03004	.03656	.02729	.02940	.03342	.02487	.02176	.03961
H-6	5000	3000	1000		.03242	.03004	.03679	.02841	.03092	.03373	.02332	.02226	.04070
H-7	7500	1500	50		.03341	.03112	.03528	.03294	.03486	.03851	.02420	.02204	.04079
H-8	7500	3000	50		.03327	.03087	.03566	.03299	.03537	.03807	.02307	.02226	.04153
H-9	7500	50	750		.03314	.03078	.03538	.02738	.02821	.03474	.02731	.02109	.03738
H-10	7500	50	1000		.03319	.03065	.03547	.02701	.02798	.03439	.02731	.02118	.03755
H-11	7500	1500	750		.03279	.02974	.03679	.02715	.02968	.03333	.02462	.02154	.03983
H-12	7500	3000	1000		.03248	.02948	.03693	.02776	.03078	.03333	.02319	.02176	.04079
H-13	10000	1500	50		.03292	.03057	.03547	.03271	.03477	.03794	.02366	.02213	.04061
H-14	10000	3000	50		.03283	.03022	.03580	.03262	.03532	.03759	.02261	.02213	.04140
H-15	10000	50	750		.03318	.03078	.03443	.02771	.02826	.03548	.02794	.02059	.03690
H-16	10000	50	1000		.03274	.03087	.03467	.02757	.02784	.03469	.02748	.02109	.03699
H-17	10000	1500	750		.03274	.03100	.03448	.02780	.02858	.03482	.02655	.02104	.03790
H-18	10000	3000	1000		.03261	.03070	.03462	.02836	.02982	.03500	.02513	.02122	.03908
H-19	12500	1500	50		.03292	.03174	.03354	.03266	.03312	.03873	.02563	.02154	.03865
H-20	12500	3000	50		.02670	.03126	.03401	.03257	.03372	.03816	.02445	.02172	.03939
H-21	12500	50	750		.03256	.03004	.03486	.02836	.02940	.03500	.02634	.02081	.03747
H-22	12500	50	1000		.03230	.02978	.03533	.02794	.02936	.03421	.02563	.02100	.03782
H-23	12500	1500	750		.03159	.03100	.03458	.02888	.02890	.03461	.02567	.02172	.03725
H-24	12500	3000	1000		.03186	.03043	.03472	.02949	.03083	.03509	.02433	.02131	.03886
H-25	15000	1500	50		.03168	.03148	.03349	.03276	.03261	.03794	.02500	.02213	.03777
H-26	15000	3000	50		.03142	.03104	.03415	.03276	.03326	.03732	.02370	.02240	.03869
H-27	15000	50	750		.03235	.03035	.03349	.02869	.02895	.03583	.02727	.02059	.03633
H-28	15000	50	1000		.03226	.03022	.03354	.02832	.02867	.03544	.02718	.02054	.03633
H-29	15000	1500	750		.03195	.03022	.03396	.02869	.02954	.03513	.02563	.02081	.03760
H-30	15000	3000	1000		.03195	.02996	.03406	.02902	.03060	.03526	.02445	.02081	.03865

TABLE A13
(continued)

Proximity Probe Measurements

TEST & RUN NO.	OPERATING CONDITION SHAFT SPEED (rpm)	RADIAL LOAD (lb)	THRUST LOAD (lb)	PROBE NO.	RMS DISTANCE FROM PROBE TO MEASURED SURFACE 1 In.	2 In.	3 In.	4 In.	5 In.	6 In.	7 In.	8 In.	9 In.
H-31	17500	1500	50		.03177	.02965	.03373	.03065	.03202	.03636	.02441	.02072	.03847
H-32	17500	3000	50		.03173	.02935	.03401	.03084	.03271	.03605	.02315	.02091	.03917
H-33	17500	50	750		.03190	.02983	.03311	.02921	.02954	.03579	.02668	.02036	.03616
H-34	17500	50	1000		.03164	.03004	.03335	.02907	.02895	.03526	.02655	.02086	.03585
H-35	17500	1500	750		.03080	.02957	.03453	.02958	.03032	.03425	.02399	.02150	.03777
H-36	17500	3000	1000		.03106	.02926	.03434	.02967	.03147	.03465	.02298	.02561	.03891

TABLE A13
(continued)

BEARING DRAG TORQUE, MEASURED CAGE AND SHAFT SPEED DATA

TEST & RUN NO.	OPERATING CONDITION SHAFT SPEED (rpm)	RADIAL LOAD (lb)	THRUST LOAD (lb)	CAGE SPEED (rpm)	SHAFT SPEED (rpm)	CAGE SPEED/SHAFT SPEED RATIO	PERCENT SLIP BASED ON NO SLIP RATIO OF 0.40300 (%)	DRAG TORQUE (in-oz)
H-1	5000	1500	50	1998.1	5013.0	0.39958	0.85	60
H-2	5000	3000	50	1998.6	5004.0	0.39940	0.89	60
H-3	5000	50	750	555.3	5011.5	0.11081	72.5	100
H-4	5000	50	1000	601.1	4996.5	0.12029	70.2	150
H-5	5000	1500	750	682.5	4996.0	0.13661	66.1	110
H-6	5000	3000	1000	1966.9	4989.5	0.39421	2.18	125
H-7	7500	1500	50	2991.8	7516.0	0.39806	1.23	80
H-8	7500	3000	50	2995.9	7508.0	0.39903	0.98	89
H-9	7500	50	750	3021.6	7518.5	0.40188	2.76	94
H-10	7500	50	1000	3031.1	7514.0	0.40372	-0.18	94
H-11	7500	1500	750	3001.3	7508.0	0.39975	0.81	85
H-12	7500	3000	1000	2986.9	7498.5	0.39833	1.16	106
H-13	10000	1500	50	3977.1	10019.5	0.39693	1.51	89
H-14	10000	3000	50	3986.9	10001.5	0.39863	1.08	105
H-15	10000	50	750	4012.4	10004.0	0.40087	0.54	106
H-16	10000	50	1000	4032.9	10002.5	0.40318	-0.04	114
H-17	10000	1500	750	3997.3	9997.5	0.39983	0.79	105
H-18	10000	3000	1000	3991.7	9990.0	0.39957	0.85	106
H-19	12500	1500	50	49603	12509.5	0.39652	1.61	100
H-20	12500	3000	50	4977.9	12498.0	0.39830	1.17	132
H-21	12500	50	750	4976.9	12519.5	0.39754	1.35	116
H-22	12500	50	1000	5025.5	12504.0	0.40191	-0.27	116
H-23	12500	1500	750	4990.2	12497.0	0.39931	0.92	126
H-24	12500	3000	1000	4980.7	12486.5	0.39889	1.02	166
H-25	15000	1500	50	5932.4	15019.0	0.39499	1.99	118
H-26	15000	3000	50	5968.4	14998.5	0.39793	1.26	-
H-27	15000	50	750	5955.8	15034.0	0.39615	1.70	132
H-28	15000	50	1000	6019.1	15014.5	0.40089	0.52	133
H-29	15000	1500	750	5984.7	15006.0	0.39882	1.04	-
H-30	15000	3000	1000	5985.1	14995.5	0.39912	0.96	-

TABLE A13
(continued)

TEST & RUN NO.	OPERATING CONDITION SHAFT SPEED (rpm)	RADIAL LOAD (lb)	THRUST LOAD (lb)	CAGE SPEED (rpm)	SHAFT SPEED (rpm)	CAGE SPEED/SHAFT SPEED RATIO	PERCENT SLIP BASED ON NO SLIP RATIO OF 0.40300 (%)	DRAG TORQUE (in-oz)
H-31	17500	1500	50	6930.0	17530.0	0.39538	1.89	-
H-32	17500	3000	50	6967.6	17516.0	0.39778	1.30	-
H-33	17500	50	750	6892.5	17554.5	0.39263	2.57	-
H-34	17500	50	1000	7003.3	17524.0	0.39964	0.83	-
H-35	17500	1500	750	6981.9	17517.5	0.39856	1.10	-
H-36	17500	3000	1000	6979.5	17505.0	0.39871	1.06	-

APPENDIX B

TEST BEARINGS MEASURED DIMENSIONS

Radial Looseness

Brg. 01	Brg. 02	Brg. 03	Brg. 06
99 µm	75 µm	77 µm	75 µm

Inner Ring Roller Groove Radius (Axial)

	Brg. 01	Brg. 02	Brg. 03	Brg. 06
SS	39.550 mm	39.700 mm	40.751	41.400 mm
PS	40.000	40.100	40.747	41.200

Outer Ring Roller Groove Radius (Axial)

Brg. 01	Brg. 02	Brg. 03	Brg. 06
40.370 mm	40.350 mm	40.345 mm	40.380 mm

Roller Diameter

Roller	Brg. 01	Brg. 02	Brg. 03	Brg. 06
#1	12.998 mm	13.002 mm	12.998 mm	13.012 mm
#2	13.003	12.996	12.997	13.011
#3	13.001	12.999	13.000	13.009

Roller Out-of-Roundness

Roller	Brg. 01	Brg. 02	Brg. 03	Brg. 06
#1	2µm	1µm	1µm	-
#2	1	1	1	-
#3	2	1	1	-

Roller Axial Radius

Roller	Brg. 01	Brg. 02	Brg. 03	Brg. 06
#1	39.000 mm	39.000 mm	39.000 mm	39.600 mm
#2	39.100	38.995	38.750	39.600
#3	39.000	38.750	39.000	39.550

Roller Sphere End Radius

Roller	Brg. 01	Brg. 02	Brg. 03	Brg. 06
#1	152.00 mm	143.00 mm	146.00 mm	141.00 mm
#2	146.00	146.00	146.00	141.00
#3	147.00	148.00	149.00	141.00

Roller Length

Roller	Brg. 01	Brg. 02	Brg. 03	Brg. 06
#1	11.986 mm	12.043 mm	11.954 mm	11.992 mm
#2	11.989	11.941	11.986	12.038
#3	11.993	11.929	11.970	12.026

Inner Ring Roller Paths

Surface Finish - µin. "AA"

Brg.		Readings 1	2	3	Avg.
#1	SS	2.7-2.8	2.6-2.8	2.8-3.1	2.8
	PS	2.6-2.8	2.6-2.8	2.6-2.8	2.7
#2	SS	2.4-2.7	2.8-3.1	2.7-2.9	2.8
	PS	2.2-2.4	2.2-2.4	2.5-2.6	2.4
#3	SS	2.7-3.0	2.5-2.8	2.3-2.7	2.7
	PS	2.4-2.6	2.5-2.6	2.5-2.7	2.6
#6	SS	5.1-5.6	4.2-4.3	5.6-5.8	5.1
	PS	5.4-5.6	4.5-4.7	4.7-4.8	5.0

Outer Ring Roller Path

Surface Finish - μin. "AA"

Brg.	Reading	1	2	3	Avg.
#1		9.4-10.4	11.0-11.8	11.0-11.6	10.9
#2		10.7-11.7	10.3-10.7	9.4-10.6	10.6
#3		10.3-11.5	10.4-11.9	10.4-12.2	11.1
#6		5.2-5.5	5.3-5.6	4.6-6.5	5.5

Roller Outer Diameter (Axially)

Surface Finish - μIn. "AA"

Brg.	Roller	Reading	1	2	3	Avg.
#1	1		3.4-3.6	3.5-3.7	2.5-2.8	3.2
	2		2.8-3.0	2.3-2.7	2.8-3.1	2.8
	3		3.6-4.1	3.7-3.8	2.5-2.6	3.4
#2	1		2.4-2.6	2.3-2.5	2.9-3.1	2.6
	2		3.6-3.8	3.5-3.7	3.0-3.2	3.5
	3		2.6-2.8	2.8-2.9	2.7-3.1	2.8
#3	1		2.4-2.5	3.5-3.8	2.8-3.0	3.0
	2		2.3-2.5	2.4-2.7	2.6-2.8	2.6
	3		2.1-2.4	1.8-2.1	2.3-2.6	2.2
#6	1		4.1-4.4	4.4-4.5	3.8-3.9	4.2
	2		4.1-4.5	4.4-4.6	3.5-3.7	4.2
	3		4.4-4.5	4.8-4.9	4.1-4.3	4.5

Across Roller Finished End

Surface Finish - µin. "AA"

Brg.	Roller	Reading	1	2	3	Avg.
#1	1		2.7-2.9	3.0-3.3	3.4-4.1	3.2
	2		3.0-3.5	2.7-2.9	2.7-3.0	3.0
	3		3.2-3.4	3.6-4.1	3.2-3.7	3.5
#2	1		2.6-3.0	2.7-3.0	2.7-3.1	2.9
	2		2.7-3.2	2.9-3.4	2.5-3.3	3.0
	3		2.7-3.4	3.1-3.6	2.8-3.3	3.2
#3	1		2.8-3.5	2.8-3.5	3.9-4.6	3.5
	2		2.7-3.4	2.9-3.4	2.8-3.4	3.1
	3		2.9-3.4	2.8-3.3	2.7-3.1	3.0
#6	1		3.4-3.7	3.6-4.0	3.5-4.1	3.7
	2		3.9-4.3	3.5-4.0	4.4-5.5	4.3
	3		3.3-3.7	3.5-3.9	3.2-3.6	3.5